



HAL
open science

Boronic acid catalysts in amide synthesis: experimental and computational investigations

Fatima Almetwali

► **To cite this version:**

Fatima Almetwali. Boronic acid catalysts in amide synthesis: experimental and computational investigations. Organic chemistry. Normandie Université, 2023. English. NNT: 2023NORMC214 . tel-04238275

HAL Id: tel-04238275

<https://theses.hal.science/tel-04238275>

Submitted on 12 Oct 2023

HAL is a multi-disciplinary open access archive for the deposit and dissemination of scientific research documents, whether they are published or not. The documents may come from teaching and research institutions in France or abroad, or from public or private research centers.

L'archive ouverte pluridisciplinaire **HAL**, est destinée au dépôt et à la diffusion de documents scientifiques de niveau recherche, publiés ou non, émanant des établissements d'enseignement et de recherche français ou étrangers, des laboratoires publics ou privés.



Normandie Université



UNIVERSITÉ
CAEN
NORMANDIE

THÈSE

Pour obtenir le diplôme de doctorat

Spécialité CHIMIE

Préparée au sein de l'Université de Caen Normandie

Boronic Acid Catalysts in Amide Synthesis: Experimental and Computational Investigations

Présentée et soutenue par
FATIMA ALMETWALI

Thèse soutenue le 07/07/2023
devant le jury composé de

M. JEAN - MARC CAMPAGNE	Professeur des universités, Université de Montpellier	Rapporteur du jury
M. CLAUDIA LALLI	Professeur des universités, UNIVERSITE RENNES 1	Membre du jury
M. ARNAUD MARTEL	Professeur des universités, IUT LE MANS UNIVERSITE LE MANS	Président du jury
M. JÉRÔME BLANCHET	Chargé de recherche au CNRS, ENSICAEN	Directeur de thèse
M. JACQUES ROUDEN	Professeur des universités, ENSICAEN	Co-directeur de thèse

Thèse dirigée par **JÉRÔME BLANCHET (Laboratoire de chimie moléculaire et thio-organique (Caen))** et **JACQUES ROUDEN (Laboratoire de chimie moléculaire et thio-organique (Caen))**



A toi Maman

Acknowledgments

I would like to begin by expressing my gratitude to the members of my thesis committee: Pr. Jean-Marc Campagne (ENSCM, Montpellier), Pr. Arnaud Martel (IMMM, Le Mans), and Dr. Claudia Lalli (ISCR, Rennes). I am deeply honored by their willingness to evaluate my doctoral dissertation and research work.

Furthermore, I would like to extend my heartfelt appreciation to my thesis supervisors, Dr. Jérôme Blanchet and Pr. Jacques Rouden, for their daily availability, and valuable scientific discussions. Their mentorship and dedication have been pivotal in shaping both this dissertation and my personal growth as a researcher. Additionally, I am grateful for their meticulous review of this manuscript and the insightful feedback they provided.

I would also like to express my gratitude to the NMR analysis personnel, Hussein Elsiblani, and Rémi Legay, for the countless hours of engaging discussions. They not only provided valuable scientific insights but also brought joy and laughter. I am also thankful to Karine Jarsale for her patience and willingness to handle ten mass spectra samples at a time!

Also, I want to thank the administrative staff, Mme. Marie-Cecile Helaine and Mme. Janine Amice. Their dedication, professionalism, and commitment to addressing any concerns have been instrumental in ensuring a smooth administrative experience.

Moreover, I am delighted to have had the opportunity to meet and interact with several professors and doctors at LCMT. First and foremost, I would like to thank Dr. Jérôme Baudoux, and Dr. Bénédicte Lepoittevin from our research group for their support and the nice small-talks that we had. Furthermore, I am grateful for having had the opportunity to meet Pr. Jean-Luc Renaud, Dr. Isabelle Dez, and Dr. Jean-Francois, whose presence enhanced my academic journey.

I am incredibly appreciative of my colleagues at the JR group, namely Aimar Gonzalo-Barquero, Ava Boussetat, Jihen Ben Hadj Salem, and Clémence Nicolas, for their support and belief in my abilities. Their constant encouragement has been a tremendous source of inspiration and motivation. I also send my best wishes to Aimar and Jihen, who are on the verge of completing their Ph.D.

Furthermore, I thoroughly enjoyed getting to know and connect with colleagues and friends beyond our immediate group. Firstly, I express my deep appreciation to Jawad Fayek for his

presence during the most challenging moments, both professionally and personally. Moreover, I wholeheartedly value my friends Malak, Aziz, Audrey, Aurore, Nicholas, Julien, Pierre, Deborah, Iliia, Charles, and Lilia for the wonderful moments we have shared. I consider myself incredibly fortunate to have had the privilege of spending these three years of my life with such kind individuals.

I am equally glad for meeting with former students at LCMT, namely Dr. Fatima Rammal and Dr. Abdoul Diallo. Their kind-hearted nature has left a lasting impact on me.

Moreover, I would like to acknowledge my dad and siblings, for their unwavering love, encouragement, and patience.

Lastly, I want to express my infinite gratitude and love for my late mother, who taught me how to be strong, patient, hard-working, passionate, and kind. Without her, I wouldn't be the person I am today. While she won't witness me achieve this significant milestone in my life, I'm confident she'll be proud.

List of abbreviations

Å	Angstrom
Ac	Acetyl
AIBN	Azobisisobutyronitrile
Aq	Aqueous
Ar	Argon
Bn	Benzyl
Boc	<i>Tert</i> -butyloxycarbonyl
Bu	Butyl
°C	Degree Celsius
CH₃CN	Acetonitrile
CHCl₃	Chloroform
COMU	(1-Cyano-2-ethoxy-2-oxoethylideneaminoxy)dimethylamino-morpholino-carbenium hexafluorophosphate
CPME	Cyclopentyl methyl ether
Cy	Cyclohexane
D₂O	Deuterated water
DATB	1,3-Dioxa-5-aza-2,4,6-triborinane
DCC	<i>N,N'</i> -dicyclohexylcarbodiimide
DCE	Dichloroethane
DCM	Dichloromethane
DFT	Density functional theory
DIC	<i>N,N'</i> -diisopropylcarbodiimide
DIPEA	<i>N,N</i> -Diisopropylethylamine
DMAPO	4-(Dimethylamino)pyridine <i>N</i> -oxide
DMF	Dimethylformamide
DMG	Direct metalation group
DMSO	Dimethylsulfoxide
dr	Diastereomeric ratio
DVB	Divinylbenzene
EDC	1-Ethyl-3-(3'-dimethylaminopropyl)- carbodiimide
ee	Enantiomeric excess

eq/equiv	Equivalents
ESI	Electrospray ionization
Et	Ethyl
Et₂O	Diethylether
EtOAc	Ethyl acetate
EWG	Electron withdrawing group
FIA	Fluoride ion affinity
Fmoc	Fluorenylmethoxycarbonyl
HATU	<i>N</i> -[(dimethylamino)-1 <i>H</i> -1,2,3-triazolo[4,5- <i>b</i>]-pyridin-1-ylmethylene]- <i>N</i> -methylmethanaminium hexafluorophosphate <i>N</i> -oxide
HBTU	<i>N,N,N',N'</i> -Tetramethyl- <i>O</i> -(1 <i>H</i> -benzotriazol-1-yl)uronium hexafluorophosphate
HCl	Hydrochloric acid
HOAt	1-hydroxy-7-azabenzotriazole
HOBt	<i>N</i> -hydroxybenzotriazole
HOMO	Highest occupied molecular orbital
HRMS	High-resolution mass spectrometry
Hz	hertz
<i>i</i>-Bu	<i>Iso</i> -butyl
<i>i</i>-Pr	<i>Iso</i> -propyl
IR	Infrared spectroscopy
LA	Lewis acid
LUMO	Lowest unoccupied molecular orbital
M	Mol.L ⁻¹
Me	Methyl
MeOH	Methanol
mg	Milligram
μL	Microliter
MIBA	5-Methoxy-2-iodophenylboronic acid
min	Minute
mL	Millilitre
mmol	Millimole
mol%	Mole percent
MOM	Methoxymethyl ether

MS	Molecular sieves
Ms	Methanesulfonate
MTM	Methyltrimethoxysilane
NMP	<i>N</i> -Methylpyrrolidone
NMR	Nuclear magnetic resonance spectroscopy
Oxone	Potassium peroxymonosulfate
Oxyma	Ethyl cyanohydroxyiminoacetate
PAA	Phenylacetic acid
Ph	Phenyl
PhF	Fluorobenzene
PhMe	Toluene
Pin	Pinacol
ppm	Parts per million
rt	Room temperature
sat	Saturated
S_NA_r	Nucleophilic aromatic substitution
T	Temperature
TAME	<i>Tert</i> -amyl methyl ether
<i>t</i>-Bu	<i>Tert</i> -butyl
tBuOAc	<i>Tert</i> -butyl acetate
Tf	Trifluoromethanesulfonate
THF	Tetrahydrofuran
TMEDA	Tetramethylethylenediamine
TMS	Trimethylsilyl
TMSCN	Trimethylsilyl cyanide

Table of Contents

General introduction.....	14
Chapter 1. A literature review of amide bond formation strategies	18
1.1 Importance of the amide bond and its applications.....	20
1.2 Strategies for amide bond formation.....	21
1.2.1 Stoichiometric amidation methods.....	23
1.2.1.1 Acyl halides and anhydrides	23
1.2.1.2 Coupling via activated esters.....	24
1.2.1.3 Silicon-based coupling reagents.....	26
1.2.1.4 Boron-based reagents	27
1.2.2 Catalytic amide bond formation strategies.....	28
1.2.2.1 Organoboron catalysis.....	28
1.2.2.1.1 Boronic acid catalysts.....	29
1.2.2.1.2 Diboronic acids: A special case of boronic acid catalysis	48
1.2.2.1.3 Boric acid	50
1.2.2.1.4 Borate esters	51
1.2.2.1.5 Diboron reagents	52
1.2.2.1.6 Boron-Nitrogen heterocycles	53
1.2.2.2 Organocatalysis	55
1.2.2.3 Metal-catalysis	56
1.2.2.4 Photocatalysis.....	58
1.2.2.5 Biocatalysis	59
1.3 An overview of the current advancements and limitations in the boron-catalyzed direct amidation reaction.....	60
1.4 Project Objectives	63

Chapter 2. Cyclic borinic acids and biarylether-based boronic acids as promoters for direct amides synthesis.....	64
2.1 Catalytic application of borinic acids in amide synthesis	67
2.1.1 Introduction	67
2.1.2 Cyclic borinic acids in amidation reactions	68
2.1.2.1 Preliminary results.....	68
2.1.2.2 Preparation of cyclic borinic acid: sulfonylboraanthracene.....	70
2.1.2.3 Catalytic activity and stability studies of cyclic borinic acids	73
2.2 Biarylether-based boronic acids in the direct amidation reaction	77
2.2.1 Introduction and Objective.....	77
2.2.2 Preparation of aryloxyphenylboronic acids.....	78
2.2.3 Kinetic studies for catalytic activity evaluation	81
2.2.3.1 The case of 2-(aryloxy)phenylboronic acids	82
2.2.3.2 The case of 2,4-disubstituted derivatives	83
2.2.3.3 The case of 2,6-disubstituted derivatives	85
2.2.4 Comparative catalytic activity study with the state-of-the-art boronic acids.....	87
2.2.5 Examination of the scope of the reaction	89
2.2.6 Conclusion.....	89
2.3 Experimental Section	91
2.3.1 General Methods	91
2.3.2 Synthetic protocol and characterization for sulfonylboraanthracene.....	92
2.3.3 Synthetic protocol and characterization of oxaboraanthracene.....	94
2.3.4 Synthetic protocol and characterization of borinic acids' protodeborylation products	95
2.3.5 Procedure for the protodeboration experiments	97
2.3.5.1 Protodeboration of sulfonylboraanthracene	97
2.3.5.2 Protodeboration of oxaboraanthracene.....	98

2.3.6 Synthetic protocols and characterization for 2-(aryloxy)phenyl]boronic acids and their intermediates	98
2.3.6.1 General procedure A for the preparation of 2-aryloxyphenyl iodides	98
2.3.6.2 General procedure B for the preparation of 2-aryloxyphenyl boronic acids.....	98
2.3.6.3 Corresponding characterization data	99
2.3.7 Synthetic protocols and characterization for [2,4-bis(aryloxy)phenyl]boronic acids and their intermediates	106
2.3.7.1 General procedure C for the preparation of 2,4-aryloxybenzenes	106
2.3.7.2 General procedure D for the preparation of 2,4-aryloxybenzene bromides.....	106
2.3.7.3 General procedure E for the preparation of 2,4-aryloxybenzene boronic acids.	106
2.3.7.4 Corresponding chatacterization data	107
2.3.8 Synthetic protocols and characterization for [2,6-bis(aryloxy)phenyl]boronic acid and its intermediates.....	113
2.3.9 General procedure of kinetic experiments and raw kinetic data	117
2.3.10 Amides synthesis and characterization	118
Chapter 3. Lewis acidity quantification of arylboronic acids	120
3.1 Literature review of Lewis acidity quantification methods	122
3.1.1 Introduction	122
3.1.2 Classification of Lewis acidity metrics	122
3.1.3 Lewis acidity scaling methods	123
3.1.3.1 Effective Lewis acidity metrics	123
3.1.3.1.1 Spectroscopic metrics.....	124
3.1.3.1.2 Fluorescence-based technique	126
3.1.3.2 Intrinsic Lewis acidity metrics	128
3.1.3.3 Global Lewis acidity metrics.....	129
3.1.4 Lewis acidity determination of boronic acids	131
3.1.5 Conclusion.....	133

3.2 Results and discussion.....	134
3.2.1 Methodology for boronic acid catalyst selection/design in the literature	134
3.2.2 Lewis acidity assessment for a library of boronic acids.....	135
3.2.2.1 The choice of the FIA.....	135
3.2.2.2 Selection of DFT method	136
3.2.2.3 Anchoring agent for FIA calculations	137
3.2.2.4 Evaluation of Lewis acidity of biarylether-based boronic acids	138
3.2.2.5 Design of a new group of boronic acid catalysts	141
3.2.2.5.1 Key elements in catalyst design	141
3.2.2.5.2 FIA calculation for the new group of arylboronic acids	143
3.3 Conclusion.....	145
3.4 Experimental Section	146
3.4.1 Cartesian coordinates and energies of the studied molecules	146
3.4.2 Determination of reaction rates	160
Chapter 4. Novel class of (sulfonate)-functionalized arylboronic acid catalysts for amide bond formation	162
4.1 Introduction	165
4.2 Preparation of the (sulfonyloxy)phenylboronic acids	166
4.2.1 Mono-substituted-(sulfonyloxy)phenylboronic acids	166
4.2.2 2,6-Bis(sulfonyloxy)phenylboronic acids	169
4.2.3 2,4-Bis(sulfonyloxy)phenylboronic acid.....	178
4.2.4 2,4,6-Tris-(sulfonyloxy)phenylboronic acid	179
4.3 Kinetic Studies for catalytic activity evaluation	180
4.3.1 Catalytic activity assessment of mono-substituted arylboronic acids.....	180
4.3.2 Catalytic activity assessment of di-substituted arylboronic acids.....	182
4.3.3 Comparative catalytic activity study with the state-of-the-art boronic acids.....	183
4.4 Investigation of the catalyst stability during the amidation reaction	185

4.4.1 The case of 2-(triflyloxy)phenylboronic acid.....	185
4.4.2 The case of 2,6-bis(triflyloxy)phenylboronic acid.....	187
4.5 Selection of catalyst for scope examination.....	189
4.6 Optimization of reaction conditions for low-temperature amide synthesis	190
4.6.1 Effect of the nature of molecular sieves.....	190
4.6.2 Catalyst loading.....	195
4.7 Scope and limitations of low-temperature amide synthesis.....	196
4.8 Optimization of high-temperature amidation conditions	198
4.8.1 Effect of catalyst loading.....	198
4.8.2 Effect of the solvent	199
4.8.3 Effect of the solvent concentration.....	201
4.9 Scope of the high-temperature amides synthesis	202
4.10 Mechanistic investigation.....	204
4.11 Conclusions	211
4.12 Future Perspective	212
4.13 Experimental Section	214
4.13.1 General Methods	214
4.13.2 Preparation and characterization of <i>ortho</i> -(sulfonyloxy)phenylboronic acids.....	215
4.13.2.1 General procedure A for the preparation of 2-(sulfonyloxy)phenylboronic acid pinacol ester.....	215
4.13.2.2 General procedure B for the deprotection of 2-(sulfonyloxy)phenylboronic acid pinacol ester with NaIO ₄	215
4.13.2.3 General procedure C for the deprotection of 2-(sulfonyloxy)phenylboronic acid pinacol ester with diethanolamine.....	216
4.13.3 Preparation and characterization of <i>para</i> -(sulfonyloxy)phenylboronic acid and its pinacol ester.....	224
4.13.4 Synthesis and characterization of 2,6-bis(sulfonyloxy)phenylboronic acid and its synthetic intermediates	226

4.13.5 Synthesis and characterization of 2,4-bis(mesyloxy)phenylboronic acid.....	235
4.13.6 General procedure for kinetic studies and raw kinetic data	239
4.13.7 Synthesis of the protodeboronation products	240
4.13.8 Scope of the low-temperature amides synthesis	242
4.13.8.1 General procedure D for Low-temperature amide synthesis	242
4.13.8.2 Synthesis and characterization of amide substrates	242
4.13.9 Scope of the High-temperature amide synthesis	253
4.13.9.1 General procedure E for amide synthesis under azeotropic reflux	253
4.13.9.2 Synthesis and characterization of amide substrates	253
4.13.10 Synthesis and characterization of mixed anhydride intermediates	261
General Conclusion	265

General introduction

The amides are an essential class of compounds in modern chemistry due to their versatility. Importantly, the amide bond can be found in proteins, pharmaceuticals, and polymeric materials. The condensation of carboxylic acid and amine is one of the most direct routes for amide bond formation with water being the sole byproduct. However, when amines and carboxylic acids react directly, they form a stable ammonium carboxylate salt that requires very high temperatures (110 °C to 300 °C) to be converted into the amide. Consequently, this transformation often requires pre-activation of the carboxylic acid using a stoichiometric coupling reagent. Although coupling reagents facilitate amides synthesis under mild conditions, the method has some drawbacks, such as low atom economy, the generation of wastes, and, in certain cases, toxicity.

Alternatively, the catalytic direct amidation enables the formation of amide bonds without the need for pre-activation or stoichiometric reagents. Several non-metal and metal catalysts have shown potential in catalyzing this transformation. In particular, arylboronic acids have been one of the most investigated groups of catalysts in this active research area due to their versatility where they can be modified with various substituents to fine-tune their reactivity. Moreover, many arylboronic acid catalysts enable the condensation of carboxylic acids and amines at room temperature, which lowers the energy barrier of this process and permits a broad substrate scope.

In this thesis, our objective is to explore arylboronic acids that can catalyze the direct condensation of carboxylic acids and amines at room temperature and that compete favorably with the existing state-of-the-art boronic acids. Moreover, we are interested in probing the Lewis acidity of arylboronic acids through a computationally derived metric and understanding the relationship between their catalytic performance and Lewis acidity.

This manuscript is divided into four chapters:

- Firstly, in chapter I, an overview of the different methods for direct amide bond formation is presented. Moreover, special attention is given to the arylboronic acid-catalyzed approaches.
- Next, chapter II discusses our initial work on cyclic borinic acids. Also, it covers our study on a group of biarylether-based boronic acids in terms of their synthesis and application as catalysts for amide synthesis
- In chapter III, the different metrics for Lewis acidity quantification are presented. Additionally, this chapter presents our work on the determination of Lewis acidity of

biarylether-based boronic acids of chapter II, using the computational fluoride-ion affinity, and the design of a new group of *ortho*-(sulfonate)benzeneboronic acids.

- Lastly, chapter IV describes the preparation of the *ortho*-(sulfonate)benzeneboronic acids and the examination of their catalytic efficiency in the direct amide bond formation reaction. Mechanistic investigations are discussed as well.

Chapter 1. A literature review of amide bond formation strategies

Table of Contents

1.1 Importance of the amide bond and its applications.....	20
1.2 Strategies for amide bond formation.....	21
1.2.1 Stoichiometric amidation methods.....	23
1.2.1.1 Acyl halides and anhydrides	23
1.2.1.2 Coupling via activated esters.....	24
1.2.1.3 Silicon-based coupling reagents.....	26
1.2.1.4 Boron-based reagents	27
1.2.2 Catalytic amide bond formation strategies.....	28
1.2.2.1 Organoboron catalysis.....	28
1.2.2.1.1 Boronic acid catalysts.....	29
1.2.2.1.2 Diboronic acids: A special case of boronic acid catalysis	48
1.2.2.1.3 Boric acid	50
1.2.2.1.4 Borate esters	51
1.2.2.1.5 Diboron reagents	52
1.2.2.1.6 Boron-Nitrogen heterocycles	53
1.2.2.2 Organocatalysis	55
1.2.2.3 Metal-catalysis	56
1.2.2.4 Photocatalysis.....	58
1.2.2.5 Biocatalysis	59
1.3 An overview of the current advancements and limitations in the boron-catalyzed direct amidation reaction.....	60
1.4 Project Objectives	63

1.1 Importance of the amide bond and its applications

One of the most pertinent linkages in organic chemistry is the amide bond. It constitutes a key functional group in biologically important proteins and serves as the foundation of the pharmaceutical industry. Furthermore, according to a survey conducted in 2016, amide bond formation was one of the top five chemical transformations appearing in medicinal chemistry manuscripts over three decades, from 1984 to 2014.¹ Some examples of commercially available amide-based drugs include Paracetamol **1.1** (treatment of mild pain and fever), Tigan **1.2** (prevents nausea and vomiting), and Penicillin G **1.3** (treatment of bacterial infections) (Figure 1).

This class of molecules is not only used in medicinal chemistry, but it additionally has applications in materials science. Polyamides, which are polymers made of amide linkages, are extremely important due to their numerous applications. Some examples include Nomex® **1.4** and Kevlar® **1.5** (Figure 1), which are high-performance materials used in fields such as transportation, optically active materials, and smart materials.² Other examples range from simple everyday materials like nylon (6,6) **1.6** to more complicated and advanced applications such as polypeptide membranes for therapeutic delivery and surgical sealants.³

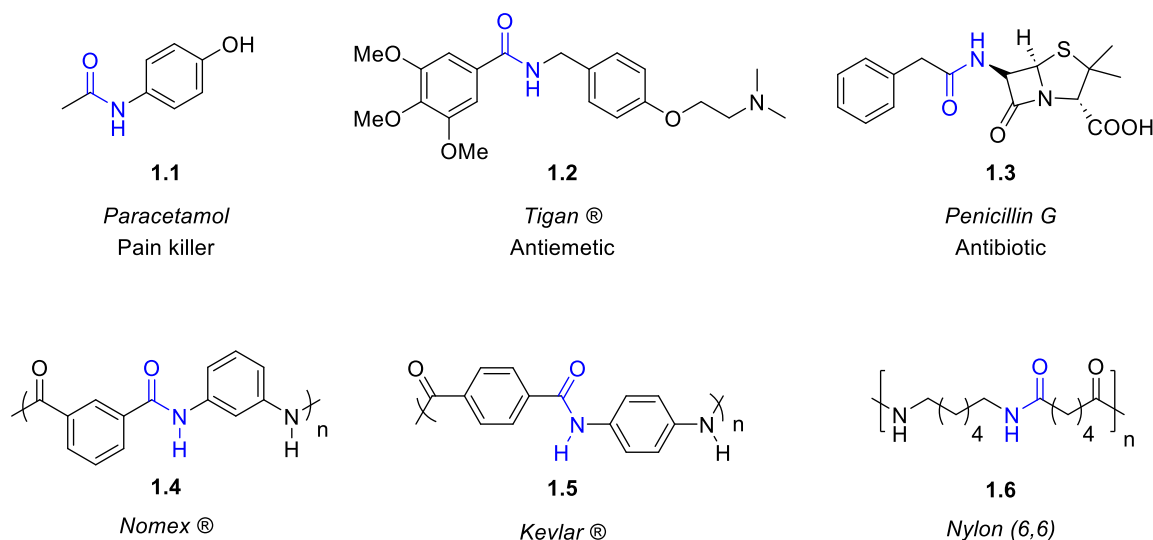


Figure 1

¹ Brown, D. G.; Boström, J. J. *Med. Chem.* **2016**, *59*, 4443–4458.

² (a) Marchildon, K. *Macromol. React. Eng.* **2011**, *5*, 22–54. (b) Reglero Ruiz, J. A.; Trigo-López, M.; García, F. C.; García, J. M. *Polymers* **2017**, *9*, 414.

³ Deming, T. J. *Prog. Polym. Sci.* **2007**, *32*, 858–875.

1.2 Strategies for amide bond formation

Carboxamide formation has been extensively studied over the last century, as a result, several methods have been developed, each having its advantages and disadvantages. The simplest way to construct amides would be the direct condensation of carboxylic acid and amine. Nevertheless, such condensation necessitates extremely high temperatures (160-180°C) to transform the unreactive ammonium carboxylate salt into the amide.⁴ As a consequence, such a procedure is restricted and not compatible with sensitive substrates, such as epimerization-prone amino acid residues or thermally sensitive compounds.⁵

To circumvent the employment of high temperatures, amides are mainly accessed via a condensation reaction between a carboxylic acid and an amine, mediated by a stoichiometric activating agent, otherwise known as a coupling reagent (Scheme 1).⁶ These reagents are highly efficient, as witnessed by their incredible success in peptide synthesis, however, the process suffers from poor atom economy and waste generation. In fact, in 2018, the American Chemical Society Green Chemistry Institute Pharmaceutical Roundtable (ACS GCIPR) published an update on the most relevant and promising green chemistry research areas within the pharmaceutical industry. Importantly, the subject of “general methods for catalytic/ sustainable (direct) amide or peptide formation” was identified as one of the top priority research areas.⁷ This has driven the interest in finding more green and sustainable routes for accessing these scaffolds.

In view of this, the challenge in amide synthesis is to devise sustainable strategies that avoid poor reactivity, racemization, low yield, large amounts of byproducts, poor selectivity, and complicated purification. Catalytic direct amidation (the coupling of a carboxylic acid and an amine) offers the possibility of lowering the energy requirements of these reactions and broadening the substrate scope. It is achieved *via* boron-based catalysts, transition metals, or organocatalysts (Scheme 1). This active research area has been covered by several reviews,

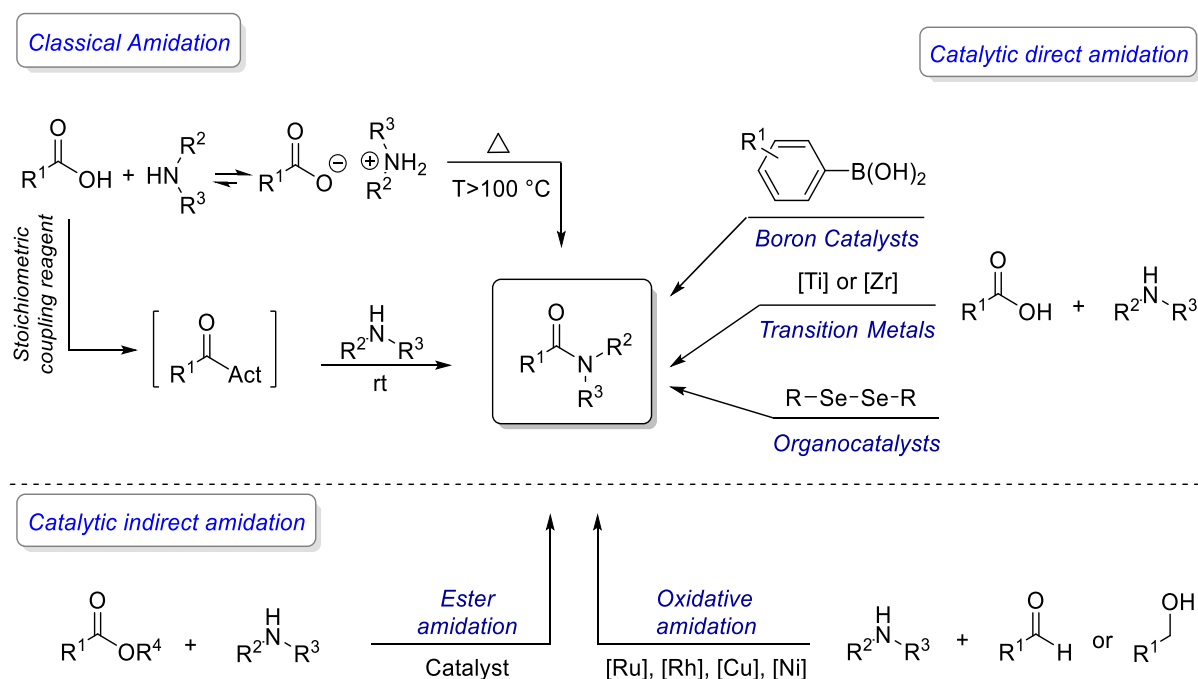
⁴ (a) Jursic, B. S.; Zdravkovski, Z. *Synth. Commun.* **1993**, *23*, 2761–2770. (b) Gooßen, L. J.; Ohlmann, D. M.; Lange, P. P. *Synthesis* **2009**, *2009*, 160–164.

⁵ Charville, H.; Jackson, D.; Hodges, G.; Whiting, A. *Chem. Commun.* **2010**, *46*, 1813–1823.

⁶ Valeur, E.; Bradley, M. *Chem. Soc. Rev.* **2009**, *38*, 606–631.

⁷ Bryan, M. C.; Dunn, P. J.; Entwistle, D.; Gallou, F.; Koenig, S. G.; Hayler, J. D.; Hickey, M. R.; Hughes, S.; Kopach, M. E.; Moine, G.; Richardson, P.; Roschangar, F.; Steven, A.; Weiberth, F. J. *Green Chem.* **2018**, *20*, 5082–5103.

one of which is Perrin's review which discusses the latest advances in catalytic amidation reactions.⁸ Moreover, indirect amidation (the coupling of other partners resulting in an amide bond), such as ester amidation or redox-coupled amidation, is one of the solutions for improving the poor sustainability of the current methods (Scheme 1). A number of reviews that discuss the developments in the field of indirect amidation reactions have been published. One key example is a review that covers the advances in the formation of amides from non-activated substrates and it highlights several ester and oxidative amidation strategies.⁹



Scheme 1

Given that our research work revolves around the development of catalytic amidation strategies starting from carboxylic acids and amines, only the direct amidation approaches will be presented in this chapter. The organoboron-mediated direct condensation of carboxylic acids and amines will be given special attention due to its relevance to our research area.

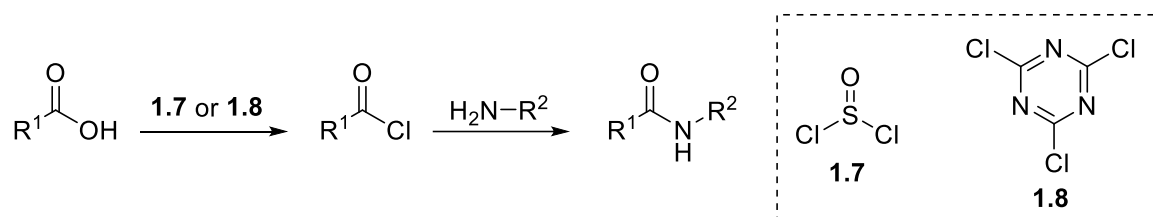
⁸ Todorovic, M.; Perrin, D. M. *Pept. Sci.* **2020**, *112*, e24210.

⁹ Ojeda-Porras, A.; Gamba-Sánchez, D. *J. Org. Chem.* **2016**, *81*, 11548–11555.

1.2.1 Stoichiometric amidation methods

1.2.1.1 Acyl halides and anhydrides

One of the classical approaches to activate a carboxylic acid is transforming it into an acid chloride.¹⁰ Several reagents can be used for the preparation of acid chlorides, among which are thionyl chloride¹¹ **1.7** and cyanuric chloride **1.8** (Scheme 2).¹² The high reactivity of acid chlorides toward amines generally results in fast reactions, which can be useful in the case of sterically hindered substrates. Nonetheless, their use for amide and peptide bond formation has been limited due to their ease of hydrolysis, cleavage of the acid-labile protecting groups, and racemization of α -amino acid chlorides. Acyl fluorides, on the other hand, may serve as a more stable substitute for acid chlorides, however, the generation of toxic hydrogen fluoride during their preparation is a major concern.¹³



Scheme 2

The reaction of an anhydride and an amine is another commonly used strategy for amide bond synthesis, with several possibilities of symmetrical and mixed anhydrides that can be utilized depending on the substrate and conditions to be employed.¹⁴ One way to prepare mixed anhydrides is using *iso*-butyl chloroformate¹⁵ (IBCF, **1.9**), which allows for a regioselective addition of the amine into the carboxy group of the carboxylic-carbonic anhydride (Scheme 3).

¹⁰ Williams, J. M. J. 5.01 - Acid Halides. In *Comprehensive Organic Functional Group Transformations*; Katritzky, A. R., Meth-Cohn, O., Rees, C. W., Eds.; Elsevier Science: Oxford, **1995**; pp 1–21.

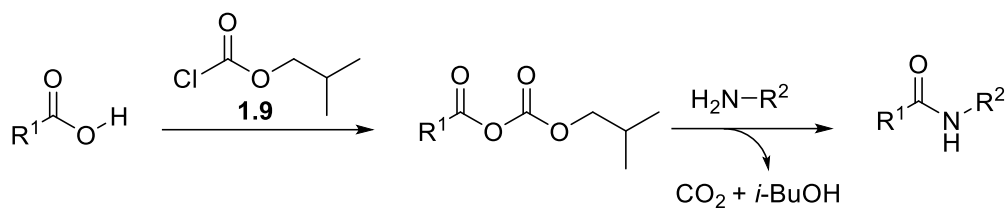
¹¹ Zuffanti, Saverio. *J. Chem. Educ.* **1948**, *25*, 481.

¹² Venkataraman, K.; Wagle, D. R. *Tetrahedron Lett.* **1979**, *20*, 3037–3040.

¹³ (a) Gonay, M.; Batisse, C.; Paquin, J.-F. *Synthesis* **2021**, *53*, 653–665. (b) Aigueperse, J.; Mollard, P.; Devilliers, D.; Chemla, M.; Faron, R.; Romano, R.; Cueur, J. P. Fluorine Compounds, Inorganic. In *Ullmann's Encyclopedia of Industrial Chemistry*; John Wiley & Sons, Ltd, **2000**; pp 404-405.

¹⁴ Montalbetti, C. A. G. N.; Falque, V. *Tetrahedron* **2005**, *61*, 10827–10852.

¹⁵ Chaudhary, A.; Girgis, M. J.; Prashad, M.; Hu, B.; Har, D.; Repič, O.; Blacklock, T. J. *Org. Process Res. Dev.* **2003**, *7*, 888–895.



Scheme 3

Other notable reagents include *n*-propanephosphonic acid anhydride¹⁶ (T3P), which is widely used since it is suitable with epimerization-prone substrates¹⁷ and it generates easily removable, water-soluble byproducts.

Aside from the fact that anhydrides are particularly useful for *N*-acylation of amines, when symmetrical anhydrides are used, only half of the starting acid is coupled with the amine, making such a process limited and not cost- or time-effective. Additionally, regioselectivity issues may arise in some cases, such as the case of carboxylic-acetic mixed anhydrides.

1.2.1.2 Coupling via activated esters

One of the customary ways to activate a carboxylic acid before its reaction with an amine is to transform it into an active ester. One approach is to utilize carbodiimides, which activate the carboxylic acid through an *O*-acylisourea intermediate, that can be viewed as a carboxylic ester with an activated leaving group. Moreover, they have been widely employed as coupling reagents for efficient amide formation reactions since the seminal report on *N,N*-dicyclohexylcarbodiimide (DCC, **1.10**) in 1955.¹⁸ Since then, a plethora of carbodiimides has been reported, including DIC **1.11** and EDC.HCl **1.12** (Scheme 4).¹⁹ In most cases, carbodiimides are used in conjugation with an *N*-hydroxy-containing additive (Scheme 4), such as HOBt **1.13**, HOAt **1.14**, or Oxyma **1.15**,²⁰ to increase the rate of the reaction and suppress racemization pathways.

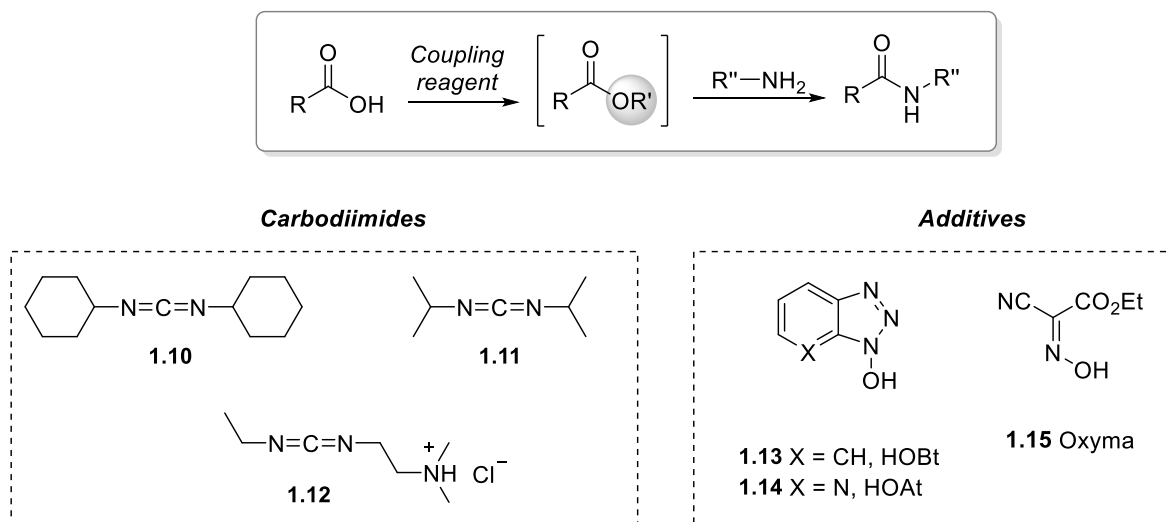
¹⁶ (a) Wissmann, H.; Kleiner, H.-J. *Angew. Chem., Int. Ed. Engl.* **1980**, *19*, 133–134. (b) Waghmare, A. A.; Hindupur, R. M.; Pati, H. N. *Rev. J. Chem.* **2014**, *4*, 53–131.

¹⁷ Dunetz, J. R.; Xiang, Y.; Baldwin, A.; Ringling, J. *Org. Lett.* **2011**, *13*, 5048–5051.

¹⁸ Sheehan, J. C.; Hess, G. P. *J. Am. Chem. Soc.* **1955**, *77*, 1067–1068.

¹⁹ Rich, D. H.; Singh, J. Chapter 5 - The Carbodiimide Method. In *Major Methods of Peptide Bond Formation*; Gross, E., Meienhofer, J., Eds.; Academic Press, **1979**; Vol. 1, pp 241–261.

²⁰ Subirós-Funosas, R.; Prohens, R.; Barbas, R.; El-Faham, A.; Albericio, F. *Chem. Eur. J.* **2009**, *15*, 9394–9403.



Scheme 4

Another notable family of reagents developed for the formation of active esters are the uronium/guanidinium salts. Several reagents have been created in association with various activators (Figure 2), comprising HBTU **1.16**,²¹ HATU **1.17**, and COMU **1.18**.²² Importantly, COMU **1.18** have demonstrated higher coupling efficiency, reduced epimerization, and a less hazardous safety profile than the benzotriazole-based reagents HBTU/HATU.²³

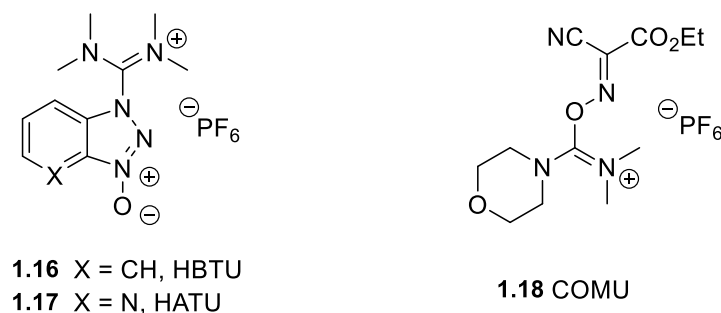


Figure 2

It's worth noting that phosphonium salts can be similarly employed as coupling reagents to uronium/guanidinium reagents. Nonetheless, it has been pointed out, in a review that discusses the applicability of amide coupling reagents for large-scale applications,²⁴ that these reagents are rarely used in process chemistry. The reason behind their limited use is that they generate a

²¹ Dourtoglou, V.; Ziegler, J.-C.; Gross, B. *Tetrahedron Lett.* **1978**, *15*, 1269–1272.

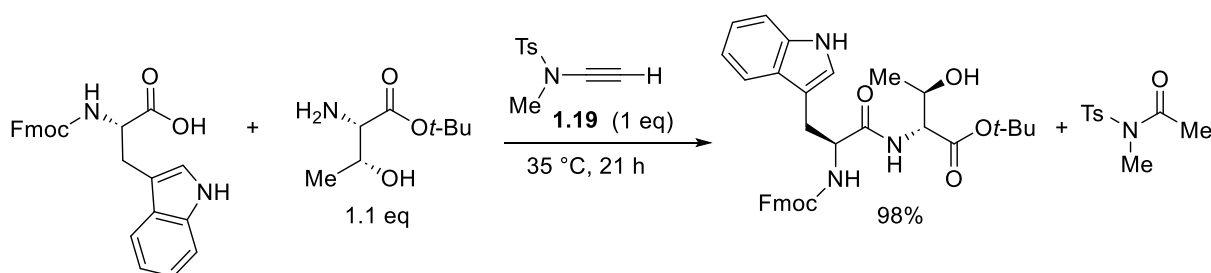
²² For a review on peptide coupling reagents, see: El-Faham, A.; Albericio, F. *Chem. Rev.* **2011**, *111*, 6557–6602.

²³ El-Faham, A.; Subirós Funosas, R.; Prohens, R.; Albericio, F. *Chem. Eur. J.* **2009**, *15*, 9404–9416.

²⁴ Dunetz, J. R.; Magano, J.; Weisenburger, G. A. *Org. Process Res. Dev.* **2016**, *20*, 140–177.

carcinogenic byproduct, hexamethylphosphoramide (HMPA), and due to the high cost associated with the use of relatively safer derivatives.²⁴

Importantly, ynamide **1.19** has been described as a highly efficient coupling reagent for the one-pot synthesis of amides and peptides, under mild conditions.²⁵ Also, it was used for peptide segment condensation. Interestingly, no racemization was detected for chiral substrates, and high functional group tolerance was demonstrated by the compatibility of side chains bearing alcohol, thiol, or indole moieties (Scheme 5).



Scheme 5

Although amide coupling reagents are highly competent, as evidenced by their enormous success in the field of peptide synthesis,²⁶ the process typically suffers from poor atom economy, waste generation, and, in many cases, toxicity and safety issues.

1.2.1.3 Silicon-based coupling reagents

Silicon-based reagents have shown promise as useful tools for organic synthesis due to their versatile reactivity, and wide availability. Several of these reagents have also displayed potential as stoichiometric amide coupling reagents (Figure 3). Chan *et al.* pioneered the work on silicon-based reagents for direct amidation with their report on silicon tetrachloride **1.20** in 1969.²⁷ Additionally, Ruan and colleagues reported on the use of commercially available and structurally simple phenylsilane **1.21** that mediates amide synthesis via the formation of an active silylester.²⁸ The latter methodology was later upgraded by Blanchet *et al.* and it was

²⁵ Hu, L.; Xu, S.; Zhao, Z.; Yang, Y.; Peng, Z.; Yang, M.; Wang, C.; Zhao, J. *J. Am. Chem. Soc.* **2016**, *138*, 13135–13138.

²⁶ Chandrudu, S.; Simerska, P.; Toth, I. *Molecules* **2013**, *18*, 4373–4388.

²⁷ Chan, T.-H.; Wong, L. T. L. *J. Org. Chem.* **1969**, *34*, 2766–2767.

²⁸ Ruan, Z.; Lawrence, R. M.; Cooper, C. B. *Tetrahedron Lett.* **2006**, *47*, 7649–7651.

effectively used to construct dipeptides, tripeptides, and Weinreb amides.²⁹ Another notable example is the recent work of Braddock and colleagues, who reported an amide synthesis strategy that is operationally concise and employs the use of inexpensive and relatively safe methyltrimethoxysilane (MTM, **1.22**).³⁰ In relation to the topic of orthosilicate reagents, a new study has revealed the efficiency of novel hexamethoxydisilane **1.23** and dodecamethoxyneopentasilane **1.24** for a solvent-free amide synthesis.³¹

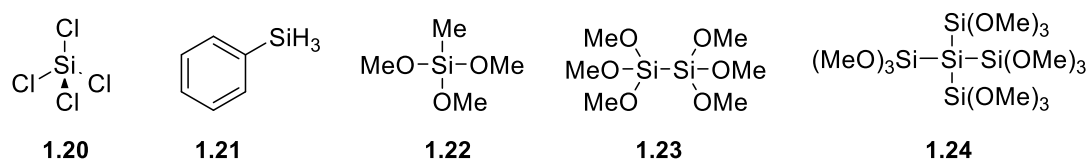


Figure 3

In a recent review, the advances in the field of silicon-based reagents as stoichiometric amide coupling reagents were highlighted, and the advantages as well as the limitations of each method were discussed.³²

1.2.1.4 Boron-based reagents

Pelter and Nelson initiated the work on organoboron-mediated amidation reactions in 1965 with the use of tris(dialkylamino)boranes for converting carboxylic acids to amides, under refluxing benzene conditions (80 °C).³³

Moreover, the stoichiometric use of catecholborane **1.25** has been described for the synthesis of amides and macrocyclic lactams (Figure 4).³⁴ Later, Wang described the solid-supported catecholborane **1.26** as an efficient boron reagent for the room-temperature synthesis of amide bonds (Figure 4).³⁵

²⁹ Morisset, E.; Chardon, A.; Rouden, J.; Blanchet, J. *Eur. J. Org. Chem.* **2020**, 2020, 388–392.

³⁰ Braddock, D. C.; Davies, J. J.; Lickiss, P. D. *Org. Lett.* **2022**, 24, 1175–1179.

³¹ Lainer, T.; Czerny, F.; Haas, M. *Org. Biomol. Chem.* **2022**, 20, 3717–3720.

³² Davies, J. J.; Braddock, D. C.; Lickiss, P. D. *Org. Biomol. Chem.* **2021**, 19, 6746–6760.

³³ Nelson, P.; Pelter, A. *J. Chem. Soc.* **1965**, 5142–5144.

³⁴ Collum, D. B.; Chen, S.-C.; Ganem, B. *J. Org. Chem.* **1978**, 43, 4393–4394.

³⁵ Yang, W.; Gao, X.; Springsteen, G.; Wang, B. *Tetrahedron Lett.* **2002**, 43, 6339–6342.

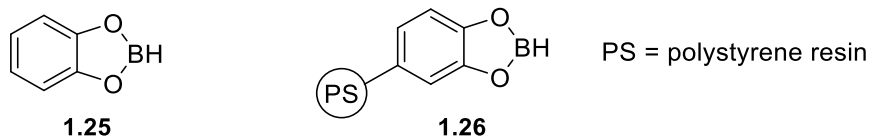
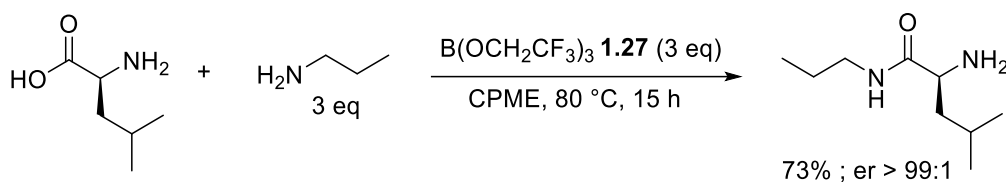


Figure 4

In 2016, Sheppard demonstrated the utility of the commercially available trifluoroethylborate **1.27** for the direct amidation of unprotected α -amino acids with a broad range of amines, in cyclopentyl methyl ether (CPME), at 80 °C (Scheme 6).³⁶ The reactions of the amino acids with both primary and secondary amines proceeded effectively, with very low levels of racemization.



Scheme 6

Moreover, a catalytic version of the trifluoroethylborate-mediated amidation was developed and is discussed in the upcoming section.

1.2.2 Catalytic amide bond formation strategies

1.2.2.1 Organoboron catalysis

One of the most eminent classes of molecules studied for catalytic amide bond formation is organoboron catalysts. Several reviews have been published in this context that discuss, not exclusively but in great part, the organoboron-based catalytic systems for amidation reactions and provide valuable insights into the current state-of-the-art in the field. An example is the review by Shimizu and Sawamura which has placed major emphasis on the newly emerging multinuclear boron catalysts.³⁷ Another notable review is that published by Campagne *et al.* and it discusses the catalytic, mechanistic, and scope generality aspects of organoboron catalysts.³⁸ Additionally, Perrin *et al.* have highlighted several boron-based approaches and

³⁶ Lanigan, R. M.; Karaluka, V.; Sabatini, M. T.; Starkov, P.; Badland, M.; Boulton, L.; Sheppard, T. D. *Chem. Commun.* **2016**, 52, 8846–8849.

³⁷ Sawamura, M.; Shimizu, Y. *Eur. J. Org. Chem.* **2023**, 26, e202201249.

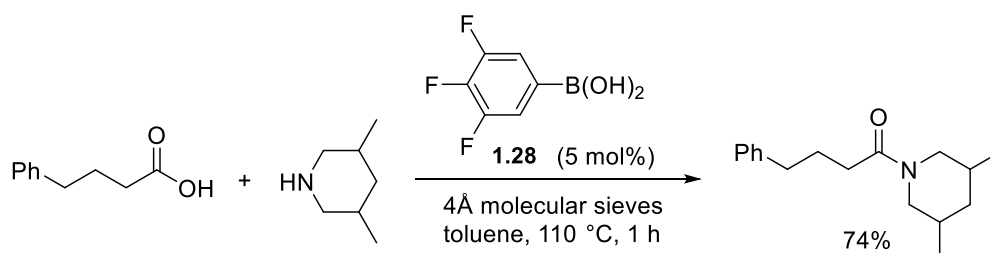
³⁸ Taussat, A.; de Figueiredo, R. M.; Campagne, J.-M. *Catalysts* **2023**, 13, 366.

their applicability for amino acid coupling.⁸ Sheppard and colleagues have also reviewed the green chemistry aspects of catalytic amidation strategies, among which were the organoboron-catalyzed methods.³⁹ Other key reviews include those of Raines⁴⁰ and Taylor⁴¹ which discuss organoboron acids and their catalytic applications.

Aside from the above-mentioned ones, some of the important literature reviews that detailed the boronic acid catalysis include the review of D.G. Hall which presents the numerous catalytic applications of boronic acids,⁴² and another by de Figueiredo and Campagne, which illustrates all reported boronic acid catalysts until 2015.⁴³ In the next section, several boronic acid catalysts are depicted.

1.2.2.1.1 Boronic acid catalysts

Arylboronic acids have been extensively studied as catalysts for direct amide bond formation since their Lewis acidity can be finely tuned through the modulation of substituents, allowing for the optimization of the catalytic condensation between free carboxylic acids and amines. The applicability of boronic acids as catalysts for the direct amidation reaction became known after Yamamoto's seminal work on the utility of electron-deficient arylboronic acids in amide synthesis. Following a screening of various arylboronic acids decorated with various electron-withdrawing groups (EWG), it was discovered that 3,4,5-trifluorophenylboronic acid **1.28** is the most active catalyst.⁴⁴ The boronic acid **1.28** was exploited for the condensation of carboxylic acids with various amine classes, including anilines (Scheme 7).



Scheme 7

³⁹ Sabatini, M. T.; Boulton, L. T.; Sneddon, H. F.; Sheppard, T. D. *Nat Catal* **2019**, 2, 10–17.

⁴⁰ Graham, B. J.; Raines, R. T. *J. Org. Chem.* **2022**.

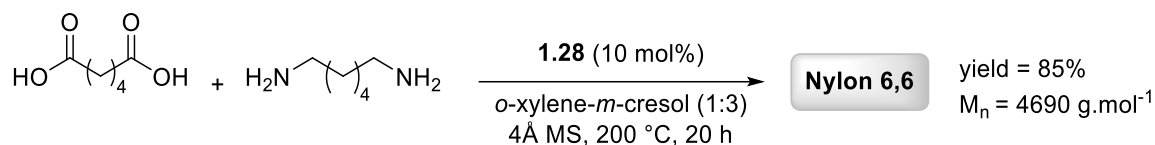
⁴¹ Dimitrijević, E.; Taylor, M. S. *ACS Catal.* **2013**, 3, 945–962.

⁴² Hall, D. G. *Chem. Soc. Rev.* **2019**, 48, 3475–3496.

⁴³ de Figueiredo, R. M.; Suppo, J.-S.; Campagne, J.-M. *Chem. Rev.* **2016**, 116, 12029–12122.

⁴⁴ Ishihara, K.; Ohara, S.; Yamamoto, H. *J. Org. Chem.* **1996**, 61, 4196–4197.

Interestingly, the applicability of boronic acid **1.28** was also explored for catalyzing the direct polycondensation of diacids and diamines to form polyamides (Scheme 8).⁴⁵ This process has enabled the formation of aliphatic polyamides (e.g., nylon 6,6) and aramids in good to excellent yields. Such a strategy is restricted by the difficulty to achieve high-molecular-weight polyamides and the use of elevated reaction temperatures (> 200 °C). However, to this date, this protocol represents the only organoboron-catalyzed approach for polyamide synthesis.



Scheme 8

The group of Yamamoto has made additional contributions to this field by developing arylboronic acids whose activities are not diminished in polar solvents. They developed *N*-alkyl-4-boronopyridinium salt (**1.29**) that can operate in polar solvents such as *N*-methylpyrrolidinone (NMP) (Figure 5).⁴⁶ The boronic acid **1.29** was used in a biphasic toluene-ionic liquid medium, which allowed for a significant improvement in the catalytic activity and enabled catalyst recovery. Nonetheless, at 120 °C, **1.29** underwent gradual protodeborylation. Polymer-supported versions of this catalyst were also developed as heterogeneous and recyclable amidation catalysts (Figure 5). It is worth noting that polystyrene-bound 3-boronopyridinium chloride **1.31**, developed by Wang,⁴⁷ is unstable and deboronates into boric acid, as opposed to Yamamoto's more stable 4-boronopyridinium chloride **1.30**.⁴⁰

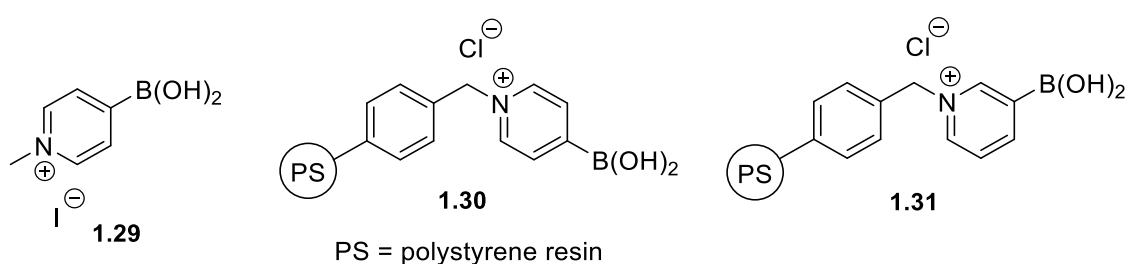


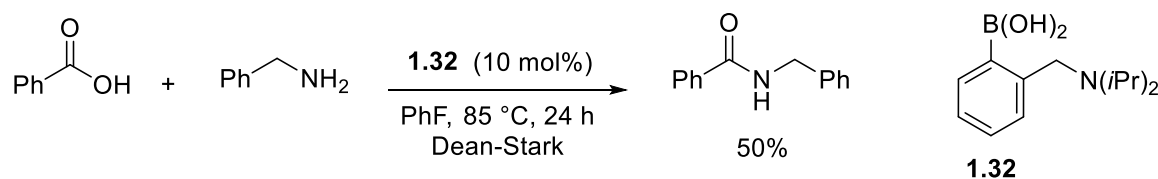
Figure 5

⁴⁵ Ishihara, K.; Ohara, S.; Yamamoto, H. *Macromolecules* **2000**, *33*, 3511–3513.

⁴⁶ Maki, T.; Ishihara, K.; Yamamoto, H. *Org. Lett.* **2005**, *7*, 5043–5046.

⁴⁷ Latta, R.; Springsteen, G.; Wang, B. *Synthesis* **2001**, *2001*, 1611–1613.

After considerable effort to reduce dehydrative amidation reaction temperatures below that of refluxing toluene (bp =110 °C), Whiting *et al.* reported on the utility of bifunctional aminoboronic acid catalysts in refluxing fluorobenzene (85 °C).⁴⁸ It was revealed that *N,N*-diisopropylbenzylamine-2-boronic acid **1.32** demonstrated utility for less reactive substrates, such as aromatic carboxylic acids, at lower temperatures (85 °C) (Scheme 9). To investigate the effect of the Lewis acidity of **1.32** on its catalytic activity, two derivatives of **1.32** were tested, where the *N,N*-di-isopropylaminobenzyl function was retained.⁴⁹ It was revealed that the addition of an *ortho*-methoxy group resulted in a significant decrease in the reaction rate, however, a *para*-trifluoromethyl group has enabled slightly faster reactions. Although it is evident that decreasing the electron density on **1.32** improved its catalytic activity, it is not obvious whether the drop in the activity with the *ortho*-methoxy substituted derivative is due to its lower Lewis acidity only, or if there is a contribution of steric hindrance from the *ortho*-position.



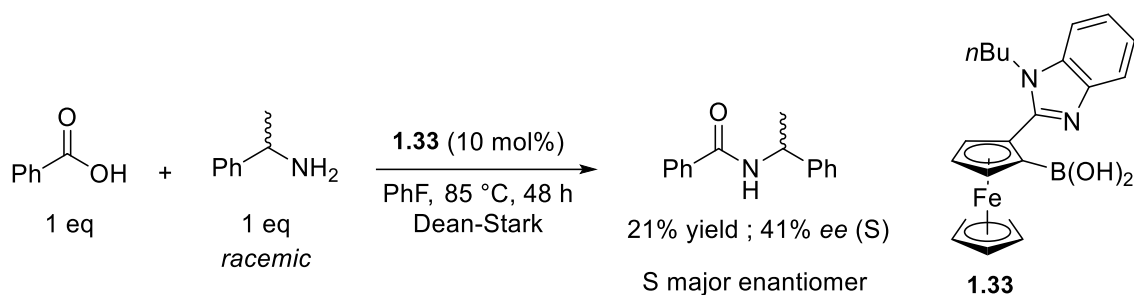
Scheme 9

After unraveling this class of aminoboronic acids, Whiting and coworkers investigated chiral aminoboronic acids with ferrocene backbone to achieve kinetic resolution of amines.⁵⁰ It was discovered that catalyst **1.33** enabled the coupling of benzoic acid to one enantiomer of chiral, α -substituted benzylamine with low yield and low enantiomeric excess (Scheme 10). This protocol, however, represents the only example of an asymmetric direct amidation to date.

⁴⁸ Arnold, K.; Davies, B.; Giles, R. L.; Grosjean, C.; Smith, G. E.; Whiting, A. *Adv. Synth. Catal.* **2006**, *348*, 813–820.

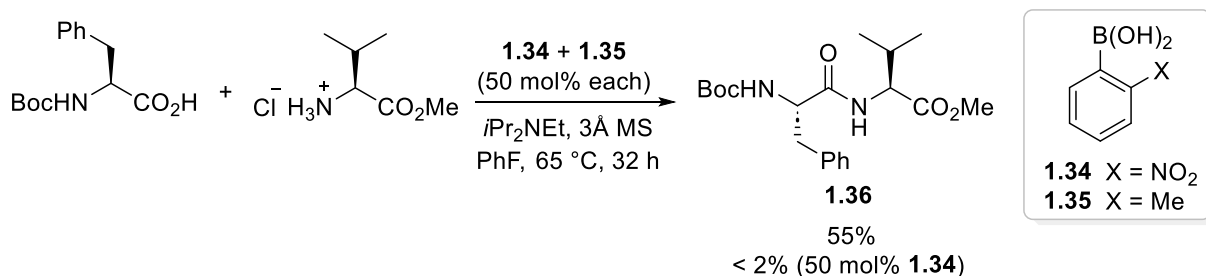
⁴⁹ Arnold, K.; Batsanov, A. S.; Davies, B.; Whiting, A. *Green Chem.* **2008**, *10*, 124–134.

⁵⁰ Arnold, K.; Davies, B.; Hérault, D.; Whiting, A. *Angew. Chem. Int. Ed. Engl.* **2008**, *47*, 2673–2676.



Scheme 10

None of the boronic acid-mediated amidation strategies listed so far was examined on peptide synthesis, and this could be attributed to the high temperatures employed, thus, limiting their use on the epimerization-prone amino acid substrates. Nonetheless, Whiting *et al.* have studied the efficacy of a binary arylboronic acid catalyst system composed of a 1:1 mixture of 2-nitro-**1.34** and 2-methyl-**1.35** phenylboronic acids in the amidation of α -amino acids at 65 °C (Scheme 11).⁵¹ This synergistic system was especially useful for the least reactive amino acid combinations. For example, dipeptide **1.36** was synthesized in 55% yield using **1.34** and **1.35**, each with 50 mol% loading, whereas the use of **1.34** (50 mol%) provided a 2% yield only (Scheme 11). On the other hand, this protocol is hampered by the high catalyst loadings.

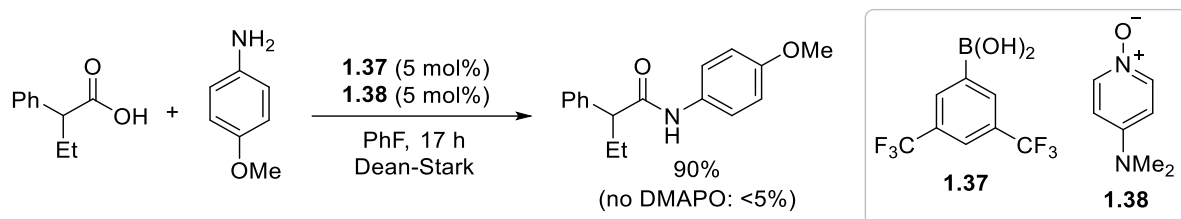


Scheme 11

Another example of a cooperative catalytic system comprises the use of arylboronic acid **1.37** and 4-(*N,N*-dimethylamino)pyridine *N*-oxide (DMAPO, **1.38**).⁵² The use of DMAPO co-catalyst allowed for significantly improving the results with challenging carboxylic acids, such as aromatic, α -branched, and conjugated substrates (Scheme 12).

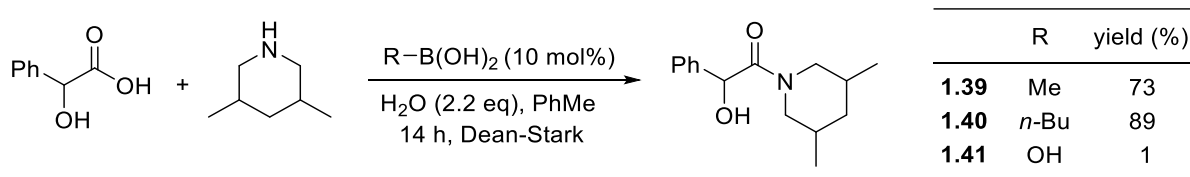
⁵¹ Liu, S.; Yang, Y.; Liu, X.; Ferdousi, F. K.; Batsanov, A. S.; Whiting, A. *Eur. J. Org. Chem.* **2013**, 2013, 5692–5700.

⁵² Ishihara, K.; Lu, Y. *Chem. Sci.* **2016**, 7, 1276–1280.



Scheme 12

Generally, the reports on boronic acid-assisted amide synthesis are dominated by the implementation of arylboronics due to the feasibility of functionalizing their aromatic ring. Nevertheless, Ishihara *et al.* reported on the use of alkylboronic acids, particularly methyl- **1.39** and *n*-butyl- **1.40** boronic acids, as highly competent catalysts for the coupling of α -hydroxycarboxylic acids (Scheme 13).⁵³ Notably, α -hydroxycarboxylic acids are unsuccessful substrates for arylboronic acid catalysts such as **1.28** and **1.32**. Moreover, the possibility of background boric acid catalysis, which could result from protodeboronation of **1.39** or **1.40**, was ruled out since only traces of amide product (1%) were obtained when boric acid **1.41** was used (Scheme 13).



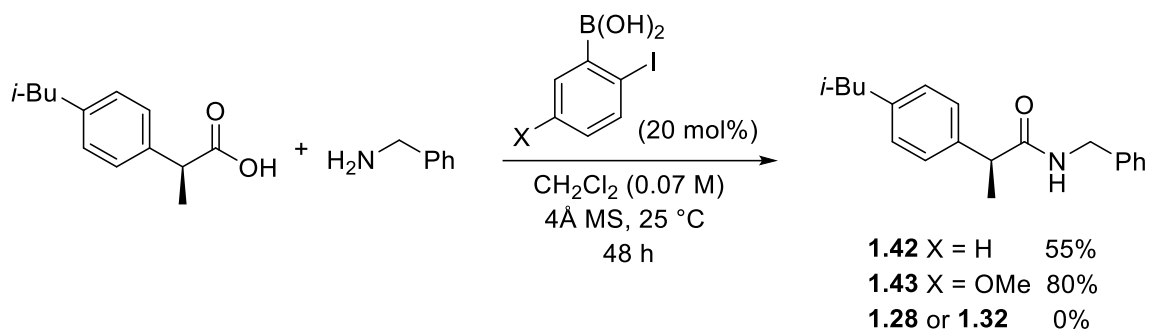
Scheme 13

All of the aforementioned strategies require elevated temperatures ranging from 65 °C to 165 °C. In 2008, Hall *et al.* accomplished room-temperature boronic acid-catalyzed amidation with the use of *ortho*-iodophenylboronic acid **1.42**.⁵⁴ An extensive list of 45 *ortho*-functionalized arylboronic acids was screened, among which *ortho*-iodophenylboronic acid **1.42** was the best performing. Shortly after, the same authors reported the kinetically more active 5-methoxy-2-iodophenylboronic acid (MIBA, **1.43**) (Scheme 14).⁵⁵ Both of these catalysts significantly outperformed Yamamoto's **1.28** and Whiting's **1.32** boronic acids, both of which did not produce the amide product at room temperature (Scheme 14).

⁵³ Yamashita, R.; Sakakura, A.; Ishihara, K. *Org. Lett.* **2013**, *15*, 3654–3657.

⁵⁴ Al-Zoubi, R. M.; Marion, O.; Hall, D. G. *Angew. Chem., Int. Ed. Engl.* **2008**, *47*, 2876–2879.

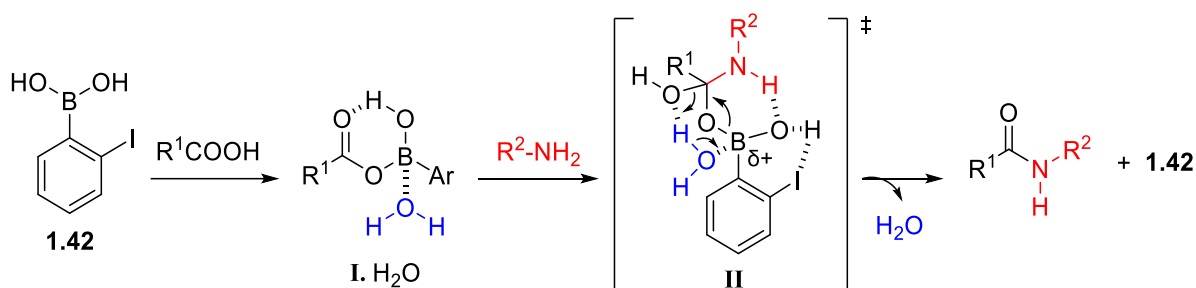
⁵⁵ Gernigon, N.; Al-Zoubi, R. M.; Hall, D. G. *J. Org. Chem.* **2012**, *77*, 8386–8400.



Scheme 14

The mild reaction conditions employing MIBA **1.43** has allowed the coupling of functionalized acids and amines carrying phenol, pyridine, and indole units. On the contrary, aromatic acids produced low to moderate yields, even at 50 °C and with 20 mol% **1.43**.⁴⁹

Upon the examination of the catalytic activity of the *ortho*-(halo)phenylboronic acids, it was observed that the trend of reactivity in this series was in the decreasing order of I > Br > Cl > F. This reverse trend was difficult to rationalize given that the 2-fluorophenylboronic acid is more electron-deficient than the 2-iodo **1.42**. Intrigued by this observation, Marcelli investigated the role of this *ortho*-iodine group using density functional theory (DFT).⁵⁶ It was postulated that the iodine acts as a Lewis basic site that forms hydrogen bonds with the boron-bound hydroxy group in the orthoaminal transition state **II** (Scheme 15). This hydrogen-iodine bonding favors the breakdown of the transition state **II** by a water molecule and the release of the amide.

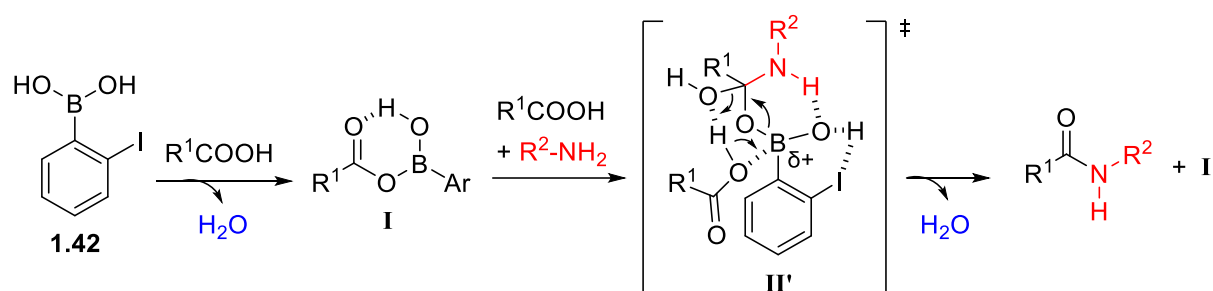


Scheme 15

The requirement of a water molecule for the orthoaminal breakdown contradicts the fact that these reactions operate under rigorously anhydrous conditions. Accordingly, Hall *et al.* have proposed an alternative mechanism that is in line with the experimental findings.⁵⁵ First, it was stated that a "premix" of the carboxylic and boronic acids with the molecular sieves was critical

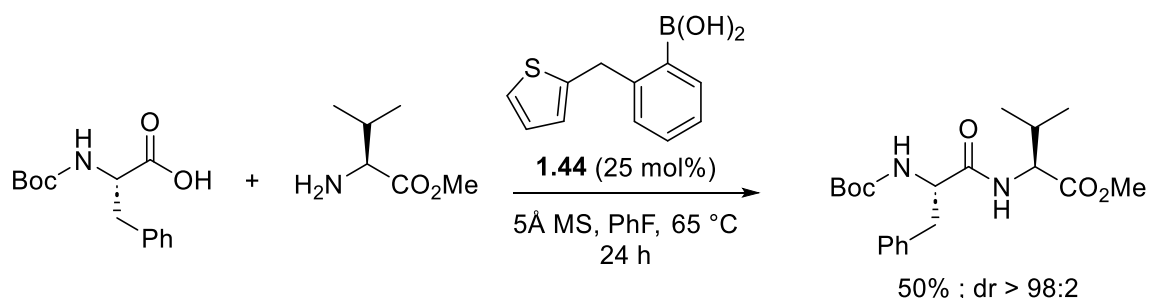
⁵⁶ Marcelli, T. *Angew. Chem., Int. Ed.* **2010**, *49*, 6840–6843.

before the amine addition since control reactions with the simultaneous addition of both substrates and the catalyst yielded less than 5% amide product.⁵⁵ Following this observation, they proposed that the acid activation phase of the catalytic cycle necessitates the formation of a non-hydrated acylboronate **I**, the formation of which can be inhibited in the presence of an amine (Scheme 16). The acylating species **I** can later react with the amine forming the transition structure **II'**, whose collapse is assisted by a carboxylic acid molecule rather than water (Scheme 16). Herein, the iodine also serves to form halogen–hydrogen bonding and renders the boron more electrophilic.



Scheme 16

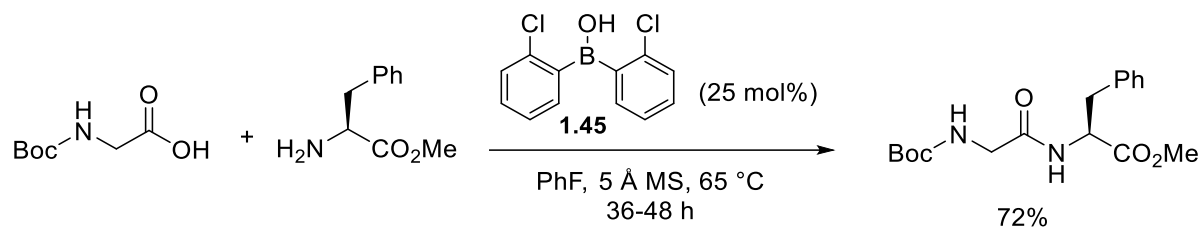
Following Hall's work, researchers were eager to uncover more boronic acids that operate at room temperature. In this context, our research group has developed an arylboronic acid with a thiophene moiety **1.44**, which is active at 25 °C.⁵⁷ Applying this approach, a range of carboxylic acids and amines were successfully coupled using 10 mol% **1.44** at 25 °C, with slight warming (45 °C) required for more challenging ones. Moreover, catalyst **1.44** was used for the synthesis of a dipeptide in 50% yield with minimal racemization (Scheme 17). This example represented the first catalytic use of boronic acid for dipeptide formation.



Scheme 17

⁵⁷ Mohy El Dine, T.; Erb, W.; Berhault, Y.; Rouden, J.; Blanchet, J. *J. Org. Chem.* **2015**, *80*, 4532–4544.

Next, our group reported the use of borinic acid **1.45** as a more effective catalyst for the synthesis of several dipeptides.⁵⁸ Fourteen dipeptides were prepared in useful yields (40-80%) without detectable racemization, under relatively mild conditions (65 °C) (Scheme 18).



Scheme 18

It was suggested that the *ortho*-chlorine group in **1.45** is vital because it contributes to mild hydrogen-halogen bonding that might stabilize the transition state (Figure 6).⁵² Additionally, the Lewis-basicity of this chlorine group supports the collapse of this transition state to release the amide product.

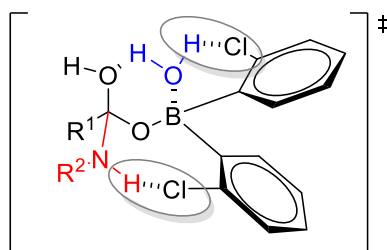
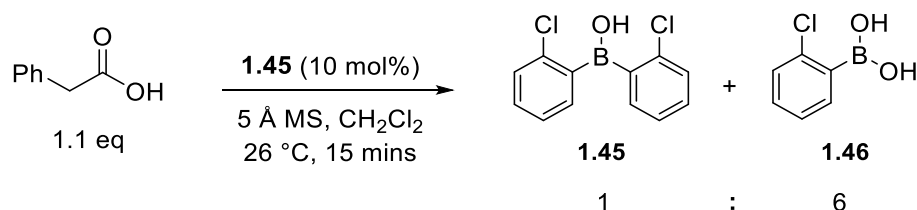


Figure 6

Later, Whiting and Sheppard discovered that borinic acid **1.45** is a *pre*-catalyst that protodeboronates *in situ* into the respective boronic acid.⁵⁹ An experiment where borinic acid **1.45** and phenylacetic acid were stirred for 15 minutes with 5 Å molecular sieves yielded a 1:6 ratio of borinic **1.45** to boronic **1.46** species (Scheme 19).

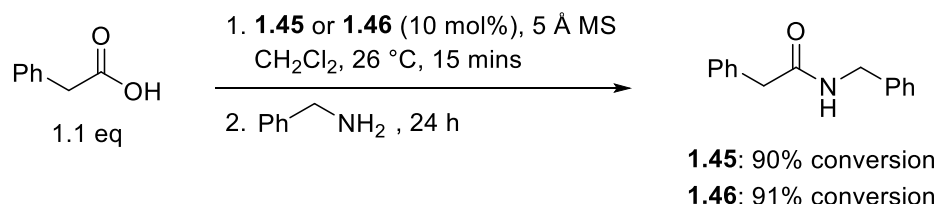


Scheme 19

⁵⁸ Mohy El Dine, T.; Rouden, J.; Blanchet, J. *Chem. Commun.* **2015**, 51, 16084–16087.

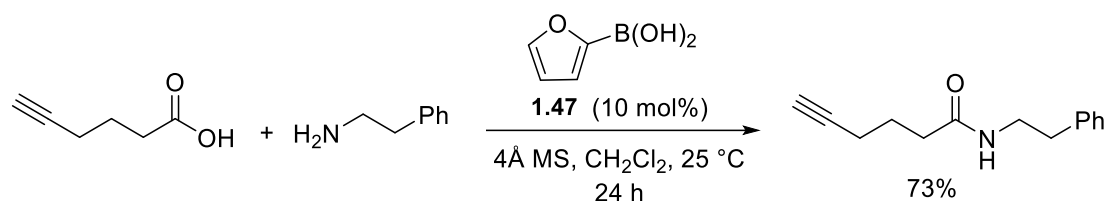
⁵⁹ Arkhipenko, S.; Sabatini, M. T.; Batsanov, A. S.; Karaluka, V.; Sheppard, T. D.; Rzepa, H. S.; Whiting, A. *Chem. Sci.* **2018**, 9, 1058–1072.

To confirm this observation, the authors conducted two separate amidation experiments, one with boronic acid **1.45** and another with boronic acid **1.46**, and found similar yields in both cases (Scheme 20).⁵⁹ This demonstrates that the boronic acid acts as a *pre*-catalyst that generates the boronic acid *in situ*, which in turn facilitates amides synthesis.



Scheme 20

Furthermore, Tam has explored the use of 2-furanylboronic acid **1.47**, as a commercially available, low-cost, and efficient catalyst for direct amidation at 25 °C.⁶⁰ This methodology worked well on a wide variety of aliphatic carboxylic acids and amines (Scheme 21), yet, aromatic and sterically hindered substrates represented a limitation.

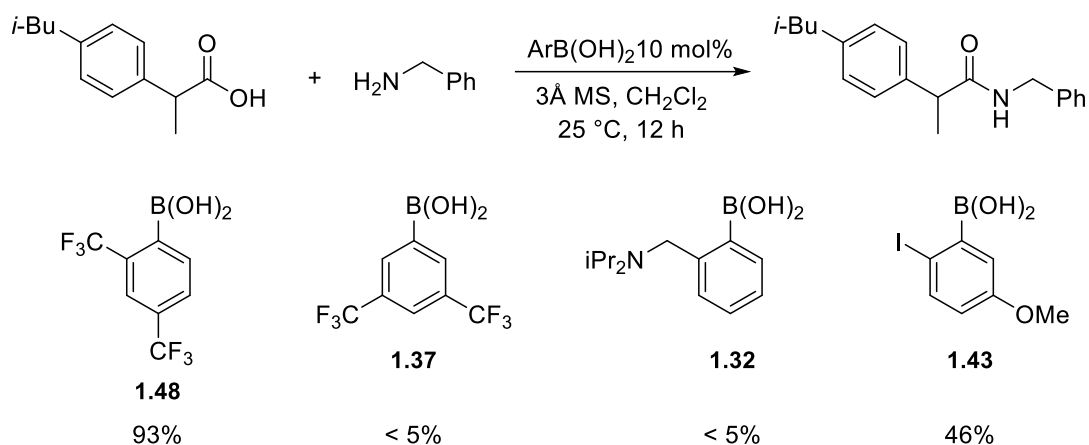


Scheme 21

In 2018, Ishihara *et al.* studied the utility of commercially available 2,4-bis(trifluoromethyl)phenylboronic acid **1.48**.⁶¹ Initially, a series of arylboronic acids were screened on the model reaction of coupling of racemic ibuprofen and benzylamine, and their catalytic efficiency was compared to those of amino-boronic acid **1.32** and MIBA **1.43**. It was discovered that **1.48** was the superior catalyst (Scheme 22).

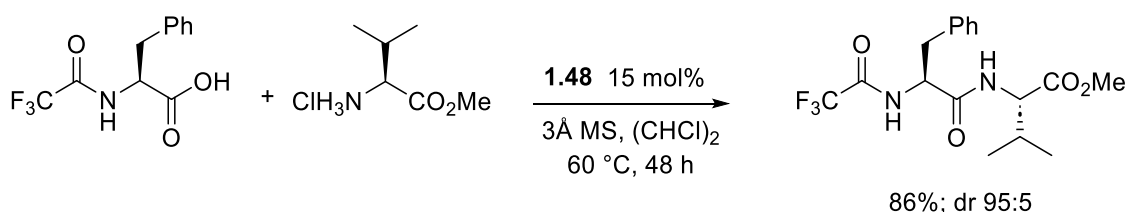
⁶⁰ Tam, E. K. W.; Rita; Liu, L. Y.; Chen, A. *Eur. J. Org. Chem.* **2015**, 2015, 1100–1107.

⁶¹ Wang, K.; Lu, Y.; Ishihara, K. *Chem. Commun.* **2018**, 54, 5410–5413.



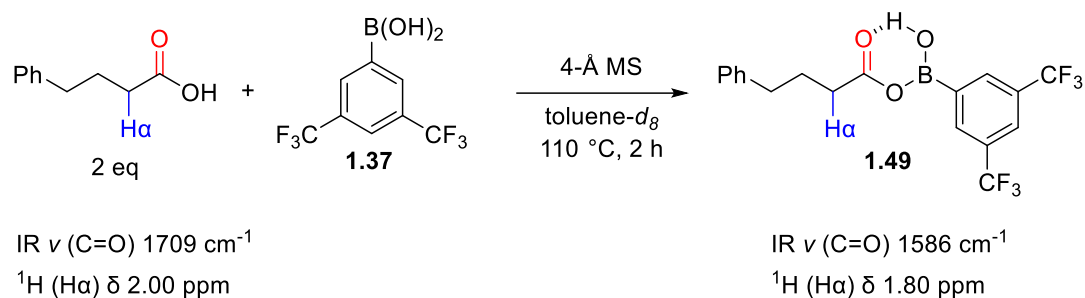
Scheme 22

The generality of the direct amidation using **1.48** was demonstrated further by coupling various aliphatic and aromatic substrates, however, temperatures of 85-110 °C were required for aromatic ones.⁵⁵ Moreover, several dipeptides were efficiently synthesized from α -aminoacids and aminoester hydrochlorides (Scheme 23). In this case, the specific use of *N*-trifluoroacetyl protecting group was suggested to avoid catalyst deactivation.



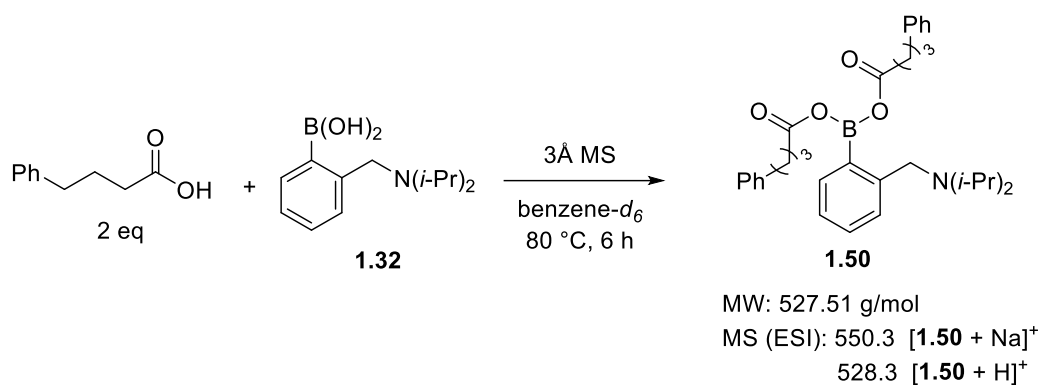
Scheme 23

A general feature in most of the highly performant arylboronic acids, such as **1.48** and **1.43**, is the presence of an *ortho*-substituent. However, the role of this substituent has not been explained by the initially proposed mechanism for boronic acid-catalyzed amidation reaction. Originally, Yamamoto proposed that the active acylating agent is a monoacyl boronate intermediate. In fact, the monoacylboronate **1.49** was synthesized, *in situ*, from boronic acid **1.37** and 4-phenylbutyric acid and it was characterized by ¹H NMR and IR analyses (Scheme 24).⁴⁴



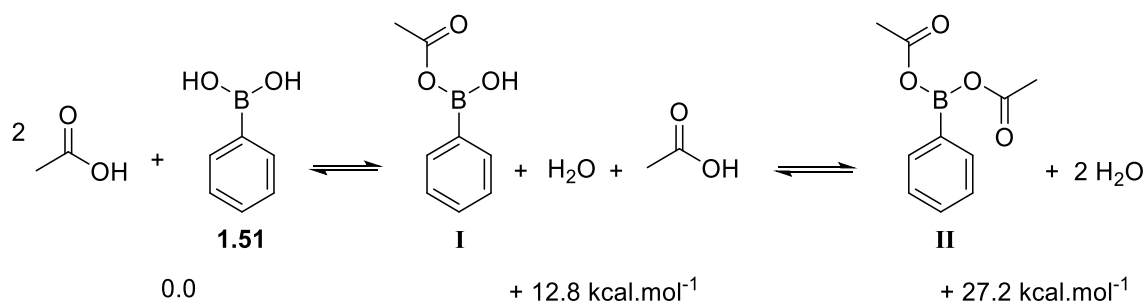
Scheme 24

On the other hand, Whiting reported that diacylboronate intermediate **1.50** was observed by ESI/MS when boronic acid **1.32** was used (Scheme 25), and it was proposed to be the active acylating species. In this case, the monoacylboronate intermediate was not detected.⁴⁸



Scheme 25

Moreover, computational studies by Wang revealed that the formation of monoacyl intermediate **I**, from acetic acid and phenylboronic acid **1.51**, required lower energy (+12.8 kcal.mol⁻¹) than that of intermediate **II** (+27.2 kcal.mol⁻¹), and it was suggested that diacylboronate **II** should not be formed during the reaction (Scheme 26).⁶²

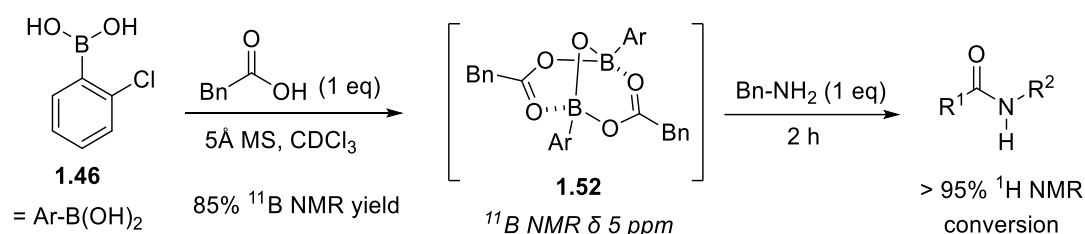


Scheme 26

⁶² Wang, C.; Yu, H.-Z.; Fu, Y.; Guo, Q.-X. *Org. Biomol. Chem.* **2013**, *11*, 2140–2146.

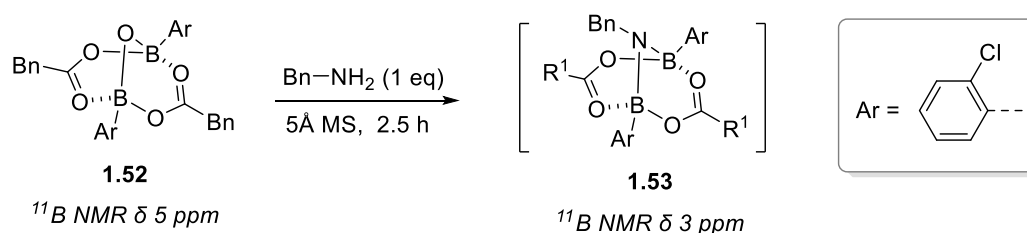
Overall, the above-mentioned mechanism has not been fully elucidated, with only scattered experimental and computational data reported that do not explain the role of the *ortho*-substituent.

In 2018, Whiting and Sheppard investigated the mechanism of the boron-catalyzed amidation reaction by studying the interactions between carboxylic acid, amine, and boronic acid.⁵⁹ First, the reaction between 2-chlorophenylboronic acid **1.46** and phenylacetic acid, in the presence of 5 Å MS, resulted in the formation of a new complex which was assigned the structure of dimeric anhydride **1.52** based on NMR (¹H, ¹³C, ¹¹B) and IR characterizations (Scheme 27). Subsequent addition of the amine into complex **1.52** led to > 95% conversion into the amide within 2 h, signifying that **1.52** is a catalytically active intermediate.



Scheme 27

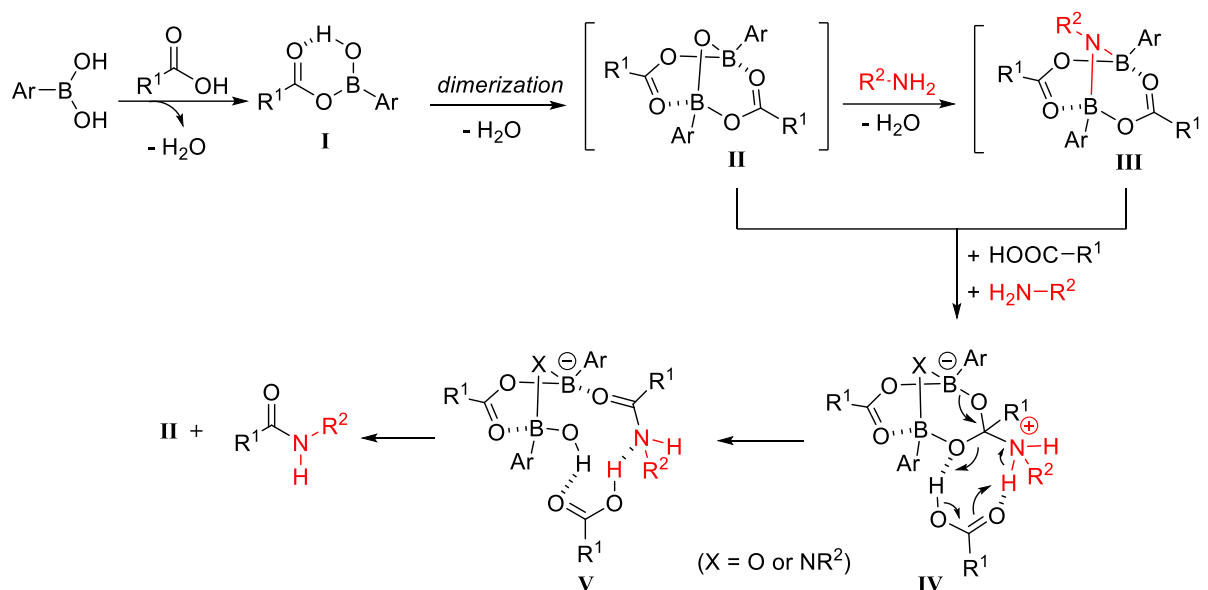
Moreover, the addition of benzylamine (1 eq) to isolated complex **1.52** caused the appearance of a new signal at 3 ppm in ¹¹B NMR (Scheme 28). The new species was provisionally attributed to the structure of complex **1.53** since it was formed from the reaction of **1.52** with benzylamine under dehydrative conditions. It is worth noting that the signal at 3 ppm in ¹¹B NMR was also detected in amidation reaction mixtures.



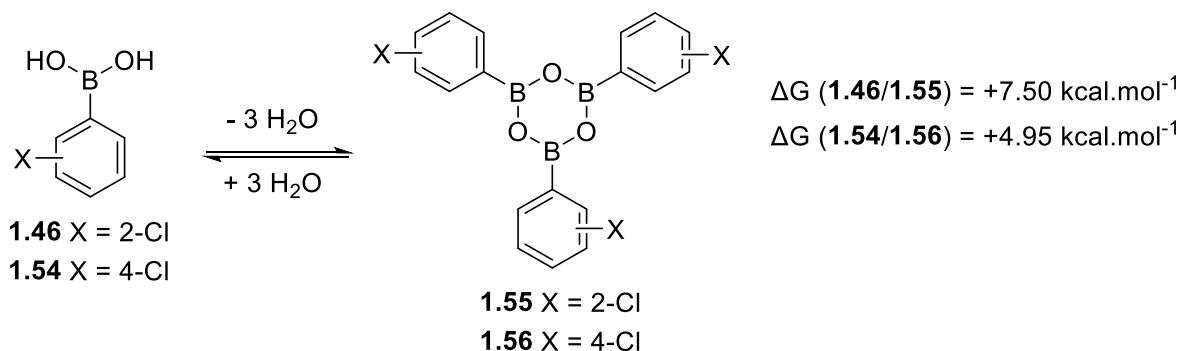
Scheme 28

Accordingly, in the newly postulated mechanism, the condensation of boronic acid with a carboxylic acid leads to the formation of a monoacyloxyboron intermediate **I**, which then self-condenses/dimerizes under dehydrative conditions, into bicyclic intermediate **II** (Scheme 29). Next, in the presence of an amine, a new complex can form and it was attributed to complex **III**. The intermediate **II** or **III** can subsequently react with the amine to give the amide (Scheme

29). Computationally, different mechanisms were studied to explain the formation of the amide from intermediates **II** and **III**, but no favored pathway has been identified.⁵³

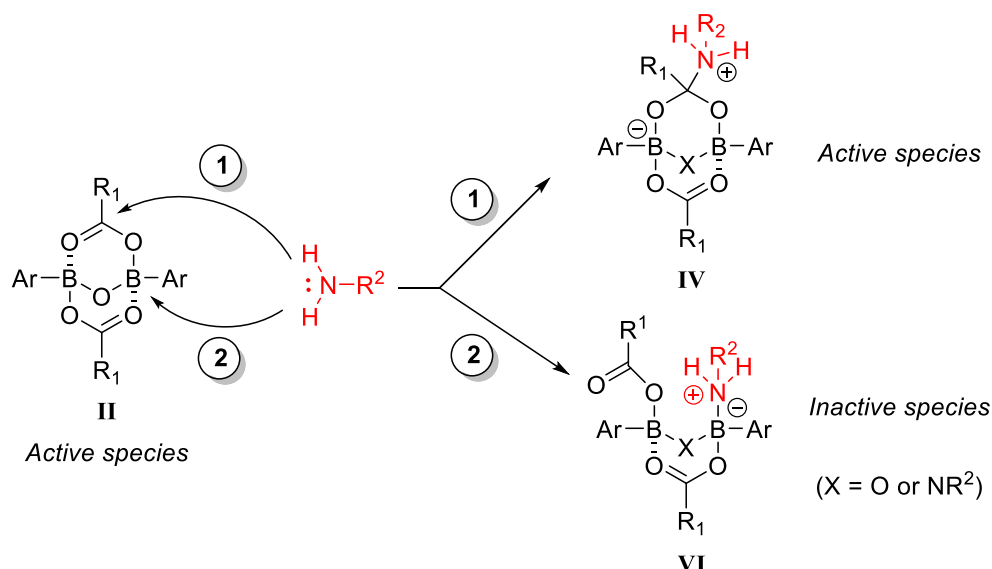


Notably, the role of the *ortho*-substitution was explained by the above mechanism. To emphasize, the relative free energy calculations showed that the formation of boroxine **1.55** from 2-chlorophenylboronic acid **1.46** requires 2.55 kcal/mol more energy than the formation of boroxine **1.56** from 4-chlorophenyl boronic acid **1.54** (Scheme 30). Therefore, the boroxine of an *ortho*-substituted boronic acid is destabilized by steric repulsion. In this case, the formation of dimeric, catalytically active complex **II** is more favorable than that of trimeric boroxine, which is considered an off-cycle resting state of the catalyst.



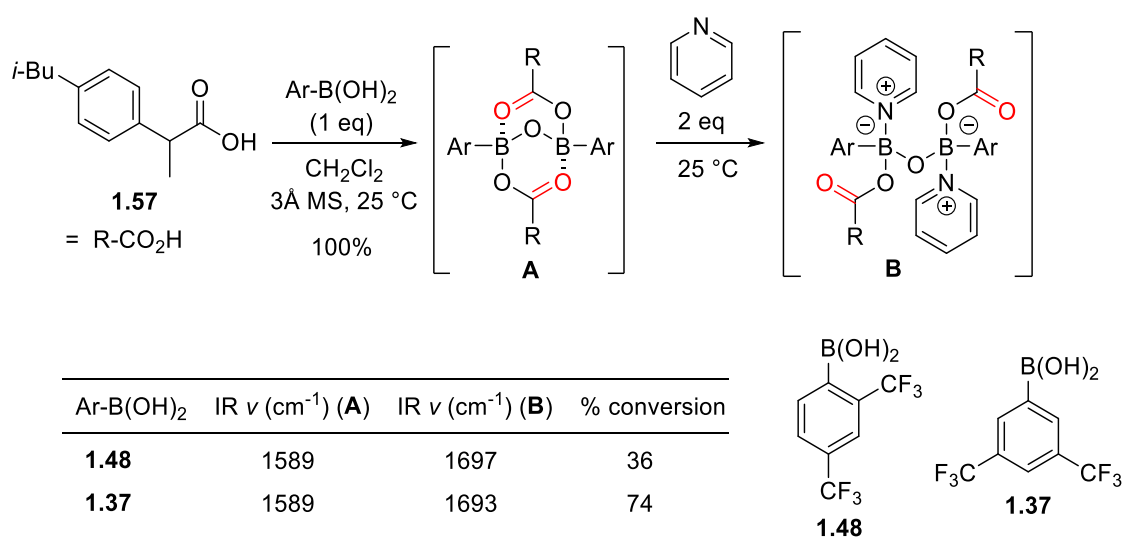
Furthermore, Ishihara has studied the significance of the *ortho*-trifluoromethyl group on the catalytic activity of boronic acid **1.48**. It was presumed that this *ortho*-substituent prevents the

amine from adding to the boron center of **II**, thus disfavoring the formation of a stable, inactive intermediate **VI** (Scheme 31; path 2) and favoring the amine's attack on the carboxylic acid (Scheme 31; path 1). The latter path leads to the formation of the amide.



Scheme 31

To accomplish this goal, *in situ* infrared analyses were carried out to track the stretching vibration of the carbonyl groups of the intermediates generated from boronic acid **1.48** and its 3,5-regioisomer **1.37** (Scheme 32). First, the boronic acid and ibuprofen **1.57** reacted, in the presence of 3Å molecular sieves, to produce the intermediate **A**. Following complete conversion, two equivalents of pyridine were introduced and the conversion into the pyridine-complexes **B** was determined from *in situ* IR analysis of the carbonyl peaks of **A** and **B**.

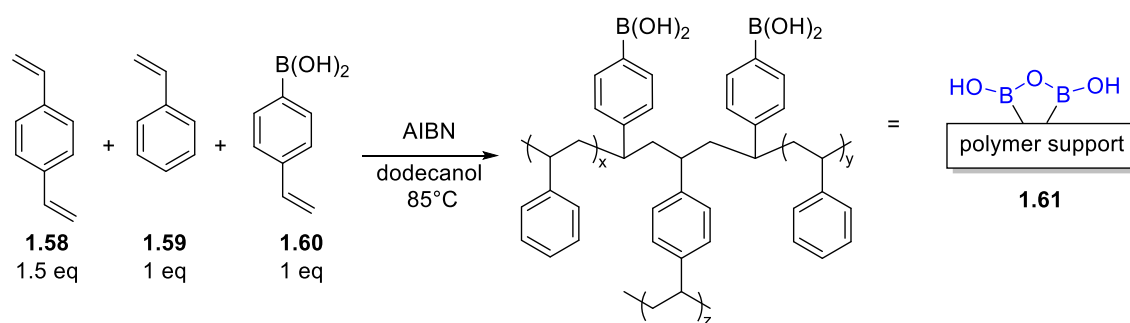


Scheme 32

In the case of 2,4-disubstituted boronic acid **1.48**, a 36% conversion from **A** to **B** was detected (Scheme 32). On the other hand, the use of boronic acid **1.37** resulted in a higher conversion of 74% (Scheme 32). These results show that the *ortho*-trifluoromethyl group shields the trigonal boron center of **A** from the addition of the amine, thus favoring the amide's formation.

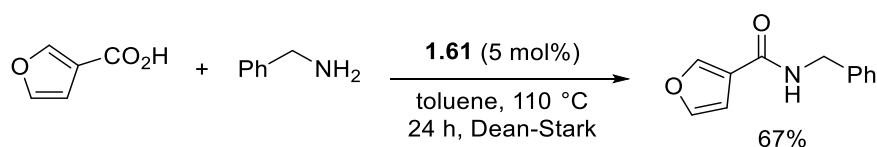
The mechanistic investigations of Whiting and Ishihara have sparked an interest in *ortho*-substituted arylboronic acids. Moreover, given the importance of the B-O-B motif in the catalytically active species, catalysts based on B-O-B linkage were developed.

To exemplify, Whiting later designed a novel polymer-supported boronic acid catalyst **1.61** carrying a *pre*-organized B-O-B motif (Scheme 33).⁶³ This catalyst was prepared by heating a mixture of 1,4-divinylbenzene **1.58** (1.5 eq), styrene **1.59** (1 eq), and 4-vinylphenylboronic acid **1.60** (1 eq) at 85°C in the presence of AIBN initiator (Scheme 33).



Scheme 33

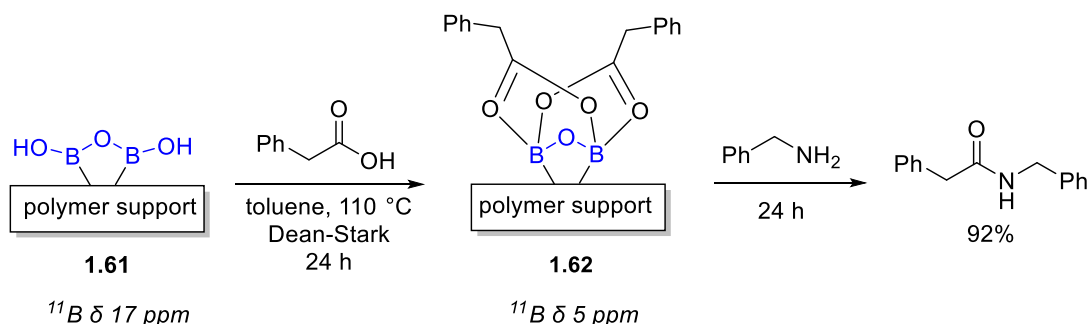
The resulting polystyrene-bound catalyst **1.61** was used for the condensation of benzylamine with aliphatic and aromatic carboxylic acids (Scheme 34). The yields were variable (5-92%) depending on the carboxylic acid used. However, the reaction of benzoic acid with aniline was low yielding (15%), which is a limitation of this method.



Scheme 34

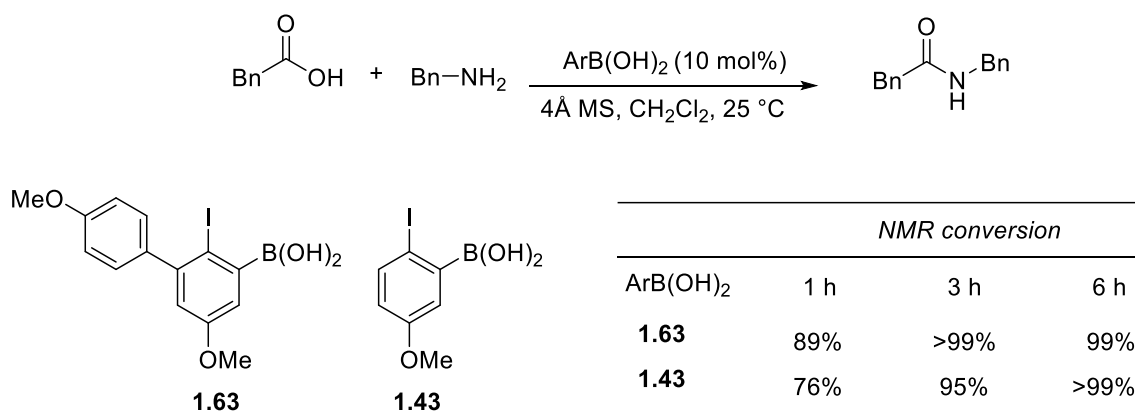
⁶³ Du, Y.; Barber, T.; Lim, S. E.; Rzepa, H. S.; Baxendale, I. R.; Whiting, A. *Chem. Commun.* **2019**, 55, 2916–2919.

Furthermore, the catalyst recyclability was examined and it was shown that catalyst **1.61** displayed high reproducibility in up to 5 cycles. Eventually, the authors looked into the activation route of **1.61** using solid-state ^{11}B NMR, and a diagnostic ^{11}B chemical shift at 5 ppm was detected suggesting the presence of dimeric species **1.62** (Scheme 35).⁵⁷



Scheme 35

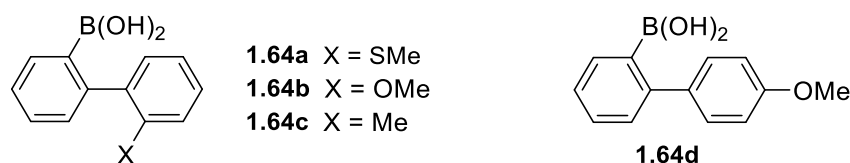
Recently, Al-Zoubi *et al.* reported on the synthesis and application of *ortho*-iodo-biphenylboronic acids.⁶⁴ These boronic acids were anticipated to enhance the catalytic activity over the parent MIBA **1.43** by tuning the proximity of the iodine and boronic acid group. Notably, when iodo-biphenylboronic **1.63** was examined on the model reaction of synthesis of *N*-benzyl-2-phenylacetamide, it provided a minor enhancement in the catalytic activity over **1.43** (Scheme 36). Several derivatives of **1.63** were tested too, however, they all exhibited reduced activity compared to MIBA. Even though boronic acid **1.63** provided a little improvement over MIBA, its synthetic utility has not been well demonstrated yet since it has been used for the synthesis of 6 amides only, and no examples of challenging aromatic acids/amines were reported.



Scheme 36

⁶⁴ Al-Zoubi, R. M.; Al-Jammal, W. K.; McDonald, R. *New J. Chem.* **2020**, *44*, 3612–3623.

It can be noticed that anilines are challenging substrates for the catalytic direct amidation reaction, typically giving low yields. To address this issue, Hall studied the utility of a group of 2-biphenylboronic acids substituted with a basic heteroatom moiety, among which are **1.64a** and **1.64b** (Scheme 37).⁶⁵ Also, examined for control studies, were a boronic acid without a basic group (**1.64c**) and another that lacks an *ortho*-substitution (**1.64d**) (Scheme 37). Noticeably, boronic acid **1.64a** performed best while the two control structures, **1.64c** and **1.64d**, showed no activity, indicating the importance of the basicity of the substituent and the *ortho*-position, respectively.



Scheme 37

The rationale behind designing these catalysts is that the Lewis basic moiety (SMe, or OMe) could encourage hydrogen bonding to the amine, thus increasing its nucleophilicity, and enhancing the electrophilicity of the boron center (Figure 7).⁶⁵ Moreover, it assists in bringing the amine closer to the carboxylic group. This mode of interaction relates strongly to the aminoboronic acid **1.32** where the diisopropylamino group forms a hydrogen bond with the hydroxy group of the boronic acid, thus increasing its Lewis acidity (Figure 7).^{66,48} Another explanation is that the Lewis basic moiety donates electrons to the antibonding orbital of the boron Lewis acid, thus reducing its electron density and facilitating the activation of the carboxylic acid. This electron donation to the antibonding orbital also destabilizes the B-O bond of the transition state, hence promoting the release of the amide product.

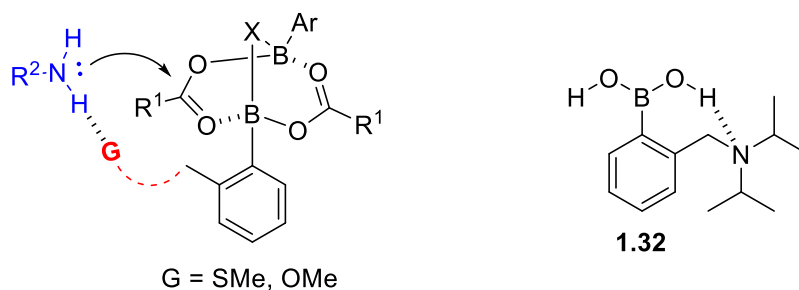
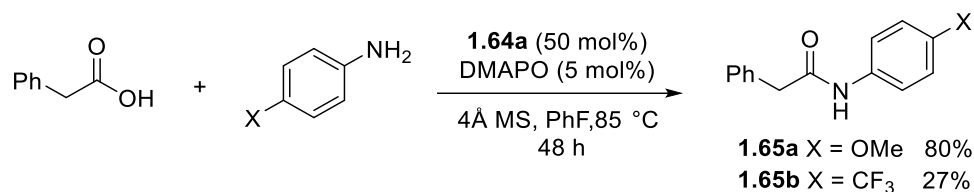


Figure 7

⁶⁵ Zhou, J.; Paladino, M.; Hall, D. G. *Eur. J. Org. Chem.* **2022**, 2022, e202201050.

⁶⁶ Georgiou, I.; Ilyashenko, G.; Whiting, A. *Acc. Chem. Res.* **2009**, 42, 756–768.

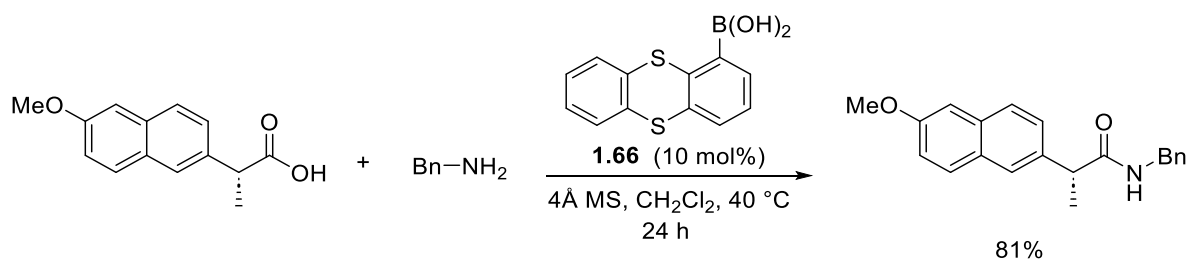
Upon screening of various reaction conditions, it was revealed that 50 mol% of **1.64a** is required to achieve acceptable yields and that the addition of DMAPO co-catalyst (5 mol%) is advantageous.⁶⁵ Amides resulting from the coupling of neutral and electron-rich anilines with aliphatic acids were efficiently synthesized, such as amide **1.65a** (80%). However, the electron-poor 4-trifluoromethyl aniline provided the amide **1.65b** in a low yield (27%) (Scheme 38).



Scheme 38

Overall, this methodology can be useful to guide the design of boronic acid catalysts that may activate the amine as well as the carboxylic acid. Nonetheless, the current protocol is constrained by high catalyst loading, the requirement for an additive, and racemization with chiral substrates.

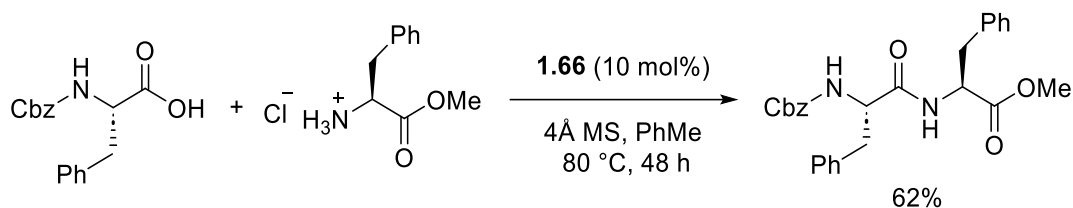
A very recent study reported the application of boronic acid **1.66** based on a thianthracene scaffold.⁶⁷ This catalyst was selected as the most active among a list of 14 commercial heterocyclic boronic acids. Moreover, it was suggested that the heterocycle stabilizes the active acylating intermediate and assists amidation. The catalyst **1.66** enabled the efficient coupling of aliphatic and aromatic acids with aliphatic amines (Scheme 39). Nonetheless, the reactions involving sterically hindered secondary amines and anilines are an identified limitation.



Scheme 39

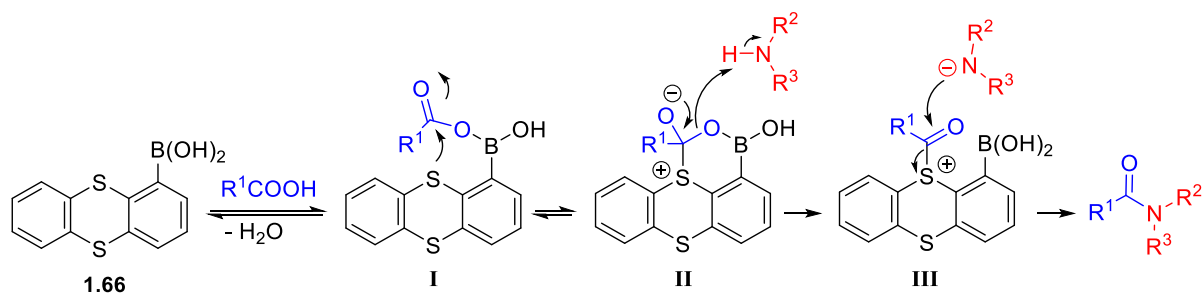
Interestingly, dipeptide synthesis was also investigated starting from protected α -aminoacids and aminoester hydrochlorides, at 80 °C (Scheme 40).

⁶⁷ Pan, B.; Huang, D.-M.; Sun, H.-T.; Song, S.-N.; Su, X.-B. *J. Org. Chem.* **2023**, *88*, 2832–2840.



Scheme 40

To understand the role of boronic acid **1.66** in facilitating the amidation reaction, the authors suggested two possible pathways, however, no experimental or computational evidence was provided for either of them. The first one replicates Whiting's mechanistic proposal, in which a B-O-B bridged bicyclic intermediate is formed as the active acylating species.⁵⁹ An alternative route entails the formation of a monoacyloxy-boron species **I**, followed by the attack of the sulfur on the carboxy group to form a six-membered ring **II** (Scheme 41).⁶⁷ The sulfur's nucleophilicity and the reduced intramolecular strain favor this attack. Finally, an activated acid in the form of an acylsulfonium ion **III** can be easily approached by the amine to form the amide.



Scheme 41

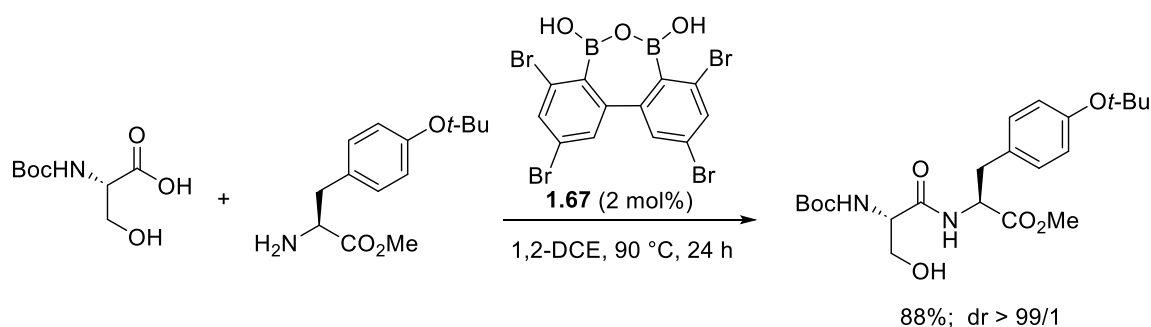
To sum up this section, boronic acid catalysis is among the atom-efficient methods for the dehydrative condensation of carboxylic acids and amines. They have an advantage in that the only byproduct of this reaction is water. Furthermore, the aromatic ring of arylboronic acid can be functionalized in a variety of ways, allowing the alteration of activity via structural modulation. Despite the fact that boronic acids have been extensively studied, several other boron-based catalysts have been reported and are covered in the following sections.

1.2.2.1.2 Diboronic acids: A special case of boronic acid catalysis

The elucidation of the mechanism of the boronic acid-catalyzed amidation reaction and the identification of key reactive intermediates by Whiting and co-workers has encouraged exploring potential catalysts bearing a B-O-B motif.

In this context, Shimada reported the application of biphenyl-based diboronic acid **1.67**, which served as a highly efficient catalyst for the direct amidation of a wide range of β -hydroxycarboxylic acids.⁶⁸ Interestingly, in some cases, the catalyst loading was reduced to 0.01 mol%, with a turnover number of 7,500, which is the highest ever reported for an organoboron-catalyzed amidation reaction.⁶⁸

Moreover, catalyst **1.67** has been applied for dipeptide synthesis from β -hydroxy- α -amino acids in high yields with high functional group tolerance (phenol, sulfides, indole, etc.) and minimal epimerization (Scheme 42).⁶⁹

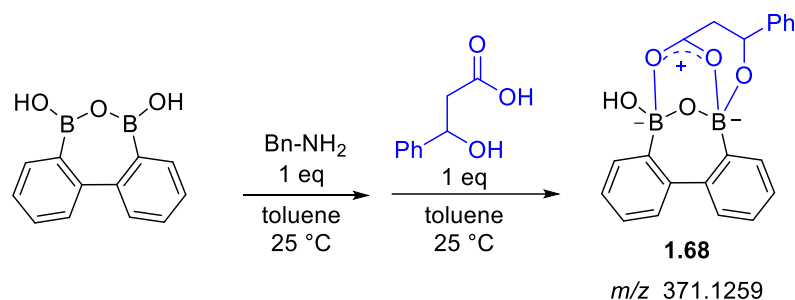


Scheme 42

Concerning the activation route of **1.67**, the acyloxydiboronate **1.68** (Scheme 43) was detected by negative ESI mass spectrometry, and in line with previous studies,⁵⁹ it was proposed as the active acylating intermediate.

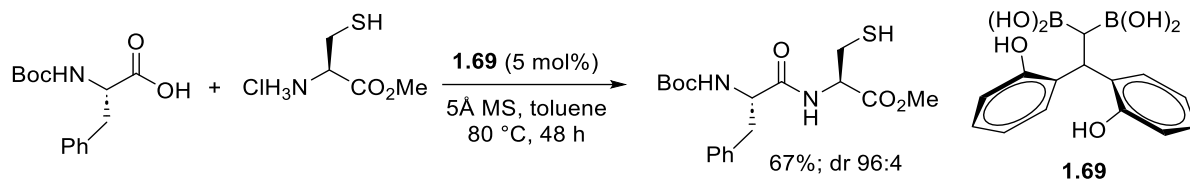
⁶⁸ Shimada, N.; Hirata, M.; Koshizuka, M.; Ohse, N.; Kaito, R.; Makino, K. *Org. Lett.* **2019**, *21*, 4303–4308.

⁶⁹ Koshizuka, M.; Makino, K.; Shimada, N. *Org. Lett.* **2020**, *22*, 8658–8664.



Scheme 43

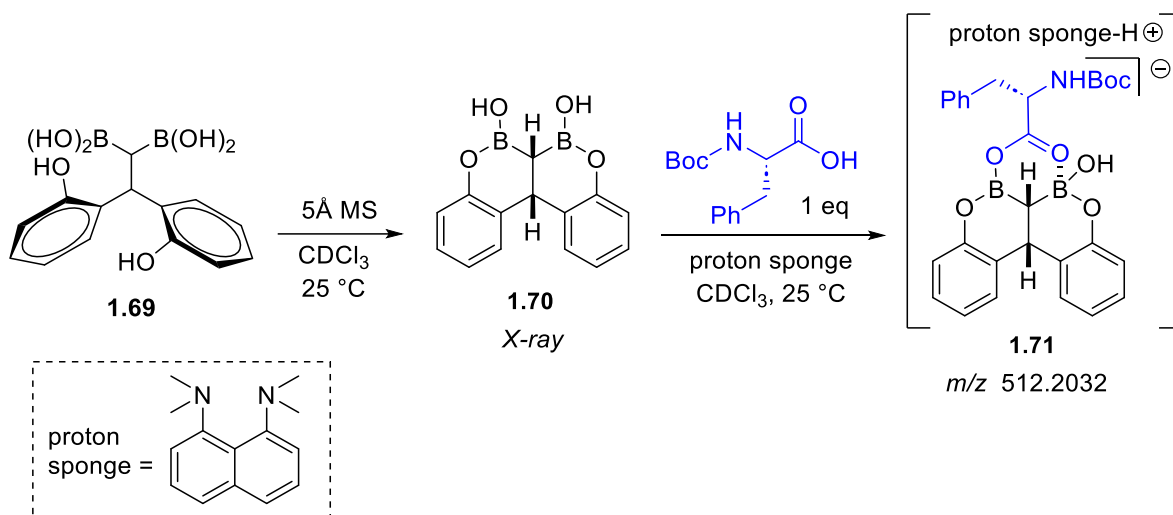
Furthermore, Takemoto described the novel geminal diboronic acid **1.69**, which incorporates a B-C-B linkage, as an amidation catalyst.⁷⁰ Notably, catalyst **1.69** was competent for the condensation of functionalized α -amino acids bearing phenol, thiol, or heterocyclic moieties, with aminoester hydrochlorides, with minimal racemization (Scheme 44). Remarkably, switching from the standard Boc-protection to an *N*-trifluoroacetyl protecting group has enabled the catalytic peptide synthesis at 25 °C, for the first time. However, in this case, a long reaction time of 120 h and 20 mol% of **1.69** were needed to achieve a moderate yield.⁷⁰



Scheme 44

Mechanistic studies have revealed that catalyst **1.69** rapidly transforms into the bicyclic structure **1.70** when added to 5 Å molecular sieves, which was determined by X-ray analysis (Scheme 45). Moreover, the organoboron species **1.70** gives rise to the carboxylic-bound complex **1.71** (detected by ESI-MS) upon the addition of an α -amino acid, in the presence of proton sponge[®] (Scheme 45).

⁷⁰ Michigami, K.; Sakaguchi, T.; Takemoto, Y. *ACS Catal.* **2020**, *10*, 683–688.

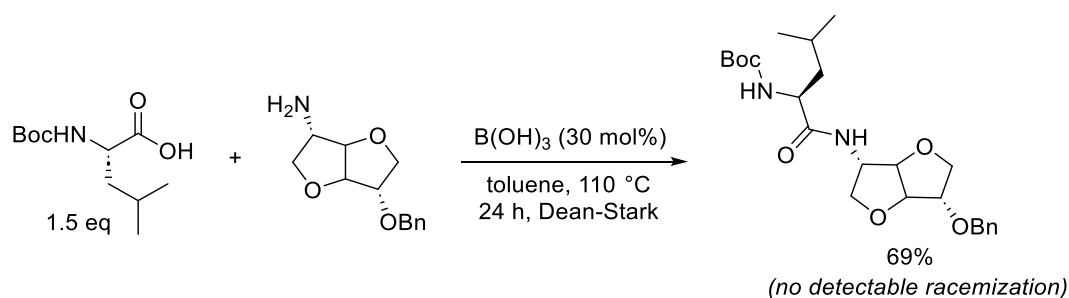


Scheme 45

1.2.2.1.3 Boric acid

In 2005, Tang reported the use of boric acid as a catalyst for the direct amidation of carboxylic acids and amines.⁷¹ By using this reagent at 5 mol% loading, in refluxing toluene (110 °C), benzylamines and cyclic aliphatic amines reacted efficiently, nevertheless, anilines required higher catalyst loading of 25 mol%. Importantly, the simplicity of the operational conditions permitted large-scale applications.⁷²

The synthetic utility of boric acid was illustrated by the synthesis of amido-isohexides, obtained from a renewable source (starch).⁷³ This approach was carried out successfully with various functionalized substrates in moderate to excellent yields (Scheme 46).



Scheme 46

⁷¹ Tang, P. *Org. Synth.* **2005**, 81, 262–172.

⁷² Anderson, J. E.; Davis, R.; Fitzgerald, R. N.; Haberman, J. M. *Synth. Commun.* **2006**, 36, 2129–2133.

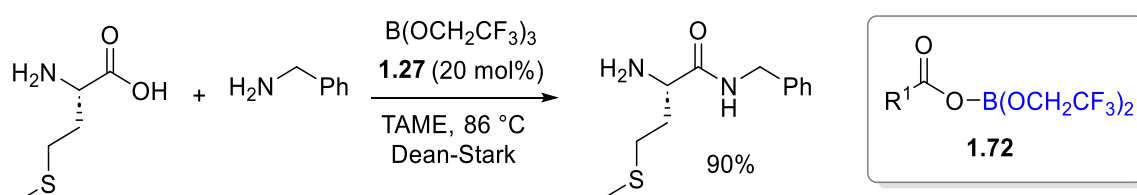
⁷³ Janvier, M.; Moebis-Sanchez, S.; Popowycz, F. *Eur. J. Org. Chem.* **2016**, 2016, 2308–2318.

Overall, boric acid is a useful catalyst for amide synthesis due to its low cost and practicality, however, it is only active at a high temperature (110 °C), thus limiting the range of amides that can be synthesized using this methodology. Additionally, it poses reproductive toxicity issues at high doses.⁷⁴

1.2.2.1.4 Borate esters

Sheppard investigated the utility of the commercially available tris(2,2,2-trifluoroethyl)borate **1.27** as a catalyst for the dehydrative amidation reaction.⁷⁵

The borate catalyst **1.27** enabled the coupling of functionalized, unprotected α -amino acids with a diverse selection of amines in a chemoselective manner (Scheme 47).⁷⁵ It's worth mentioning that these processes performed best in *tert*-amyl methyl ether (TAME, 86 °C), which allowed for lowering the reaction temperature below 110 °C. Another appealing feature of this method is the ease of amide isolation, where scavenger resins are used to remove unreacted acid and amine, as well as boron-based impurities, thus, eliminating the need for an extractive workup or chromatographic purification. Furthermore, the active acylating agent was assigned the structure of **1.72** since ¹⁹F NMR analysis of the Dean-Stark trap revealed the removal of less than 1 equivalent of trifluoroethanol during the amidation reaction (Scheme 47).⁷⁵ However, the work to fully elucidate the mechanism is still in progress.



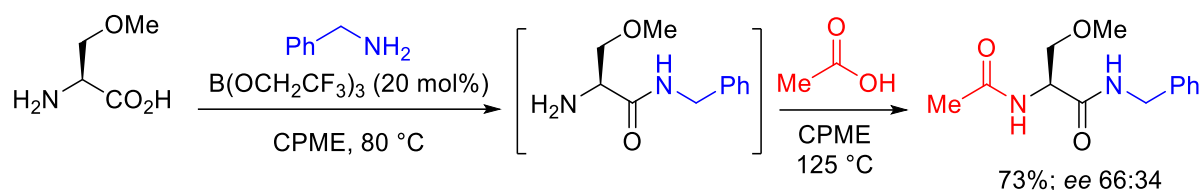
Scheme 47

Lately, Sheppard discovered that *tert*-butyl acetate is an excellent solvent for the $\text{B(OCH}_2\text{CF}_3)_3$ -catalyzed reactions, providing increased safety and sustainability over TAME, as well as higher

⁷⁴ (a) Price, C. J.; Marr, M. C.; Myers, C. B.; Seely, J. C.; Heindel, J. J.; Schwetz, B. A. *Fundam. Appl. Toxicol.* **1996**, *34*, 176–187. (b) Heindel, J. J.; Price, C. J.; Field, E. A.; Marr, M. C.; Myers, C. B.; Morrissey, R. E.; Schwetz, B. A. *Fundam. Appl. Toxicol.* **1992**, *18*, 266–277.

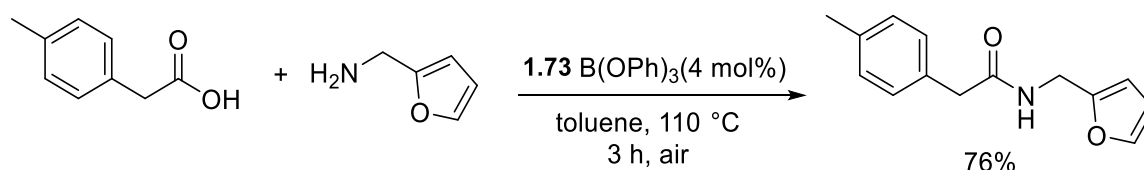
⁷⁵ Sabatini, M. T.; Boulton, L. T.; Sheppard, T. D. *Sci. Adv.* **2017**, *3*, e1701028.

yields for aromatic acids and anilines.⁷⁶ Moreover, a one-pot sequential double amidation method was devised for unprotected α -amino acids, in cyclopentylmethyl ether (CPME). Generally, good yields were obtained, however, a significant decline in enantiopurity was detected (Scheme 48).⁷⁷



Scheme 48

Besides Sheppard's reports on trifluoroethylborate, Sekar explored the use of triphenyl borate **1.73** for the direct *N*-acylation of amines.⁷⁸ With a catalyst loading of 4 mol%, aliphatic amides were produced in good yields (Scheme 49).



Scheme 49

In contrast, borate **1.73** was ineffective for sterically hindered or aromatic carboxylic acids.⁷⁸

1.2.2.1.5 Diboron reagents

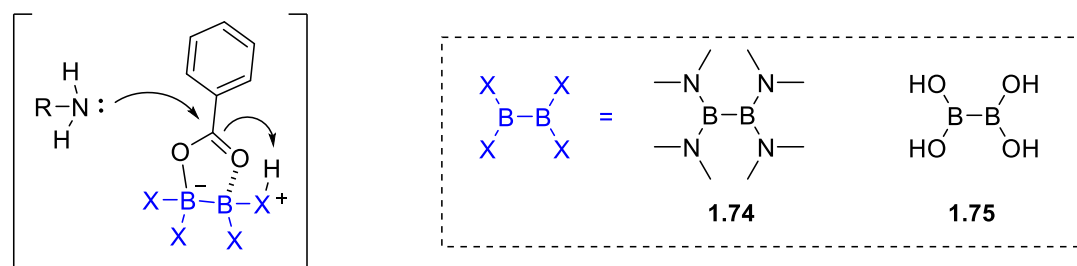
The applicability of diboron reagents in the catalytic condensation of carboxylic acids and amines has been brought to light by Saito and his coworkers. It was presumed that a diboron reagent, such as tetrakis(dimethylamino)diboron **1.74** or tetrahydroxydiboron **1.75**, could activate the carboxylate via bidentate coordination to the B-B moiety (Scheme 50).⁷⁹

⁷⁶ Coomber, C. E.; Laserna, V.; Martin, L. T.; Smith, P. D.; Hailes, H. C.; Porter, M. J.; Sheppard, T. D. *Org. Biomol. Chem.* **2019**, *17*, 6465–6469.

⁷⁷ Sabatini, M. T.; Karaluka, V.; Lanigan, R. M.; Boulton, L. T.; Badland, M.; Sheppard, T. D. *Chem. Eur. J.* **2018**, *24*, 7033–7043.

⁷⁸ Ghorpade, S. A.; Sawant, D. N.; Sekar, N. *Tetrahedron* **2018**, *74*, 6954–6958.

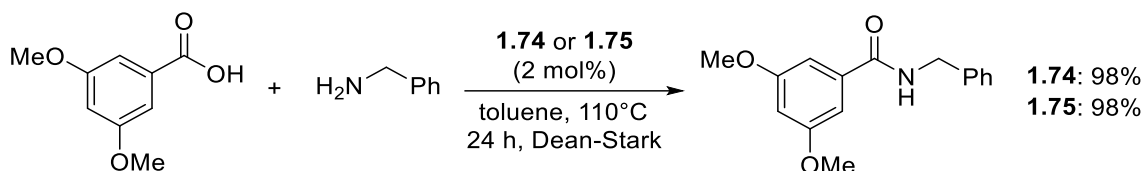
⁷⁹ Sawant, D. N.; Bagal, D. B.; Ogawa, S.; Selvam, K.; Saito, S. *Org. Lett.* **2018**, *20*, 4397–4400.



hypothesized activation mode

Scheme 50

They have demonstrated the efficiency of commercially available diboron reagents, **1.74** and **1.75**, for the coupling of aromatic substrates.⁷⁹ A selection of aromatic acids was coupled with aliphatic amines and aminoesters in high yields using a low catalyst loading of 2 mol% (Scheme 51). Nonetheless, anilines provided low yields.



Scheme 51

In most cases, **1.74** and **1.75** performed similarly, with **1.74** displaying a slightly improved reactivity for challenging aromatic acids.

1.2.2.1.6 Boron-Nitrogen heterocycles

The utility of an organoboron catalyst bearing a B₃NO₂ core was unraveled by Shibasaki and Kumagai in 2017.⁸⁰ The scope of DATB **1.76** (Figure 8) comprised undemanding aliphatic substrates (for which 0.5 mol% **1.76** was used), highly epimerizable, and sterically demanding ones. This methodology was extended to include the synthesis of peptides using Fmoc-protected amino acids, and, its synthetic potential has been illustrated by the preparation of a pentapeptide.⁸¹ Moreover, a second-generation DATB based on pyrimidines **1.77** (Pym-DATBs, Figure 8) was reported to be equally potent to **1.76**.⁸²

⁸⁰ Noda, H.; Furutachi, M.; Asada, Y.; Shibasaki, M.; Kumagai, N. *Nature Chem.* **2017**, *9*, 571–577.

⁸¹ Liu, Z.; Noda, H.; Shibasaki, M.; Kumagai, N. *Org. Lett.* **2018**, *20*, 612–615.

⁸² Opie, C. R.; Noda, H.; Shibasaki, M.; Kumagai, N. *Chem. Eur. J.* **2019**, *25*, 4648–4653.

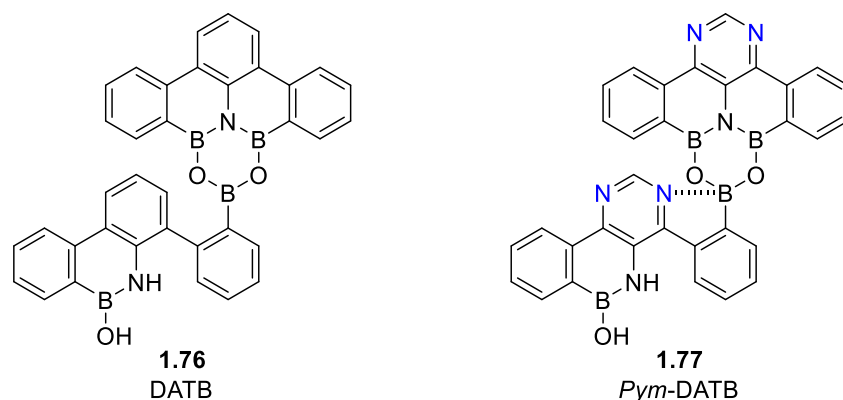
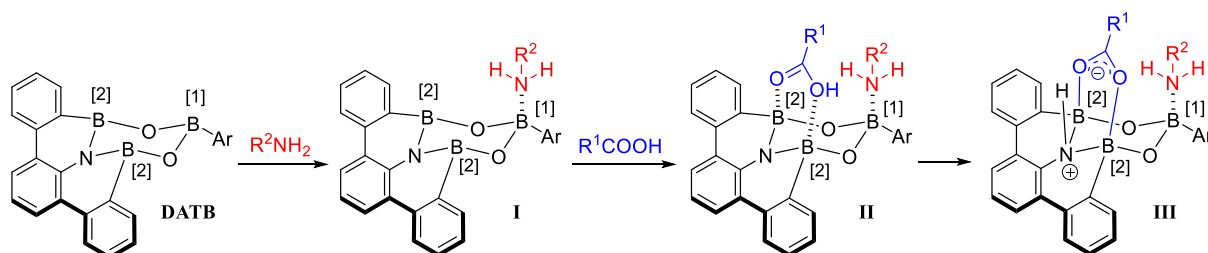


Figure 8

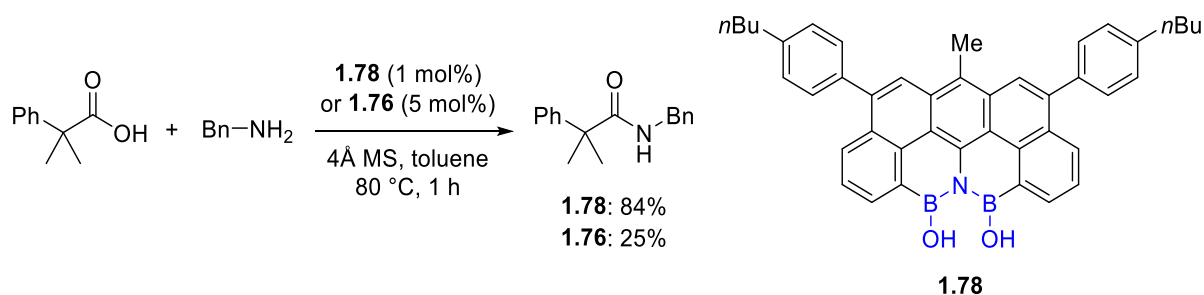
Mechanistic investigations have revealed the distinct roles of the three boron atoms of DATBs (Scheme 52).⁸³ First, the most Lewis-acidic boron atom [B1] interacts with the amine (**I**) through adduct formation. On the other hand, the boron centers [B2] of the azaborine moiety become Lewis acidic only upon the protonation of the neighboring nitrogen. Therefore, each [B2] forms a hydrogen bond with the carboxylic acid (**II**) which facilitates the protonation of the nitrogen. Then, in the cyclic complex (**III**), the carboxylic acid is activated.



More recently, Shibasaki and Kumagai disclosed a simplified catalyst **1.78** with an N(BOH)₂ configuration.⁸⁴ The latter outperformed DATB for the coupling of a variety of sterically demanding and functionalized substrates, with reduced catalyst loading of 1 mol% (Scheme 53).

⁸³ Noda, H.; Asada, Y.; Shibasaki, M.; Kumagai, N. *J. Am. Chem. Soc.* **2019**, *141*, 1546–1554.

⁸⁴ Opie, C. R.; Noda, H.; Shibasaki, M.; Kumagai, N. *Org. Lett.* **2023**, *25*, 694–697.



Scheme 53

The authors suggested that the mode of activation of **1.78** might differ from that of DATB.

1.2.2.2 Organocatalysis

Organoselenium compounds have been developed as catalysts for direct amidation reactions (Figure 9). Notable examples include Liebeskind's *ortho*-functionalized diselenide catalyst **1.79** which operates with 2.5 mol% catalyst loading, at 30 °C, and under aerobic conditions.⁸⁵ Complex and highly functionalized amides have been obtained in high yields using **1.79** and with the absence of racemization for sensitive substrates.

Following that, Arora proposed the cyclic diselenide **1.80** that incorporates a urea moiety (Figure 9). This method was subsequently used for solid-phase peptide synthesis (SPPS) from Fmoc-amino acids.⁸⁶

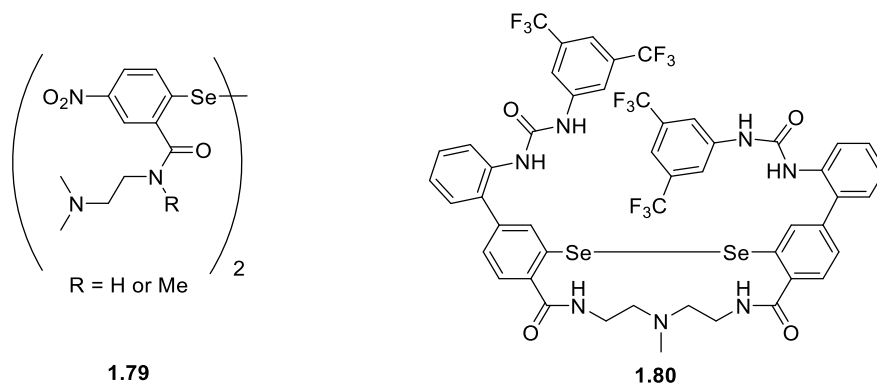


Figure 9

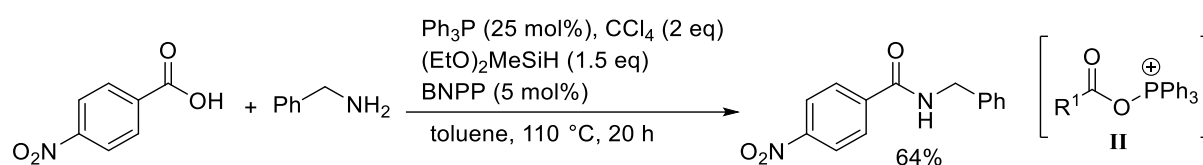
Another example involves the catalytic use of Ph_3P , with two-fold excess of CCl_4 , for the amidation of aromatic carboxylic acids and aliphatic amines (Scheme 54).⁸⁷ In this protocol,

⁸⁵ Akondi, S. M.; Gangireddy, P.; Pickel, T. C.; Liebeskind, L. S. *Org. Lett.* **2018**, *20*, 538–541.

⁸⁶ Handoko; Satishkumar, S.; Panigrahi, N. R.; Arora, P. S. *J. Am. Chem. Soc.* **2019**, *141*, 15977–15985.

⁸⁷ Lenstra, D. C.; Rutjes, F. P. J. T.; Mecinović, J. *Chem. Commun.* **2014**, *50*, 5763–5766.

the carboxylic acid is activated through a mixed anhydride **II** (Scheme 54) and the generated triphenylphosphine oxide is reduced *in situ* to triphenylphosphine in the presence of diethoxymethylsilane and bis(4-nitrophenyl)phosphate (BNPP).



Scheme 54

While this study demonstrated how phosphines can be catalytically used in amidation reactions, the stoichiometric use of toxic CCl_4 represents a major drawback.

1.2.2.3 Metal-catalysis

The field of metal-catalyzed amides synthesis has witnessed major advances since the first report of Shteinberg on $\text{Ti}(\text{O}i\text{Bu})_4$ catalysis.⁸⁸ Since then, various metal catalysts have been examined, including the inexpensive titanium (IV) isopropoxide and zirconium (IV) chloride.⁸⁹ Interestingly, the use of hafnium (IV) bis(cyclopentadienyl)bischloride **1.81** (Figure 10) has enabled the first metal-catalyzed direct amidation reaction at 26 °C.⁹⁰ Moreover, $[\text{Zr}(\text{Cp})_2(\text{OTf})_2] \cdot \text{THF}$ **1.82** (Figure 10) has recently been used as a water-tolerant homogeneous catalyst that can mediate amidation reactions at 70 °C, without the use of water-scavenging techniques.⁹¹

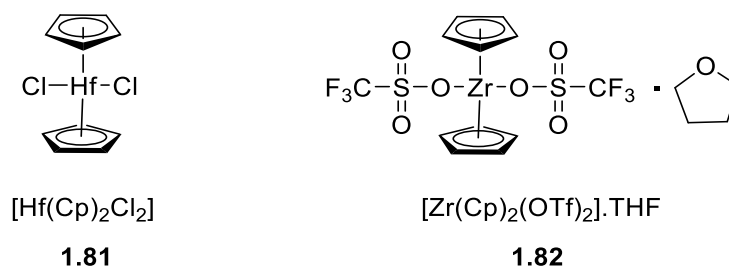


Figure 10

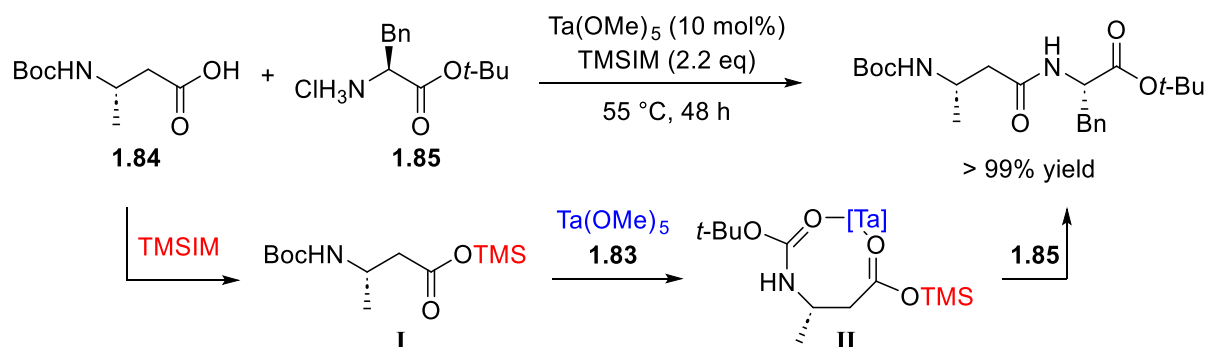
⁸⁸ L. Y. Shteinberg, S. A. Kondratov and S. M. Shein, *Zh. Org. Khim.* **1988**, 24, 1968–1972.

⁸⁹ Lundberg, H.; Tinnis, F.; Adolfsson, H. *Chem. Eur. J.* **2012**, 18, 3822–3826.

⁹⁰ Lundberg, H.; Adolfsson, H. *ACS Catal.* **2015**, 5, 3271–3277.

⁹¹ Lundberg, H.; Tinnis, F.; Adolfsson, H. *Appl. Organomet. Chem.* **2019**, 33, e5062.

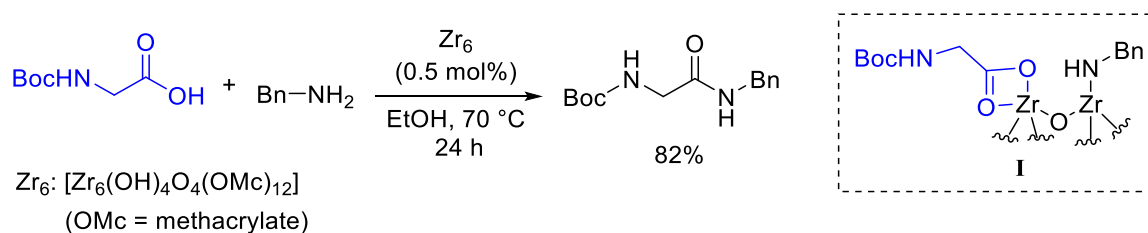
Notably, Ta(OMe)₅ **1.83** have been applied to the direct amidation of a broad range of β-amino acids with high yields and no racemization (Scheme 55).⁹² This protocol is water-tolerant, solvent-free, and requires moderate temperature (55 °C), however, it involves the use of an excess of trimethylsilyl-imidazole (TMSIM).



Scheme 55

The activation of β-amino acids occurs via an initial *in-situ* generation of a silyl ester **I** from **1.84** and TMSIM, followed by bidentate chelation of the generated silyl ester **I** with [Ta] to form the complex **II** (Scheme 55).

Furthermore, in 2023, the group of Parac-Vogt described the use of the Zr₆O₈ cluster [Zr₆] as a unique molecular catalyst for the amidation of non-activated carboxylic acids.⁹³ The reactions were conducted in ethanol, a green solvent rarely used in amidation reactions, without the need for water scavenging techniques to achieve good yields (Scheme 56).



Scheme 56

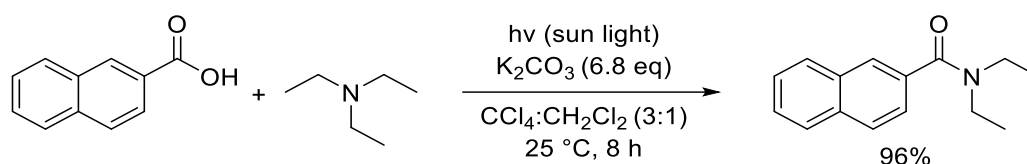
The promising reactivity of [Zr₆] was suggested to be the result of a dynamic interaction at the cluster surface (**I**), where the coordination of the acid and the amine is necessary (Scheme 56).⁹³

⁹² Muramatsu, W.; Yamamoto, H. *J. Am. Chem. Soc.* **2019**, *141*, 18926–18931.

⁹³ Zhang, Y.; Kokculer, I. Y.; Azambuja, F. de; Parac-Vogt, T. N. *Catal. Sci. Technol.* **2023**, *13*, 100–110.

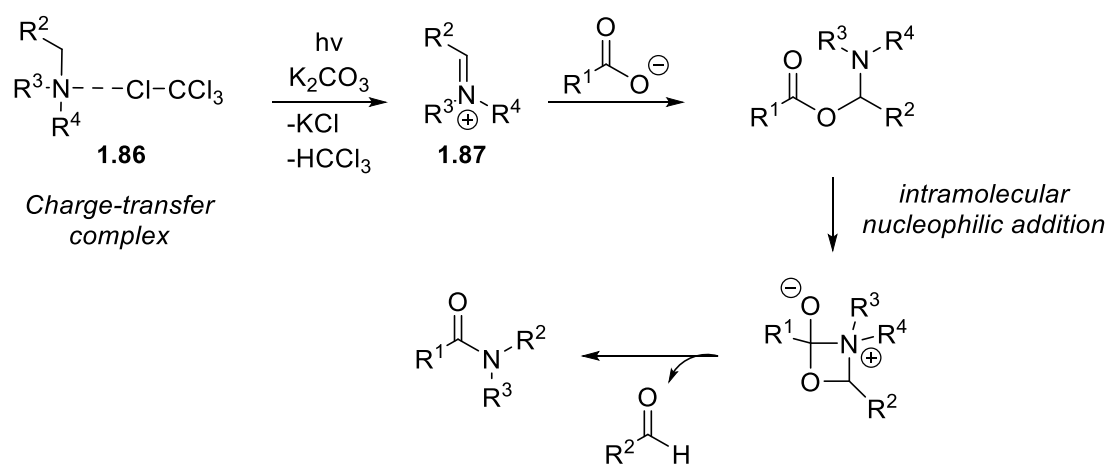
1.2.2.4 Photocatalysis

Photoredox catalysis has sparked a lot of interest in the synthetic community over the last few years. In this context, amide synthesis via photoredox catalysis has received increasing interest. Nevertheless, most reported methods have mainly focussed on substrates other than carboxylic acids, such as aldehydes, or thioacids.⁹⁴ However, Szpilman's methodology for the dealkylative condensation of amines with carboxylic acids is one of the few examples mentioning the reaction of carboxylic acids and amines (Scheme 57).⁹⁵ The dealkylative condensation of a variety of linear and cyclic trialkylamines with carboxylic acids was achieved in synthetically useful yields.



Scheme 57

It was discovered through experimental and computational studies that the amine and tetrachloromethane form a light-absorbing charge-transfer complex **1.86** (Scheme 58).⁹⁵ When irradiated with visible light, the latter causes an electron transfer between the amine (electron donor) and tetrachloromethane (electron acceptor), generating iminium ion **1.87** and chloroform.



Scheme 58

⁹⁴ For a recent review on visible-light-mediated amide synthesis, see: Lu, B.; Xiao, W.-J.; Chen, J.-R. *Molecules* **2022**, *27*, 517.

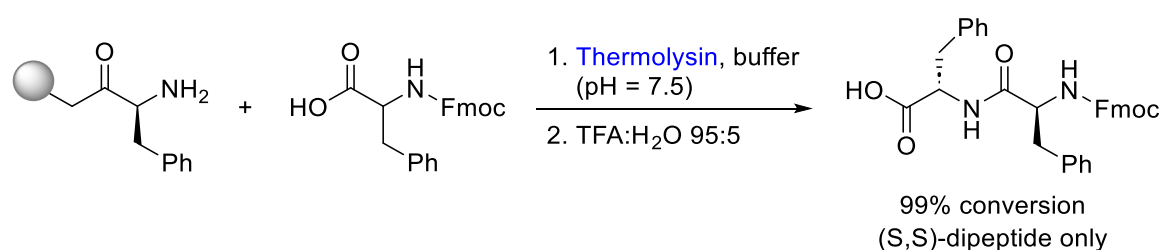
⁹⁵ Cohen, I.; Mishra, A. K.; Parvari, G.; Edrei, R.; Dantus, M.; Eichen, Y.; Szpilman, A. M. *Chem. Commun.* **2017**, *53*, 10128–10131.

The iminium ion **1.87** serves a dual role as both a dehydrating agent and a carboxylic acid activator.

1.2.2.5 Biocatalysis

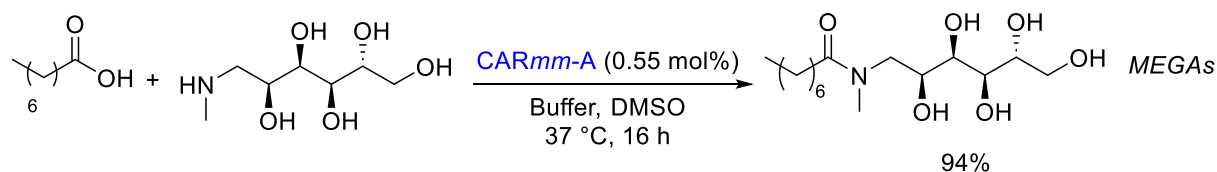
Enzyme-assisted direct amidation of carboxylic acids and amines is an attractive approach to construct this linkage since it normally proceeds with high selectivity and under mild conditions.

For instance, Thermolysin was used to achieve kinetic resolution of racemic Fmoc-phenylalanine, selectively producing the S,S-diastereomer of the dipeptide (Scheme 59).⁹⁶



Scheme 59

Recently, the production of commercially used surfactants, *N*-alkanoyl-*N*-methylglucamides (MEGAs), has been achieved using carboxylic acid reductase CARmm-A (Scheme 60).⁹⁷ Under mild conditions, the fabrication of 24 commercially relevant MEGAs was made possible using only 0.55 mol% loading of CARmm-A. Despite starting with multi-functionalized substrates, these reactions produced the amide product exclusively, with no competitive esterification side products (Scheme 60).



Scheme 60

⁹⁶ Ulijn, R. V.; Baragaña, B.; Halling, P. J.; Flitsch, S. L. *J. Am. Chem. Soc.* **2002**, *124*, 10988–10989.

⁹⁷ Lubberink, M.; Finnigan, W.; Schnepel, C.; Baldwin, C. R.; Turner, N. J.; Flitsch, S. L. *Angew. Chem. Int. Ed.* **2022**, *61*, e202205054.

Overall, biocatalysts are highly selective and efficient, however, their application is generally limited to structurally similar substrates, and reaction times can be lengthy. These factors can be optimized by structurally manipulating the catalyst through directed evolution and bioengineering.⁹⁸

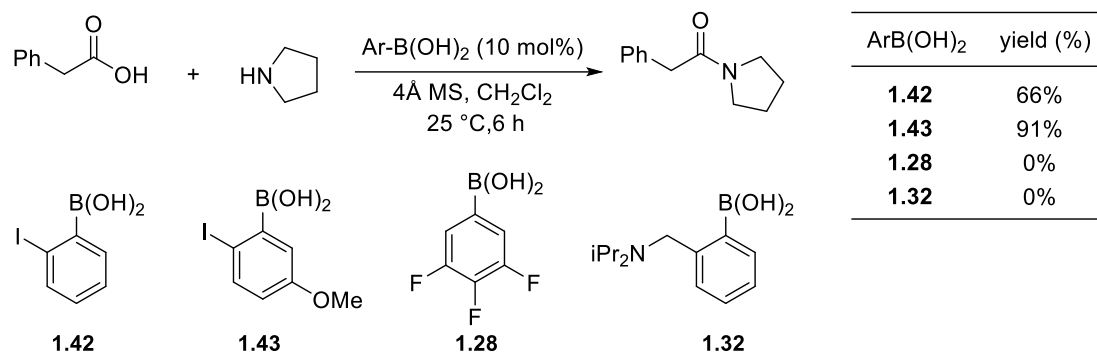
1.3 An overview of the current advancements and limitations in the boron-catalyzed direct amidation reaction

Multiple organoboron catalysts have been reported for the synthesis of amides from carboxylic acids and amines, each presenting a distinct advantage such as lower reaction temperature, broader substrate scope, or enhanced reaction rate.

Among the various classes of organoboron catalysts, arylboronic acids are the most extensively studied. This is due to the ease of manipulating the reactivity of arylboronic acids by changing the electronic and steric properties of substituents. Additionally, they can catalyze amide synthesis under mild conditions, such as at room temperature, and they are applicable for a broad substrate scope.

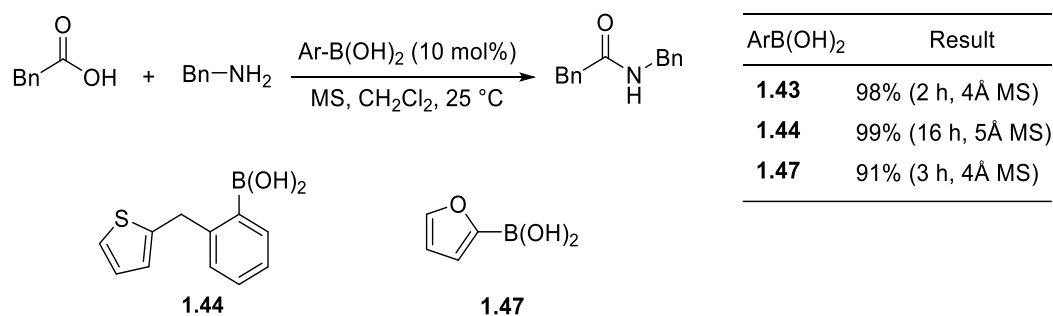
A significant breakthrough was accomplished by Hall in 2008, when he utilized 2-iodophenylboronic acid **1.42** as a catalyst for amide bond formation at 25 °C.⁵⁴ In a subsequent report, Hall presented the more efficient 2-iodo-5-methoxyphenylboronic acid **1.43**,⁵⁵ which enabled higher yields within shorter reaction times and allowed to expand the substrate scope (Scheme 61). Notably, catalyst **1.43** demonstrated applicability across a diverse range of substrates, including secondary aliphatic amines, α -branched aliphatic carboxylic acids, and aromatic acids (at 50 °C). Importantly, boronic acids **1.42** and **1.43** exhibit superior performance compared to Yamamoto's catalyst **1.28** and Whiting's aminoboronic acid **1.32**, as the latter two catalysts do not display catalytic activity at 25 °C (Scheme 61).⁵⁵

⁹⁸ Reetz, M. T. *Directed Evolution of Selective Enzymes: Catalysts for Organic Chemistry and Biotechnology*; John Wiley & Sons, 2016.



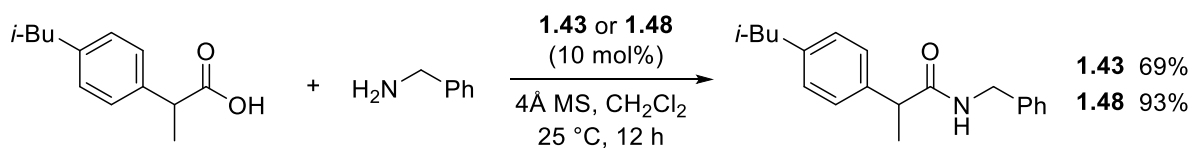
Scheme 61

Following the work on boronic acid **1.43**, the efficacy of arylboronic acids has been judged based on their ability to catalyze amide synthesis at 25 °C with comparable efficiency to **1.43**. In 2015, two catalysts, namely **1.44** and **1.47**, were identified for their ability to promote the direct amidation reaction at 25 °C (Scheme 62).^{57,60} Nevertheless, both of these catalysts demonstrated lower catalytic activity in comparison to **1.43**. They either necessitated longer reaction times or provided lower yields (Scheme 62). Even though **1.47** displayed a roughly close efficiency to **1.43**, it was unsuccessful for the coupling of aromatic or sterically hindered carboxylic acids.⁶⁰



Scheme 62

Moreover, Ishihara described the boronic acid **1.48** as a highly efficient catalyst. Based on a comparative catalytic activity study on the reaction of racemic ibuprofen and benzylamine, **1.48** provided an enhanced yield (93%) over **1.43** (69%) (Scheme 63).⁶¹



Scheme 63

Using catalyst **1.48**, only two amides were prepared at 25 °C. In contrast, higher temperatures of 85 °C or 110 °C were used for the coupling of aromatic or α -branched carboxylic acids, as well as anilines. Interestingly, **1.48** was used efficiently for the coupling of protected L-amino acids and L-amino ester hydrochlorides.⁶¹

In summary, when it comes to arylboronic acid-catalyzed direct amidation reactions, the boronic acids **1.43** and **1.48** are the best performing and represent the current state-of-the-art in this field.

While the boronic acid catalyzed amidation is efficient and well-developed, it does have certain drawbacks. The major limitation is the requirement of large amounts of molecular sieves to drive the reaction, which complicates large-scale applications. One potential solution to this issue involves replacing molecular sieves with azeotropic water removal as a dehydration protocol. However, this alternative approach requires higher temperatures of 85 °C to 110 °C.

Furthermore, new classes of organoboron catalysts have emerged in the last few years and each can offer a certain advantage. For instance, DATB^{80,81} **1.76** and pym-DATB⁸² **1.77** are very useful catalysts for the coupling of sterically hindered aliphatic acids and epimerization-prone substrates. Nonetheless, these catalysts require complicated synthesis that compromises their synthetic utility. Recently, a simplified analog **1.78**,⁸⁴ was reported and although its scope is still limited, it offered enhanced performance over DATB and enhanced practicality. Additionally, diboronic acids have been explored and they displayed interesting applications. To exemplify, diboronic acid **1.67** was used for dipeptide synthesis from β -hydroxy- α -amino acids and demonstrated high functional group tolerance.^{68,69} On the other hand, similar to DATB, the preparation of **1.67** is time-consuming and requires extensive use of reagents.

Overall, although there are several classes of organoboron catalysts developed, arylboronic acids remain one of the most developed groups in this research area where it provides several

advantages in terms of the mildness of reaction conditions, high availability, or amidation reaction scope.

1.4 Project Objectives

Given the reasons listed in the previous section, our research group has been greatly invested, over the last decade, in studying organoboron catalysis for direct amide synthesis. One of their contributions in this field was the development of a competent boronic acid catalyst carrying a thiophene moiety that is active at room temperature and allows for a broad substrate scope.⁵⁷ Another study used borinic acids as *pre*-catalysts for dipeptide synthesis.⁵⁸

In light of this, the research project presented in this manuscript aims at developing boronic acid catalysts for the direct formation of amide linkages. The general goals are to reduce the energy requirements of the process, avoid poor atom economy, and allow the preparation of a diverse selection of amides.

The research project began with a study on cyclic borinic acids. Later, a group of *ortho*-(aryloxy)phenylboronic acids, structurally derived from these cyclic borinic acids, was examined for their potential as direct amidation catalysts. The second chapter will discuss our initial work on cyclic borinic acids and the subsequent work on *ortho*-(aryloxy)phenylboronic acids.

Chapter three will discuss the Lewis acidity assessment of the *ortho*-(aryloxy)phenylboronic acids using Fluorine-ion affinity (FIA). The Lewis acidity scaling was also used to design a new group of *ortho*-(sulfonate) arylboronic acids.

In chapter four, we discuss the preparation of the *ortho*-(sulfonate) arylboronic acids and the investigations on their catalytic efficiency in amide bond formation reactions. The scope of amides synthesis, as well as mechanistic insights, are covered.

Chapter 2. Cyclic borinic acids and biarylether-based boronic acids as promoters for direct amides synthesis

Table of Contents

2.1 Catalytic application of borinic acids in amide synthesis	67
2.1.1 Introduction	67
2.1.2 Cyclic borinic acids in amidation reactions	68
2.1.2.1 Preliminary results.....	68
2.1.2.2 Preparation of cyclic borinic acid: sulfonylboraanthracene	70
2.1.2.3 Catalytic activity and stability studies of cyclic borinic acids	73
2.2 Biarylether-based boronic acids in the direct amidation reaction	77
2.2.1 Introduction and Objective.....	77
2.2.2 Preparation of aryloxyphenylboronic acids.....	78
2.2.3 Kinetic studies for catalytic activity evaluation	81
2.2.3.1 The case of 2-(aryloxy)phenylboronic acids	82
2.2.3.2 The case of 2,4-disubstituted derivatives	83
2.2.3.3 The case of 2,6-disubstituted derivatives	85
2.2.4 Comparative catalytic activity study with the state-of-the-art boronic acids.....	87
2.2.5 Examination of the scope of the reaction	89
2.3 Experimental Section	91
2.3.1 General Methods	91
2.3.2 Synthetic protocol and characterization for sulfonylboraanthracene	92
2.3.3 Synthetic protocol and characterization of oxaboraanthracene.....	94
2.3.4 Synthetic protocol and characterization of borinic acids' protodeborylation products	95
2.3.5 Procedure for the protodeboration experiments	97
2.3.5.1 Protodeboration of sulfonylboraanthracene	97
2.3.5.2 Protodeboration of oxaboraanthracene.....	98
2.3.6 Synthetic protocols and characterization for 2-(aryloxy)phenyl]boronic acids and their intermediates	98

2.3.6.1 General procedure A for the preparation of 2-aryloxyphenyl iodides	98
2.3.6.2 General procedure B for the preparation of 2-aryloxyphenyl boronic acids.....	98
2.3.6.3 Corresponding characterization data	99
2.3.7 Synthetic protocols and characterization for [2,4-bis(aryloxy)phenyl]boronic acids and their intermediates	106
2.3.7.1 General procedure C for the preparation of 2,4-aryloxybenzenes	106
2.3.7.2 General procedure D for the preparation of 2,4-aryloxybenzene bromides.....	106
2.3.7.3 General procedure E for the preparation of 2,4-aryloxybenzene boronic acids.	106
2.3.7.4 Corresponding characterization data	107
2.3.8 Synthetic protocols and characterization for [2,6-bis(aryloxy)phenyl]boronic acid and its intermediates.....	113
2.3.9 General procedure of kinetic experiments and raw kinetic data	117
2.3.10 Amides synthesis and characterization	118

2.1 Catalytic application of borinic acids in amide synthesis

2.1.1 Introduction

Borinic acids are among the least recognized organoboron derivatives,⁹⁹ nonetheless, they possess some interesting properties. One of these properties is that they exhibit higher Lewis acidity than corresponding boronic acids (Figure 11). Given that arylboronic acids can be employed as catalysts for the *N*-acylation of amines, it can be hypothesized that the more Lewis acidic borinic acids may constitute an enhanced catalytic system.

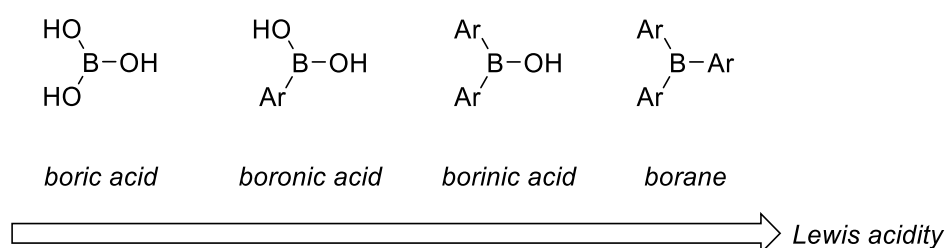
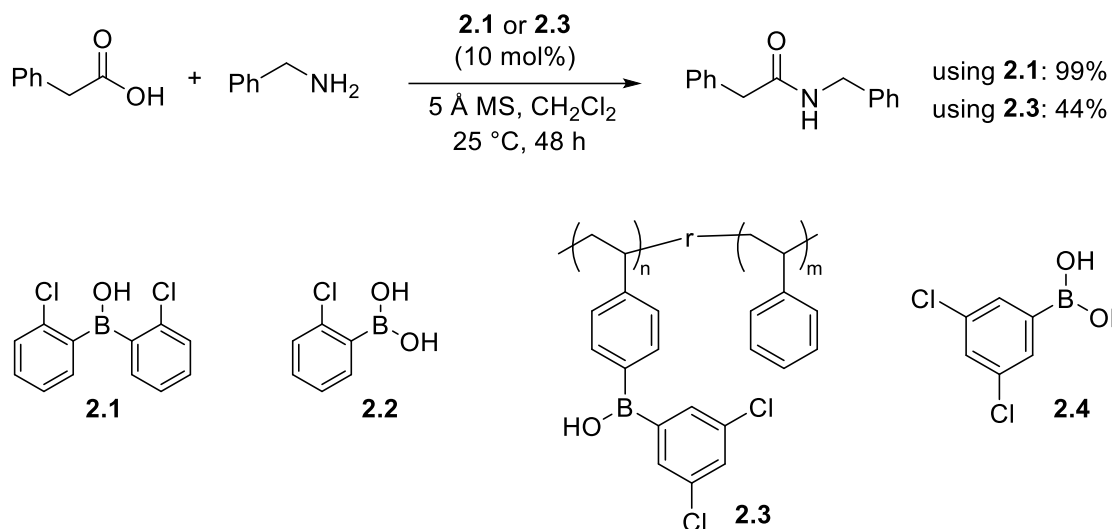


Figure 11

This class of compounds has demonstrated proficiency in catalyzing various chemical transformations, however, there have been merely two reports on their use as catalysts for the *N*-acylation of amines. One of these reports discusses the use of non-cyclic arylboronic acid **2.1** for the synthesis of dipeptides.⁵⁸ Nonetheless, Whiting and Sheppard re-examined this report and demonstrated that borinic acid **2.1** protodeboronates *in situ* to generate boronic acid **2.2** which in turn acts as the active catalyst (Scheme 64).⁵⁹ Another one describes the application of polystyrene-bound dichlorophenylborinic acid **2.3**, which is less potent than **2.1**, and it was also revealed that this borinic acid did indeed protodeboronate and release the boronic acid **2.4** responsible for the observed performance (Scheme 64).¹⁰⁰

⁹⁹ Ishihara, K.; Kurihara, H.; Yamamoto, H. *Synlett* **1997**, 597.

¹⁰⁰ Baraniak, M. K.; Lalancette, R. A.; Jäkle, F. *Chem. Eur. J.* **2019**, *25*, 13799–13810.



Scheme 64

In order to circumvent the protodeboronation issue, it was envisioned that the incorporation of the boronic acid in a cyclic structure could confer some stability. Therefore, cyclic boronic acids were investigated in terms of their application as direct amidation catalysts.

2.1.2 Cyclic boronic acids in amidation reactions

2.1.2.1 Preliminary results

Cyclic boronic acids based on a boraanthracene scaffold (**2.5-2.7**, Figure 12) have been explored for a range of applications such as regioselective activation of polyols,¹⁰¹ and ring opening of epoxyalcohols.¹⁰² Nonetheless, the potential of cyclic boronic acids as direct amidation catalysts has not yet been explored.

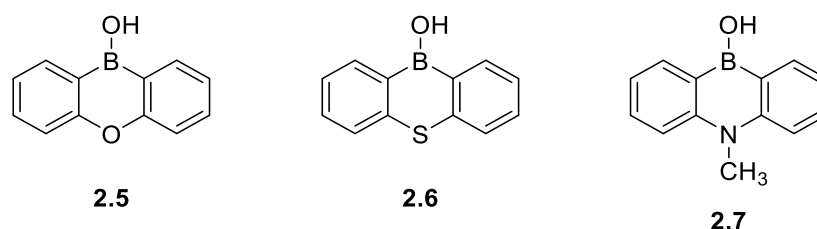
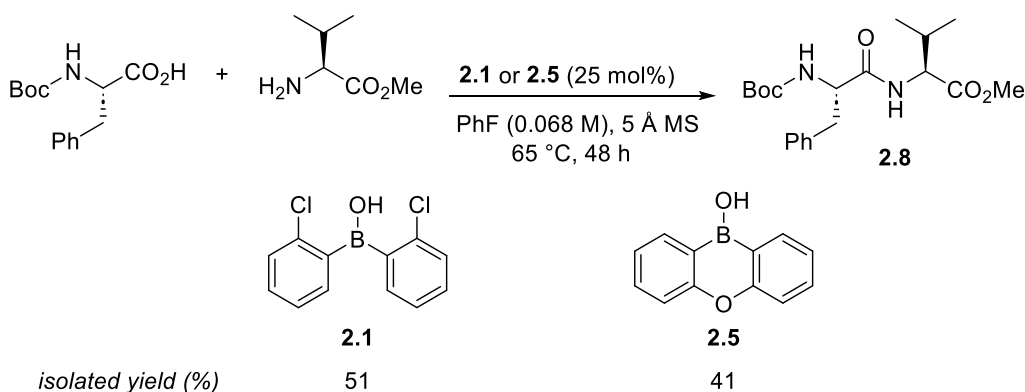


Figure 12

¹⁰¹ Dimitrijević, E.; Taylor, M. S. *Chem. Sci.* **2013**, *4*, 3298–3303.

¹⁰² Wang, G.; Taylor, M. S. *Adv. Synth. Catal.* **2020**, *362*, 398–403.

A preliminary result was obtained in our research group using the cyclic borinic acid **2.5** which enabled the coupling of *N*-Boc phenylalanine and valine methyl ester in 41% yield (Scheme 65).¹⁰³ However, dibenzoxaborininol **2.5** provided a lower yield (41%) of dipeptide **2.8** than the *pre*-catalyst **2.1** (51%).



Scheme 65

Through seeking to enhance the catalytic efficiency of dibenzoxaborininol **2.5**, we assumed that introducing an electron-withdrawing group would increase the Lewis acidity of the borinic acid and its overall efficiency. As observed earlier, only electron-rich boranthracenes **2.5-2.7** (Figure 12) have been explored as catalysts, with no precedent example of an electron-poor analog.

To identify an electron-withdrawing group of interest to incorporate into the structure of the cyclic borinic acid, we made use of Hammett's substituent constants (σ).¹⁰⁴ It is important to note that this constant applies to the *meta*- and *para*-positions, rather than the *ortho*-substitution. However, it can provide an overall indication of the relative electron-withdrawing effect. It was noted that a phenylsulfonyl group has substituent constant values of 0.62 (σ_m) and 0.68 (σ_p), which fall in between those of strongly deactivating nitro ($\sigma_m= 0.71$, $\sigma_p= 0.78$) and trifluoromethyl ($\sigma_m=0.43$, $\sigma_p=0.54$) groups (Figure 13).

¹⁰³ Mohy El Dine, T. (2016). New insights in amide bond formation mediated by boron-based catalysts [Doctoral dissertation, University of Caen Normandy]

¹⁰⁴ Hansch, Corwin.; Leo, A.; Taft, R. W. *Chem. Rev.* **1991**, *91*, 165–195.

substituent	σ_m	σ_p
NO ₂	0.71	0.78
SO ₂ C ₆ H ₅	0.62	0.68
CF ₃	0.43	0.54

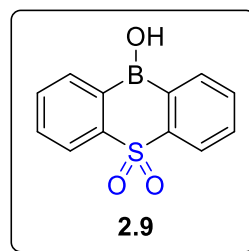
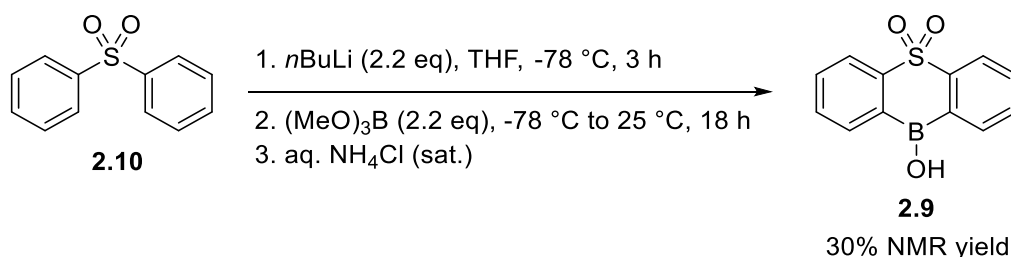


Figure 13

As a result, cyclic borinic acid **2.9**, decorated with a sulfonyl group, was identified as an interesting target to be synthesized and studied.

2.1.2.2 Preparation of cyclic borinic acid: sulfonylboraanthracene

Generally, cyclic arylborinic acids are obtained through the *ortho*-lithiation of biaryl scaffolds such as diaryl ether¹⁰⁵ or diphenyl sulfide,¹⁰¹ followed by the electrophilic trapping of the organolithium species with trialkyl borate. Given that the sulfone moiety is a good directed metalation group (DMG),^{106,107} borinic acid **2.9** was synthesized through the *ortho*-lithiation of the commercially available diphenyl sulfone **2.10** with subsequent electrophilic quench using B(OMe)₃ (Scheme 66). This has afforded the borinic acid **2.9** in an estimated 30% NMR yield. The low yield was accompanied by the formation of the boronic acid byproduct (<10%) and degradation products.



Scheme 66

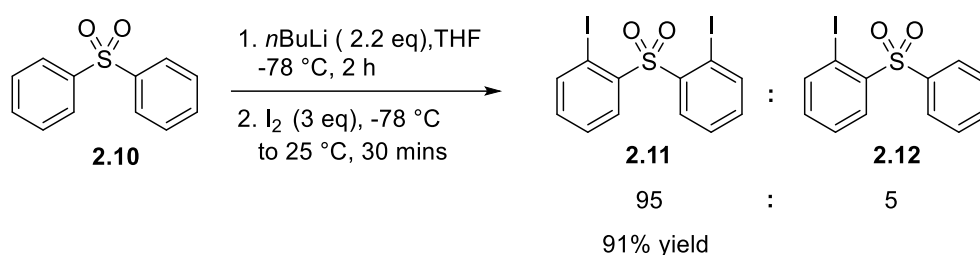
Several optimization studies were carried out at the level of the *ortho*-lithiation and electrophilic quench steps to improve the yield. First, the *ortho*-lithiation step was examined using iodine as an electrophile instead of B(OMe)₃. The desired diiodide **2.11** was obtained with high

¹⁰⁵ Niu, L.; Yang, H.; Jiang, Y.; Fu, H. *Adv. Synth. Catal.* **2013**, 355, 3625–3632.

¹⁰⁶ Leroux, F. R.; Mortier, J. Directed metalation of arenes with organolithiums, lithium amides, and superbases. In *Arene Chemistry*; John Wiley & Sons, Ltd, **2015**; pp 741–776.

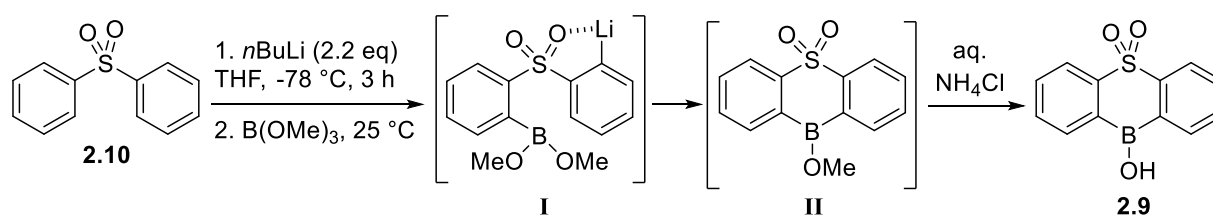
¹⁰⁷ Iwao, M.; Iihama, T.; Mahalanabis, K. K.; Perrier, H.; Snieckus, V. *J. Org. Chem.* **1989**, 54, 24–26.

selectivity (95%) and isolated yield (91%), accompanied by only 5% of the mono-iodinated product **2.12** (Scheme 67). This reveals that the boronic acid byproduct formed during the synthesis of **2.9**, is caused by the formation of 2-lithiated diphenyl sulfone during the *ortho*-lithiation step. Nonetheless, the 2,2'-dilithiated diphenyl sulfone is formed with high selectivity when 2.2 equiv. of *n*BuLi is used, therefore, the lithiation step is not the primary source of the low yield.



Scheme 67

Next, the electrophilic quench was investigated (Scheme 68). Primarily, decreasing the amount of B(OMe)₃ from 2.2 equiv. to 1.5 equiv. led to the absence of the formation of boronic acid **2.9** (Entry 2). Moreover, reducing the reaction time from 18 h (Entry 1) to 3 h (Entry 3) caused a significant drop in the NMR yield from 30% to 5%. However, an excess of 4 equiv. of B(OMe)₃ proved to be advantageous providing a 40% NMR yield of **2.9** (Entry 4). Yet, increasing this excess to 6 equiv. provided no further improvement (Entry 5). Overall, the NMR yield never exceeded 40%.



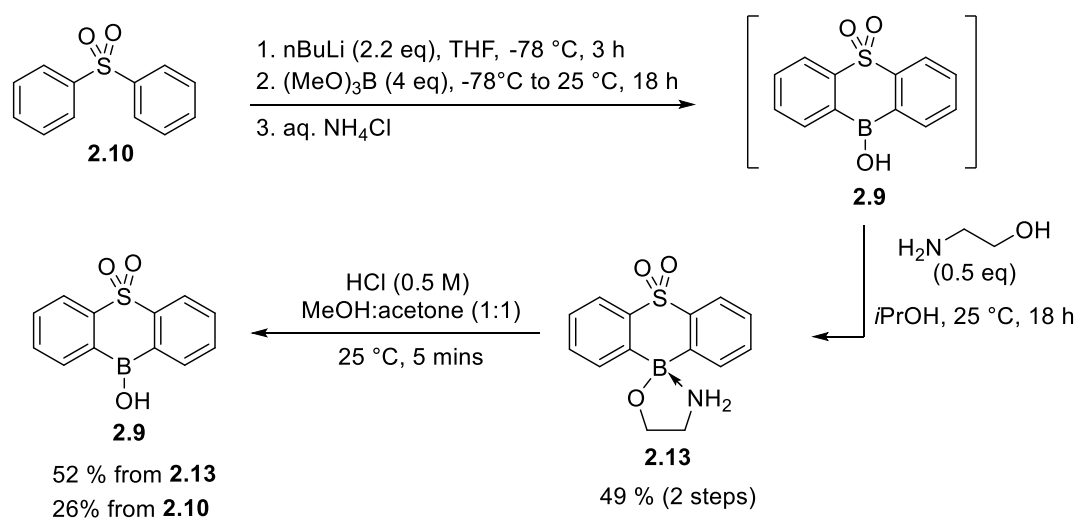
Entry	N ^o eq B(OMe) ₃	Time (h)	% NMR yield ^(a)
1	2.2	18	30
2	1.5	18	0
3	2.2	3	5
4	4	18	40
5	6	18	40

^(a) determined from ¹H NMR

Scheme 68

It could be presumed that the borylation step is hampered by the difficulty of the cyclization of the second aryl lithium on the intermediate boron species **I** (Scheme 68). To emphasize, the stabilization of the intermediate boronate species **I** via lithium-oxygen interaction could slow down the second addition onto the boron center. This might explain the need for excess borate reagent to react with the aggregated organolithium species. It is worth noting that the addition of a Lewis base additive, TMEDA, to break down organolithium aggregates did not provide any enhancement. To sum up, the optimal outcome of 40% NMR yield was achieved using a slight excess of *n*BuLi (2.2 equiv.) and 4 equiv. of B(OMe)₃ for an 18 h reaction (Entry 4, Scheme 68).

Furthermore, it was observed that borinic acid **2.9** degraded on silica-gel upon chromatographic purification. Therefore, its purification required a two-step protocol through an aminoethanol complex **2.13** (Scheme 69). Under the optimized reaction conditions, sulfonylboraanthracene **2.9** was synthesized with an overall 26% yield over two steps (Scheme 69). This result is comparable with the low yield reported by Taylor for the sulfide derivative **2.6** that was synthesized in 20% yield.¹⁰¹

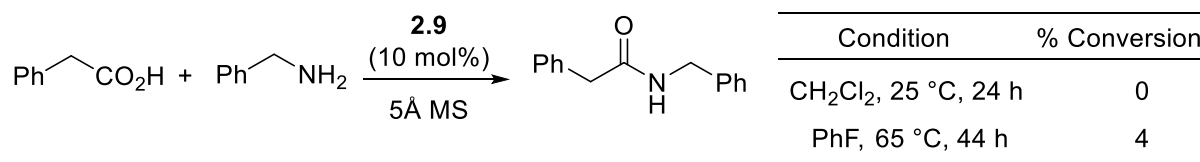


Scheme 69

As a result, with this new electron-deficient borinic acid **2.9** in hand, its catalytic activity was evaluated.

2.1.2.3 Catalytic activity and stability studies of cyclic borinic acids

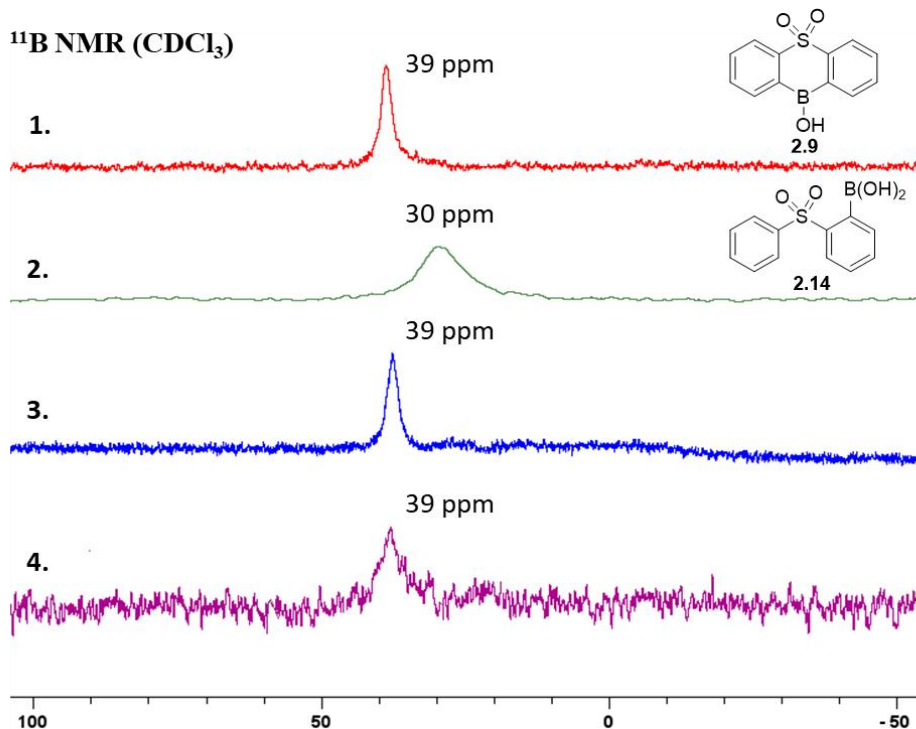
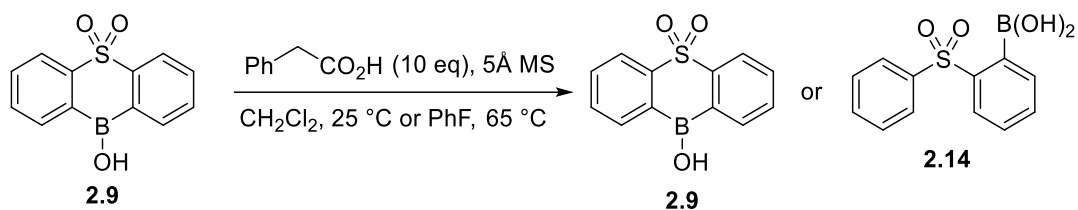
The catalytic efficiency of borinic acid **2.9** was assessed on the direct amidation reaction of phenylacetic acid and benzylamine. At 25 °C, no conversion was observed after 24 h. Moreover, forcing the conditions by heating the reaction at 65 °C for 44 h provided a 4% conversion only (Scheme 70).



Scheme 70

At first, it was hypothesized that the absence of catalytic activity with borinic acid **2.9** was caused by the generation of less reactive boronic acid. Therefore, its stability was examined at 25 °C and 65 °C using ¹¹B NMR (Scheme 71). It should be noted that ¹H NMR analyses did not allow a clear interpretation since the aromatic proton signals of phenylacetic acid overlap with those of **2.9**. Additionally, the 2-(phenylsulfonyl)benzeneboronic acid **2.14**, which is the deboronation byproduct of **2.9**, was synthesized to help recognize its presence in the reaction mixture.

First, borinic acid **2.9** was added to phenylacetic acid (PAA) and 5 Å powdered activated molecular sieves at 25 °C. In this case, a signal was observed at 39 ppm in ¹¹B NMR, after 30 mins, which corresponds to **2.9** (Entry 3, Scheme 71). Therefore, no protodeborylation took place at 25 °C. Moreover, the addition of **2.9** to phenylacetic acid and 5 Å activated molecular in PhF at 65 °C for 3 h, resulted in the appearance of a major signal at 39 ppm in ¹¹B NMR (Entry 4, Scheme 71). Hence, borinic acid **2.9** is the major compound at 65 °C.

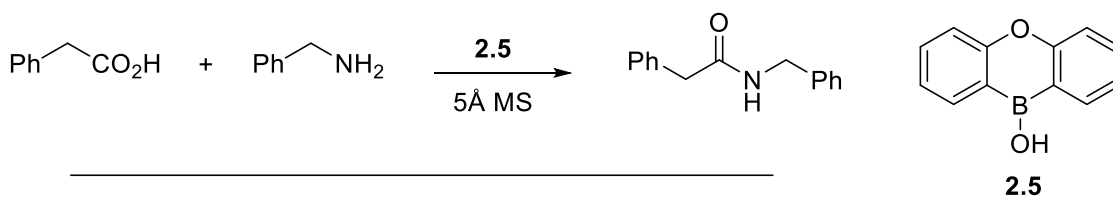


Reaction conditions: **1.** Pure borinic **2.9** ; **2.** Pure boronic **2.14** ; **3.** Borinic **2.9** (0.05 mmol), PAA (10 eq), 5Å MS (1 g), CH₂Cl₂, 25 °C, 30 mins ; **4.** Borinic **2.9** (0.05 mmol), PAA (10 eq), 5Å MS (1 g), PhF, 65 °C, 3 h

Scheme 71

Therefore, according to ¹¹B NMR analyses, borinic acid **2.9** does not undergo deboronation when added to carboxylic acid and 5Å MS at 25 °C or 65 °C.

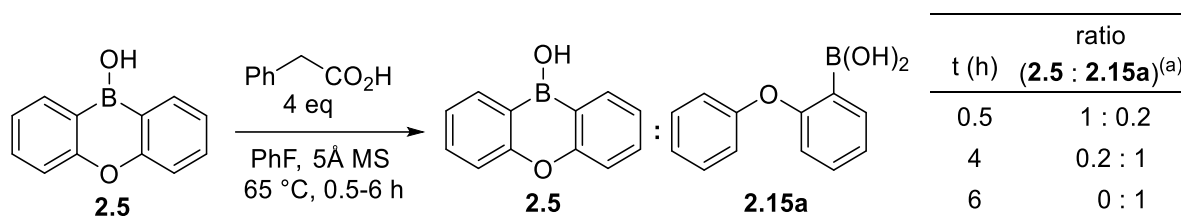
Following that, the catalytic performance of borinic acid **2.5** was examined for the synthesis of *N*-benzylphenylacetamide, at 25 °C, in an attempt to correlate it with the behavior observed with borinic acid **2.9**. At 25 °C, no amide product was obtained even after 45 h (Entry 1, Scheme 72). Nonetheless, when the coupling of phenylacetic acid and benzylamine was conducted in PhF at 65 °C and with a 25 mol% loading of **2.5**, a 57% yield was obtained (Entry 2, Scheme 72).



Entry	Condition	% yield
1	10 mol% 2.5 , CH ₂ Cl ₂ , 25 °C, 45 h	0
2	25 mol% 2.5 , PhF, 65 °C, 44 h	57

Scheme 72

Since protodeboronation is a common phenomenon for borinic acids,^{59,100} the activity observed for borinic acid **2.5** at 65 °C was investigated further to seek out possible protodeboronation (Scheme 73). To accomplish this, 2-(phenoxy)phenylboronic acid **2.15a**, which is the deboronation product of **2.5**, was synthesized.¹⁰⁸ First, when **2.5** was added to phenylacetic acid and 5 Å powdered activated MS at 25 °C, the formation of **2.15a** was not detected in ¹H NMR. Therefore, protodeborylation did not take place at 25 °C. Secondly, the borinic acid **2.5** was added to phenylacetic acid and activated powdered 5 Å MS at 65 °C, in PhF (Scheme 73). After 30 mins, the formation of boronic acid **2.15a** was detected by ¹H NMR. Later, the conversion of **2.5** into **2.15a** was complete in 6 h at 65 °C.

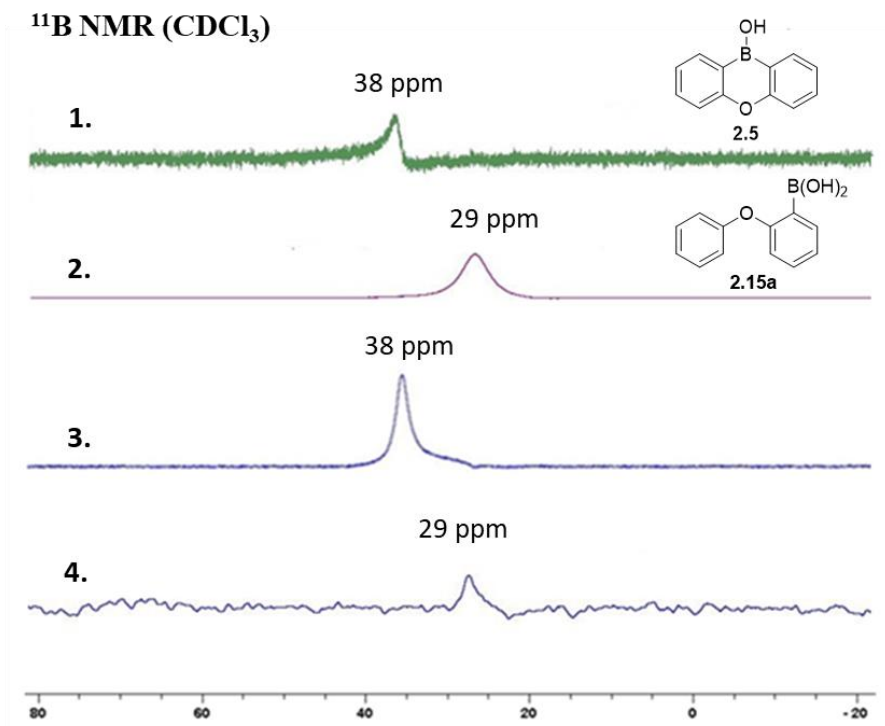


^(a) The ratio was determined from ¹H NMR analysis of samples of the reaction mixture

Scheme 73

These results were also supported by ¹¹B NMR analyses. First, at 25 °C, a signal was detected at 38 ppm which corresponded to **2.5** (Entry 3, Figure 14). Moreover, the disappearance of the signal of **2.5** in ¹¹B NMR at 38 ppm after 6 h at 65 °C and the appearance of a new signal at 29 ppm for **2.15a** (Entry 4, Figure 14), confirmed the observation that **2.5** underwent protodeboronation at 65 °C.

¹⁰⁸ Ishihara, K.; Gao, Q.; Yamamoto, H. *J. Org. Chem.* **1993**, *58*, 6917–6919.

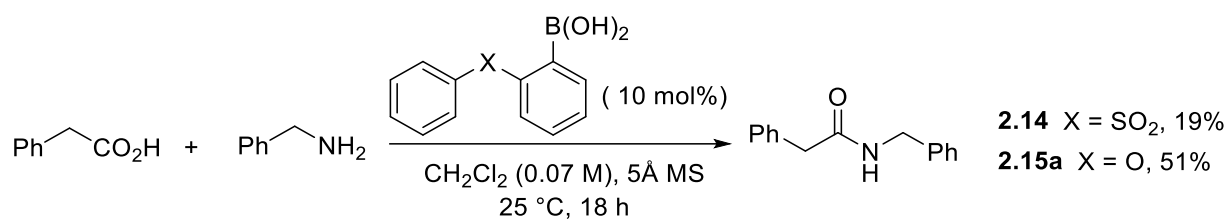


Reaction conditions: **1.** Pure boronic **2.5** ; **2.** Pure boronic **2.15a** ; **3.** Boronic **2.5** (0.055 mmol), PAA (10 eq), 5 Å MS (1 g), CH₂Cl₂, 25 °C, 30 mins ; **4.** Boronic **2.5** (0.125 mmol), PAA (4 eq), 5 Å MS (1 g), PhF, 65 °C, 6 h

Figure 14

To sum up, boronic acid **2.5** protodeboronates into boronic acid **2.15a**, in the presence of a carboxylic acid at 65 °C, and **2.15a** acts as the active catalyst. Furthermore, sulfonylboraanthracene **2.9** was found to be the major organoboron compound, even at 65 °C. This observation implies that the absence of catalytic activity using boronic acid **2.9** can be attributed to the lack of protodeborylation and the consequent absence of boronic acid **2.14**. These results are consistent with the observations of Whiting *et al.*, which demonstrated that boronic acids act as *pre*-catalysts and they do not catalyze the amidation reaction unless they protodeborylate to give the respective boronic acid.⁵⁹

Next, the boronic acids **2.14** and **2.15a** were investigated, separately, as catalysts for the direct condensation of phenylacetic acid and benzylamine (Scheme 74). Boronic acid **2.14** furnished the amide in 19% yield after 18 h at 25 °C. However, boronic acid **2.15a** afforded an encouraging 51% yield at 25 °C (Scheme 74) which matched the one observed with **2.5** at 65 °C upon its protodeborylation (Scheme 72, Entry 2).



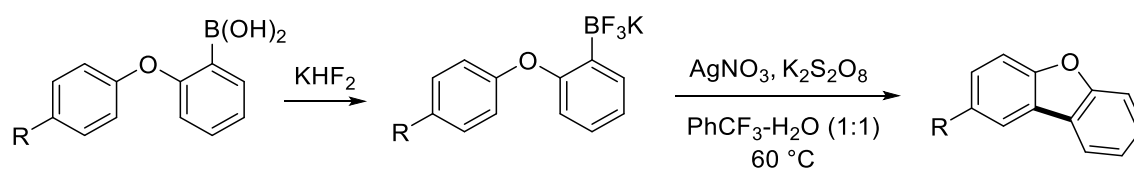
Scheme 74

The preliminary result obtained with **2.15a** prompted the further modification of the biarylether scaffold of **2.15a** to enhance its catalytic performance.

2.2 Biarylether-based boronic acids in the direct amidation reaction

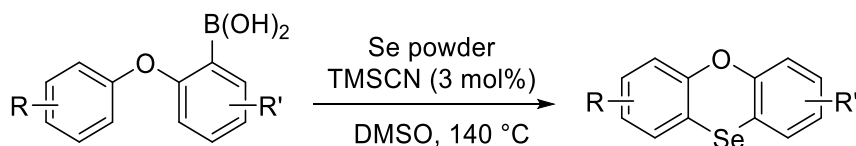
2.2.1 Introduction and Objective

Generally, biarylether boronic acids have received little attention in the literature. The few examples available comprise the use of biaryletherboronic acids to produce the respective trifluoroborates, which then serve as radical precursors in Pschorr-type cyclization (Scheme 75).¹⁰⁹



Scheme 75

Another example is the synthesis of selenaheterocycles using a three-component reaction of arylboronic acids, Se powder, and TMSCN (Scheme 76).¹¹⁰



Scheme 76

¹⁰⁹ Lockner, J. W.; Dixon, D. D.; Risgaard, R.; Baran, P. S. *Org. Lett.* **2011**, 13, 5628–5631.

¹¹⁰ Zhang, X.; Huang, X.-B.; Zhou, Y.-B.; Liu, M.-C.; Wu, H.-Y. *Chem. Eur. J.* **2021**, 27, 944–948.

Interestingly, there is no precedent for using these structures as catalysts for the direct condensation of acids and amines. Moreover, the biarylether scaffold carries some interesting features such as an *ortho*-aryloxy group, where *ortho*-substitution is common in highly performing boronic acid catalysts. Besides, it comprises two aromatic rings thus allowing for large possibilities of electronic structure modulation (Figure 15).

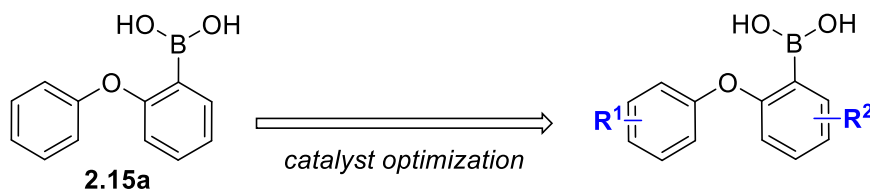


Figure 15

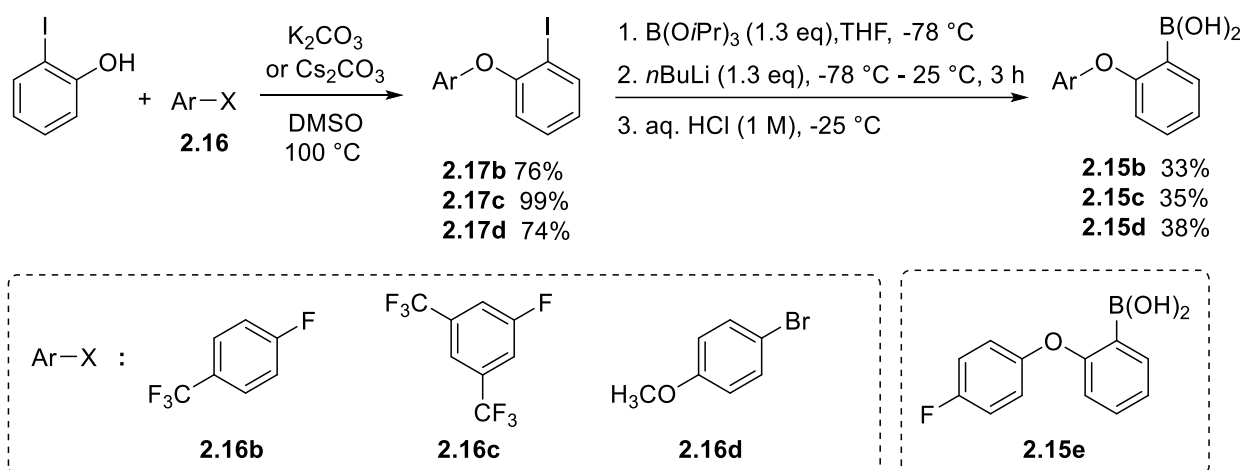
Motivated by these observations, we decided to investigate a group of functionalized biarylether-based boronic acids of varied electronic and steric properties.

2.2.2 Preparation of aryloxyphenylboronic acids

A two-step synthetic strategy was devised for constructing electron-deficient 2-aryloxyphenylboronic acids **2.15b,c** (Scheme 77), except **2.15e**, which is commercially available. Also, a boronic acid containing an electron-donating methoxy substituent **2.15d** was prepared (Scheme 77).

First, the nucleophilic aromatic substitution of 2-iodophenol with the appropriately substituted aryl halides **2.16** provided 2-aryloxyphenyliodides **2.17b-d** in 74-99% yields. Following *n*BuLi addition at -78 °C, **2.17** undergoes lithium-iodide exchange and *in situ* quench with B(O*i*Pr)₃, furnishing the boronic acids **2.15b-d** in 33-38% yields. The addition of B(O*i*Pr)₃ prior to the introduction of *n*BuLi was suggested to minimize the formation of side products since the lithium-halogen exchange is faster than the reaction between *n*BuLi and B(O*i*Pr)₃.¹¹¹

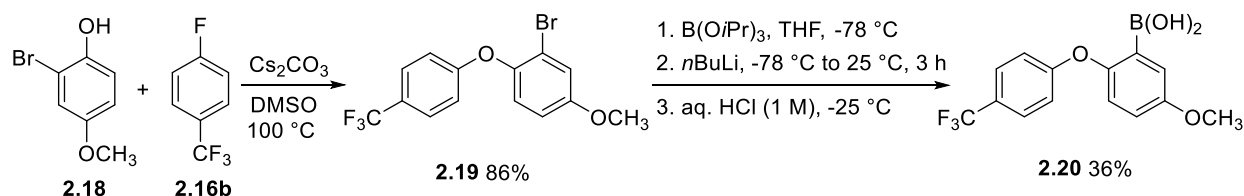
¹¹¹ Cai, D.; Larsen, R. D.; Reider, P. J. *Tetrahedron lett.* **2002**, *43*, 4285–4287.



Scheme 77

The low yield of boronic acids **2.15b-d** was accompanied by two experimental observations. Firstly, the crude mixtures contained a considerable amount of unidentified side products. However, the formation of borinic or diboronic acids, which could result from secondary deprotonation of the *ortho*-lithiated biarylether, was not observed. Although the aryloxy group has never been described as a precursor for aryne formation,¹¹² it is possible that the aryloxy group may serve as a good leaving group leading to the *in-situ* generation of highly reactive arynes, which could lead to the formation of byproducts. Secondly, a significant mass loss (30-40%) was detected during chromatographic purification, even though these boronic acids are stable on silica-gel (based on 2D TLC). This could originate from the formation of unstable side products that degraded on silica.

Furthermore, a boronic acid with a methoxy group positioned *para*- to the aryloxy moiety (**2.20**) was constructed from 2-bromo-4-methoxyphenol **2.18** and 4-fluorobenzotrifluoride **2.16b**, using the same procedure as for the boronic acids **2.15b-d** (Scheme 78). This protocol afforded the target boronic acid **2.20** in an overall yield of 31% from **2.16b**.



Scheme 78

¹¹² For a review that includes a timeline of aryne generation methods, see: Shi, J.; Li, L.; Li, Y. *Chem. Rev.* **2021**, *121*, 3892–4044.

The goal of developing this catalyst is to mimic the pattern of reactivity observed with 2-iodo-5-methoxybenzeneboronic acid (MIBA, **2.21**), in which the methoxy group reinforces the role of iodine as a hydrogen bond acceptor (Figure 16).^{55,56} In the case of **2.20**, it can be rationalized that the oxygen of the aryloxy group could act as a Lewis basic site that forms a hydrogen bond with one hydroxyl of the boronic acid group and the methoxy group supports such interaction (Figure 16).

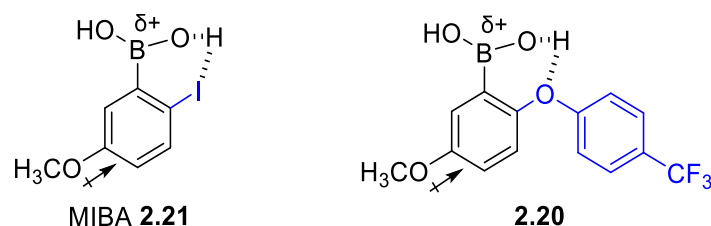
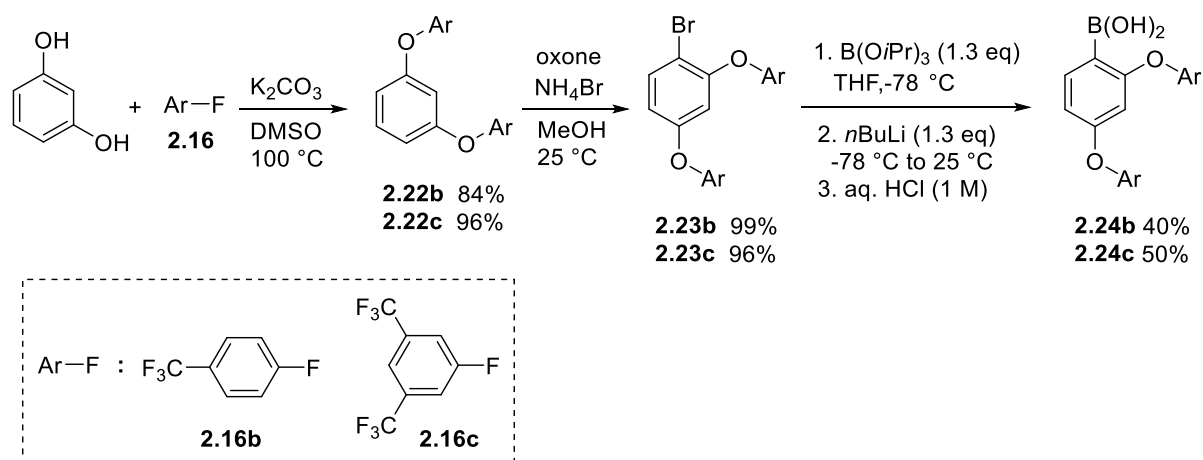


Figure 16

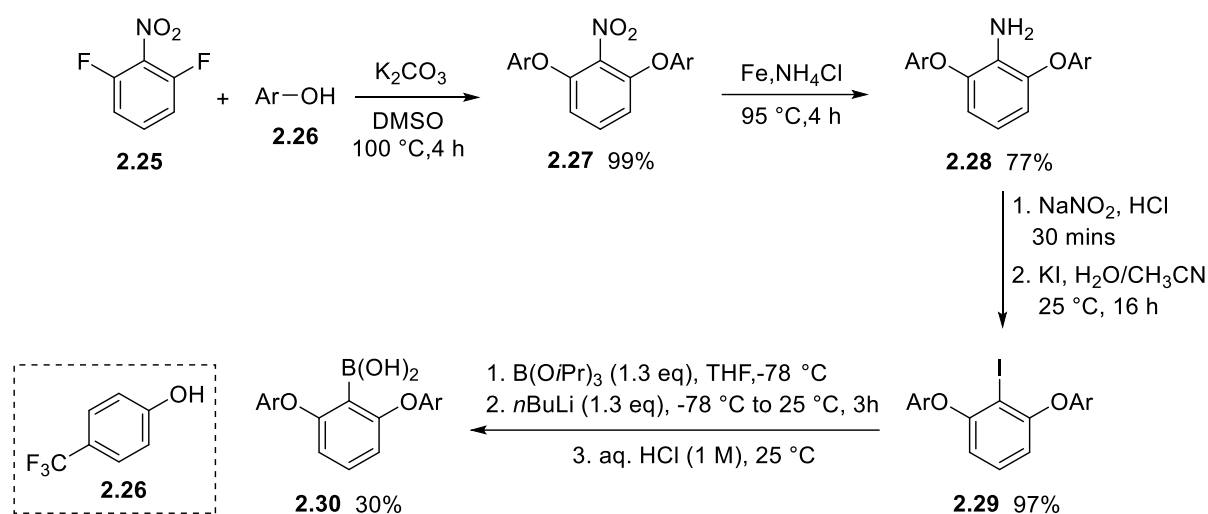
Additionally, disubstituted boronic acids were constructed to gain insight into the influence of the electronic effects and pattern of disubstitution on the catalytic performance. A simple three-step methodology was established to synthesize 2,4-disubstituted boronic acids **2.24** (Scheme 79). First, the nucleophilic aromatic substitution of the substituted fluorobenzenes **2.16b,c** with resorcinol afforded the diaryloxybenzenes **2.22b-c** in 84-96% yields. Secondly, 2,4-diaryloxyphenylbromides **2.23b-c** were obtained in 96-99% yields through a regioselective oxidative bromination of **2.22** using NH_4Br and Oxone.¹¹³ Lastly, the boronic acids **2.24b-c** were formed upon lithium-bromide exchange and *in situ* electrophilic quench with $\text{B}(\text{O}i\text{Pr})_3$ in 40-50% yields.



Scheme 79

¹¹³ Narender, N.; Mohan, K. V. V. K.; Kulkarni, S. J.; Raghavan, K. V. J. *Chem. Res.* **2003**, 2003, 597–598.

Next, to gain access to the structure of 2,6-disubstituted biarylether boronic acid **2.30**, a four-step protocol, based on reliable chemistry, was devised (Scheme 80). Starting with the nucleophilic aromatic substitution of 2,6-difluoro-nitrobenzene **2.25** with the 4-trifluoromethylphenol **2.26**, the nitrobenzene derivative **2.27** was obtained with a 99% yield. Then, the reduction of the nitrobenzene **2.27**, using iron and ammonium chloride as reducing agents, afforded the respective aniline **2.28** in 77% yield.¹¹⁴ The diazotization of the aniline derivative and subsequent substitution of the diazonium moiety with iodide furnished the iodobenzene **2.29** in 97% yield. Finally, the aryl iodide **2.29** undergoes lithium-iodine exchange and trapping with B(O*i*Pr)₃ (reverse addition) to produce boronic acid **2.30** in 30% yield.



Scheme 80

Following the synthesis of the (aryloxy)phenylboronic acid derivatives, their catalytic activity was assessed through kinetic studies.

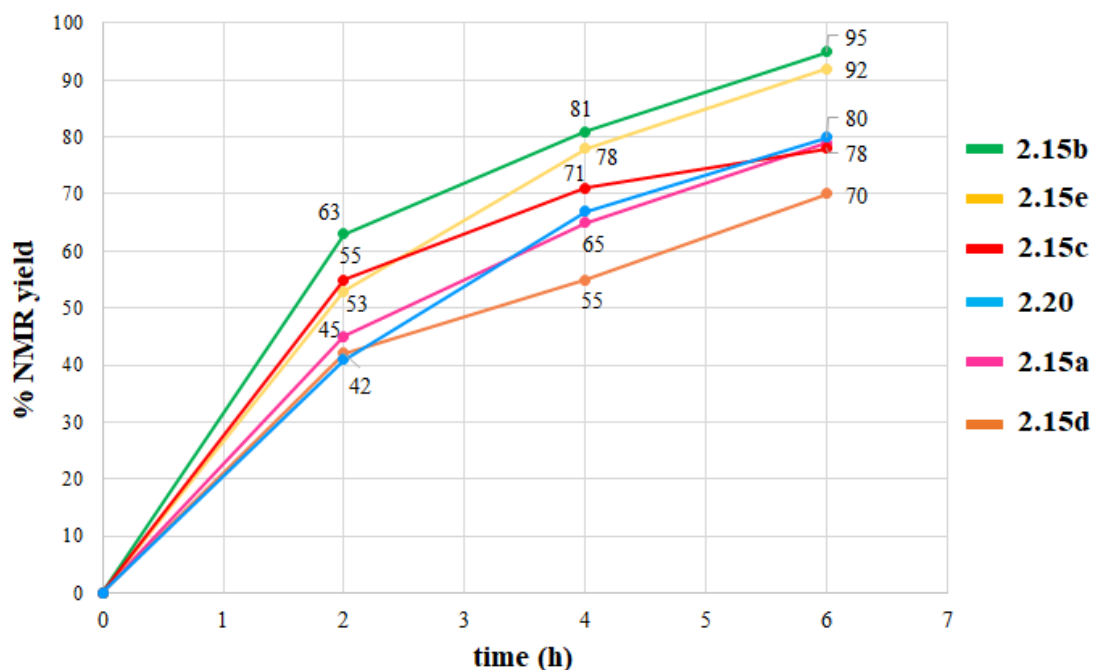
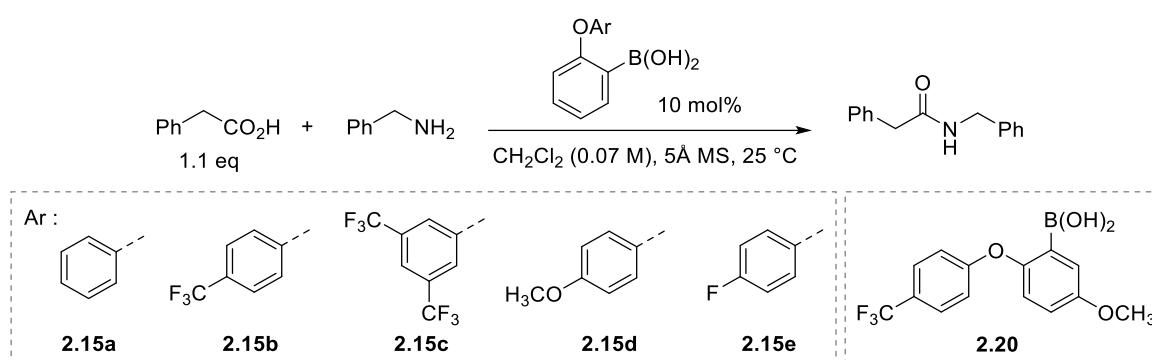
2.2.3 Kinetic studies for catalytic activity evaluation

The produced biaryletherboronic acids were subjected to an evaluation of their catalytic performance on the model dehydrative amidation reaction of phenylacetic acid and benzylamine at room temperature (25 °C). The NMR yields were determined from ¹H NMR integrations of the amide at 4.4 ppm (d, 2 H, CH₂-NH) and 3.6 ppm (s, 2 H, CH₂-C-C=O) using the internal standard 1,1,2,2-tetrachloroethane with its signal at 5.96 ppm (s, 2 H).

¹¹⁴ Vicker, N.; Bailey, H. V.; Day, J. M.; Mahon, M. F.; Smith, A.; Tutill, H. J.; Purohit, A.; Potter, B. V. L. *Molecules* **2021**, *26*, 7166.

2.2.3.1 The case of 2-(aryloxy)phenylboronic acids

Boronic acid **2.15b** bearing a 4-trifluoromethyl group provided the amide in 81% NMR yield in 4 h and 95% in 6 h (Scheme 81). Moreover, **2.15e** displayed a very close catalytic efficiency to **2.15b** where it afforded 78% NMR yield in 4 h and 92% in 6 h. Notably, the two catalysts **2.15b** and **2.15e** showed an enhanced catalytic performance over **2.15a**, which afforded a lower NMR yield of 78% in 6 h (Scheme 81). When boronic acid **2.15c** was used, a 71% NMR yield was recorded in 4 h and a 78% NMR yield in 6 h. Hence, the addition of two trifluoromethyl groups in the *meta*-positions in **2.15c** caused a drop in the reaction rate compared to **2.15b**.



Scheme 81

Moreover, the electron-rich boronic acid **2.15d** provided an even lower 55% NMR in 4 h and 70% in 6 h (Scheme 81). These results demonstrated that the electron deficiency of the aryloxy

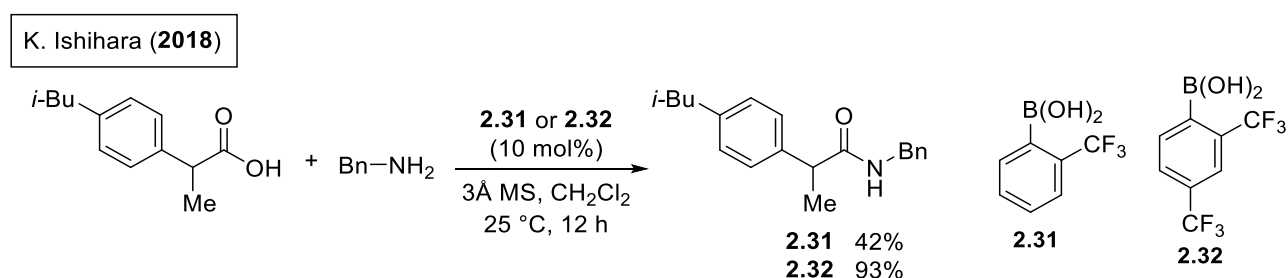
moiety has a positive influence on the catalytic efficiency and that the position of the substituents on the aryloxy group also had an impact.

Furthermore, the use of **2.20** led to a decline in the efficiency compared to **2.15b** since 80% NMR yield was recorded in 6 h, compared to 95% with **2.15b** (Scheme 81). This indicated that the original proposal of the methoxy group enhancing the role of the oxygen as a hydrogen-bond acceptor did not apply in this case, and it is possible that the methoxy substituent rendered the aryl ring electron-rich, hence, reducing the Lewis acidity of the boronic acid **2.20**.

As a result, catalyst **2.15b** is the most active among the group of 2-(aryloxy)phenylboronic acids. Next, the activity of the disubstituted derivatives was examined to study the effect of changing the electronic properties and pattern of disubstitution on the catalytic activity.

2.2.3.2 The case of 2,4-disubstituted derivatives

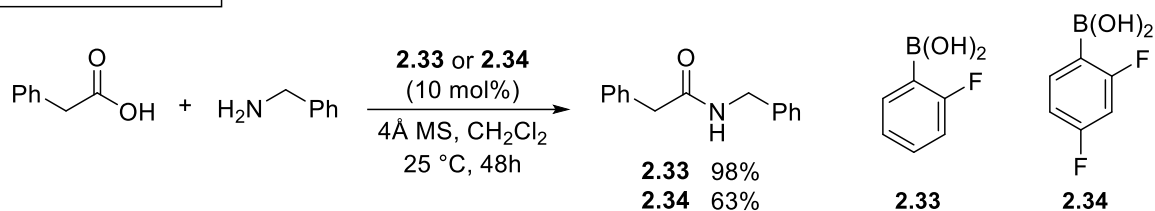
When examining the literature on boronic acid catalysts for amide synthesis, it can be noticed that 2,4-disubstituted arylboronic acids, having electron-withdrawing groups, can exhibit an enhanced catalytic performance over their 2-substituted analogs in some cases. For example, the 2,4-bis(trifluoromethyl)benzeneboronic acid **2.32** achieved the coupling of racemic ibuprofen and benzylamine in a 93% yield, meanwhile, 2-(trifluoromethyl)benzeneboronic acid **2.31** afforded a markedly lower 42% yield (Scheme 82).⁶¹



Scheme 82

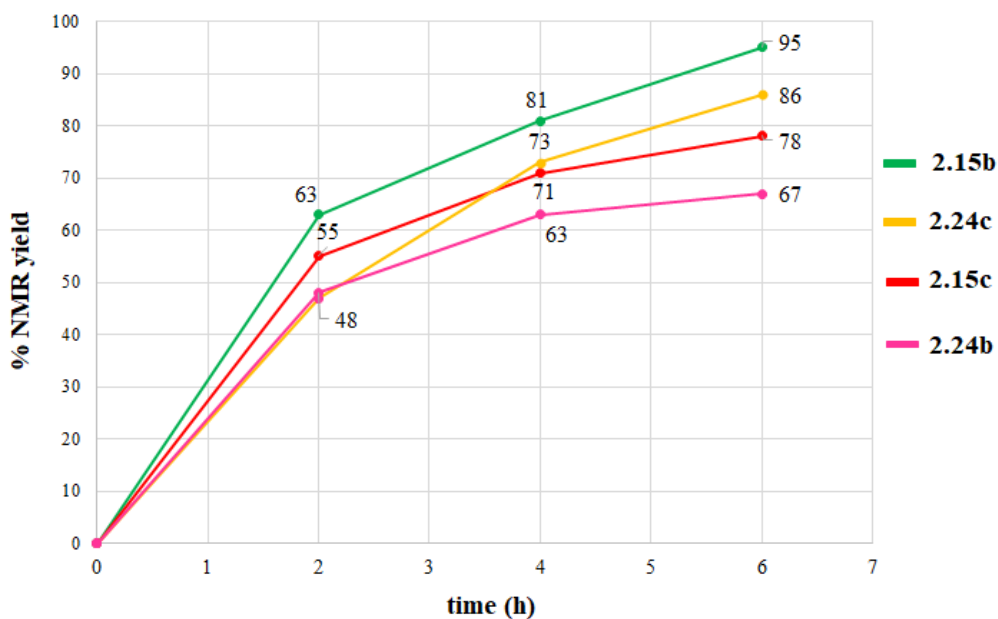
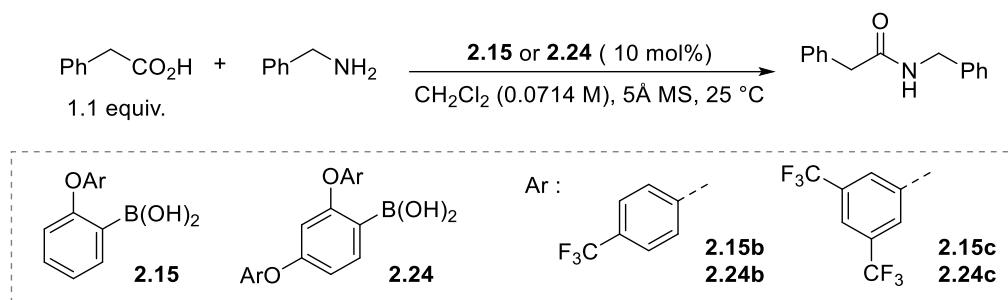
Nevertheless, this trend cannot be generalized because on some occasions the 2,4-disubstitution has led to a decline in activity. For instance, 2-fluorophenylboronic acid **2.33** provided *N*-benzylphenylacetamide in a higher 98% yield, compared to 63% yield with the 2,4-di(fluoro)phenylboronic acid **2.34** (Scheme 83).⁵⁴

D. G. Hall (2008)



Scheme 83

Accordingly, we examined the catalytic activity of the 2,4-disubstituted boronic acids **2.24** (Scheme 84). Firstly, using the boronic acid **2.24b**, 67% NMR yield was recorded in 6 h, compared to 95% NMR yield with **2.15b**. Therefore, **2.24b** displayed a considerably reduced catalytic efficiency compared to the *ortho*-substituted **2.15b**. Moreover, the catalyst **2.24c** provided a 73% NMR yield after 4 h and 86% after 6 h. The NMR yields of **2.24c** are comparable with those of **2.15c** where 71% NMR yield was achieved in 4 h and 78% in 6 h.



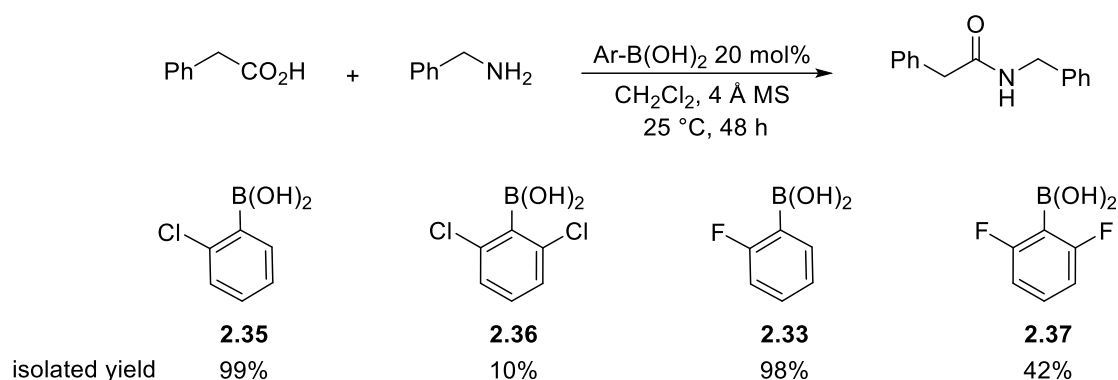
Scheme 84

Overall, in the case of biarylether-based boronic acids, the 2,4-disubstitution did not prove to be advantageous since lower catalytic efficiency was detected in the case of **2.24b**, and marginally higher performance was achieved by **2.24c**.

2.2.3.3 The case of 2,6-disubstituted derivatives

The reported boronic acids that are substituted on both *ortho* positions have displayed a diminished catalytic performance in all instances. To exemplify, Hall has reported that the 2-chlorophenylboronic acid **2.35** is an efficient catalyst at 25 °C, affording 99% yield of *N*-benzylphenylacetamide (Scheme 85).⁵⁴ On the other hand, the 2,6-dichlorobenzeneboronic acid **2.36** provided a noticeably lower 10% yield. Similarly, 2,6-difluorobenzeneboronic acid **2.37** furnished the amide in 42% yield versus 98% with **2.33** (Scheme 85).⁵⁴

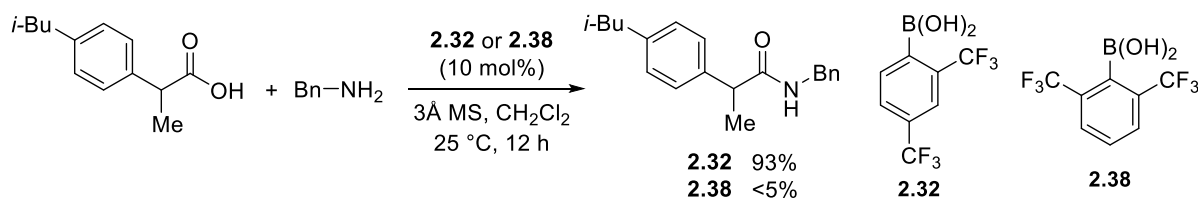
D. G. Hall (2008)



Scheme 85

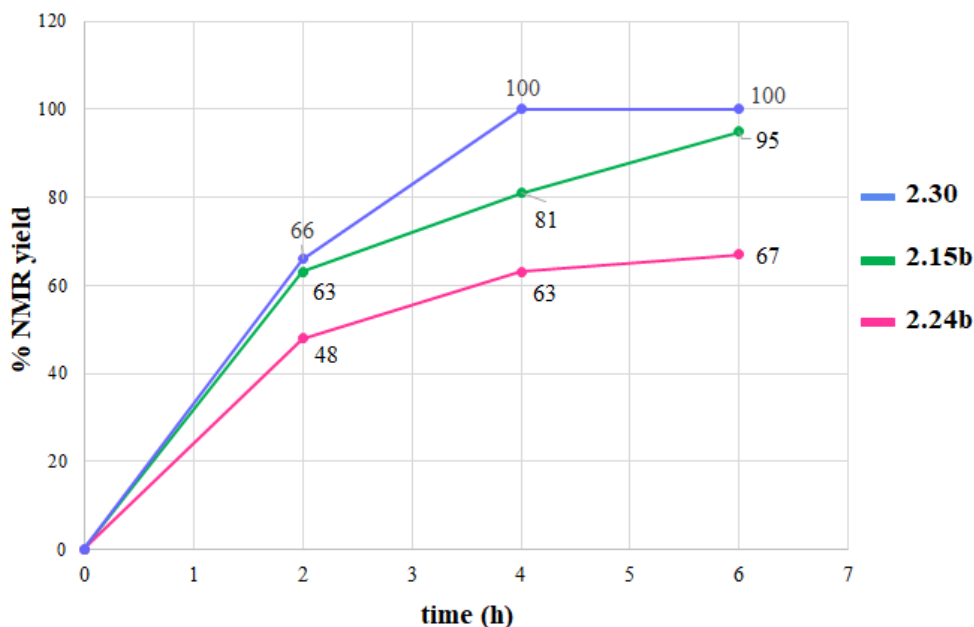
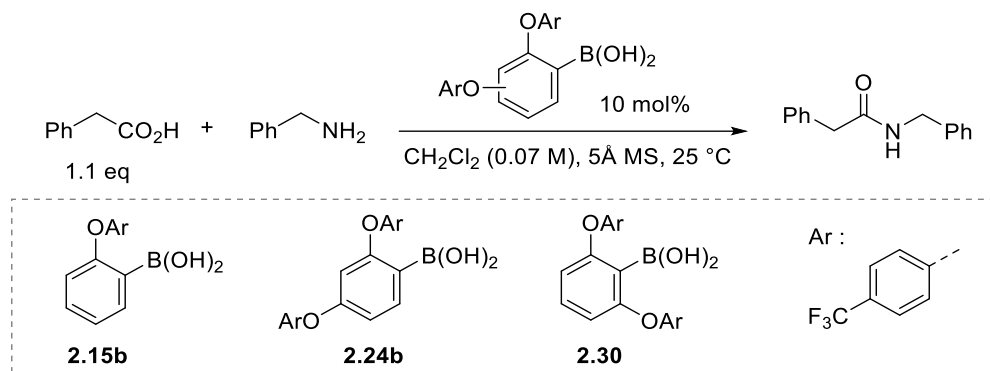
As an additional example, Ishihara has shown that catalyst **2.32** can achieve the coupling of racemic ibuprofen and benzylamine in 93% yield, which is substantially higher than that of its 2,6-regioisomer **2.38** that provided <5% yield (Scheme 86).⁶¹

K. Ishihara (2018)



Scheme 86

In this context, investigating the catalytic performance of 2,6-bis(aryloxy)phenyl boronic acid **2.30** does not appear to be promising. Unexpectedly, after 4 h, the boronic acid **2.30** afforded 100% NMR yield of *N*-benzylphenylacetamide (Scheme 87), which is higher than the NMR yields recorded for **2.15b** (81%) and **2.24b** (63%).

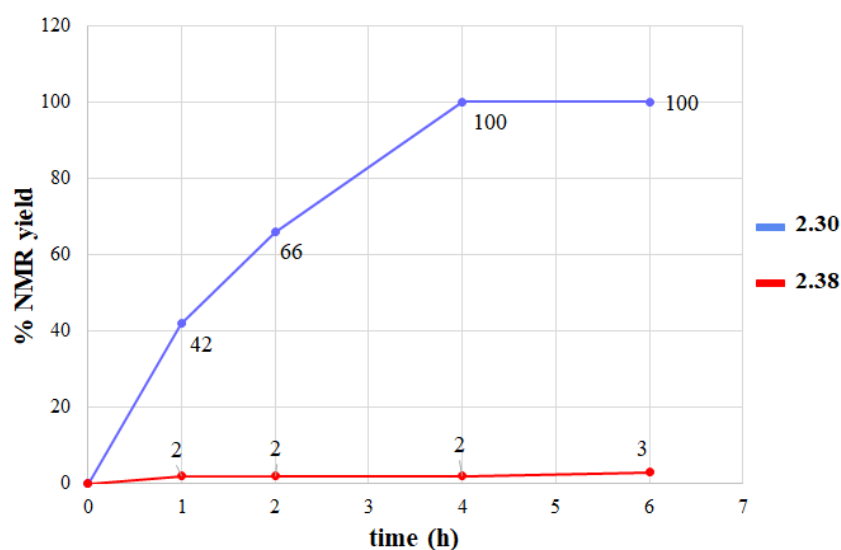
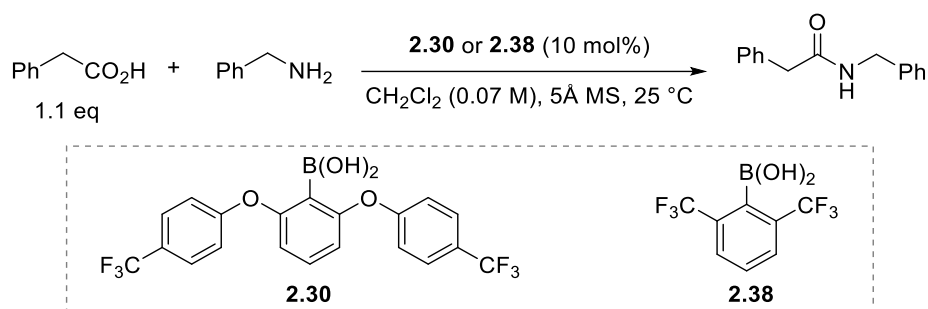


Scheme 87

As a result, **2.30** exhibited superior performance to **2.15b** and **2.24b** and it emerged to be the most catalytically active biarylether-based boronic acid.

The reported 2,6-disubstituted arylboronic acids **2.36**, **2.37**, and **2.38** were examined under slightly modified conditions than those used for catalyst **2.30**. To emphasize, boronic acid **2.38** was tested by Ishihara using 3 Å molecular sieves meanwhile, **2.30** was tested using 5 Å molecular sieves. Therefore, the kinetics of the amidation reaction was tested using **2.38** under

the same reaction conditions as **2.30**, with 5Å MS as a dehydrating agent (Scheme 88). In this case, **2.38** afforded 3% NMR yield after 6 h, which is consistent with the described data.⁶¹



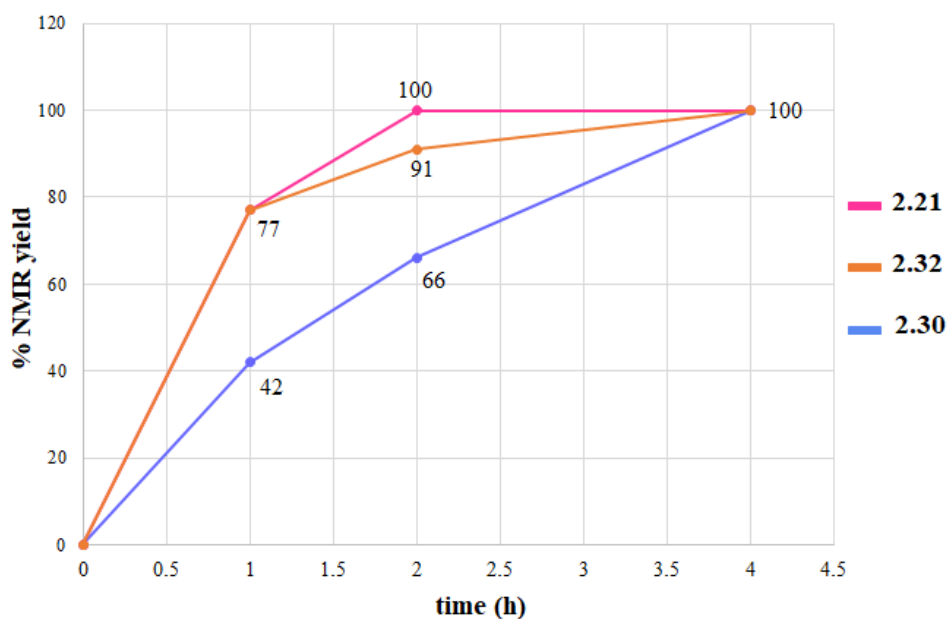
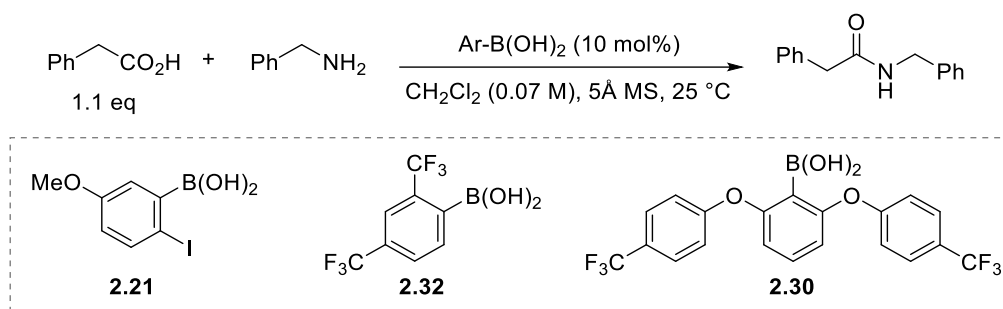
Scheme 88

As a consequence, the efficiency of catalyst **2.30** originates from its structural features where it possesses a specific combination of electronic and steric factors that contribute to its performance.

2.2.4 Comparative catalytic activity study with the state-of-the-art boronic acids

Furthermore, the catalytic efficiency of **2.30** was compared to that of two of the most efficient boronic acids for amide synthesis, 2-iodo-5-methoxyphenylboronic acid **2.21** and 2,4-trifluoromethylphenylboronic acid **2.32**, under our reaction conditions (5Å MS instead of 4Å or 3Å). After 2 h at 25 °C, the boronic acids **2.21** and **2.32** afforded 100% and 91% NMR yields, respectively (Scheme 89). However, the boronic acid **2.30** furnished a lower NMR yield of 66%

in 2 h. These results indicate that **2.30** did not compare favorably with the current state-of-the-art boronic acids.



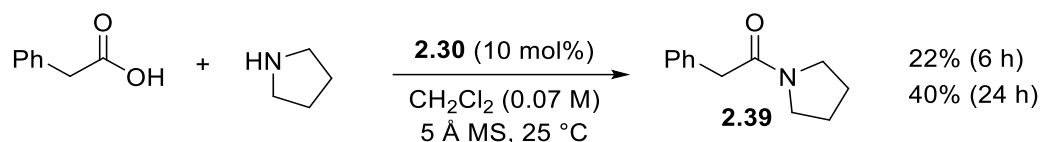
Scheme 89

Overall, the conducted kinetic studies on the biarylether-based boronic acids revealed that reducing the electron density on the aryloxy-ring provided a slight but measurable enhancement of the catalytic efficiency. Additionally, the performance of bis(aryloxy)benzeneboronic acids was affected not only by the alteration of electronic properties but also by the disubstitution pattern.

Even though the state-of-the-art boronic acids were not outperformed in this case, further studies were conducted using **2.30** to investigate the range of amide substrates that can be prepared using this catalyst.

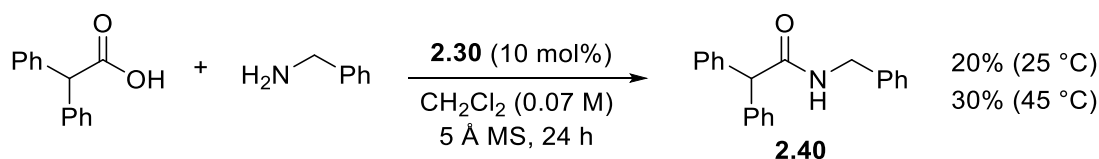
2.2.5 Examination of the scope of the reaction

First, the coupling of phenylacetic acid with pyrrolidine provided the amide **2.39** in 22% yield after 6 h (Scheme 90). The increase in the reaction time to 24 h provided a slightly improved 40% yield. These yields were significantly lower than the one reported for the same substrate with catalyst **2.21**, where **2.39** was isolated in 91% yield after 6 hours at 25 °C.⁵⁵



Scheme 90

Similarly, the amide **2.40**, resulting from the condensation of diphenylacetic acid with benzylamine, was obtained in a low yield of 20%, with a slight enhancement to 30% yield after gentle warming of the reaction mixture to 45 °C (Scheme 91).



Scheme 91

The dissatisfying yields of amides **2.39** and **2.40** showed that while boronic acid **2.30** demonstrated an interesting efficiency in the reaction of phenylacetic acid and benzylamine, its synthetic utility appeared to be limited.

2.2.6 Conclusion

While biarylether boronic acids were found to be insufficiently competent for catalyzing the room temperature direct amidation reaction, this study did highlight several interesting points. Evidently, there is a direct relationship between the aryl group's electron deficiency and the catalytic activity of the boronic acid. Additionally, it can be deduced that the catalytic performance of disubstituted arylboronic acids is influenced not only by the modification of the

electronic properties but also by the pattern of disubstitution. To exemplify, 2,4-di(aryloxy)phenylboronic acid **2.24b** exhibited lower catalytic activity compared to its 2-(aryloxy)phenylboronic acid derivative **2.15b**. Conversely, the 2,6-disubstituted boronic acid **2.30** displayed increased efficiency compared to its 2,4-regioisomer **2.24b** and its 2-(aryloxy) analog **2.15b**. The latter finding contradicts the established trend in the literature where di(*ortho*)-substitution diminishes the catalytic activity. It can be proposed that a specific combination of *ortho*-steric and *ortho*-electronic effects is required in the di(*ortho*)-substituted arylboronic acid for effective carboxylic acid activation.

2.3 Experimental Section

2.3.1 General Methods

Dry solvents (THF, dichloromethane, diethyl ether, acetonitrile, and toluene) were dried from a double-cartridge solvent purification system. Fluorobenzene and anhydrous DMF were purchased from Sigma-Aldrich. Analytical thin layer chromatographies were performed on silica gel 60 F254 plates. ^1H NMR spectra were recorded on BRUKER Avance III (500 MHz) and BRUKER NEO (600 MHz) spectrometers. ^1H NMR spectral data were recorded as follows: chemical shift in ppm from internal tetramethylsilane on the δ scale, multiplicity (s = singlet; br s = broad singlet; d = doublet; t = triplet; q = quartet; sept = septet; m = multiplet; dd = doublet of doublet; dt = doublet of triplet, etc.), coupling constant (Hz), and integration. The residual solvent protons (in ^1H NMR) were used as internal standards (CDCl_3 at 7.26 ppm, CD_3CN at 1.94 ppm, and $\text{DMSO-}d_6$ at 2.50 ppm). ^{13}C NMR spectra were taken on a BRUKER Avance III (125 MHz) and BRUKER NEO (150 MHz) spectrometers. Chemical shifts were recorded in ppm from the solvent resonance employed as the internal standard (CDCl_3 at 77.16 ppm, CD_3CN at 1.32 and 118.26 ppm, and $\text{DMSO-}d_6$ at 39.52 ppm). ^{11}B NMR spectra were taken on BRUKER Avance III (160 MHz) and BRUKER NEO (193 MHz) spectrometers. ^{19}F NMR spectra were taken on a BRUKER Avance III (470 MHz) and BRUKER NEO (565 MHz) spectrometers. Chemical shifts recorded in NMR experiments were performed in deuterated solvents (CDCl_3 with 0.04% TMS, CD_3CN , or $\text{DMSO-}d_6$) purchased from Eurisotop. In some mentioned cases, a drop of D_2O was added to minimize the formation of the corresponding boronic anhydrides. Because of their low intensity (resulting from quadrupolar coupling), ^{13}C signals arising from the quaternary carbon bearing the boronic acid group were not observed in most cases (unless otherwise mentioned).

Mass spectrometry analysis were conducted using a Q-ToF APCI analyzer equipped with an atmospheric pressure chemical ionization (APCI) source. The used instrument was the UPLC H-ClassXevo G2-XS QToF (WATERS) spectrometer. High-resolution mass spectra were recorded using either atmospheric solids analysis probe (ASAP) or electrospray ionization (ESI) techniques.

Infrared spectra were recorded using a PerkinElmer Spectrum Two Fourier Transform Infrared (FT-IR) Spectrometer equipped with a diamond attenuated total reflectance (ATR) accessory.

Measurements were conducted in the mid-infrared region (4000-450 cm^{-1}) with a resolution of 4 cm^{-1} . Each spectrum was obtained by accumulating 50 scans to improve the signal-to-noise ratio. Baseline correction was performed by acquiring a blank spectrum without the sample and subtracting it from the sample spectrum to remove any instrument or background noise. The IR spectra were reported as frequencies expressed in cm^{-1} .

5Å molecular sieves were purchased from Sigma-Aldrich (CAS 69912-79-4), reference 233676-500G (powder, undried). This reference is no longer available. 4Å molecular sieves were purchased from Sigma-Aldrich (CAS 70955-01-0), reference 688363-500G (powder, activated, -325 mesh particle size).

The molecular sieves were activated under a high vacuum (1 mbar) at 250 °C using a Kugelrohr distillation instrument for 2 hours. The oil bath technique was utilized to conduct reactions that necessitated heating.

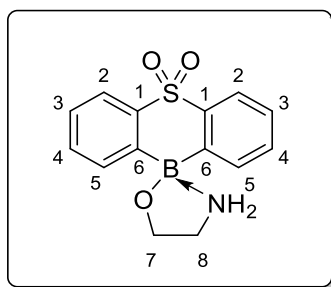
2.3.2 Synthetic protocol and characterization for sulfonylboraanthracene

Under an argon atmosphere, at -78 °C, *n*BuLi (6.16 mL, 2.5 M, 15.4 mmol, 2.2 equiv.) was added to a stirred solution of diphenyl sulfone (1.528 g, 7 mmol, 1 equiv.) in 14 mL of dry THF. This mixture was stirred at -78 °C for 3 h. Then, at -78 °C, B(OMe)₃ (3.12 mL, 2.9 g, 28 mmol, 4 equiv.) was added dropwise. The flask was left in the dry ice bath to allow a slow increase of temperature from -78 °C to 25 °C. Then, after an 18 h stirring at 25 °C, the reaction was quenched with an aqueous, saturated NH₄Cl solution (50 mL), and the aqueous layer was extracted with EtOAc (3×75 mL). The collected organic phases were washed with brine (50 mL), dried over anhydrous MgSO₄, filtered, and concentrated under reduced pressure to afford the crude residue (2.04 g, 8.35 mmol). The latter residue was dissolved in *i*PrOH (10 mL), after which ethanolamine (0.25 mL, 255 mg, 4.18 mmol, 0.5 equiv.) was added and the mixture was stirred at 25 °C for 18 h. Next, pentane (15 mL) was added until the complete precipitation of the aminoethanol complex. After filtration, the collected off-white solid was dried under vacuum to afford the pure aminoethanol complex **2.13** (986 mg, 3.46 mmol, **49% yield**).

Lastly, the pure borinate **2.13** was dissolved in acetone: methanol (1:1), then aqueous HCl (10 mL, 0.5 M) was added at 25 °C and the mixture was stirred for 5 mins, after which it was extracted with EtOAc (3×20 mL). The combined organic phases were washed with brine (10 mL) and dried over anhydrous MgSO₄, filtered, and concentrated under reduced pressure to

afford the crude residue containing **2.9** (935 mg, 3.83 mmol). The obtained residue was purified by recrystallization from EtOAc (5 mL) to afford the pure sulfonylboraanthracene **2.9** as a colorless amorphous powder (442 mg, 1.81 mmol, **52% yield**). The overall yield of synthesis of sulfonylboraanthracene **2.9** from diphenyl sulfone is **26% yield** (442 mg, 1.81 mmol).

2-(10H-Phenothiaborin-10-yloxy)ethanamine 5,5-dioxide **2.13**



$C_{14}H_{14}BNO_3S$, **M.W:** 287.14 g/mol. **M.p:** product degraded at 240 °C before melting.

1H NMR (500 MHz; $DMSO-d_6$): δ 7.85 (dd, $J = 7.6, 1.2$ Hz, 2H, H^5), 7.71 (dd, $J = 7.3, 1.3$ Hz, 2H, H^2), 7.48 (td, $J = 7.3, 1.2$ Hz, 2H, H^3), 7.39 (td, $J = 7.6, 1.3$ Hz, 2H, H^4), 6.24 (br t, $J = 6.1$ Hz, 2H, NH_2), 4.13 (t, $J = 6.1$ Hz, 2H, H^7), 2.90 (pentet, $J = 6.1$ Hz, 2H, H^8).

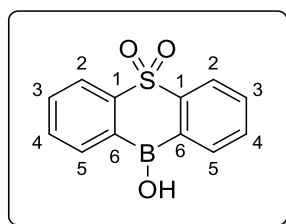
^{13}C NMR (125 MHz; $DMSO-d_6$) δ 143.4 (C_{qAr} , C^1), 131.7 (CH_{Ar} , C^5), 130.8 (CH_{Ar} , C^4), 126.5 (CH_{Ar} , C^3), 121.9 (CH_{Ar} , C^2), 64.9 (CH_2 , C^7), 42.3 (CH_2 , C^8). C^6 was not observed due to quadrupolar relaxation.

^{11}B NMR (160 MHz, $DMSO-d_6$) δ 0.16.

HRMS (ASAP-TOF) m/z : $[M + H]^+$ Calcd for $C_{14}H_{15}NO_3SB$: 288.0866 ; Found: 288.0864.

IR (neat)/ cm^{-1} ν_{max} 3500 (br), 3257, 3048, 1431, 1373, 1330, 1276, 1174, 1151, 1084, 735, 716.

10-hydroxy-10H-dibenzo[b,e][1,4]thiaborinine 5,5-dioxide **2.9**



C₁₂H₉BO₃S, **M.W:** 244.07 g/mol. **M.p:** 222-226 °C.

➤ In DMSO-*d*₆:

¹H NMR (600 MHz, DMSO-*d*₆): δ 7.95 (dd, *J* = 7.3, 1.3 Hz, 2H, H⁵), 7.87 (dd, *J* = 7.7, 1.1 Hz, 2H, H²), 7.52 (td, *J* = 7.3, 1.2 Hz, 2H, H⁴), 7.45 (td, *J* = 7.6, 1.3 Hz, 2H, H³).

¹³C NMR (150 MHz, DMSO-*d*₆) δ 147.5 (br C_{qAr}, C⁶), 143.7 (C_{qAr}, C¹), 131.8 (CH_{Ar}, C⁵), 130.9 (CH_{Ar}, C⁴), 127.5 (CH_{Ar}, C³), 122.0 (CH_{Ar}, C²).

¹¹B NMR (193 MHz, DMSO-*d*₆) δ 5.65 (DMSO complexes **2.9**).

➤ In CDCl₃:

¹H NMR (600 MHz, CDCl₃): δ 8.19 (d, *J* = 7.8 Hz, 2H, H²), 7.95 (d, *J* = 7.4 Hz, 2H, H⁵), 7.73 (td, *J* = 7.8, 1.1 Hz, 2H, H³), 7.63 (td, *J* = 7.4, 1.0 Hz, 2H, H⁴).

¹³C NMR (150 MHz, CDCl₃) δ 147.6 (C_{qAr}, C¹), 133.2 (CH_{Ar}, C²), 132.3 (CH_{Ar}, C³), 132.2 (CH_{Ar}, C⁴), 123.9 (CH_{Ar}, C⁵). C⁶ was not observed due to quadrupolar relaxation.

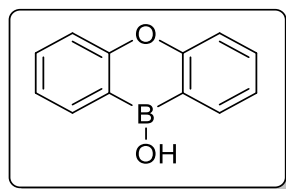
¹¹B NMR (192.5 MHz, CDCl₃) δ 38.5.

HRMS (ASAP-TOF) *m/z*: [M - H]⁻ Calcd for C₁₂H₈BO₃S: 243.0287; Found: 243.0290.

IR (neat)/cm⁻¹ *v*_{max} 3450, 2971, 1588, 1439, 1375, 1301, 1277, 1152, 1092, 865, 744.

2.3.3 Synthetic protocol and characterization of oxaboraanthracene

10H-Dibenzo[*b,e*][1,4]oxaborinin-10-ol **2.5**



To a solution of diphenyl ether (170 mg, 1 mmol, 1 equiv.) in 2 mL of dry THF, under argon, was added dropwise *n*BuLi in hexane (1.2 mL, 2.5 M, 3 mmol, 3 equiv.) at -78°C, and the mixture was stirred at 25°C for 3 h. The resulting solution was cooled to -78°C, then, B(OMe)₃ (0.33 mL, 312 mg, 3 mmol, 3 equiv.) was added dropwise. After a 16h stirring at 25 °C, aqueous saturated NH₄Cl (15 mL) was added and the aqueous layer was extracted with EtOAc (3×25

mL). The combined organic phase was dried over anhydrous MgSO_4 , filtered, and concentrated under reduced pressure to give the crude residue (391 mg). The residue was purified by flash silica gel column chromatography using Cy/EtOAc (80:20) to give the pure product as a colorless amorphous powder (127 mg, 0.65 mmol, **65% yield**). The ^1H , ^{13}C , and ^{11}B NMR spectra match the reported ones.^{101,105}

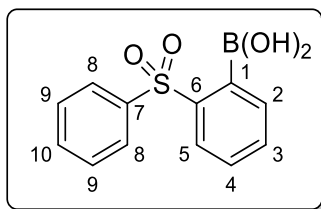
^1H NMR (600 MHz; $\text{DMSO}-d_6$): δ 9.87 (br s, 1H), 8.15 (dd, $J = 7.8, 1.5$ Hz, 2H), 7.67 (d, $J = 8.3, 7.3, 1.5$ Hz, 2H), 7.43 (d, $J = 8.3$ Hz, 2H), 7.28 (t, $J = 7.3, 1.0$ Hz, 2H).

^{13}C NMR (125 MHz; CDCl_3) δ 160.8, 133.3, 131.9, 122.2, 117.1. C-B was not observed due to quadrupolar relaxation.

^{11}B NMR (160 MHz, CDCl_3) δ 38.4.

2.3.4 Synthetic protocol and characterization of borinic acids' protodeborylation products

2-(phenylsulfonyl)benzeneboronic acid **2.14**



Diphenylsulfone (218.3 mg, 1 mmol, 1 equiv.) was dissolved in of dry THF (2 mL), under argon. At -78°C , $n\text{BuLi}$ (0.44 mL, 1.1 mmol, 2.5 M, 1.1 equiv.) was added dropwise, then, this mixture was stirred at 25°C for 3 h. Next, at -78°C , B(OMe)_3 (123 μL , 1.1 mmol, 1.1 equiv.) was added dropwise and the reaction mixture was stirred for 18 h at 25°C . The reaction was quenched with aqueous HCl (10 mL, 1 M), and the mixture was extracted with EtOAc (3×10 mL). The combined EtOAc phase was washed with brine (15 mL), dried over MgSO_4 , filtered and concentrated under reduced pressure to afford the crude residue (270 mg). The residue was purified by crystallization from toluene (5 mL) to afford the pure boronic acid **2.14** as a colorless amorphous powder (230 mg, 0.88 mmol, **88% yield**).

$\text{C}_{12}\text{H}_{11}\text{BO}_4\text{S}$, **M.W:** 262.09 g/mol. **M.p:** 133-137 $^\circ\text{C}$.

¹H NMR (600 MHz; DMSO-*d*₆): δ 8.24 (br s, 2H, OH), 8.08-8.04 (m, 2H, H⁸), 7.84 (d, *J* = 7.7 Hz, 1H, H²), 7.65 (tt, *J* = 7.4, 1.8 Hz, 1H, H¹⁰), 7.62-7.56 (m, 3H, H⁹⁺⁴), 7.51 (dd, *J* = 7.7, 1.2 Hz, 1H, H⁵), 7.49 (td, *J* = 7.7, 1.2 Hz, 1H, H³).

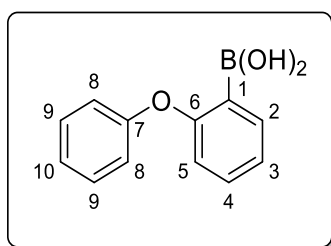
¹³C NMR (150 MHz; DMSO-*d*₆) δ 142.4 (C_{qAr}, C⁶), 141.6 (C_{qAr}, C⁷), 139.8 (br C_{qAr}, C¹), 133.4 (CH_{Ar}, C¹⁰), 132.4 (CH_{Ar}, C⁴), 132.1 (CH_{Ar}, C³), 129.3 (2CH_{Ar}, C⁹), 128.8 (CH_{Ar}, C⁵), 127.9 (CH_{Ar}, C²), 127.7 (2CH_{Ar}, C⁸).

¹¹B NMR (192.5 MHz, DMSO-*d*₆) δ 29.6 ppm.

HRMS (ASAP-TOF) *m/z*: [M - H]⁻ Calcd for C₁₂H₁₀BO₄S 261.0343; Found: 261.0352.

IR (neat)/cm⁻¹ v_{max} 3455, 3332, 3060, 1584, 1448, 1365, 1292, 1155, 1085, 842, 763.

[2-(phenoxy)phenyl]boronic acid **2.15a**



Diphenyl ether (0.47 mL, 511 mg, 3 mmol, 1 equiv.) was dissolved in dry THF (6 mL), under argon. At -78°C, *n*BuLi (1.32 mL, 3.3 mmol, 2.5 M, 1.1 equiv.) was added dropwise and the mixture was stirred at -78°C to 25 °C for 3 h. Then, at -78°C, B(OMe)₃ (0.37 mL, 3.3 mmol, 1.1 equiv.) was added and the mixture was stirred at 25 °C for 18 h. HCl (1 M, 10 mL) was added to quench the reaction and the mixture was extracted with Et₂O (3 × 20 mL). The Et₂O phases were collected, dried over MgSO₄, filtered, and concentrated under reduced pressure to afford the crude mixture (701 mg). The latter was purified by crystallization from Cy/EtOAc (90:10) to afford the pure boronic acid in the form of needle-like colorless crystals (340 mg, 1.59 mmol, **53% yield**).¹⁰⁸

R_f (Cy/EtOAc 90:10) = 0.25

C₁₂H₁₁BO₃, **M.W.**: 214.03 g/mol. **M.p.**: 110 °C.

¹H NMR (500 MHz, CDCl₃): δ 7.94 (dd, *J* = 7.4, 1.8 Hz, 1H, H²), 7.40 (t, *J* = 7.6 Hz, 2H, H⁹), 7.36 (ddd, *J* = 8.3, 7.4, 1.8 Hz, 1H, H⁴), 7.21 (t, *J* = 7.6 Hz, 1H, H¹⁰), 7.13 (t, *J* = 7.4 Hz, 1H, H³), 7.10 (d, *J* = 7.6 Hz, 2H, H⁸), 6.73 (d, *J* = 8.3 Hz, 1H, H⁵), 6.01 (br s, 2H, OH).

¹³C NMR (125 MHz, CDCl₃) δ 163.5 (C_{qAr}, C⁶), 155.6 (C_{qAr}, C⁷), 137.1 (CH_{Ar}, C²), 132.9 (CH_{Ar}, C⁴), 130.2 (2CH_{Ar}, C⁹), 124.9 (CH_{Ar}, C¹⁰), 123.2 (CH_{Ar}, C³), 120.4 (2CH_{Ar}, C⁸), 116.3 (CH_{Ar}, C⁵). C¹ was not observed due to quadrupolar relaxation.

¹¹B NMR (160.5 MHz, CDCl₃) δ 29.2 ppm.

HRMS (ASAP-TOF) *m/z*: [M - H]⁻ Calcd for C₁₂H₁₀BO₃ 213.0723; Found: 213.0727.

IR (neat)/cm⁻¹ *v*_{max} 3500, 3323, 1604, 1565, 1491, 1474, 1442, 1386, 1333, 1226, 1144, 1105, 1070, 1009, 872, 795, 749, 642.

2.3.5 Procedure for the protodeboronation experiments

2.3.5.1 Protodeboronation of sulfonylboraanthracene

At T = 25 °C: Under argon, sulfonylboraanthracene **2.9** (12.2 mg, 0.05 mmol, 1 equiv.), phenylacetic acid (68 mg, 0.5 mmol, 10 equiv.) and activated 5 Å molecular sieves (1 g) were introduced, then 7 mL of dry CH₂Cl₂ (0.07 M) were added. The mixture was vigorously stirred for 30 minutes at 25 °C, then, it was filtered through a celite pad (1 cm) and washed with CH₂Cl₂ (2×10 mL) and EtOAc (2×10 mL). The filtrate was concentrated under reduced pressure to afford a residue (82 mg) that was analyzed by ¹H and ¹¹B NMR in DMSO-*d*₆. In this case, no protodeboronation was observed (¹¹B NMR δ = 39 ppm). In ¹H NMR the signals of phenylacetic acid and **2.9** are overlapping, therefore, ¹¹B NMR results were considered.

At T = 65 °C: Under argon, sulfonylboraanthracene **2.9** (12.2 mg, 0.05 mmol, 1 equiv.), phenylacetic acid (68 mg, 0.5 mmol, 10 equiv.) and activated 5 Å molecular sieves (1 g) were introduced, then 7 mL of dry PhF (0.07 M) were added. The mixture was vigorously stirred for 3 h at 65 °C, then, it was filtered through a celite pad (1 cm) and washed with CH₂Cl₂ (2×10 mL) and EtOAc (2×10 mL). The filtrate was concentrated under reduced pressure to afford a residue (80 mg) that was analyzed by ¹H and ¹¹B NMR in DMSO-*d*₆. In this case, no protodeboronation was observed (¹¹B NMR δ = 39 ppm). In ¹H NMR the signals of phenylacetic acid and **2.9** are overlapping, therefore, ¹¹B NMR results were considered.

2.3.5.2 Protodeboronation of oxaboraanthracene

At T = 25 °C: Under argon, oxaboraanthracene **2.5** (10.8 mg, 0.055 mmol, 1 equiv.), phenylacetic acid (75 mg, 0.55 mmol, 10 equiv.) and activated 5 Å molecular sieves (1 g) were introduced, then 7 mL of dry CH₂Cl₂ (0.078 M) were added. The mixture was vigorously stirred for 30 minutes at 25 °C, then, it was filtered through a celite pad (1 cm) and washed with CH₂Cl₂ (2×10 mL) and EtOAc (2×10 mL). The filtrate was concentrated under reduced pressure to afford a residue (86 mg) that was analyzed by ¹H and ¹¹B NMR in DMSO-*d*₆. In this case, no protodeboronation was observed in ¹¹B NMR (δ = 38 ppm) (confirmed by ¹H NMR).

At T = 65 °C: Under argon, oxaboraanthracene **2.5** (24.5 mg, 0.125 mmol, 1 equiv.), phenylacetic acid (68 mg, 0.5 mmol, 4 equiv.) and activated 5 Å molecular sieves (1 g) were introduced, then 6.4 mL of PhF (0.078 M) were added. The mixture was vigorously stirred at 65 °C and 100 μL samples of the reaction mixture were taken at different times (t = 0.5, 4, 6 h) and analyzed by ¹H and ¹¹B NMR in DMSO-*d*₆. In this case, protodeboronation was observed (confirmed by ¹H and ¹¹B NMR) and it was completed after 6 hours at 65 °C.

2.3.6 Synthetic protocols and characterization for 2-(aryloxy)phenylboronic acids and their intermediates

2.3.6.1 General procedure A for the preparation of 2-aryloxyphenyl iodides

In an oven-dried flask, under argon, 2-iodophenol (1.3 equiv.), substituted-fluoro/bromo benzene (1 equiv.), K₂CO₃ (1.3 equiv.) and DMSO (technical grade; 1 M) were added. The mixture was stirred at 100 °C until the haloarene is consumed. After cooling down to 25 °C, aqueous NaOH (1 M) was added and the mixture was extracted with Et₂O (3×50 mL). The Et₂O phases were collected, washed with brine (30 mL), dried over MgSO₄, and concentrated under reduced pressure to afford the 2-aryloxyiodide.

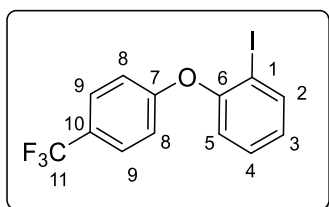
2.3.6.2 General procedure B for the preparation of 2-aryloxyphenyl boronic acids

2-Aryloxyphenyl iodide (1 equiv.) was dissolved in dry THF (2 mL), under argon. At -78 °C, B(O*i*Pr)₃ 98% (1.3 equiv.) was added and the mixture was stirred at this temperature for 20 mins. Next, *n*-BuLi (2 M, 1.3 equiv.) was added, and the mixture was stirred at -78 °C for 30 mins then, at 25 °C for 3 h. The reaction medium was quenched with aqueous HCl (1 M, 10

mL) at -40 °C then stirred at 25 °C for 15 mins. After, it was extracted with EtOAc (3×30 mL), and the organic phases were washed with brine (30 mL), dried over MgSO₄, and concentrated under reduced pressure to afford the crude residue. The latter was purified by flash silica-gel column chromatography using Cy/EtOAc 80:20 to afford the pure boronic acid as an amorphous powder.

2.3.6.3 Corresponding characterization data

1-Iodo-2-(4-(trifluoromethyl)phenoxy)benzene **2.17b**



The title compound was prepared from 2-iodophenol (981 mg, 4.46 mmol, 1.3 equiv.) and 4-fluorobenzotrifluoride (435 μ L, 563 mg, 3.43 mmol), and K₂CO₃ (616 mg, 4.46 mmol, 1.3 equiv.) in DMSO (3.4 mL, 1 M), after a 24 h reaction, according to general procedure **A**. After extractive workup, the pure **2.17b** was obtained as a pale-yellow oil (950 mg, 2.61 mmol, **76% yield**).

The ¹H and ¹³C NMR data match those reported in the literature.¹¹⁵

Rf (Cy 100%) = 0.35.

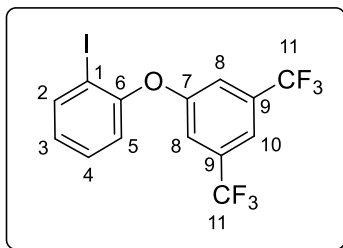
¹H NMR (500 MHz, CDCl₃): δ 7.90 (dd, $J = 7.9, 1.5$ Hz, 1H, H²), 7.59 (d, $J = 8.6$ Hz, 2H, H⁹), 7.36 (ddd, $J = 8.8, 7.9, 1.5$ Hz, 1H, H⁴), 7.04-6.94 (m, 4H, H^{8,3,5}).

¹³C NMR (125 MHz, CDCl₃) δ 160.0 (C_{qAr}, C⁷), 155.3 (C_{qAr}, C⁶), 140.4 (CH_{Ar}, C²), 130.1 (CH_{Ar}, C⁴), 127.3 (q, ³ $J_{C-F} = 3.8$ Hz, C⁹), 126.8 (CH_{Ar}, C^{3/5}), 125.3 (q, ² $J_{C-F} = 32.8$ Hz, C¹⁰), 124.3 (q, ¹ $J_{C-F} = 271.7$ Hz, C¹¹), 121.2 (CH_{Ar}, C^{3/5}), 117.5 (CH_{Ar}, C⁸), 89.9 (C_{qAr}, C¹).

¹⁹F NMR (470 MHz, CDCl₃) δ -61.7 ppm.

¹¹⁵ Lockner, J. W.; Dixon, D. D.; Risgaard, R.; Baran, P. S. *Org. Lett.* **2011**, *13*, 5628–5631.

1-Iodo-2-(3,5-bis(trifluoromethyl)phenoxy)benzene **2.17c**



The title compound was prepared from 2-iodophenol (1.144 g, 5.2 mmol, 1.3 equiv.) and 1,3-trifluoromethyl-5-fluorobenzene (928 mg, 4 mmol), and K_2CO_3 (719 mg, 5.2 mmol, 1.3 equiv.) in DMSO (4 mL, 1 M), after a 24 h reaction, according to general procedure **A**. After extractive workup, the pure **2.17c** was obtained as a yellow oil (1.71 g, 3.96 mmol, **99% yield**).

Rf (Cy/EtOAc 95:5) = 0.8

$C_{14}H_7F_6IO$, **M.W:** 432.10 g/mol.

1H NMR (600 MHz, $CDCl_3$): δ 7.93 (dd, $J = 7.7, 1.5$ Hz, 1H, H^2), 7.60 (s, 1H, H^{10}), 7.42 (ddd, $J = 8.0, 7.7, 1.5$ Hz, 1H, H^4), 7.33 (s, 2H, H^8), 7.03 (d, $J = 8.0$ Hz, 1H, H^5), 7.02 (td, $J = 7.7, 1.5$ Hz, 1H, H^3).

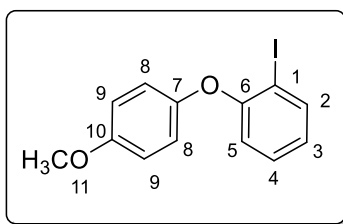
^{13}C NMR (150 MHz, $CDCl_3$) δ 158.2 (C_{qAr} , C^7), 154.6 (C_{qAr} , C^6), 140.7 (CH_{Ar} , C^2), 133.5 (q, $^2J_{C-F} = 33.8$ Hz, C^9), 130.4 (CH_{Ar} , C^4), 127.5 (CH_{Ar} , C^3), 123.0 (q, $^1J_{C-F} = 272.7$ Hz, C^{11}), 121.1 (CH_{Ar} , C^5), 117.5 (qq, $^3J_{C-F} = 3.8, 1.01$ Hz, C^8), 116.6 (septet, $^3J_{C-F} = 3.8$ Hz, C^{10}), 89.7 (C_{qAr} , C^1).

^{19}F NMR (565 MHz, $CDCl_3$) δ -63.0 ppm.

HRMS (ASAP-TOF) m/z: $[M + H]^+$ Calcd for $C_{14}H_7OF_6I$ 431.9446; Found: 431.9451.

IR (neat)/ cm^{-1} ν_{max} 3068, 1614, 1576, 1461, 1368, 1276, 1172, 1130, 1089, 1022, 951, 880, 766, 701.

1-Iodo-2-(4-(methoxy)phenoxy)benzene **2.17d**



The title compound was prepared from 2-iodophenol (1.0 g, 4.58 mmol, 1.3 equiv.), 4-bromoanisole (442 μ l, 658 mg, 3.52 mmol), and Cs_2CO_3 (1.49 g, 4.58 mmol, 1.3 equiv.) in DMSO (3.5 mL, 1 M), after a 48 h reaction, according to general procedure **A**. After extractive workup, the crude residue (1.50 g) was purified by flash silica gel column chromatography using Cy/EtOAc (95:5) to afford the pure **2.17e** as a colorless oil (850 mg, 2.60 mmol, **74% yield**).

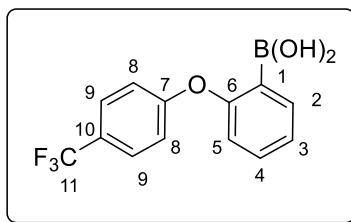
The ^1H and ^{13}C NMR data match those reported in the literature.¹¹⁶

Rf (Cy/EtOAc 95:5) = 0.35.

^1H NMR (500 MHz, CDCl_3): δ 7.80 (dd, $J = 7.8, 1.5$ Hz, 1H, H^2), 7.19 (ddd, $J = 8.2, 7.8, 1.5$ Hz, 1H, H^4), 6.93 (d, $J = 9.1$ Hz, 2H, H^8), 6.85 (d, $J = 9.1$ Hz, 2H, H^9), 6.77 (td, $J = 7.8, 1.3$ Hz, 1H, H^3), 6.73 (dd, $J = 8.2, 1.3$ Hz, 1H, H^5), 3.75 (s, 3H, H^{11}).

^{13}C NMR (125 MHz, CDCl_3) δ 157.6 (C_{qAr} , C^6), 156.1 (C_{qAr} , C^{10}), 150.0 (C_{qAr} , C^7), 139.8 (CH_{Ar} , C^2), 129.5 (CH_{Ar} , C^4), 124.6 (CH_{Ar} , C^3), 120.4 (2CH_{Ar} , C^8), 117.8 (CH_{Ar} , C^5), 115.0 (2CH_{Ar} , C^9), 87.8 (C_{qAr} , C^1), 55.7 (CH_3 , C^{11}).

(2-(4-(Trifluoromethyl)phenoxy)phenyl)boronic acid **2.15b**



The title compound was prepared from **2.17b** (910 mg, 2.5 mmol), $n\text{BuLi}$ (1.63 mL, 2 M, 3.25 mmol, 1.3 equiv.), and $\text{B}(\text{O}i\text{Pr})_3$ 98% (766 μ L, 624 mg, 3.316 mmol, 1.3 equiv.) in THF (5

¹¹⁶ Tietze, L. F.; Hungerland, T.; Diefert, A.; Objartel, I.; Stalke, D. *Chem. Eur. J.* **2012**, *18*, 3286–3291.

mL, 0.5 M), using general procedure **B**. After extractive workup, the crude residue (772 mg) was purified by flash silica gel column chromatography using Cy/EtOAc (80:20) to afford the pure boronic acid as a beige amorphous powder (233 mg, 0.83 mmol, **33% yield**).

The ^1H and ^{13}C NMR data match those reported in the literature.¹⁴

$\text{C}_{13}\text{H}_{10}\text{BF}_3\text{O}_3$, **M.W:** 282.03 g/mol. **M.p:** 104-107 °C.

Rf (Cy/EtOAc 80:20) = 0.25

^1H NMR (600 MHz, CDCl_3): δ 7.96 (dd, $J = 7.4, 1.8$ Hz, 1H, H^2), 7.64 (d, $J = 8.4$ Hz, 2H, H^9), 7.42 (ddd, $J = 8.3, 7.4, 1.8$ Hz, 1H, H^4), 7.21 (td, $J = 7.4, 0.7$ Hz, 1H, H^3), 7.15 (d, $J = 8.4$ Hz, 2H, H^8), 6.80 (dd, $J = 8.3, 0.7$ Hz, 1H, H^5), 5.54 (br s, 2H, OH).

^{13}C NMR (150 MHz, CDCl_3) δ 162.0 (C_{qAr} , C^6), 158.9 (q, $^5J_{\text{C-F}} = 1.3$ Hz, C^7), 137.4 (CH_{Ar} , C^2), 133.2 (CH_{Ar} , C^4), 127.6 (q, $^3J_{\text{C-F}} = 3.7$ Hz, C^9), 126.7 (q, $^2J_{\text{C-F}} = 32.9$ Hz, C^{10}), 124.4 (CH_{Ar} , C^3), 124.1 (q, $^1J_{\text{C-F}} = 271.7$ Hz, C^{11}), 119.7 (2CH_{Ar} , C^8), 117.6 (CH_{Ar} , C^5). C^1 was not observed due to quadrupolar relaxation.

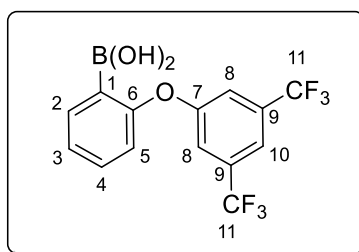
^{19}F NMR (565 MHz, CDCl_3) δ -62.0 ppm.

^{11}B NMR (192.5 MHz, CDCl_3) δ 28.9 ppm.

HRMS (ASAP-TOF) m/z : $[\text{M} - \text{H}]^-$ Calcd for $\text{C}_{13}\text{H}_9\text{BF}_3\text{O}_3$ 281.0597; Found: 281.0598.

IR (neat)/ cm^{-1} ν_{max} 3529 (br), 3376 (br), 1605, 1573, 1478, 1448, 1414, 1322, 1227, 1157, 1063, 855, 746.

(2-(3,5-bis(trifluoromethyl)phenoxy)phenyl)boronic acid **2.15c**



The title compound was prepared from **2.17c** (230 mg, 0.532 mmol), *n*BuLi (0.35 mL, 2 M, 0.69 mmol, 1.3 equiv.), and B(O*i*Pr)₃ 98% (163 μL , 132.8 mg, 0.706 mmol, 1.3 equiv.) in THF (2 mL, 0.27 M), using general procedure **B**. After extractive workup, the crude residue (182

mg) was purified by flash silica gel column chromatography using Cy/EtOAc (80:20) to afford the pure boronic acid as a colorless amorphous powder (65 mg, 0.186 mmol, **35% yield**).

R_f (Cy/EtOAc 80:20) = 0.35

C₁₄H₉BF₆O₃, **M.W:** 350.02 g/mol. **M.p:** 99-103 °C.

(one drop of D₂O is added to the NMR tube to shift the equilibrium of the boronic + boroxine into boronic acid only)

¹H NMR (600 MHz; CDCl₃ + D₂O): δ 7.99 (dd, *J* = 7.5, 1.7 Hz, 1H, H²), 7.68 (s, 1H, H¹⁰), 7.50 (s, 2H, H⁸), 7.46 (ddd, *J* = 8.3, 7.5, 1.7 Hz, 1H, H⁴), 7.27 (t, *J* = 7.5 Hz, 1H, H³), 6.78 (d, *J* = 8.3 Hz, 1H, H⁵).

Note: in CDCl₃ the signal of B-(OH)₂ is at 5.28 ppm (br s, 2H, OH)

¹³C NMR (150 MHz; CDCl₃+ D₂O) δ 161.4 (C_{qAr}, C⁶), 157.2 (C_{qAr}, C⁷), 137.7 (CH_{Ar}, C²), 133.8 (q, ²*J*_{C-F} = 34.0 Hz, C⁹), 133.5 (CH_{Ar}, C⁴), 125.0 (CH_{Ar}, C³), 122.8 (q, ¹*J*_{C-F} = 272.7 Hz, C¹¹), 119.8 (qq, *J*_{C-F} = 3.8 Hz, 1.0 Hz, C⁸), 118.1 (septet, ³*J*_{C-F} = 3.8 Hz, C¹⁰), 117.3 (CH_{Ar}, C⁵). C¹ was not observed due to quadrupolar relaxation.

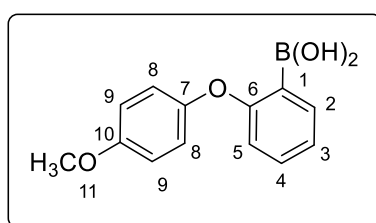
¹⁹F NMR (565 MHz, CDCl₃ + D₂O) δ -63.0 ppm.

¹¹B NMR (192.5 MHz, CDCl₃ + D₂O) δ 28.8 ppm.

HRMS (ESI-TOF) *m/z*: [M - H]⁻ Calcd for C₁₄H₈BO₃F₆ 349.0471; Found: 349.0477.

IR (neat)/cm⁻¹ *v*_{max} 3324 (br), 1606, 1570, 1459, 1446, 1370, 1275, 1227, 1185, 1123, 1017, 950, 879, 777.

(2-(4-(methoxy)phenoxy)phenyl)boronic acid **2.15d**



The title compound was prepared from **2.17d** (815 mg, 2.5 mmol), *n*BuLi (1.63 mL, 2 M, 3.25 mmol, 1.3 equiv.), and B(O*i*Pr)₃ 98% (766 μL, 624 mg, 3.316 mmol, 1.3 equiv.) in THF (5

mL, 0.5 M), using general procedure **B**. After extractive workup, the crude residue (690 mg) was purified by flash silica gel column chromatography using Cy/EtOAc (80:20) to afford the pure boronic acid as a beige amorphous powder (232 mg, 0.95 mmol, **38% yield**).

$C_{13}H_{13}BO_4$, **M.W**: 244.05 g/mol. **M.p**: 100-105 °C.

Rf (Cy/EtOAc 80:20) = 0.2

1H NMR (600 MHz; $CDCl_3$): δ 7.91 (dd, $J = 7.4, 1.8$ Hz, 1H, H^2), 7.32 (ddd, $J = 8.5, 7.4, 1.8$ Hz, 1H, H^4), 7.09 (td, $J = 7.4, 0.7$ Hz, 1H, H^3), 7.04 (d, $J = 9.0$ Hz, 2H, H^8), 6.92 (d, $J = 9.0$ Hz, 2H, H^9), 6.65 (d, $J = 8.5$ Hz, 1H, H^5), 6.06 (br s, 2H, OH), 3.83 (s, 3H, H^{11}).

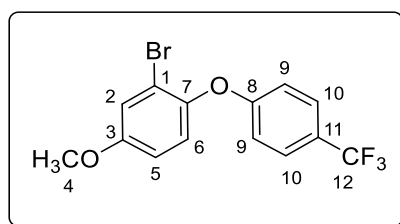
^{13}C NMR (150 MHz; $CDCl_3$) δ 164.5 (C_{qAr} , C^6), 156.9 (C_{qAr} , C^{10}), 148.5 (C_{qAr} , C^7), 137.0 (CH_{Ar} , C^2), 132.9 (CH_{Ar} , C^4), 122.7 (CH_{Ar} , C^3), 122.0 (2 CH_{Ar} , C^8), 115.3 (2 CH_{Ar} , C^9), 115.1 (CH_{Ar} , C^5), 55.8 (CH_3 , C^{11}). C^1 was not observed due to quadrupolar relaxation.

^{11}B NMR (192.5 MHz, $CDCl_3$) δ 29.18 ppm.

HRMS (ASAP-TOF) m/z: $[M - H]^-$ Calcd for $C_{13}H_{12}BO_4$ 243.0829; Found: 243.0830.

IR (neat)/ cm^{-1} ν_{max} 3472 (br), 3360 (br), 1602, 1574, 1504, 1477, 1443, 1401, 1336, 1207, 1157, 1083, 1032, 839, 747.

1-bromo-2-(4-(trifluoromethyl)phenoxy)-5-methoxybenzene **2.19**



The title compound was prepared from 2-bromo-4-methoxyphenol (609 mg, 3 mmol, 1 equiv.), 4-fluorobenzotrifluoride (985 mg, 6 mmol, 2 equiv.), Cs_2CO_3 (1.95 g, 6 mmol, 2 equiv.) and DMSO (5 mL) after a 16 h reaction, using general procedure **A**. After extractive workup, the pure product was obtained as a pale-yellow oil (890 mg, 2.56 mmol, **86% yield**).

Rf (Cy/EtOAc 90:10) = 0.55

$C_{14}H_{10}BrF_3O_2$, **M.W**: 347.13 g/mol.

¹H NMR (500 MHz; CDCl₃): δ 7.54 (d, *J* = 8.5 Hz, 2H, H¹⁰), 7.19 (d, *J* = 3.0 Hz, 1H, H²), 7.04 (d, *J* = 8.9 Hz, 1H, H⁶), 6.92 (d, *J* = 8.5 Hz, 2H, H⁹), 6.89 (dd, *J* = 8.9, 3.0 Hz, 1H, H⁵), 3.82 (s, 3H, H⁴).

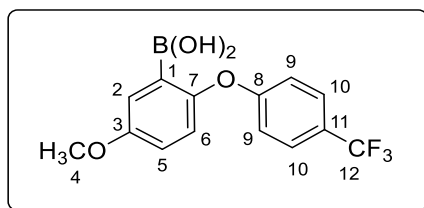
¹³C NMR (125 MHz; CDCl₃) δ 160.8 (C_{qAr}, C⁸), 157.6 (C_{qAr}, C³), 145.5 (C_{qAr}, C⁷), 127.2 (q, ³*J*_{C-F} = 3.8 Hz, C¹⁰), 124.6 (q, ²*J*_{C-F} = 32.9 Hz, C¹¹), 124.3 (q, ¹*J*_{C-F} = 271.0 Hz, C¹²), 123.5 (CH_{Ar}, C⁶), 118.9 (CH_{Ar}, C²), 116.7 (C_{qAr}, C¹), 116.3 (2CH_{Ar}, C⁹), 115.0 (CH_{Ar}, C⁵), 56.0 (CH₃, C⁴).

¹⁹F NMR (470 MHz, CDCl₃) δ -61.66 ppm.

HRMS (ASAP-TOF) *m/z*: [M + H]⁺ Calcd for C₁₄H₁₀BrF₃O₂ 345.9816; Found: 345.9820.

IR (neat)/cm⁻¹ *v*_{max} 1615, 1597, 1579, 1486, 1440, 1324, 1254, 1220, 1162, 1118, 1065, 1040, 945, 838, 778.

(2-(4-(Trifluoromethyl)phenoxy)-5-methoxy)phenylboronic acid **2.20**



The title compound was prepared from **2.19** (500 mg, 1.44 mmol, 1 equiv.), *n*BuLi (0.94 mL, 2 M, 1.87 mmol, 1.3 equiv.) and B(O*i*Pr)₃ 98% (441 μL, 362 mg, 1.91 mmol, 1.3 equiv.) in THF (3 mL, 0.5 M), using general procedure **B**. After extractive workup, the crude residue (512 mg) was purified by flash silica gel column chromatography using Cy/EtOAc (70:30) to afford the pure boronic acid as a colorless amorphous powder (163 mg, 0.52 mmol, **36% yield**).

R_f (Cy/EtOAc 70:30) = 0.3

C₁₄H₁₂BF₃O₄, **M.W**: 312.05 g/mol. **M.p**: 89-92 °C.

¹H NMR (600 MHz; CDCl₃): δ 7.60 (d, *J* = 8.6 Hz, 2H, H¹⁰), 7.44 (d, *J* = 3.2 Hz, 1H, H²), 7.09 (d, *J* = 8.6 Hz, 2H, H⁹), 6.98 (dd, *J* = 8.9, 3.2 Hz, 1H, H⁵), 6.80 (d, *J* = 8.9 Hz, 1H, H⁶), 5.57 (br s, 2H, OH), 3.85 (s, 3H, H⁴).

¹³C NMR (150 MHz; CDCl₃) δ 159.9 (q, ⁵J_{C-F} = 1.3 Hz, C⁸), 156.3 (Cq_{Ar}, C³), 155.0 (Cq_{Ar}, C⁷), 127.5 (q, ³J_{C-F} = 3.8 Hz, C¹⁰), 126.0 (q, ²J_{C-F} = 32.9 Hz, C¹¹), 124.1 (q, ¹J_{C-F} = 271.5 Hz, C¹²), 120.2 (CH_{Ar}, C²), 120.0 (CH_{Ar}, C⁶), 119.6 (CH_{Ar}, C⁵), 118.5 (2CH_{Ar}, C⁹), 55.9 (CH₃, C⁴). C¹ was not observed due to quadrupolar relaxation.

¹⁹F NMR (565 MHz, CDCl₃) δ -61.91 ppm.

¹¹B NMR (192.5 MHz, CDCl₃) δ 28.79 ppm.

HRMS (ESI-TOF) m/z: [M - H]⁻ Calcd for C₁₄H₁₁BO₄F₃ 311.0702; Found: 311.0712.

IR (neat)/cm⁻¹ ν_{max} 3395 (br), 3309 (br), 1613, 1575, 1482, 1441, 1411, 1322, 1223, 1159, 1122, 1105, 1064, 837, 723.

2.3.7 Synthetic protocols and characterization for [2,4-bis(aryloxy)phenyl]boronic acids and their intermediates

2.3.7.1 General procedure C for the preparation of 2,4-aryloxybenzenes

In a pressure-sealed flask, resorcinol (1 equiv.), fluorobenzene derivative **2.16** (2.5 - 3 equiv.), Cs₂CO₃ (2.5 equiv.) or K₂CO₃ (finely ground; 3 equiv.) and DMSO (5 mL) were added. The mixture was stirred at 100 °C until reaction completion. After cooling down to 25 °C, NaOH (1.25 M, 30 mL) was added and the mixture was extracted with Et₂O (3×50 mL). The Et₂O phases were collected, washed with brine (15 mL), dried over MgSO₄, and concentrated under reduced pressure to afford the pure 2,4-aryloxybenzenes.

2.3.7.2 General procedure D for the preparation of 2,4-aryloxybenzene bromides

To a solution of 1,3-diaryloxybenzene **2.22** (1 equiv.) in MeOH (10 mL), was added NH₄Br (1.5 equiv.) and oxone® (1.5 equiv.). The resulting mixture was stirred at 25 °C until reaction completion, then MeOH was evaporated and aqueous saturated Na₂SO₃ (25 mL) and EtOAc (50 mL) were added. The organic phase was collected by extraction with EtOAc (3×50 mL) and the combined organic phases were washed with brine (50 mL), dried over MgSO₄, and concentrated under reduced pressure to afford the pure 2,4-aryloxybenzene bromides.

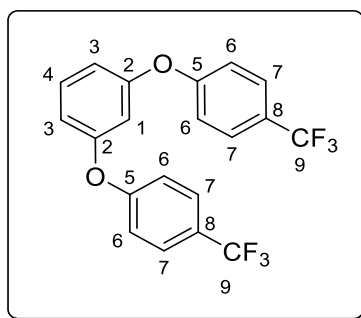
2.3.7.3 General procedure E for the preparation of 2,4-aryloxybenzene boronic acids

In an oven-dried flask, under argon, 2,4-diaryloxyphenyl bromide (1 equiv.) was dissolved in dry THF (5 mL, 0.18 M). At -78 °C, B(OiPr)₃ (1.3 equiv.) was added, and the mixture was

stirred at -78 °C for 20 mins. *n*BuLi (1.81 M, 1.3 equiv.) was then added dropwise and the mixture was stirred at -78 °C for 30 mins, then at 25 °C for 3 h. After that, the mixture was quenched with aqueous HCl (1 M, 10 mL) at -40 °C where it was left to stir at 25 °C for 30 mins. Next, it was extracted with EtOAc (3×30 mL), and the combined organic phases were washed with brine (20 mL), dried over MgSO₄, and concentrated under reduced pressure to afford the crude residue. The latter was purified by flash silica-gel column chromatography using Cy/EtOAc (80:20) to afford the pure boronic acid.

2.3.7.4 Corresponding characterization data

1,3-Bis[4-(trifluoromethyl)phenoxy]benzene **2.22b**



The title compound was prepared from resorcinol (450 mg, 4 mmol), 4-fluorobenzotrifluoride **2.16b** (1.641 g, 10 mmol, 2.5 equiv.), and Cs₂CO₃ (3.26 g, 10 mmol, 2.5 equiv.) in DMSO (5 mL), after a 16 h reaction, using general procedure **C**. After extraction, the pure **2.22b** was obtained as an orange oil (1.33 g, 3.34 mmol, **84% yield**).

R_f (Cy/EtOAc 95:5) = 0.6

C₂₀H₁₂F₆O₂, **M.W.**: 398.30 g/mol.

¹H NMR (500 MHz; CDCl₃) δ 7.60 (d, *J* = 8.45 Hz, 4H, H⁷), 7.37 (t, *J* = 8.15 Hz, 1H, H⁴), 7.09 (d, *J* = 8.45 Hz, 4H, H⁶), 6.86 (dd, *J* = 8.19, 2.36 Hz, 2H, H³), 6.76 (t, *J* = 2.30 Hz, 1H, H¹).

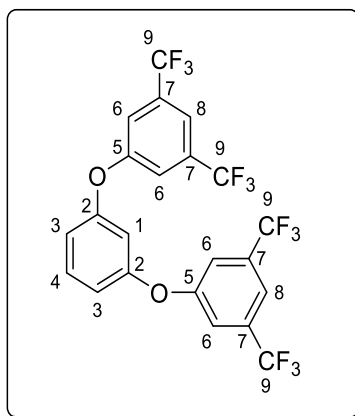
¹³C NMR (125 MHz; CDCl₃) δ 159.8 (q, ⁵*J*_{C-F} = 1.1 Hz, Cq_{Ar}, C⁵), 157.5 (2Cq_{Ar}, C²), 131.2 (CH_{Ar}, C⁴), 127.4 (q, ³*J*_{C-F} = 3.8 Hz, C⁷), 125.6 (q, ²*J*_{C-F} = 32.9 Hz, C⁸), 124.2 (q, ¹*J*_{C-F} = 271.6 Hz, C⁹), 118.5 (4CH_{Ar}, C⁶), 115.4 (2CH_{Ar}, C³), 111.3 (CH_{Ar}, C¹).

¹⁹F NMR (470 MHz, CDCl₃) δ -61.8 ppm.

HRMS (ASAP-TOF) m/z: [M + H]⁺ Calcd for C₂₀H₁₂O₂F₆ 398.0741; Found: 398.0743.

IR (neat)/cm⁻¹ ν_{\max} 1618, 1592, 1512, 1479, 1320, 1264, 1227, 1161, 1117, 1103, 1063, 1013, 965, 838, 784.

1,3-Bis[3,5-di(trifluoromethyl)phenoxy]benzene **2.22c**



The title compound was prepared from resorcinol (440 mg, 4 mmol, 1 equiv.), 1,3-trifluoromethyl-5-fluorobenzene **2.16c** (1.658 g, 12 mmol, 3 equiv.), and K₂CO₃ (finely ground; 1.658 g, 12 mmol, 3 equiv.) in DMSO (5 mL), after a 60 h reaction, using general procedure C. After extraction, the pure **2.22c** was obtained as an orange powder (2.055 g, 3.85 mmol, **96% yield**).

R_f (Cy/EtOAc 90:10) = 0.7

C₂₂H₁₀F₁₂O₂, **M.W.**: 534.30 g/mol. **M.p.**: 55-57 °C.

¹H NMR (600 MHz; CDCl₃): δ 7.62 (s, 2H, H⁸), 7.46 (t, J = 8.2 Hz, 1H, H⁴), 7.43 (s, 4H, H⁶), 6.91 (dd, J = 8.2, 2.3 Hz, 2H, H³), 6.77 (t, J = 2.3 Hz, 1H, H¹).

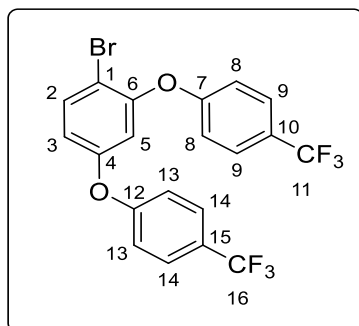
¹³C NMR (150 MHz; CDCl₃) δ 157.9 (2C_{qAr}, C⁵), 157.0 (2C_{qAr}, C²), 133.6 (q, ² J_{C-F} = 33.9 Hz, C⁷), 131.9 (CH_{Ar}, C⁴), 122.9 (q, ¹ J_{C-F} = 272.6 Hz, C⁹), 118.7 (q, ³ J_{C-F} = 3.7 Hz, C⁶), 117.2 (septet, ³ J_{C-F} = 3.9 Hz, C⁸), 115.9 (2CH_{Ar}, C³), 111.3 (CH_{Ar}, C¹).

¹⁹F NMR (565 MHz, CDCl₃) δ -63.1 ppm.

HRMS (ASAP-TOF) m/z: [M + H]⁺ Calcd for C₂₂H₁₀O₂F₁₂ 534.0489; Found: 534.0486.

IR (neat)/cm⁻¹ v_{max} 1586, 1482, 1462, 1367, 1278, 1228, 1189, 1139, 1123, 1105, 950, 867, 760, 680.

1-bromo-2,4-Bis[4-(trifluoromethyl)phenoxy]benzene 2.23b



The title compound was prepared from 1,3-diaryloxybenzene **2.22b** (833 mg, 2.09 mmol, 1 equiv.), NH₄Br (307 mg, 3.135 mmol, 1.5 equiv.) and Oxone® (1.928 g, 3.135 mmol, 1.5 equiv.) in MeOH (10 mL), after a 3 h reaction, using general procedure **D**. After extraction, the pure product was obtained as an orange amorphous solid (990 mg, 2.08 mmol, >99% yield).

R_f (Cy/EtOAc 95:5) = 0.5

C₂₀H₁₁BrF₆O₂, M.W: 477.20 g/mol. M.p: 70-72 °C.

¹H NMR (600 MHz; CDCl₃): δ 7.64 (d, *J* = 8.7 Hz, 1H, H²), 7.60 (d, *J* = 8.6 Hz, 4H, H⁹⁺¹⁴), 7.07 (d, *J* = 8.6 Hz, 2H, H⁸), 7.02 (d, *J* = 8.6 Hz, 2H, H¹³), 6.80 (dd, *J* = 8.7, 2.7 Hz, 1H, H³), 6.76 (d, *J* = 2.7 Hz, 1H, H⁵).

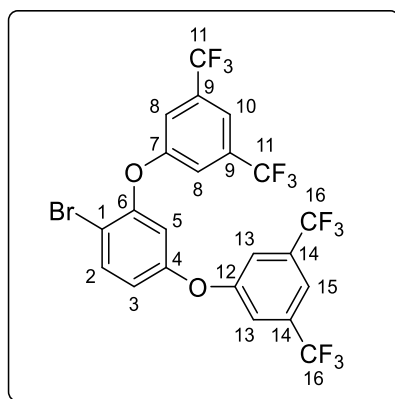
¹³C NMR (150 MHz; CDCl₃) δ 159.4 (q, ⁵*J*_{C-F} = 1.1 Hz, Cq_{Ar}, C⁷), 159.3 (q, ⁵*J*_{C-F} = 1.1 Hz, Cq_{Ar}, C¹²), 156.7 (Cq_{Ar}, C⁴), 153.5 (Cq_{Ar}, C⁶), 134.9 (CH_{Ar}, C²), 127.6 (q, ³*J*_{C-F} = 3.7 Hz, C¹⁴), 127.5 (q, ³*J*_{C-F} = 3.7 Hz, C⁹), 126.1 (q, ²*J*_{C-F} = 33.0 Hz, C¹⁰), 125.7 (q, ²*J*_{C-F} = 33.0 Hz, C¹⁵), 124.2 (q, ¹*J*_{C-F} = 272.0 Hz, C¹¹), 124.1 (q, ¹*J*_{C-F} = 272.0 Hz, C¹⁶), 118.6 (2CH_{Ar}, C⁸), 117.5 (2CH_{Ar}, C¹³), 117.2 (CH_{Ar}, C³), 113.2 (CH_{Ar}, C⁵), 110.3 (Cq_{Ar}, C¹).

¹⁹F NMR (565 MHz, CDCl₃) δ -61.83, -61.90 ppm.

HRMS (ASAP-TOF) m/z: [M + H]⁺ Calcd for C₂₀H₁₁O₂F₆Br 475.9847; Found: 475.9853.

IR (neat)/cm⁻¹ v_{max} 1616, 1585, 1511, 1471, 1408, 1321, 1277, 1224, 1161, 1118, 1104, 1064, 1039, 1013, 975, 836, 727.

1-bromo-2,4-Bis[3,5-di(trifluoromethyl)phenoxy]benzene **2.23c**



The title compound was prepared from 1,3-diaryloxybenzene **2.22c** (534 mg, 1 mmol, 1 equiv.), NH₄Br (147 mg, 1.5 mmol, 1.5 equiv.) and Oxone® (922 mg, 1.5 mmol, 1.5 equiv.) in MeOH (10 mL), after a 16 h reaction, using general procedure **D**. After extraction, the pure product was obtained as an orange amorphous solid (590 mg, 0.96 mmol, **96% yield**).

Rf (Cy/EtOAc 90:10) = 0.5

C₂₂H₉BrF₁₂O₂, **M.W**: 613.20 g/mol. **M.p**: 60-62 °C.

¹H NMR (600 MHz; CDCl₃): δ 7.73 (d, *J* = 8.8 Hz, 1H, H²), 7.63 (s, 1H, H¹⁰), 7.62 (s, 1H, H¹⁵), 7.42 (s, 2H, H⁸), 7.35 (s, 2H, H¹³), 6.87 (dd, *J* = 8.8, 2.7 Hz, 1H, H³), 6.78 (d, *J* = 2.7 Hz, 1H, H⁵).

¹³C NMR (150 MHz; CDCl₃) δ 157.53 (Cq_{Ar}, C^{7/12}), 157.52 (Cq_{Ar}, C^{7/12}), 156.1 (Cq_{Ar}, C⁴), 153.1 (Cq_{Ar}, C⁶), 135.7 (CH_{Ar}, C²), 133.8 (q, ²*J*_{C-F} = 34.0 Hz, C^{9/14}), 133.7 (q, ²*J*_{C-F} = 34.0 Hz, C^{9/14}), 122.9 (q, ¹*J*_{C-F} = 272.9 Hz, C¹⁶), 122.8 (q, ¹*J*_{C-F} = 272.9 Hz, C¹¹), 118.7 (q, ³*J*_{C-F} = 3.8 Hz, C⁸), 117.9 (CH_{Ar}, C³), 117.6 (septet, ³*J*_{C-F} = 3.8 Hz, C¹⁰), 117.5 (q, ³*J*_{C-F} = 3.8 Hz, C¹³), 117.3 (septet, ³*J*_{C-F} = 3.8 Hz, C¹⁵), 113.3 (CH_{Ar}, C⁵), 111.2 (Cq_{Ar}, C¹).

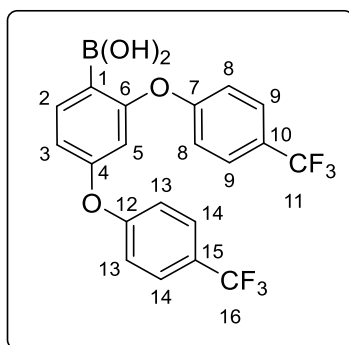
C⁹ and C¹⁴ are overlapping; C⁷ and C¹² are overlapping

¹⁹F NMR (565 MHz, CDCl₃) δ -63.0, -63.1 ppm.

HRMS (ASAP-TOF) m/z: [M + H]⁺ Calcd for C₂₂H₉O₂F₁₂Br 611.9594; Found: 611.9595.

IR (neat)/cm⁻¹ ν_{max} 1585, 1460, 1411, 1364, 1275, 1218, 1172, 1130, 1043, 987, 948, 880, 701.

2,4-Bis[4-(trifluoromethyl)phenoxy]phenyl boronic acid **2.24b**



The title compound was prepared from aryl bromide **2.23b** (422 mg, 0.885 mmol, 1 equiv.), *n*BuLi (0.64 mL, 1.81 M, 1.15 mmol, 1.3 equiv.) and B(O*i*Pr)₃ 98% (271 μ L, 222 mg, 1.174 mmol, 1.3 equiv.) in THF (5 mL, 0.18 M), using general procedure **E**. After extraction, the crude residue (450 mg) was purified by flash silica-gel column chromatography using Cy/EtOAc (80:20). The fraction containing the boronic acid (285 mg) was further purified by crystallization from cyclohexane (7 mL) to afford the pure **2.24b** as a colorless amorphous powder (157 mg, 0.355 mmol, **40% yield**).

Rf (Cy/EtOAc 80:20) = 0.25

C₂₀H₁₃BF₆O₄, **M.W.**: 442.12 g/mol. **M.p.**: 99-100 °C.

¹H NMR (600 MHz; CDCl₃): δ 7.95 (d, *J* = 8.3 Hz, 1H, H²), 7.66 (d, *J* = 8.5 Hz, 2H, H⁹), 7.58 (d, *J* = 8.5 Hz, 2H, H¹⁴), 7.19 (d, *J* = 8.5 Hz, 2H, H⁸), 7.05 (d, *J* = 8.5 Hz, 2H, H¹³), 6.80 (dd, *J* = 8.3, 2.1 Hz, 1H, H³), 6.46 (d, *J* = 2.1 Hz, 1H, H⁵), 5.41 (br s, 2H, OH) .

¹³C NMR (150 MHz; CDCl₃) δ 163.7 (C_{qAr}, C⁶), 160.1 (C_{qAr}, C⁴), 159.0 (q, ⁵*J*_{C-F} = 1.3 Hz, C_{qAr}, C¹²), 158.1 (q, ⁵*J*_{C-F} = 1.3 Hz, C_{qAr}, C⁷), 138.9 (CH_{Ar}, C²), 127.8 (q, ³*J*_{C-F} = 3.7 Hz, C⁹), 127.4 (q, ³*J*_{C-F} = 3.7 Hz, C¹⁴), 127.3 (q, ²*J*_{C-F} = 32.9 Hz, C¹⁰), 126.1 (q, ²*J*_{C-F} = 32.9 Hz, C¹⁵), 124.1 (q, ¹*J*_{C-F} = 271.7 Hz, C¹⁶), 123.9 (q, ¹*J*_{C-F} = 271.7 Hz, C¹¹), 120.0 (2CH_{Ar}, C⁸), 118.9 (2CH_{Ar}, C¹³), 114.4 (CH_{Ar}, C³), 108.3 (CH_{Ar}, C⁵). C¹ is not observed due to quadrupolar relaxation.

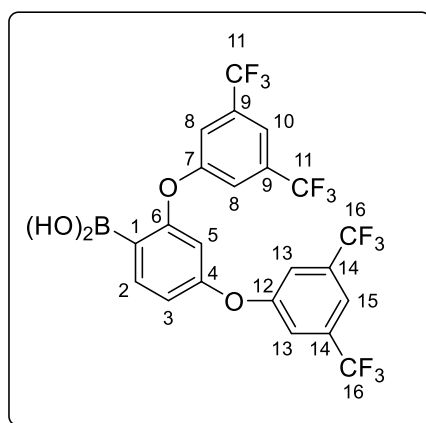
¹⁹F NMR (565 MHz, CDCl₃) δ -61.9, -62.1 ppm.

¹¹B NMR (192.5 MHz, CDCl₃) δ 28.6 ppm.

HRMS (ESI-TOF) *m/z*: [M - H]⁻ Calcd for C₂₀H₁₂BO₄F₆ 441.0733; Found: 441.0746.

IR (neat)/cm⁻¹ ν_{\max} 3380 (br), 1596, 1573, 1514, 1432, 1323, 1271, 1227, 1159, 1116, 1103, 1065, 1015, 979, 848, 769.

2,4-Bis[3,5-di(trifluoromethyl)phenoxy]phenyl boronic acid 2.24c



The title compound was prepared from aryl bromide **2.23c** (613 mg, 1 mmol, 1 equiv.), *n*BuLi (0.72 mL, 1.81 M, 1.3 mmol, 1.3 equiv.) and B(*O**i*Pr)₃ 98% (305 μ L, 250 mg, 1.33 mmol, 1.3 equiv.) in THF (6 mL, 0.18 M), using general procedure **E**. After extraction, the crude residue (631 mg) was purified by flash silica-gel column chromatography using Cy/EtOAc (80:20) to afford the pure **2.24c** as a pale-orange amorphous powder (286 mg, 0.495 mmol, **50% yield**).

R_f (Cy/EtOAc 80:20) = 0.3

C₂₂H₁₁BF₁₂O₄, **M.W**: 578.12 g/mol. **M.p**: 97-100 °C.

(One drop of D₂O is added to the NMR tube to shift the equilibrium of the boronic + boroxine into boronic acid only)

¹H NMR (600 MHz; CDCl₃ + D₂O): δ 8.04 (d, *J* = 8.3 Hz, 1H, H²), 7.73 (s, 1H, H¹⁰), 7.63 (s, 1H, H¹⁵), 7.54 (s, 2H, H⁸), 7.40 (s, 2H, H¹³), 6.87 (dd, *J* = 8.3, 2.2 Hz, 1H, H³), 6.42 (d, *J* = 2.2 Hz, 1H, H⁵), 5.31 (br s, 2H, OH).

¹³C NMR (150 MHz; CDCl₃ + D₂O) δ 163.2 (C_{qAr}, C⁶), 159.6 (C_{qAr}, C⁴), 157.2 (C_{qAr}, C¹²), 156.3 (C_{qAr}, C⁷), 139.8 (CH_{Ar}, C²), 134.2 (q, ²*J*_{C-F} = 34.0 Hz, C⁹), 133.7 (q, ²*J*_{C-F} = 34.0 Hz, C¹⁴), 122.8 (q, ¹*J*_{C-F} = 272.9 Hz, C¹⁶), 122.7 (q, ¹*J*_{C-F} = 272.9 Hz, C¹¹), 120.3 (q, ³*J*_{C-F} = 3.8 Hz, 2CH_{Ar}, C⁸), 119.1 (q, ³*J*_{C-F} = 3.8 Hz, 2CH_{Ar}, C¹³), 118.9 (septet, ³*J*_{C-F} = 3.8 Hz, C¹⁰), 117.7

(septet, $^3J_{C-F} = 3.8$ Hz, C^{15}), 115.0 (CH_{Ar} , C^3), 108.0 (CH_{Ar} , C^5). C^1 is not observed due to quadrupolar relaxation.

^{19}F NMR (565 MHz, $CDCl_3 + D_2O$) δ -63.06, -63.11 ppm.

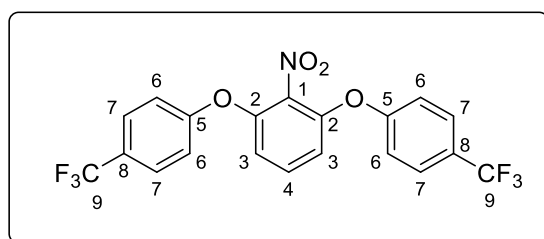
^{11}B NMR (192.5 MHz, $CDCl_3 + D_2O$) δ 28.7 ppm

HRMS (ASAP-TOF) m/z : $[M - H]^-$ Calcd for $C_{22}H_{10}BO_4F_{12}$ 577.0481; Found: 577.0492.

IR (neat)/ cm^{-1} ν_{max} 3560 (br), 3399 (br), 1598, 1576, 1460, 1428, 1365, 1277, 1175, 1125, 1019, 987, 947, 880, 702.

2.3.8 Synthetic protocols and characterization for [2,6-bis(aryloxy)phenyl]boronic acid and its intermediates

1-nitro-2,6-Bis[4-(trifluoromethyl)phenoxy]benzene 2.27



In a 100 mL flask, under argon, 4-trifluoromethylphenol **2.26** (6.824 g, 42.10 mmol, 2.5 equiv.), 2,4-difluoro-1-nitrobenzene **2.25** (2.545 g, 16 mmol, 1 equiv.), K_2CO_3 (5.528 g, 40 mmol, 2.5 equiv.) and DMSO (technical grade ; 16 mL) were added. The reaction mixture was stirred at 100 °C for 4 h. After cooling down to 25 °C, aqueous NaOH (1 M, 50 mL) was added, and the mixture was extracted with Et_2O (3×100 mL). The Et_2O phases were collected, washed with brine (20 mL), dried over $MgSO_4$, and concentrated to afford the pure nitrobenzene **2.27** as a yellow amorphous powder (7.05 g, 15.9 mmol, **99% yield**).

Rf (Cy/EtOAc 90:10) = 0.35

$C_{20}H_{11}F_6NO_4$, **M.W:** 443,30 g/mol. **M.p:** 128-130 °C.

1H NMR (500 MHz; $CDCl_3$): δ 7.66 (d, $J = 8.7$ Hz, 4H, H^7), 7.37 (t, $J = 8.5$ Hz, 1H, H^4), 7.20 (d, $J = 8.7$ Hz, 4H, H^6), 6.79 (d, $J = 8.5$ Hz, 2H, H^3).

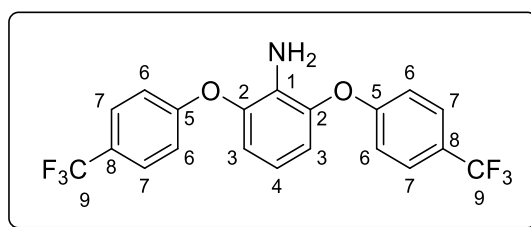
^{13}C NMR (125 MHz; CDCl_3) δ 158.4 (2Cq_{Ar}, C⁵), 149.4 (2Cq_{Ar}, C²), 136.6 (Cq_{Ar}, C¹), 131.7 (CH_{Ar}, C⁴), 127.7 (q, $^3J_{\text{C-F}} = 3.6$ Hz, C⁷), 127.2 (q, $^2J_{\text{C-F}} = 33.0$ Hz, C⁸), 123.9 (q, $^1J_{\text{C-F}} = 272.3$ Hz, C⁹), 119.3 (4CH_{Ar}, C⁶), 114.7 (2CH_{Ar}, C³).

^{19}F NMR (470 MHz, CDCl_3) δ -62.0 ppm.

HRMS (ASAP-TOF) m/z : $[\text{M} + \text{H}]^+$ Calcd for $\text{C}_{20}\text{H}_{12}\text{NO}_4\text{F}_6$ 444.0671; Found: 444.0689.

IR (neat)/ cm^{-1} ν_{max} 1616, 1591, 1526, 1511, 1468, 1421, 1364, 1321, 1246, 1212, 1158, 1106, 1064, 1029, 1014, 838, 752.

2,6-Bis[4-(trifluoromethyl)phenoxy]aniline **2.28**



Diaryloxynitrobenzene **2.27** (7.0 g, 15.8 mmol, 1 equiv.) was dissolved in EtOH: H₂O (40 mL: 4 mL). At reflux temperature (90 °C), Fe (13.24 g, 237 mmol, 15 equiv.) and NH₄Cl (1.690 g, 31.6 mmol, 2 equiv.) were added. The reaction mixture was stirred at 95 °C for 4 h. Ethanol was then evaporated and aqueous saturated NaHCO₃ (50 mL) and EtOAc (50 mL) were added to the formed residue. The mixture was extracted with EtOAc (3×50 mL) and the organic phases were collected, washed with brine (50 mL), dried over MgSO₄, and concentrated under reduced pressure to afford the pure diaryloxylaniline **2.28** as a yellow oil (5.0 g, 12.1 mmol, **77% yield**).

R_f (Cy/EtOAc 95:5) = 0.33

$\text{C}_{20}\text{H}_{13}\text{F}_6\text{NO}_2$, **M.W.**: 413.32 g/mol.

^1H NMR (500 MHz; CDCl_3): δ 7.60 (d, $J = 8.3$ Hz, 4H, H⁷), 7.09 (d, $J = 8.3$ Hz, 4H, H⁶), 6.83 (d, $J = 8.0$ Hz, 2H, H³), 6.74 (t, $J = 8.0$ Hz, 1H, H⁴), 3.94 (br s, 2H, NH₂).

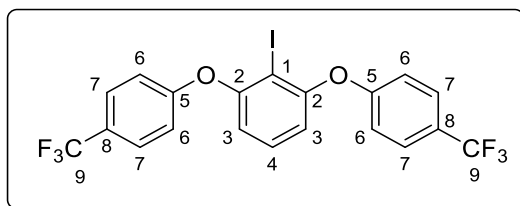
^{13}C NMR (125 MHz; CDCl_3) δ 160.0 (q, $^5J_{\text{C-F}} = 1.1$ Hz, C⁵), 143.2 (2Cq_{Ar}, C²), 132.3 (Cq_{Ar}, C¹), 127.4 (q, $^3J_{\text{C-F}} = 3.7$ Hz, C⁷), 125.2 (q, $^2J_{\text{C-F}} = 32.8$ Hz, C⁸), 124.3 (q, $^1J_{\text{C-F}} = 271.6$ Hz, C⁹), 117.7 (CH_{Ar}, C⁴), 117.3 (2CH_{Ar}, C³), 116.9 (4CH_{Ar}, C⁶).

^{19}F NMR (470 MHz, CDCl_3) δ -61.7 ppm.

HRMS (ESI-TOF) m/z: [M + H]⁺ Calcd for C₂₀H₁₄NO₂F₆ 414.0929; Found: 414.0926.

IR (neat)/cm⁻¹ ν_{\max} 3482 (br), 3391 (br), 1615, 1589, 1511, 1490, 1473, 1421, 1366, 1321, 1220, 1161, 1105, 1064, 1012, 960, 839, 728.

1-iodo-2,6-Bis[4-(trifluoromethyl)phenoxy]benzene 2.29



To a suspension of 2,6-diaryloxyaniline **2.28** (4.878 g, 11.80 mmol, 1 equiv.) in distilled H₂O (15 mL) was added HCl (32% in H₂O; 2.9 mL, 29.5 mmol, 2.5 equiv.). This mixture was stirred for 15 mins at 25 °C before being cooled down to 0 °C. Then, at 0 °C, NaNO₂ (977 mg, 14.16 mmol, 1.2 equiv.) solution in distilled H₂O (5 mL) was added dropwise and this mixture was stirred for 30 mins at 0 °C. KI (4 g, 24 mmol, 2 equiv.) solution in H₂O: CH₃CN (20 mL: 5 mL) was then introduced slowly and this mixture was stirred at 25 °C for 5 h. After reaction completion, aqueous saturated Na₂SO₃ (50 mL) was added and the mixture was extracted with EtOAc (3×75 mL). The combined organic phases were washed with brine (50 mL), dried over MgSO₄, and concentrated under reduced pressure to afford the pure diaryloxyiodide **2.29** as an orange amorphous solid (5.9 g, 11.26 mmol, **95% yield**).

R_f (Cy/EtOAc 95:5) = 0.6

C₂₀H₁₁F₆IO₂, **M.W:** 524.20 g/mol. **M.p:** 102-105 °C.

¹H NMR (600 MHz; CDCl₃): δ 7.62 (d, J = 8.5 Hz, 4H, H⁷), 7.34 (t, J = 8.2 Hz, 1H, H⁴), 7.07 (d, J = 8.5 Hz, 4H, H⁶), 6.82 (d, J = 8.2 Hz, 2H, H³).

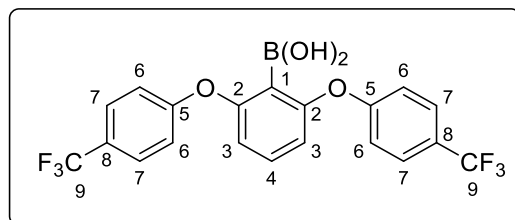
¹³C NMR (150 MHz; CDCl₃) δ 159.6 (q, $^5J_{C-F}$ = 1.3 Hz, C⁵), 157.6 (2Cq_{Ar}, C²), 130.7 (CH_{Ar}, C⁴), 127.5 (q, $^3J_{C-F}$ = 3.8 Hz, C⁷), 125.7 (q, $^2J_{C-F}$ = 32.8 Hz, C⁸), 124.2 (q, $^1J_{C-F}$ = 271.7 Hz, C⁹), 117.9 (4CH_{Ar}, C⁶), 116.5 (2CH_{Ar}, C³), 86.1 (Cq_{Ar}, C¹).

¹⁹F NMR (565 MHz, CDCl₃) δ -61.8 ppm.

HRMS (ASAP-TOF) m/z: [M + H]⁺ Calcd for C₂₀H₁₁F₆IO₂ 523.9708; Found: 523.9718.

IR (neat)/cm⁻¹ ν_{\max} 1614, 1593, 1511, 1480, 1453, 1423, 1321, 1267, 1234, 1154, 1103, 1064, 1011, 994, 834, 795, 615.

2,6-Bis[4-(trifluoromethyl)phenoxy]phenyl boronic acid **2.30**



In an oven-dried flask, under argon, aryl iodide **2.29** (5 g, 9.538 mmol, 1 equiv.) was dissolved in 20 mL of dry THF. At -78 °C, B(OiPr)₃ (98%; 2.92 mL, 2.38 g, 12.65 mmol, 1.3 equiv.) was added and the resulting mixture was stirred for 20 mins. Then, *n*BuLi (6.2 mL, 12.4 mmol, 2 M, 1.3 equiv.) was added at -78 °C for 20 mins. Next, this mixture was stirred for 4 h at 25 °C before being quenched with aqueous HCl (1 M, 20 mL) at -40 °C. After stirring at 25 °C for 20 mins, the mixture was extracted with EtOAc (3×50 mL). The EtOAc phases were washed with brine (50 mL), dried over MgSO₄, and concentrated under reduced pressure to afford the crude residue (4.50 g). The crude residue was purified by flash silica-gel column chromatography using Cy/EtOAc (80:20) and the fraction containing the boronic acid (1.356 g) was further purified by crystallization from cyclohexane (10 mL) to afford the pure boronic acid **2.30** as a pale-yellow amorphous powder (1 g, 2.26 mmol, **24% yield**).

Rf (Cy/EtOAc 80:20) = 0.35

C₂₀H₁₃BF₆O₄, **M.W.**: 442.12 g/mol. **M.p.**: 124-126 °C.

¹H NMR (600 MHz; CDCl₃): δ 7.68 (d, *J* = 8.4 Hz, 4H, H⁷), 7.32 (t, *J* = 8.3 Hz, 1H, H⁴), 7.20 (d, *J* = 8.4 Hz, 4H, H⁶), 6.61 (d, *J* = 8.3 Hz, 2H, H³), 6.53 (br s, 2H, OH).

¹³C NMR (150 MHz; CDCl₃) δ 163.2 (2C_{qAr}, C²), 158.2 (q, ⁵*J*_{C-F} = 1.2 Hz, C⁵), 133.3 (CH_{Ar}, C⁴), 127.8 (q, ³*J*_{C-F} = 3.7 Hz, C⁷), 127.3 (q, ²*J*_{C-F} = 33.0 Hz, C⁸), 124.0 (q, ¹*J*_{C-F} = 271.6 Hz, C⁹), 120.1 (4CH_{Ar}, C⁶), 113.6 (2CH_{Ar}, C³). C¹ is not observed due to quadrupolar relaxation.

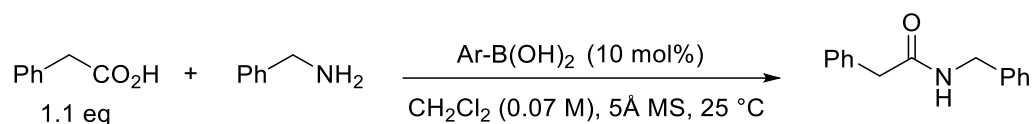
¹⁹F NMR (565 MHz, CDCl₃) δ -62.1 ppm.

¹¹B NMR (192.5 MHz, CDCl₃) δ 28.7 ppm.

HRMS (ESI-TOF) m/z: [M - H]⁻ Calcd for C₂₀H₁₂BO₄F₆ 441.0733; Found: 441.0746.

IR (neat)/cm⁻¹ ν_{\max} 3446 (br), 3381 (br), 1606, 1565, 1513, 1447, 1422, 1322, 1230, 1154, 1105, 1066, 1012, 991, 834, 746.

2.3.9 General procedure of kinetic experiments and raw kinetic data



In a 25 mL flask, under argon, phenylacetic acid 98.50% (76 mg, 0.55 mmol, 1.1 equiv.), boronic acid (0.05 mmol, 10 mol%), and 1 g of activated powdered 5 Å molecular sieves were introduced. To this mixture, 1,1,2,2-tetrachloroethane (53 μ L, 0.50 mmol, 1 equiv.) and dry CH₂Cl₂ (7 mL, 0.07 M) were added, and the mixture was stirred vigorously for 15 minutes at 25 °C. Next, benzylamine 99% (55 μ L, 0.50 mmol, 1 equiv.) was introduced and the reaction was stirred at 25 °C.

The sampling was performed by taking 0.10 mL of the reaction mixture at each time. To each sample, 0.35 mL of CDCl₃ was added and the % NMR yield was determined from ¹H NMR integrations. The % NMR yield was determined by integrating the peak at δ 5.96 ppm (s, 2H) for the internal standard (1,1,2,2-tetrachloroethane) and the signals of the amide at δ 4.4 ppm (d, 2H, CH₂-NH), and 3.6 ppm (s, 2H, CH₂-C-C=O).

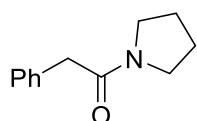
❖ **Raw kinetic data:**

Ar-B(OH) ₂	% NMR yield			
	1 h	2 h	4 h	6 h
2.15a	28	45	65	79
2.15b	41	63	81	95
2.15c	30	55	71	78
2.15d	30	42	55	70
2.15e	37	53	78	92
2.20	24	41	67	80
2.24b	28	48	63	67
2.24c	26	47	73	86
2.30	42	66	100	100
2.21	77	100	100	100
2.32	77	91	100	100
2.38	2	2	2	3

2.3.10 Amides synthesis and characterization

General procedure for the amidation reaction: In a 25 mL flask, under argon, the carboxylic acid (0.55 mmol, 1.1 equiv.), boronic acid **2.30** (22 mg, 0.05 mmol, 10 mol%), and 1 g of 5 Å powdered activated molecular sieves were introduced. Then dry CH₂Cl₂ (7 mL, 0.07 M) was added, and the mixture was stirred vigorously for 15 minutes at 25 °C. Next, the amine (0.50 mmol, 1 equiv.) was added, and the mixture was stirred under argon. After t (h), the reaction was stopped and the mixture was filtered through a celite pad (~1 cm) and washed with EtOAc (2×10 mL) and CH₂Cl₂ (2×10 mL). The filtrate was concentrated under reduced pressure to give a crude residue. The latter was purified by flash silica-gel column chromatography to afford the pure amide.

2-Phenyl-1-(1-pyrrolidinyl)ethanone **2.39**



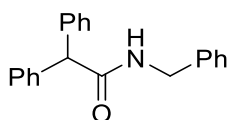
The title compound was prepared from phenylacetic acid 98.50% (76 mg, 0.55 mmol, 1.1 equiv.) and pyrrolidine 99% (41.5 μ L, 36 mg, 0.50 mmol, 1 equiv.) at 25 °C using the general procedure and purified by flash silica-gel column chromatography using Cy/EtOAc 70:30 (**Rf** = 0.3) to afford the pure amide as a colorless oil. The amide was obtained in **22% yield** (21 mg, 0.11 mmol) after a 6 h reaction and **40% yield** (38 mg, 0.2 mmol) with a 24 h reaction.

The ^1H and ^{13}C NMR data are consistent with those reported in the literature.¹¹⁷

^1H NMR (500 MHz, CDCl_3) δ 7.31-7.20 (m, 5H), 3.68 (s, 2H), 3.49 (t, J = 6.6 Hz, 2H), 3.41 (t, J = 6.5 Hz, 2H), 1.95-1.77 (m, 4H).

^{13}C NMR (125 MHz, CDCl_3) δ 169.3, 134.7, 128.8, 128.4, 126.5, 46.7, 45.7, 42.1, 25.9, 24.2.

***N*-Benzyl-2,2-diphenylacetamide 2.40**



The title compound was prepared from diphenylacetic acid 99% (118 mg, 0.55 mmol, 1.1 equiv.) and benzylamine 99% (55 μ L, 54 mg, 0.50 mmol, 1 equiv.) after 24 h using the general procedure and purified by flash silica-gel column chromatography using Cy/EtOAc 80:20 (**Rf** = 0.35) to afford the pure amide as a colorless powder. The amide was obtained in **20% yield** (30 mg, 0.10 mmol) at 25 °C and **30% yield** (45 mg, 0.15 mmol) at 45 °C.

The ^1H and ^{13}C NMR data are consistent with those reported in the literature.¹¹⁸

^1H NMR (500 MHz, CDCl_3) δ 7.29-7.17 (m, 13H_{Ar}), 7.12 (dd, J = 6.6, 1.6 Hz, 2H_{Ar}), 6.32 (br s, 1H, NH), 4.91 (s, 1H), 4.34 (d, J = 5.8 Hz, 2H).

^{13}C NMR (125 MHz, CDCl_3) δ 172.0, 139.5, 138.2, 128.9, 128.7, 128.6, 127.6, 127.4, 127.2, 58.8, 43.7.

HRMS (ESI-TOF) m/z : $[\text{M} + \text{H}]^+$ Calcd for $\text{C}_{21}\text{H}_{20}\text{NO}$ 302.1545; Found: 302.1544.

¹¹⁷ Morimoto, H.; Fujiwara, R.; Shimizu, Y.; Morisaki, K.; Ohshima, T. *Org. Lett.* **2014**, *16*, 2018–2021.

¹¹⁸ Mohy El Dine, T.; Erb, W.; Berhault, Y.; Rouden, J.; Blanchet, J. *J. Org. Chem.* **2015**, *80*, 4532–4544.

Chapter 3. Lewis acidity quantification of arylboronic acids

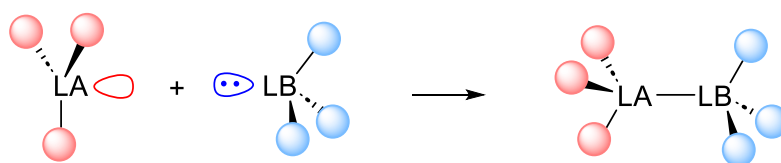
Table of Contents

3.1 Literature review of Lewis acidity quantification methods	122
3.1.1 Introduction	122
3.1.2 Classification of Lewis acidity metrics	122
3.1.3 Lewis acidity scaling methods	123
3.1.3.1 Effective Lewis acidity metrics	123
3.1.3.1.1 Spectroscopic metrics.....	124
3.1.3.1.2 Fluorescence-based technique.....	126
3.1.3.2 Intrinsic Lewis acidity metrics	128
3.1.3.3 Global Lewis acidity metrics.....	129
3.1.4 Lewis acidity determination of boronic acids	131
3.1.5 Conclusion.....	133
3.2 Results and discussion.....	134
3.2.1 Methodology for boronic acid catalyst selection/design in the literature	134
3.2.2 Lewis acidity assessment for a library of boronic acids.....	135
3.2.2.1 The choice of the FIA.....	135
3.2.2.2 Selection of DFT method	136
3.2.2.3 Anchoring agent for FIA calculations	137
3.2.2.4 Evaluation of Lewis acidity of biarylether-based boronic acids	138
3.2.2.5 Design of a new group of boronic acid catalysts	141
3.2.2.5.1 Key elements in catalyst design	141
3.2.2.5.2 FIA calculation for the new group of arylboronic acids	143
3.3 Conclusion.....	145
3.4 Experimental Section	146
3.4.1 Cartesian coordinates and energies of the studied molecules	146
3.4.2 Determination of reaction rates	160

3.1 Literature review of Lewis acidity quantification methods

3.1.1 Introduction

Since Gilbert Lewis introduced the universal concept of the reactivity of Lewis acids and bases in 1923, the concept of Lewis acidity has been extensively utilized.¹¹⁹ A Lewis acid (LA) was defined as a chemical species that contains an empty orbital which is capable of accepting an electron pair from a Lewis base (LB) to form a Lewis adduct (Scheme 92).¹¹⁹



Scheme 92

Lewis acids are one of the most utilized classes of reagents with applications ranging from catalysis to materials.^{119,120} The use of main group Lewis acid catalysis (boron, silicon, aluminum, etc.) has advanced dramatically over the last few decades,^{121,122} prompting the development of methods for assessing the strength of Lewis acidity to facilitate the fine-tuning of the catalyst. In this section, various methods of quantifying the Lewis acidity, both experimental and computational, are discussed and only the case studies on boron-based Lewis acids are covered.

3.1.2 Classification of Lewis acidity metrics

In a 2018 review, Lutz Greb proposed to classify the existing criteria for the determination of Lewis acidity into three categories: effective, intrinsic, and global (Scheme 93).¹²³

¹¹⁹ Lewis, G. N. *Valence and the Structure of Atoms and Molecules*; The Chemical Catalog Company, Inc.: New York, **1923**.

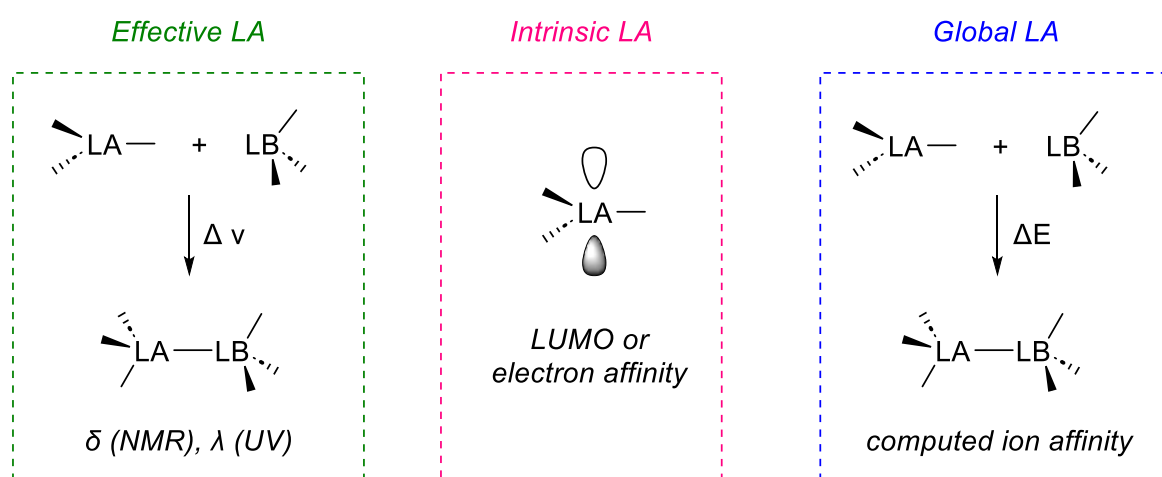
¹²⁰ Yamamoto, Y. *J. Org. Chem.* **2007**, *72*, 7817–7831.

¹²¹ Leitao, E. M.; Jurca, T.; Manners, I. *Nature Chem.* **2013**, *5*, 817–829.

¹²² Stephan, D. W. *Science* **2016**, *354*, aaf7229.

¹²³ Greb, L. *Chem. Eur. J.* **2018**, *24*, 17881–17896.

- Firstly, the effective Lewis acidity (eLA) measures the change in physicochemical properties of a Lewis acid upon its interaction with a Lewis basic probe using NMR spectroscopy or optical techniques (UV-Vis/ fluorescence).
- Secondly, the intrinsic Lewis acidity (iLA) considers the electronic properties of the uncoordinated, free Lewis acid such as LUMO energies, global electrophilicity index, or electron affinity.
- Thirdly, the global Lewis acidity (gLA) considers the entire adduct formation process and provides thermodynamic output such as intramolecular coordination and deformation energies. The gLA can be measured using the computed ion-affinities, such as fluorine-ion affinity (FIA), or experimental techniques, such as solution phase studies of association equilibria.



Scheme 93

The most frequently used scaling methods for each type of Lewis acidity (eLA, iLA, and gLA) are discussed in the following section.

3.1.3 Lewis acidity scaling methods

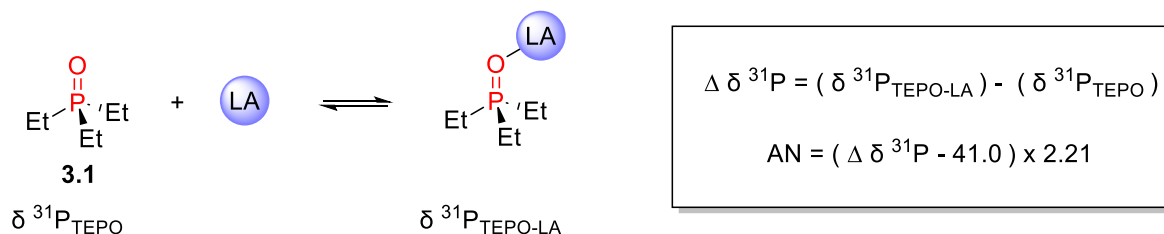
3.1.3.1 Effective Lewis acidity metrics

Representative methods for determining the eLA include those studied through NMR spectroscopy (^{31}P and ^1H NMR) and others studied through optical spectroscopy techniques (fluorescence, chromaticity).

3.1.3.1.1 Spectroscopic metrics

The Gutmann-Beckett (GB) method is the most frequently used in this category. It measures the change in the chemical shift in ^{31}P NMR of triethylphosphine oxide (TEPO, **3.1**) upon coordinating a Lewis acid (Scheme 94).¹²⁴

To illustrate, the Lewis basic oxygen atom of TEPO forms an adduct with the Lewis acid, resulting in the deshielding of the phosphorus atom which can be measured by ^{31}P NMR. The difference in the chemical shift between TEPO and its Lewis acid adduct is used to determine the acceptor number (AN). The AN is then utilized to create the Lewis acidity scale where higher values indicate higher Lewis acidity and it is calculated based on the equation in Scheme 94.¹²⁵



Scheme 94

Recently, Greb re-examined the GB method, supporting his experimental findings with computational studies.¹²⁶ It was proposed that the binding of a LA with TEPO is governed not only by the Lewis acidity strength but also by the thermodynamics of adduct formation, solubility, and possible side interactions. In short, the change in the TEPO chemical shift is influenced by the experimental conditions. For example, a Lewis acid might induce a small chemical shift in ^{31}P NMR of TEPO and be considered “weak”, meanwhile this change could be the result of incomplete adduct formation due to insufficient concentrations or when a low LA: TEPO ratio is employed.

In terms of application, the GB method has been employed on a wide range of boron-based Lewis acids, namely boranes, borates, and boron trihalides. For instance, Beckett utilized the

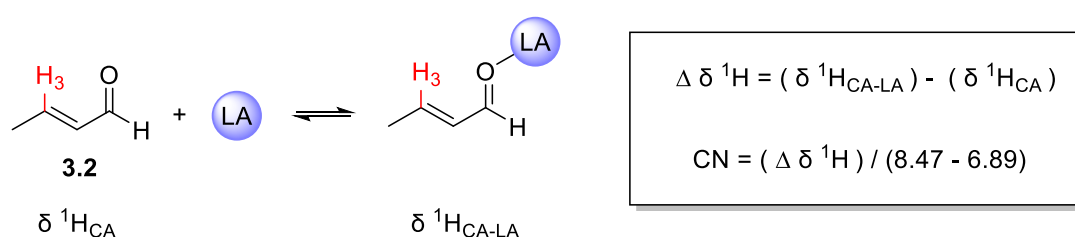
¹²⁴ Mayer, U.; Gutmann, V.; Gerger, W. *Monatsh. Chem.* **1975**, *106*, 1235–1257.

¹²⁵ The acceptor-number scale has two reference points which correspond to the ^{31}P NMR chemical shift of TEPO in the weakly Lewis acidic hexane (^{31}P δ = 41.0 ppm, AN 0) and the strongly Lewis acidic SbCl_5 (^{31}P δ = 86.1 ppm, AN 100).

¹²⁶ Erdmann, P.; Greb, L. *Angew. Chem. Int. Ed.* **2022**, *61*, e202114550.

GB method for scaling the Lewis acidity of boron trihalides and trialkyl borates and correlated this scale with the reaction rates of the Lewis acid-initiated polymerization of phenyl glycidyl ether (PGE).¹²⁷

Furthermore, an analogous approach is the Childs method, which correlates Lewis acidity to changes in ¹H NMR resonance of crotonaldehyde **3.2** upon complexation to a Lewis acid (Scheme 95).¹²⁸ In this method, the relative acidity scale is based on the Childs number (CN) which is calculated from the change in ¹H NMR chemical shift ($\Delta\delta$ ¹H) of H₃ of **3.2** and two reference values, according to the equation in Scheme 95. The reference values are those of the strong Lewis acid BBr₃ (¹H δ = 8.47 ppm, CN = 1) and hexane (¹H δ = 6.89 ppm, CN = 0).



Scheme 95

In most reports of the Lewis acidity scaling of boron Lewis acids, the Gutmann-Beckett and Childs methods are performed simultaneously for a comparative examination of the relative Lewis acidities.^{129,130} As an example, Stephan studied the Lewis acidity scaling of several boranes and catechol boronates,¹³¹ based on AN and CN. It was discovered that the GB method suggests increasing Lewis acidity of the order **3.5** < **3.4** < **3.3** < **3.6**, whereas the Childs method ranks the same Lewis acids in the order of **3.3** < **3.5** < **3.4** < **3.6** (Scheme 96). This different trend of Lewis acidity, except for **3.6**, was explained by the fact that the Lewis acids **3.3-3.6** are relatively hard, therefore their interaction with the hard donor phosphine oxide **3.1** is stronger than their interaction with the soft donor crotonaldehyde **3.2**, thus resulting in different rankings.

¹²⁷ Beckett, M. A.; Strickland, G. C.; Holland, J. R.; Sukumar Varma, K. *Polymer* **1996**, *37*, 4629–4631

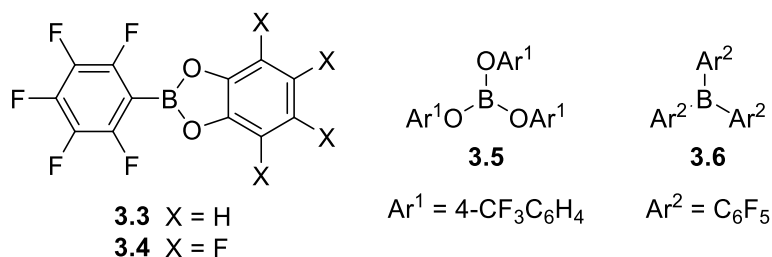
¹²⁸ Childs, R. F.; Mulholland, D. L.; Nixon, A. *Can. J. Chem.* **1982**, *60*, 809–812.

¹²⁹ Beckett, M. A.; Brassington, D. S.; Coles, S. J.; Hursthouse, M. B. *Inorg. Chem. Commun.* **2000**, *3*, 530–533.

¹³⁰ Britovsek, G. J. P.; Ugolotti, J.; White, A. J. P. *Organometallics* **2005**, *24*, 1685–1691.

¹³¹ Neu, R. C.; Ouyang, E. Y.; Geier, S. J.; Zhao, X.; Ramos, A.; Stephan, D. W. *Dalton Trans.* **2010**, *39*, 4285–4294.

LA	AN ^(a)	CN ^(b)
3.3	65.2	0.04
3.4	64.1	0.31
3.5	62.5	0.05
3.6	65.9	0.71



(a) Acceptor number; (b) Childs number

Scheme 96

A less established method for the experimental determination of Lewis acidity includes a method by Nödling and Hilt, which uses ²H NMR spectroscopy to measure the change in the *para*-deuterium signal of pyridine-*d*₅.¹³² However, the latter method has not been reported for boron Lewis acids.¹³²

To conclude, the GB and Childs methods show a strong dependence on HSAB effects,¹³³ however, the quantitative representation of Lewis adduct formation should not be explained merely on this principle whereby contributions from dispersion interaction and deformation energy could be at play too.¹²⁶ Among the GB and Childs methods, the GB is more widely employed since it has been well-correlated with theoretical calculations and experimental results.¹³⁴ Overall, these two methods remain among the most utilized metrics for Lewis acidity quantification due to their experimental ease.

3.1.3.1.2 Fluorescence-based technique

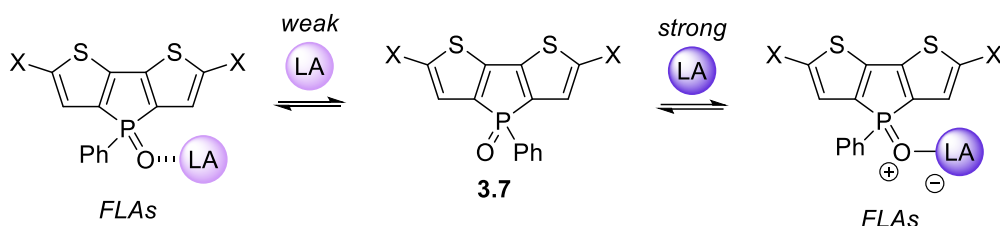
In 2019, Baumgartner and Caputo described the dithienophosphole oxides **3.7** probes that form fluorescent Lewis adducts (FLAs) with acids and can be used to scale Lewis acidity (Scheme 97).¹³⁵ The complexation of the dithienophosphole oxides with a Lewis acid induces the polarization of the P=O bond with different degrees, depending on the strength of the LA, resulting in a change in the emission wavelength (Scheme 97). A strong LA, for instance, would significantly increase the polarity of the P=O bond, thus lowering the energy of the LUMO, and causing a red-shifted emission.

¹³² Hilt, G.; Nödling, A. *Eur. J. Org. Chem.* **2011**, 2011, 7071–7075.

¹³³ Pearson, R. G. *J. Am. Chem. Soc.* **1963**, 85, 3533–3539.

¹³⁴ Sivaev, I. B.; Bregadze, V. I. *Coord. Chem. Rev.* **2014**, 270–271, 75–88.

¹³⁵ Gaffen, J. R.; Bentley, J. N.; Torres, L. C.; Chu, C.; Baumgartner, T.; Caputo, C. B. *Chem* **2019**, 5, 1567–1583.



Scheme 97

The difference in the bathochromic shift ($\Delta\lambda_{em}$) between probe **3.7** and FLAs was used for a qualitative scaling of the Lewis acidity since relying on a single probe caused variations in the relative Lewis acidity strength.¹³⁵ Based on the $\Delta\lambda_{em}$ values (Scheme 98), when probe **3.7a** was used, the increasing order of the Lewis acidity is **3.8** < **3.6** < **3.9**, whereas probe **3.7b** provided a different trend where the relative Lewis acidity order is **3.8** < **3.9** < **3.6**.



	Lewis acid	$\Delta\lambda_{em}$ (3.7a)	$\Delta\lambda_{em}$ (3.7b)
3.8	BF ₃	48 nm	56 nm
3.9	BCl ₃	68 nm	76 nm
3.6	B(C ₆ F ₅) ₃	63 nm	77 nm

Scheme 98

As a consequence, a base-independent method was used for a quantitative evaluation of the Lewis acidity where each LA is tested with three dithienophosphole oxide probes, then mathematical functions are generated for both the probes and FLAs which allow the strength of the Lewis acid to be quantified in terms of Lewis acidity unit (LAU).¹³⁵ Triarylboranes and boron trihalides were the only boron-based compounds studied using this method.

Overall, this method has shown a strong correlation between the emission spectra and the Lewis acidity strength, nonetheless, the requirement for the use of three Lewis basic probes for each Lewis acid, followed by the generation of parabolic functions, to obtain a quantitative Lewis acidity scale renders this procedure less user friendly than the GB method.

3.1.3.2 Intrinsic Lewis acidity metrics

On the contrary to eLA, intrinsic metrics reflect the electronic properties of the free Lewis acid, regardless of its interaction with a Lewis base.

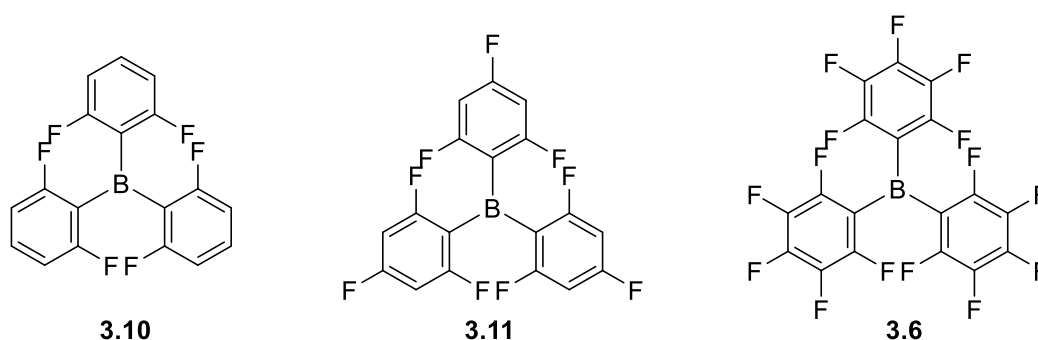
The global electrophilicity index (GEI) is the principal method of this category and it is based on calculations related to the Lewis acid's tendency to accept electrons.¹³⁶ GEI values (ω) are calculated from the chemical potential (μ), and chemical hardness (η), which are in turn calculated from the energies of the highest occupied molecular orbital (E_{HOMO}) and lowest unoccupied molecular orbital (E_{LUMO}), according to Equations 1-3.^{136,137}

$$(1) \omega = \mu^2/2\eta$$

$$(2) \mu = \frac{1}{2}(E_{\text{HOMO}} + E_{\text{LUMO}})$$

$$(3) \eta = (E_{\text{LUMO}} - E_{\text{HOMO}})$$

In 2018, Stephan and Johnstone used the GEI to estimate the Lewis acidity of various fluorinated triarylboranes.¹³⁷ Fluorotriarylboranes **3.6**, **3.10**, and **3.11** showed an increasing GEI in the order **3.10** < **3.11** < **3.6**, in line with the increasing number of electronegative fluorine substituents (Scheme 99).



Lewis acid	E_{HOMO}	E_{LUMO}	GEI (eV)
3.10	-9.366	1.039	0.833
3.11	-9.798	0.780	0.961
3.6	-10.494	-0.249	1.408

Scheme 99

¹³⁶ Parr, R. G.; Szentpály, L. v.; Liu, S. *J. Am. Chem. Soc.* **1999**, *121*, 1922–1924

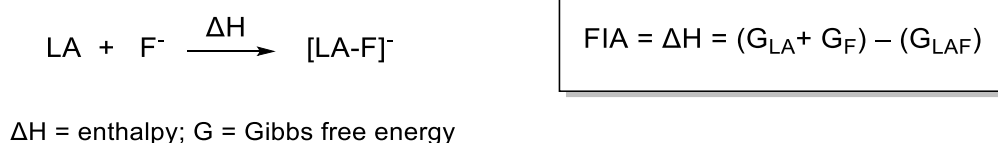
¹³⁷ Jupp, A. R.; Johnstone, T. C.; Stephan, D. W. *Dalton Trans.* **2018**, *47*, 7029–7035.

To sum up, the GEI method could be convenient for a preliminary evaluation of the Lewis acidity, however, factors that arise from an interaction with a Lewis base, such as deformation energy or repulsive forces are not considered. Therefore, it should only be used to compare compounds with very similar structures. Overall, the relevance of GEI as a quantitative measure of Lewis acidity has mostly been understudied.

3.1.3.3 Global Lewis acidity metrics

The third criterion is the global Lewis acidity (gLA) which considers the whole adduct formation process and provides thermodynamic numbers (ΔH , ΔG) as output.

The most frequent method in this class is the fluorine ion affinity (FIA), a computationally derived metric, which is the calculated change in enthalpy (ΔH) associated with the coordination of fluoride ion to the Lewis acid (Scheme 100).¹³⁸ The selection of the fluoride is based on its small size and high basicity, in short, its ability to form adducts with any LA.



Scheme 100

Triarylboranes, triarylborates, and boron trihalides are regarded as hard Lewis acids.^{131,139} Therefore, the FIA, which employs a hard fluoride Lewis base, was typically used to study their Lewis acidity.

Moreover, hydride ion affinity (HIA)¹⁴⁰ has been examined for scaling boranes Lewis acidity in the context of FLP activation of hydrogen,¹⁴¹ and it reflects a measure of soft Lewis acidity using a soft hydride Lewis base.¹⁴² A 2023 study compared the Lewis acidity assessment of triarylborates using the computed FIA and HIA, and experimental Gutmann-Beckett.¹³⁹ According to the fluoride and hydride ion affinities (Scheme 101), the triarylborates **3.12** and

¹³⁸ Christe, K. O.; Dixon, D. A.; McLemore, D.; Wilson, W. W.; Sheehy, J. A.; Boatz, J. A. *J. Fluor. Chem.* **2000**, *101*, 151–153.

¹³⁹ Alharbi, M. M.; Ingen, Y. van; Roldan, A.; Kaehler, T.; Melen, R. L. *Dalton Trans.* **2023**, 52, 1820–1825.

¹⁴⁰ Mock, M. T.; Potter, R. G.; Camaioni, D. M.; Li, J.; Dougherty, W. G.; Kassel, W. S.; Twamley, B.; DuBois, D. L. *J. Am. Chem. Soc.* **2009**, *131*, 14454–14465.

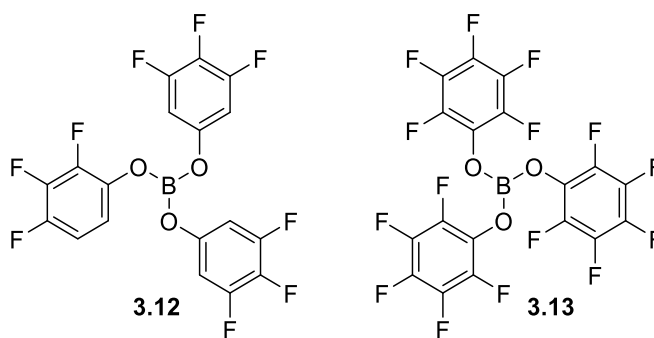
¹⁴¹ Rokob, T. A.; Hamza, A.; Pápai, I. *J. Am. Chem. Soc.* **2009**, *131*, 10701–10710.

¹⁴² Clark, E. R.; Del Grosso, A.; Ingleson, M. J. *Chem. Eur. J.* **2013**, *19*, 2462–2466.

3.12 and **3.13** were found to be weaker Lewis acids than $B(C_6F_5)_3$ **3.6**. In contrast, **3.12** and **3.13** are considered more Lewis acidic than **3.6** according to the GB method (Scheme 101).

Lewis acid	FIA	HIA	$\Delta^{31}P$ TEPO
3.12	433	414	26.6
3.13	431	411	34.5
3.6	454	497	25.5

(FIA and HIA are in $\text{kJ}\cdot\text{mol}^{-1}$)

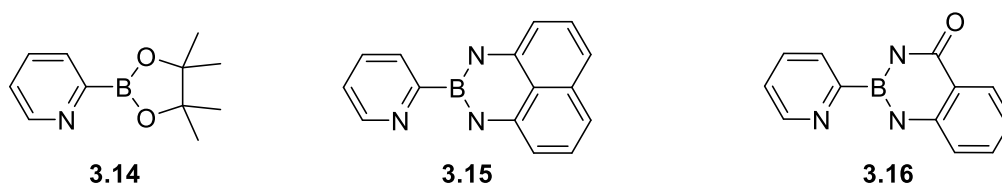


Scheme 101

The discrepancy between the theoretical and experimental Lewis acidity scales was rationalized by the contribution of steric and dispersion effects during the formation of Lewis adduct with TEPO in the GB method.¹³⁹ Such effects are almost neglected with computed FIA and HIA considering the small size of fluoride and hydride anions.¹²³

Other computed affinities have been explored for ranking the Lewis acidity, including NH_3 ,¹⁴³ methyl ion,¹⁴⁴ and chloride ion,¹⁴⁴ but they are much less studied than FIA.

In 2023, Yoshida detailed the computation of Lewis acidity of organoboronate **3.14** and organoboronamides **3.15-3.16** using ammonia affinity (AA) (Scheme 102).¹⁴³ The AA was correlated with the experimental stability of the organoboron derivatives towards hydrolysis. Interestingly, AA provided a Lewis acidity ranking of **3.14-3.16** which agreed well with the experimental stability data. In contrast, the FIA scale was found to be inconsistent with experimental results where it caused an overestimation of the Lewis acidity due to the fluoride ion forming closely contact adducts.



Scheme 102

¹⁴³ Tanaka, H.; Nakamoto, M.; Yoshida, H. *RSC Adv.* **2023**, *13*, 2451–2457.

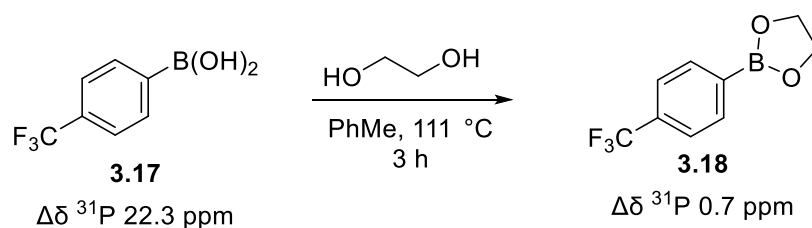
¹⁴⁴ Böhrer, H.; Trapp, N.; Himmel, D.; Schleep, M.; Krossing, I. *Dalton Trans.* **2015**, *44*, 7489–7499.

In summary, FIA has been predominantly used as a boron Lewis acidity quantification system, mainly on triarylboranes and triarylborates, with no known examination of a boronic acid to the best of our knowledge.

3.1.4 Lewis acidity determination of boronic acids

Lewis acidity estimation has been performed on triarylboranes,¹³¹ boron trihalides,¹²⁷ triarylborates,¹³⁹ and boric acid.¹⁴¹ Nonetheless, there are two reports only that concern the determination of Lewis acidity of boronic acids. These two examples are covered in this section.

Recently, Franz examined a series of Brønsted acids using the Gutmann-Beckett method in the context of the catalysis of a Friedel-Crafts reaction.¹⁴⁵ This study included several boronic acids. It was suggested that the boronic acid activation in this case proceeded majorly through hydrogen-bonding, with only minor contribution of the boron Lewis acidity. This was demonstrated by the decrease of the relative ³¹P chemical shift from boronic acid **3.17** ($\Delta\delta$ ³¹P 22.3 ppm) to ester **3.18** ($\Delta\delta$ ³¹P 0.7 ppm) (Scheme 103).



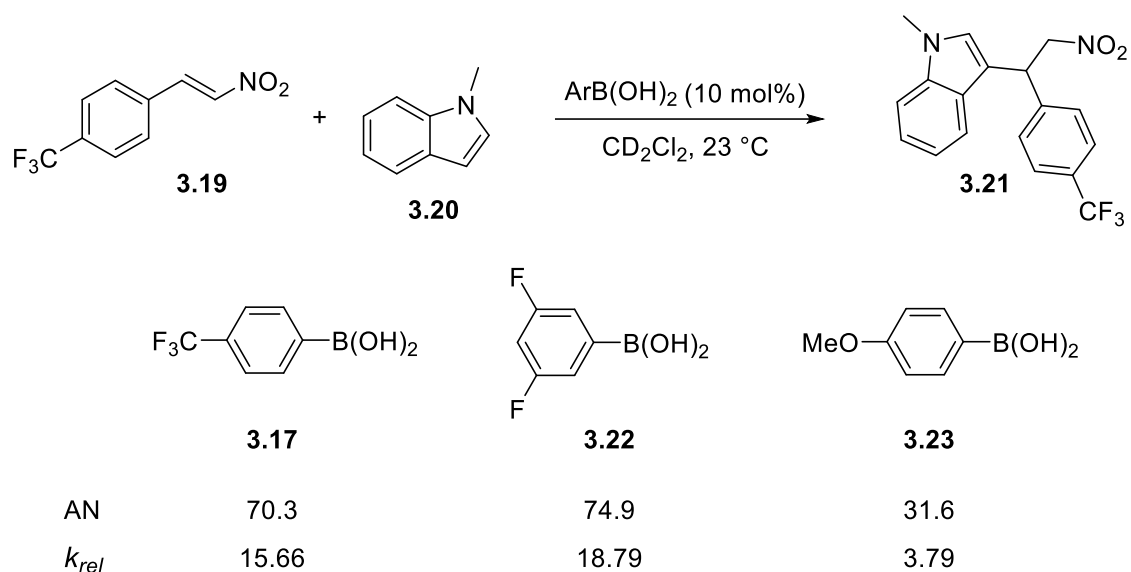
Scheme 103

Considering that the above-mentioned study represents one of only two studies on boronic acids and taking into account the presence of a minor effect of the boronic Lewis acidity, it was included and discussed in this section.

Several arylboronic acids substituted with groups of various electronic effects and on different positions were examined (Scheme 104).¹⁴⁵ It was observed that the electron-deficient boronic acids **3.17** (AN = 70.3) and **3.22** (AN = 74.9) enhanced the binding interaction with TEPO **3.1** compared to the electron-rich **3.23** (AN = 31.6). Importantly, the AN scale correlated positively with the relative reaction rates (k_{rel}) of the catalyzed Friedel-Crafts reaction since catalysts **3.17**

¹⁴⁵ Diemoz, K. M.; Franz, A. K. *J. Org. Chem.* **2019**, *84*, 1126–1138.

and **3.22** enabled significant rate enhancement ($k_{rel} = 15.66$ and 18.79 respectively) over **3.23** ($k_{rel} = 3.79$) (Scheme 104).



Scheme 104

Moreover, the Lewis acidity of boronic acids was lately examined based on their interaction with neighboring arene substituents.¹⁴⁶ First, 2,6-diarylphenylboronic acids **3.24-3.26** (Scheme 105) were prepared to examine the influence of the electronic properties of the two adjacent aryl rings on the through-space polar- π interactions between the B(OH)₂ group and the aryl rings. Next, the boronate formation energies ($\Delta E_{boronate}$) were determined by DFT calculations, with higher ΔE values indicating stronger through-space polar- π interactions and higher Lewis acidity. Moreover, the $\Delta E_{boronate}$ scale was correlated with Hammett sigma values (σ) to determine the dependence of the Lewis acidity on Hammett's substituents constant. Lastly, experimental pK_a values were also determined.

¹⁴⁶ Jian, J.; Hammink, R.; McKenzie, C. J.; Bickelhaupt, F. M.; Poater, J.; Mecinović, J. *Chem. Eur. J.* **2022**, *28*, e202104044.



	X	σ	$\Delta E_{\text{boronate}}^{(a)}$	$\text{pK}_a^{(b)}$
3.24	p-CF ₃	0.54	47.0	12.49
3.25	H	0	47.1	12.36
3.26	p-OMe	-0.27	47.8	12.36

^(a) $\Delta E_{\text{boronate}}$ is in kcal.mol⁻¹; ^(b)pK_a is determined in H₂O/CH₃CN (3:1)

Scheme 105

It was observed that boronic acid **3.24** bearing a *para*-CF₃ group ($\sigma = 0.54$) have slightly lower $\Delta E_{\text{boronate}}$ (47.0 kcal.mol⁻¹) compared to the non-substituted **3.25** (47.1 kcal.mol⁻¹) and the electron-rich **3.26** (47.8 kcal.mol⁻¹) (Scheme 105). Therefore, the variation of the electronic properties of the substituent resulted in a slight variation in the $\Delta E_{\text{boronate}}$ and therefore caused an insignificant change in the Lewis acidity of the boronic acid. Moreover, the solutions of **3.25** and **3.26** in CH₃CN/H₂O (1:3) had similar pK_a of 12.36, which is slightly lower than that of **3.24** (pK_a = 12.49) (Scheme 105).

Consequently, it was concluded that the $\Delta E_{\text{boronate}}$ and pK_a values remained approximately constant as a function of the Hammett sigma values. Overall, this study is interesting in the sense that it combined computational and analytical analyses, however, it did not permit to scale the Lewis acidity of the studied boronic acids.

3.1.5 Conclusion

Amongst the various reported Lewis acidity metrics, only the Guttmann-Beckett method, and the computed boronate formation energies were applied for boronic acid substrates. Nonetheless, the GB was applied to boronic acids as a measure of hydrogen-bonding ability, with a minor effect of their Lewis acidity. Hence, it was not used in the context of Lewis acidity estimation of boronic acids.

On the other hand, the computed boronate formation energies of the 2,6-diarylborynic acids remained unchanged as a function of the electronic properties of the boronic acids. As a

result, this method was unable to establish a comparative scale for the Lewis acidity of different boronic acids, taking into account their electronic effects.

In the context of our ongoing efforts to identify the next best boronic acid catalyst for amides synthesis, it was of interest to find a method that could predict the relative Lewis acidity strength of potential catalyst candidates, allowing the conception of reactivity trends and assisting in catalyst design. Since the GB method requires the production of the LA before its testing, it is ineffective for guiding catalyst design. Consequently, the computationally derived FIA was selected to achieve the objective of generating a Lewis acidity scale of boronic acids of interest.

3.2 Results and discussion

3.2.1 Methodology for boronic acid catalyst selection/design in the literature

In this project, our interest is to discover arylboronic acid catalysts that could compare favorably with the current state-of-the-art boronic acids for the direct amidation reaction. Typically, finding a highly active boronic acid catalyst relies on a trial and error strategy and the screening of available candidates. Mostly these candidates have electron-withdrawing groups or heterocycles since such groups increase the Lewis acidity of the boron center. For example, the highly efficient boronic acid **3.28** was selected from a screening of various commercial boronic acids such as **3.27** and **3.29** (Figure 17).⁶¹ Moreover, the 2-furanylboronic acid **3.31**, efficient at room temperature, was discovered after examining the activity of several commercial heterocyclic boronic acids among which are **3.30** and **3.32** (Figure 17).⁶⁰

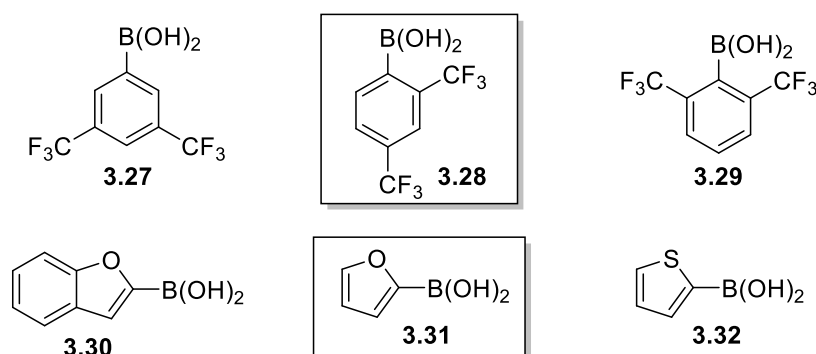


Figure 17

Alternatively, in some cases, the arylboronic acid catalyst was developed using a rational approach that relied on the understanding of the reaction mechanism. For instance, Hall

designed the catalyst **3.33** based on the rationalization that the basic, heteroatom moiety (-SMe) can encourage hydrogen bonding to the amine, and helping to bring it nearer to the carboxylic acid group of the B–O–B bridged intermediate (Figure 18).⁶⁵

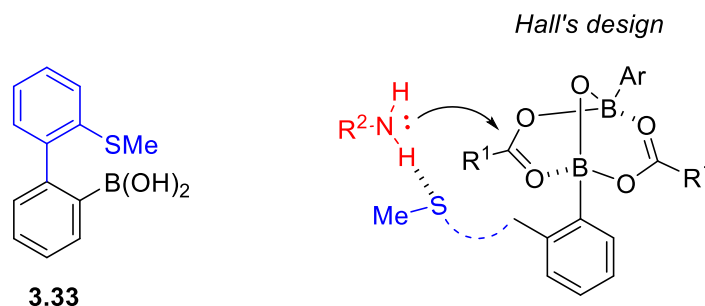


Figure 18

In this study, we aim to devise a strategy that could allow to envisage whether an arylboronic acid catalyst could be an interesting candidate or not. To do so, first, the Lewis acidity is evaluated for a group of arylboronic acids of interest. Next, the candidates with relatively high Lewis acidities are selected for further examination as direct amidation catalysts.

3.2.2 Lewis acidity assessment for a library of boronic acids

All the DFT calculations and FIA determinations were conducted by Dr. Jérôme Blanchet.

3.2.2.1 The choice of the FIA

Among the different methods for the theoretical determination of relative Lewis acidities of boron derivatives, fluoride-ion affinity (FIA) is the most utilized. This is attributed to the fact that the fluoride ion exhibits high basicity and small size, hence, it can coordinate almost all Lewis acids.¹²³ Additionally, the examined LAs which are boron trihalides, triarylboranes, and triarylborates were categorized as hard Lewis acids (LAs).^{131,137,139} Therefore, according to the HSAB principle,¹³³ they react faster and form stronger bonds with a hard Lewis base (fluoride) over a soft one (hydride). As a result, we chose FIA as a method to explore the Lewis acidity of boronic acids.

3.2.2.2 Selection of DFT method

Since no reference system is defined for the theoretical FIA computations for boronic acid substrates, we started by determining the DFT method that could provide accurate energies and allow the generation of a quantitative scale.

Among DFT functionals, ω B97XD falls into the category of "range-separated" functionals which are a type of hybrid functionals that divide the exchange-correlation energy into short-range and long-range contributions.^{147,148} The short-range contribution is calculated using the local-density approximations exchange-correlation functional, while the long-range contribution is calculated using a dispersion correction term. This approach allows ω B97XD to accurately describe short-range interactions, such as ionic, covalent, and hydrogen bonds, and long-range electronic interactions, such as dipole-dipole, dipole-induced dipole, and dispersion forces. Since boronic acids interact intermolecularly via hydrogen bonds and dispersion forces, and given that the ω B97XD considers those interactions in the calculation, it was chosen as the functional for the DFT method.

Moreover, Greb mentioned some recommendations for the computation of the FIA in the supporting information of his review.¹²³ Regarding the choice of the basis set, he suggested that the selected basis sets should take the diffuse orbitals of the fluoride adducts into consideration.

Based on this statement, the 6-31++G(d, p) basis set seems a good option because it includes two diffuse functions (++) and polarization functions (d, p), which increases its accuracy and makes it suitable for an extended range of molecular systems. Compared to smaller Pople basis sets like 6-31G(d), 6-31++G(d,p) is more favored because it has more basis functions that can provide a better description of the shape of molecular orbitals and the distribution of electron density. This can lead to improved accuracy in the calculations of vibrational frequencies and bond lengths. Therefore, the 6-31++G(d, p) basis set was selected.

As a result, the ω B97XD/6-31++G(d,p) was selected as the level of theory for geometry optimizations and frequency calculations. The Gaussian 09 software was used to perform the

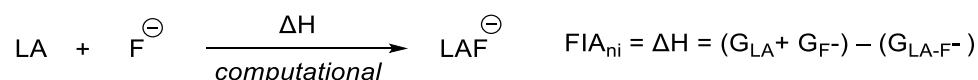
¹⁴⁷ Chai, J.-D.; Head-Gordon, M. *Phys. Chem. Chem. Phys.* **2008**, *10*, 6615–6620.

¹⁴⁸ For a review on DFT methods with dispersion corrections, see: Grimme, S. *Wiley Interdiscip. Rev. Comput. Mol. Sci.* **2011**, *1*, 211–228.

calculations and the absence of imaginary frequencies in each calculation indicated that the system is at a local minimum.

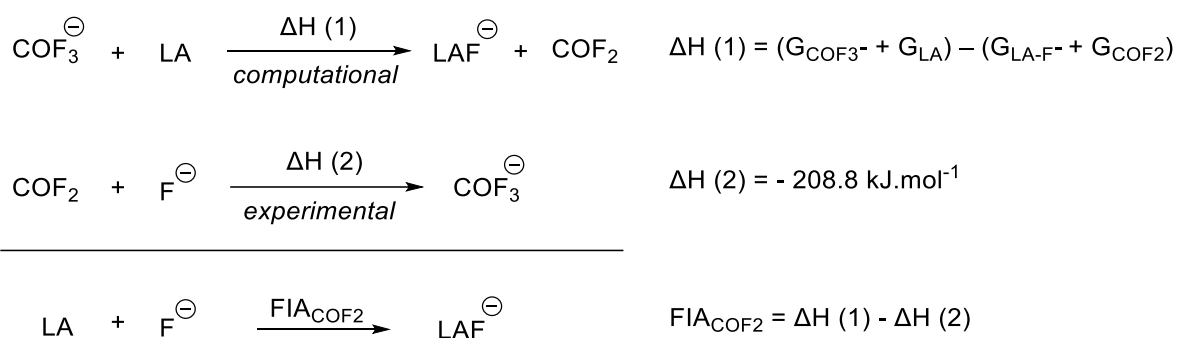
3.2.2.3 Anchoring agent for FIA calculations

The fluoride ion affinity (FIA) was first introduced as the released enthalpy by binding a LA with a fluoride ion (F^-).¹⁴⁹ This FIA is known as the non-isodesmic FIA (FIA_{ni}) and it is calculated based on the equation in Scheme 106.



Scheme 106

However, to avoid the problems that appear by the calculation of a “naked fluoride ion”, this approach was improved by using the experimental FIA of difluoroketone (COF_2) as an anchor point in a pseudo-isodesmic reaction.^{138,150} The FIA anchored to COF_2 (FIA_{COF_2}) is calculated based on the equations in Scheme 107.



Scheme 107

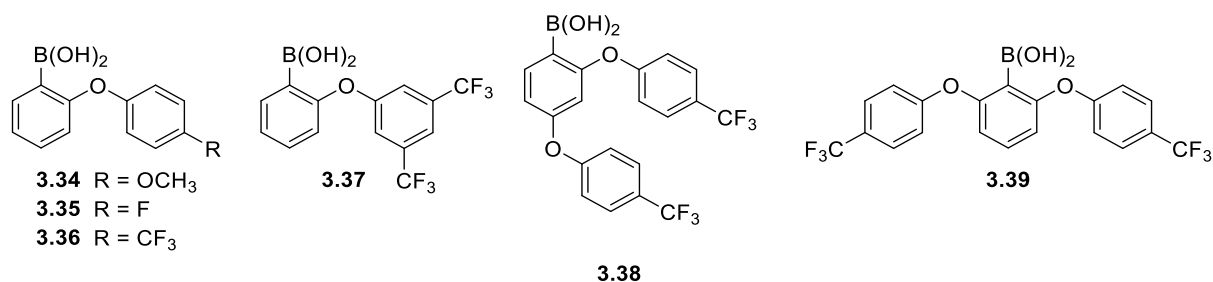
Both the non-isodesmic FIA and COF_2 -anchoring FIA were calculated, in order to validate if both FIAs will produce the same trend of Lewis acidity.

¹⁴⁹ Mallouk, T. E.; Rosenthal, G. L.; Mueller, G.; Brusasco, R.; Bartlett, N. *Inorg. Chem.* **1984**, *23*, 3167–3173.

¹⁵⁰ Erdmann, P.; Leitner, J.; Schwarz, J.; Greb, L. *ChemPhysChem* **2020**, *21*, 987–994.

3.2.2.4 Evaluation of Lewis acidity of biarylether-based boronic acids

First, the Gibbs free energies of the biarylether boronic acids **3.34-3.39** (G_{BA}) and their fluoride adducts (G_{BA-F}) were obtained using the previously described DFT methodology with the ω B97XD functional and 6-31++G(d,p) basis set, and they are presented in Table 1.



Boronic acid	G_{BA} (a.u.)	G_{BA-F} (a.u.)
3.34	-828.633042	-928.545614
3.35	-813.392501	-913.310571
3.36	-1051.144696	-1151.067402
3.37	-1388.111653	-1488.041899
3.38	-1694.214970	-1794.150030
3.39	-1694.214445	-1794.149665

Table 1

The energy values in Table 1 were used to calculate the FIA_{ni} , according to the equation in Scheme 106, and FIA_{COF_2} based on the equations in Scheme 107.

The Lewis acidity scale of biarylether-based boronic acids **3.34-3.39** (Figure 19) shows that the boronic acid **3.34** bearing a methoxy group has the lowest FIA values ($FIA_{ni} = 186.7 \text{ kJ.mol}^{-1}$, $FIA_{COF_2} = 213.2 \text{ kJ.mol}^{-1}$). Hence, it is the least Lewis acidic in this series. Additionally, arylboronic acids **3.35-3.37** display a FIA_{ni} range of 201.1-233.1 kJ.mol^{-1} and a FIA_{COF_2} range of 227.7-259.5 kJ.mol^{-1} , which are higher values compared to those of **3.34**. This supports the fact that the addition of an electron-withdrawing group lowers the electron density and enhances the Lewis acidity of the arylboronic acid.

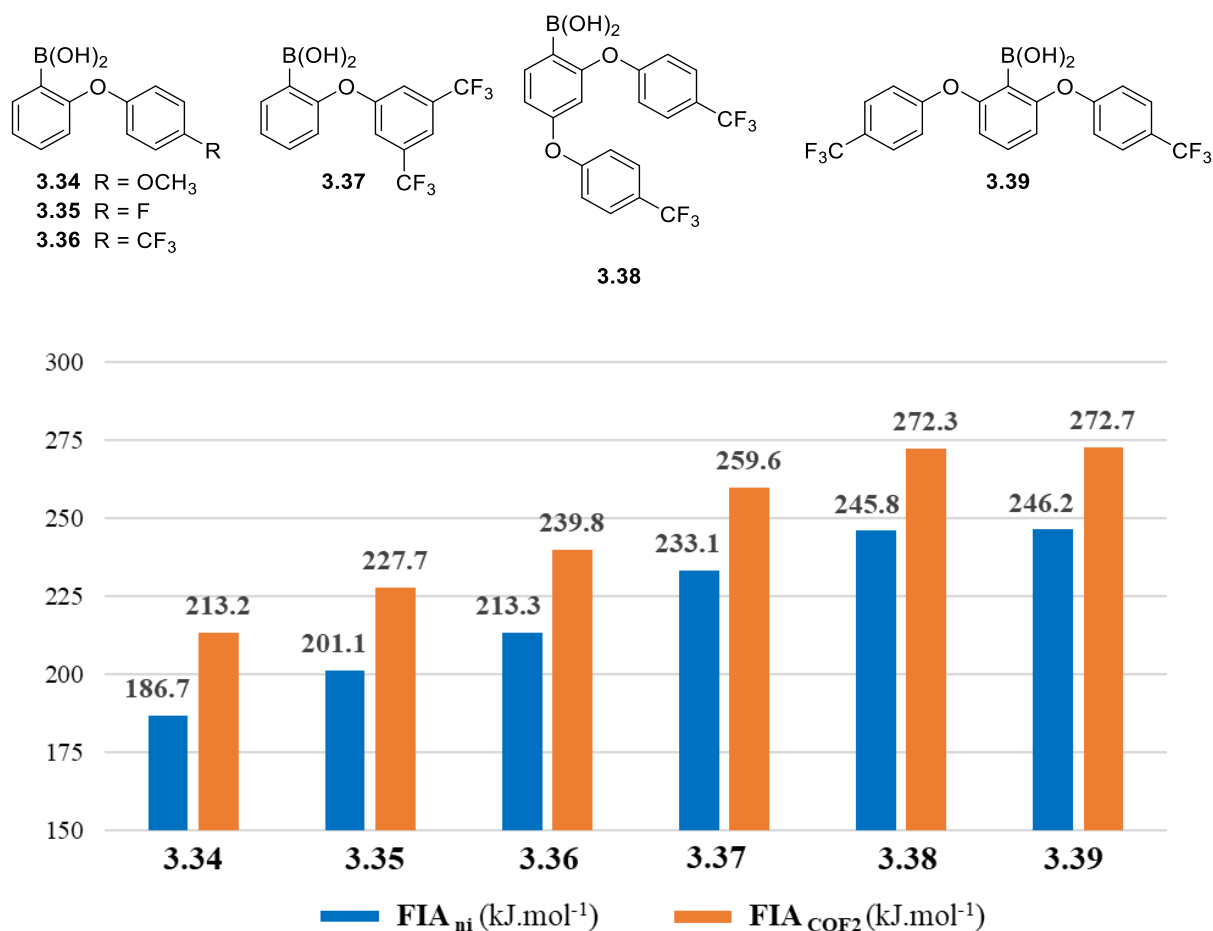


Figure 19

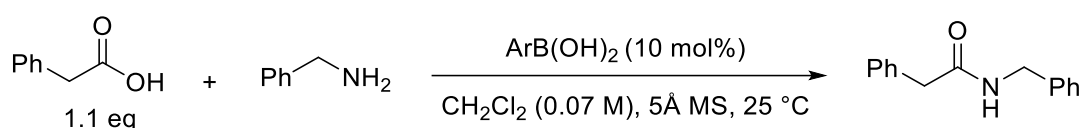
Furthermore, the fluoride-ion affinities of boronic acid **3.38** (FIA_{ni} = 245.8 kJ·mol⁻¹, FIA_{COF₂} = 272.3 kJ·mol⁻¹) are very similar to those of **3.39** (FIA_{ni} = 246.2 kJ·mol⁻¹ and FIA_{COF₂} = 272.7 kJ·mol⁻¹) (Figure 19). Therefore, the pattern of disubstitution did not result in a difference in the Lewis acidity, where the 2,4-disubstituted **3.38** and 2,6-disubstituted **3.39** boronic acids show a marginal difference in their FIA (FIA_{ni} and FIA_{COF₂}) of 0.4 kJ·mol⁻¹.

In addition, it can be observed that the FIA values of **3.38** and **3.39** are 32-33 kJ·mol⁻¹ higher than those of boronic acid **3.36** (Figure 19). This suggests that adding a second 4-trifluoromethoxyphenoxy group caused an increase in Lewis acidity.

Next, to examine whether there is a direct correlation between the Lewis acidity scale and catalytic activity, the trend of FIA_{COF₂} was compared with that of the reaction rates (Scheme 108). The rates were determined for the reaction of coupling of phenylacetic acid and benzylamine at 25 °C. To determine the reaction rates, samples of the reaction mixture were collected at different time points (t = 1 h, 2 h). These samples were then analyzed using ¹H NMR, where the % NMR yields were determined by integrations of the amide signals at 4.4

ppm (d, 2 H, CH₂-NH) and 3.6 ppm (s, 2 H, CH₂-C-C=O) using the internal standard 1,1,2,2-tetrachloroethane with its signal at 5.96 ppm (s, 2 H). Next, the % NMR yields were used to determine the concentration of the amide. Lastly, the change in amide concentration over time was plotted, and the reaction rate was determined as the intercept of the resulting trendline.

It is important to mention that in the literature a more precise method is used for determining reaction rates.^{55,151,152} Such a method involves slowing down the reaction by cooling and taking multiple samples within the first few minutes or even seconds. The yield of the amide is then determined using HPLC. In our case, the method employed is not as precise, however, it can still provide an indication of the trend of catalytic efficiency.



ArB(OH) ₂	FIA _{COF2} (kJ.mol ⁻¹)	Reaction rate (M.h ⁻¹)
3.34	213.2	0.0163
3.36	239.8	0.0239
3.39	272.7	0.0249
3.38	272.3	0.0177

Scheme 108

Among the examined boronic acids (Scheme 108), boronic acid **3.34** exhibited the lowest FIA_{COF2} of 213.2 kJ.mol⁻¹ and it displayed the lowest reaction rate of 0.0163 M.h⁻¹. The catalyst **3.36**, with higher FIA_{COF2} (239.8 kJ.mol⁻¹) than **3.34**, enabled a faster reaction compared to **3.34** with a rate of 0.0239 M.h⁻¹. Interestingly, boronic acid **3.39**, had the highest FIA_{COF2} (272.7 kJ.mol⁻¹) among the biarylether boronic acids, and it displayed the highest reaction rate of 0.0249 M.h⁻¹ (Scheme 108). It can be noticed that the 2,4-(aryloxy)phenylboronic acid **3.38** has

¹⁵¹ Diemoz, K. M.; Hein, J. E.; Wilson, S. O.; Fettingner, J. C.; Franz, A. K. *J. Org. Chem.* **2017**, *82*, 6738–6747.

¹⁵² Deem, M. C.; Cai, I.; Derasp, J. S.; Prieto, P. L.; Sato, Y.; Liu, J.; Kukor, A. J.; Hein, J. E. *ACS Catal.* **2023**, *13*, 1418–1430.

a very close FIA_{COF2} (272.3 kJ.mol⁻¹) to **3.39** (272.7 kJ.mol⁻¹), however, it displayed a lower reaction rate of 0.0177 M.h⁻¹ (Scheme 108).

For boronic acids **3.34**, **3.36**, and **3.39**, there was a positive correlation between the Lewis acidity scale and catalytic efficiency, where higher FIA_{COF2} values were associated with increased reaction rates. However, the relationship between Lewis acidity and catalytic behavior was not always linear, as demonstrated by the case of **3.38**.

These results suggest that the FIA can provide valuable information on Lewis acidity trends and identifying potential catalyst candidates. However, as mentioned by Greb¹⁵³ and observed in our study, it is not suitable to rely on the FIA for predicting trends in catalytic activity. This is because the efficiency of a catalyst is influenced by factors such as steric effects, London dispersion forces, and secondary interactions, which are not accounted for in the FIA calculations.

3.2.2.5 Design of a new group of boronic acid catalysts

3.2.2.5.1 Key elements in catalyst design

In order to enhance the catalytic efficiency of biarylether-based boronic acids **3.34-3.39**, our objective was to develop novel boronic acids capable of surpassing the existing state-of-the-art catalysts in the direct dehydrative amidation reaction, exemplified by 2,4-bis(trifluoromethyl)phenylboronic acid **3.28**. This design effort was guided by the insights derived from the previously studied Lewis acidity and catalytic activity assessments for biarylether-based boronic acids.

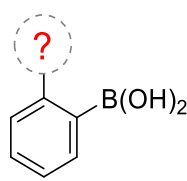
One of the key elements is the *ortho*-functionalization of the arylboronic acid with groups that increase the Lewis acidity of the boron center. Additionally, the reported boronic acid **3.28** has CF₃- groups installed directly on the aromatic ring bearing the boronic moiety. This suggests

¹⁵³ Greb has stated in a footnote in his paper (Ref. 150): “It is always important to keep in mind, that the FIA, like every other Lewis acidity scale, is only one-dimensional. There is no need, that the FIA ranking has to match with complex properties like e.g. the catalytic activity of a Lewis acid, as this might be governed by orbital perturbations of a substrate (soft Lewis acidity) or disturbed by steric repulsion”.

that introducing the EWG on the boronic-bound phenyl ring rather than on an adjacent aryl group could have a more profound impact on increasing the Lewis acidity and thus, could be a key element in catalyst design. Another key finding is the positive impact of the 2,6-disubstitution on the catalytic performance, which has been supported by both FIA and kinetic studies on **3.39**. Therefore, we decided to design new arylboronic acids functionalized with one or two electron-withdrawing groups on *ortho*-position.

Initially, we had to identify an appropriate *ortho*-substituent, hence, we referred to Hammett substituent constant (σ). The latter is a parameter that quantifies the electronic effects of a substituent,¹⁵⁴ and it applies to *para*- (σ_p) and *meta*-substitution (σ_m) rather than *ortho*-substitution due to the interference of the steric effects from the *ortho*-position.¹⁵⁵ Nevertheless, these constants remain valuable for assessing the relative influence of various substituents.

Based on the σ_p values, it can be observed that a triflate group (OSO_2CF_3 , $\sigma_p = 0.53$) and a trifluoromethyl group (CF_3 , $\sigma_p = 0.54$) have comparable electron-withdrawing effects (Figure 20). Additionally, a mesyl-substituent (OSO_2Me , $\sigma_p = 0.36$) exhibits an electron-drawing effect that is slightly lower than that of the CF_3 -group ($\sigma_p = 0.54$). Furthermore, the analysis of the σ_m values show an increasing electron-withdrawing effect of $\text{OMs} < \text{CF}_3 < \text{OTf}$ (Figure 20).



substituent	σ_p	σ_m
OSO_2CF_3	0.53	0.56
CF_3	0.54	0.43
OSO_2Me	0.36	0.39

Figure 20

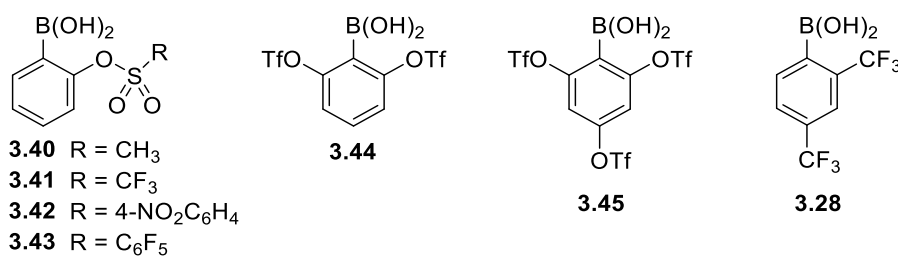
Therefore, a sulfonate group seems suitable to reduce the electron density and increase the Lewis acidity of arylboronic acid. Also, there is a variety of structurally different sulfonate groups, including mesylate, triflate, and nosylate, among others, which offers the opportunity to explore boronic acids with varying electronic and steric properties. As a result, a Lewis acidity assessment was conducted on a group of arylboronic acids decorated with an *ortho*-sulfonate moiety.

¹⁵⁴ Hansch, Corwin.; Leo, A.; Taft, R. W. *Chem. Rev.* **1991**, *91*, 165–195.

¹⁵⁵ Exner, O. A Critical Compilation of Substituent Constants. In *Correlation Analysis in Chemistry: Recent Advances*; Chapman, N. B., Shorter, J., Eds.; Springer US: Boston, MA, **1978**; pp 439–540.

3.2.2.5.2 FIA calculation for the new group of arylboronic acids

The Lewis acidity estimation of sulfonate-substituted arylboronic acids (**3.40-3.45**) was performed using the fluorine ion affinity (FIA). The Gibbs free energies of the target boronic acids (G_{BA}) **3.40-3.45** and their fluoride-adducts (G_{BA-F}) were determined by DFT calculations at the ω B97XD/6-31++(d,p) level of theory, and they are displayed in Table 2. For the sake of comparison, the energies of the reference boronic acid **3.28** were also determined (Table 2).



Boronic acid	G_{BA} (a.u.)	G_{BA-F} (a.u.)
3.40	-1188.900522	-1288.826970
3.41	-1368.715185	-1468.642034
3.42	-1467.125260	-1567.062398
3.43	-1758.742436	-1858.685125
3.44	-2329.358708	-2429.296429
3.45	-3289.998718	-3389.947945
3.28	-1082.003555	-1181.937702

Table 2

Afterward, the non-isodesmic FIA (FIA_{ni}) and COF₂-anchoring FIA (FIA_{COF_2}) were determined (Figure 21). Firstly, the boronic acid **3.40** has an FIA_{ni} of 213.9 kJ.mol⁻¹, and FIA_{COF_2} of 240.5 kJ.mol⁻¹, which are the lowest among the group of *ortho*-(sulfonate)benzene boronic acids **3.40-3.45**. Moreover, the boronic acid **3.41**, which has an *ortho*-triflate group, displayed higher FIA ($FIA_{ni} = 224.2$ kJ.mol⁻¹, $FIA_{COF_2} = 250.7$ kJ.mol⁻¹) than **3.40**. Nonetheless, both of the boronic acids **3.40** and **3.41** have lower Lewis acidity than Ishihara's boronic acid **3.28** ($FIA_{ni} = 243.4$ kJ.mol⁻¹, $FIA_{COF_2} = 269.9$ kJ.mol⁻¹). Additionally, they possessed Lower FIA than **3.39** ($FIA_{ni} = 246.2$ kJ.mol⁻¹, $FIA_{COF_2} = 272.7$ kJ.mol⁻¹).

Importantly, it was observed that the 2-(nosyl)phenylboronic acid **3.42** has higher FIA ($FIA_{ni} = 251.2 \text{ kJ.mol}^{-1}$ and $FIA_{COF_2} = 277.7 \text{ kJ.mol}^{-1}$) than **3.40** and **3.41** (Figure 21). Similarly, the addition of a pentafluorobenzene group in boronic acid **3.44** allowed an increase in the FIA ($FIA_{ni} = 265.8 \text{ kJ.mol}^{-1}$, $FIA_{COF_2} = 292.3 \text{ kJ.mol}^{-1}$) compared to **3.40-3.42**. Notably, the catalyst candidates **3.42** and **3.43** have higher Lewis acidity than boronic acid **3.28**.

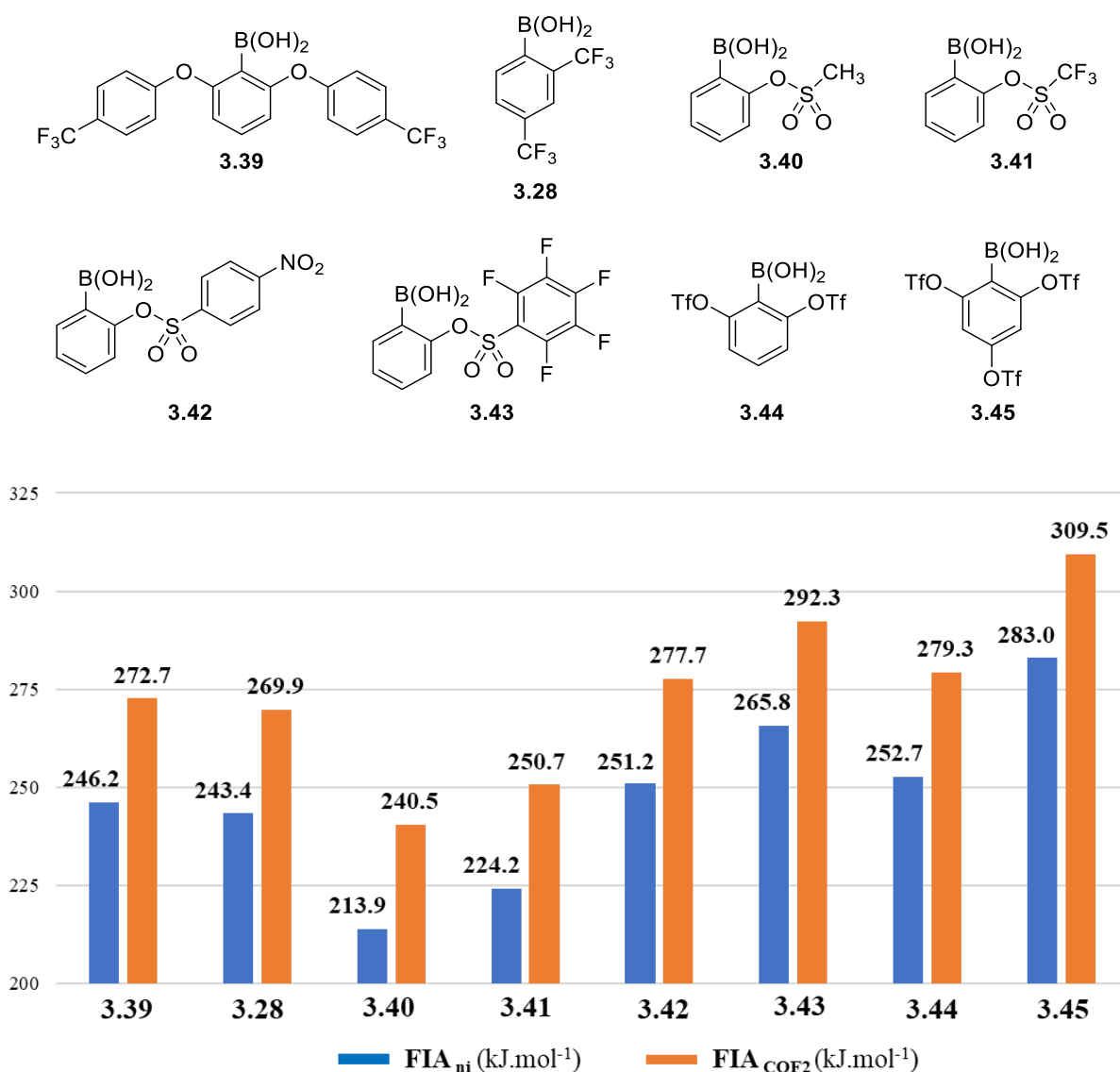


Figure 21

Furthermore, the Lewis acidity estimation of 2,6-disubstituted boronic acid **3.44** was performed and it exhibited higher FIA ($FIA_{ni} = 252.7 \text{ kJ.mol}^{-1}$, $FIA_{COF_2} = 279.3 \text{ kJ.mol}^{-1}$) than those of boronic acids **3.28** and **3.39** (Figure 21). Lastly, the boronic acid **3.45**, which has three triflate

groups showed the highest FIA ($FIA_{ni} = 283.0 \text{ kJ}\cdot\text{mol}^{-1}$, $FIA_{COF_2} = 309.5 \text{ kJ}\cdot\text{mol}^{-1}$) among the sulfonate-phenylboronic acids **3.40-3.45** (Figure 21).

Overall, the analysis of the FIA scale reveals that boronic acids **3.42-3.45** have higher global Lewis acidity than **3.28**, which represents one of the current-state-of-the-art boronic acid catalysts for amides synthesis. Additionally, **3.42-3.45** showed higher Lewis acidity than the optimal (aryloxy)phenylboronic acid **3.39**. This interesting Lewis acidity profile encouraged the preparation and investigation of the *ortho*-sulfonate-benzene boronic acids **3.42-3.45**. Additionally, although **3.40-3.41** showed lower Lewis acidity than **3.28**, they were prepared and studied as well. The preparation and catalytic efficiency examination of boronic acids **3.40-3.45** is discussed in chapter 4.

3.3 Conclusion

The quantification of a Lewis acid's strength is an especially significant strategy for guiding the design of Lewis acidic systems for a variety of applications. Many metrics have been developed, the most common of which is the spectroscopically monitored alteration of a probe molecule (effective Lewis acidity). Furthermore, computationally derived metrics have been developed. These metrics can be based on the intrinsic properties of the uncoordinated Lewis acid (intrinsic Lewis acidity) or on the adduct formation enthalpies when the Lewis acid is coordinated by a Lewis base (global Lewis acidity). The latter has been primarily represented by the application of fluorine-ion affinity (FIA). Although there are numerous measurement systems for quantifying the Lewis acidity, they have rarely been applied to boronic acid substrates.

In this study, the computed FIA was utilized as a practical method to evaluate the Lewis acidity of a set of biarylether-based boronic acids. The resulting FIA profiles enabled the identification of the main factors influencing the Lewis acidity of these boronic acids. Furthermore, it was discovered that while the Lewis acidity scale can provide an indication of whether a boronic acid may be an efficient catalyst, the FIA trend should not be used as a scale of catalytic efficiency. Moreover, computational studies were implemented for designing new boronic acid catalysts. First, guided by Hammett's substituent constant, a sulfonate-group was selected as a suitable electron-withdrawing substituent for the new class of arylboronic acids. Next, the Lewis acidity estimation of (sulfonyloxy)-substituted catalyst candidates revealed that some of

the boronic acids in this class have higher Lewis acidity than one of the current state-of-the-art boronic acids.

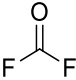
3.4 Experimental Section

3.4.1 Cartesian coordinates and energies of the studied molecules

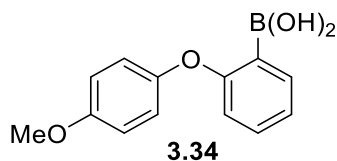
FIA_{ni} : FIA corresponding to the non-isodesmic reaction: $A + F^- \rightarrow AF^e$

FIA_{iCOF₂} : FIA corresponding to the isodesmic reaction: $A + COF_3^- \rightarrow AF^- + COF_2$. $FIA(COF_2)_{exp} = 208.8 \text{ kJ.mol}^{-1}$

Fluorine			
ωB97xd/6-31++g(d,p)			
Charge -1			
F	0.00000000	0.00000000	0.00000000
no imaginary frequencies	-99.841457	-99.841456	

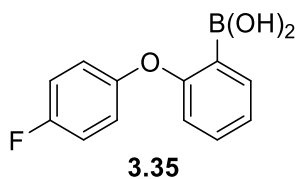
							
ωB97xd/6-31++g(d,p)							
Carbonyl fluoride		Charge 0		Trifluoromethoxide		Charge -1	
C	0.00000000	0.14239100	0.00000000	C	-0.18996500	-0.00242500	0.00155100
F	-1.06433700	-0.63368600	0.00000000	F	0.47348700	-1.22144800	-0.33549100
F	1.06440000	-0.63333400	0.00000000	F	0.44184400	0.90665400	-0.90073800
O	-0.00007000	1.31860500	0.00000000	F	0.46647400	0.33229200	1.22499800
				O	-1.41205700	-0.01786700	0.01147100
no imaginary frequencies	-312.949333			no imaginary frequencies		-412.860196	

FIA _{ni} (kJ.mol ⁻¹)	182.3
---	-------



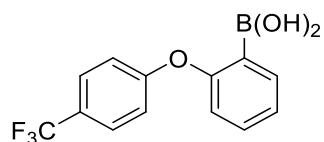
ω B97xd/6-31++g(d,p)							
Lewis acid		Charge 0		Fluorine complex		Charge -1	
C	-1.93007400	-0.70909200	0.46908000	C	-1.34450900	-0.81934000	0.60315200
C	-2.90980200	-1.68068900	0.29268200	C	-1.30179800	-2.21172700	0.66767600
C	-4.08632900	-1.35968500	-0.37883400	C	-2.27928900	-2.96021800	0.01799900
C	-4.27099600	-0.07653400	-0.88586300	C	-3.28592100	-2.29621800	-0.68209200
C	-3.27740900	0.88246700	-0.69971200	C	-3.29723000	-0.90195400	-0.72301600
C	-2.09232500	0.60055400	-0.00529900	C	-2.33124700	-0.10957000	-0.08364100
O	-0.80307000	-1.09114700	1.16201500	O	-0.35995100	-0.13929600	1.32292400
C	0.42784500	-0.84129000	0.59568500	C	0.86951500	0.00664500	0.77132500
C	0.65889500	-0.98536400	-0.77404700	C	1.91179000	0.32424000	1.64624400
C	1.92832700	-0.76172400	-1.28651900	C	3.20791900	0.48340300	1.16490200
C	2.98156700	-0.40578600	-0.43918100	C	3.46699700	0.32619300	-0.19273600
C	2.74885500	-0.27691900	0.93118700	C	2.42597600	0.02972200	-1.06842000
C	1.46875800	-0.49167300	1.44240900	C	1.12762900	-0.12722700	-0.59568600
B	-1.05028000	1.75953100	0.24281000	B	-2.37798600	1.53572800	-0.20587400
O	-0.59445600	2.55702100	-0.77666100	O	-3.56055600	2.00327800	-0.95401000
O	-0.64133600	2.04270400	1.50980600	O	-1.16291600	1.96512600	-0.87070700
H	-2.73294600	-2.67768400	0.68169300	H	-0.50062100	-2.69154900	1.22368200
H	-4.85177000	-2.11758400	-0.51357400	H	-2.25398200	-4.04629400	0.06292000
H	-5.18334500	0.17847100	-1.41516100	H	-4.05770600	-2.86425000	-1.19716100
H	-3.44059000	1.88824300	-1.08115600	H	-4.07358500	-0.38017400	-1.27766800
H	-0.15287800	-1.27023000	-1.43556200	H	1.68510300	0.45118100	2.69961900
H	2.12565900	-0.86941100	-2.34760200	H	4.02274400	0.73623100	1.83721300
H	3.54430000	-0.00202600	1.61362100	H	2.63202800	-0.05353200	-2.13172400
H	1.26733900	-0.37248900	2.50089700	H	0.30679100	-0.30255200	-1.28006000
H	-0.84945500	2.24617100	-1.64798000	H	-4.22596100	2.24382600	-0.30665100
H	0.00804300	2.75250100	1.52558600	H	-1.30404600	2.86355800	-1.17728500
O	4.18742900	-0.20962500	-1.04079400	O	4.75934200	0.49105200	-0.67241500
C	5.28326700	0.15572400	-0.23095400	C	5.45708100	-0.72790700	-0.81438200
H	6.13326900	0.25847200	-0.90543000	H	6.44304300	-0.48901600	-1.22123300
H	5.10600500	1.11285000	0.27573900	H	5.57547300	-1.23291300	0.15494700
H	5.50575200	-0.61650700	0.51615300	H	4.93667700	-1.40884400	-1.50180600
				F	-2.49609700	2.09312700	1.14114300
no imaginary frequencies		-828.633042		no imaginary frequencies		-928.545614	

FIA _{ni} (kJ.mol ⁻¹)	186.7
FIA _{/COF₂} (kJ.mol ⁻¹)	213.2



ω B97xd/6-31++g(d,p)							
Lewis acid				Fluorine complex			
Charge 0				Charge -1			
C	-1.51115100	-0.76594900	0.42359200	C	-1.14232000	0.98435900	-0.43826600
C	-2.42540000	-1.78885600	0.19582000	C	-1.49104900	2.31380600	-0.18783100
C	-3.64714300	-1.50162700	-0.40618300	C	-2.65968100	2.60267200	0.50596500
C	-3.94232300	-0.19699200	-0.79135800	C	-3.46567300	1.54786600	0.93690800
C	-3.01030300	0.81189800	-0.56011500	C	-3.08798400	0.23543000	0.66858700
C	-1.77902500	0.56315900	0.06422200	C	-1.91285500	-0.10440700	-0.02738700
O	-0.34497900	-1.12122200	1.06538800	O	0.01691800	0.82841300	-1.20763000
C	0.86257500	-0.81315100	0.49291200	C	1.19567800	0.53225700	-0.59807500
C	1.04264900	-0.71016000	-0.88526000	C	2.35039500	0.86048600	-1.31279800
C	2.30892700	-0.42951300	-1.39790100	C	3.61071800	0.60022100	-0.78093300
C	3.36604100	-0.27140700	-0.51965600	C	3.69064700	0.01525000	0.47087600
C	3.20584500	-0.38467400	0.85400800	C	2.56016000	-0.32660500	1.19311100
C	1.94097400	-0.65401400	1.36156400	C	1.30040600	-0.07259600	0.65703000
B	-0.80405200	1.76922300	0.35326600	B	-1.56369300	-1.71455600	-0.20436000
O	-0.58269500	2.75657700	-0.57412300	O	-0.52858200	-2.04345400	-1.17717200
O	-0.20340400	1.88553100	1.56781800	O	-1.14421600	-2.20288900	1.10475700
H	-2.16473200	-2.79875900	0.49378200	H	-0.83531200	3.10210700	-0.54706500
H	-4.36327100	-2.29897600	-0.57809400	H	-2.93658200	3.63515000	0.70364300
H	-4.89188500	0.03427100	-1.26262800	H	-4.38746200	1.75058100	1.47750100
H	-3.26301700	1.83174400	-0.84298700	H	-3.72335100	-0.58054200	1.00192900
H	0.20373100	-0.84740400	-1.55887500	H	2.24368500	1.32157400	-2.28910600
H	2.47435500	-0.34074900	-2.46551600	H	4.51609600	0.85026500	-1.32374500
H	4.05906400	-0.25371400	1.50985500	H	2.66048900	-0.80876800	2.15945500
H	1.76933600	-0.73118900	2.42882400	H	0.41219200	-0.39964900	1.18706000
H	-0.96575800	2.57517800	-1.43493900	H	-0.81650300	-1.79473500	-2.05672400
H	0.38371300	2.64670200	1.60842900	H	-0.69921300	-3.04167800	0.95924900
F	4.59526100	0.00193400	-1.01408000	F	4.92295500	-0.23723700	1.00401300
				F	-2.81842000	-2.34615300	-0.61880800
no imaginary frequencies				no imaginary frequencies			
-813.392501				-913.310571			

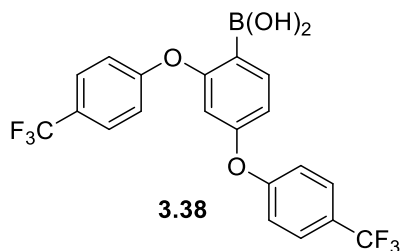
FIA _{ni} (kJ.mol ⁻¹)	201.1
FIA _{COF₂} (kJ.mol ⁻¹)	227.7



3.36

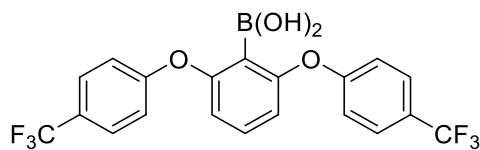
ω B97xd/6-31++g(d,p)							
Lewis acid				Fluorine complex			
Charge 0				Charge -1			
C	-2.22887300	-0.59150900	-0.56331600	C	2.05490800	0.82123100	0.56081400
C	-2.45397200	-1.96350300	-0.60954600	C	2.18576600	2.20731500	0.57860000
C	-3.52633000	-2.50389300	0.09268900	C	3.21911300	2.79641700	-0.14465700
C	-4.36979000	-1.66992200	0.82408300	C	4.09585500	1.98099700	-0.86092000
C	-4.13310000	-0.29857300	0.84449400	C	3.93050900	0.59654400	-0.84745700
C	-3.05169000	0.27726700	0.15875400	C	2.90026700	-0.03827300	-0.13688600
O	-1.20437500	-0.06984000	-1.33275600	B	2.71111900	-1.68175800	-0.14692400
C	0.07456900	-0.11059000	-0.85966500	O	1.03063900	0.28350200	1.36351300
C	0.40333100	-0.48090400	0.44361000	C	-0.22348300	0.21144500	0.86803200
C	1.73738600	-0.48052800	0.83349100	C	-1.23892300	-0.04888600	1.79525500
C	2.73739600	-0.11709700	-0.06500600	C	-2.55788500	-0.13315100	1.37786500
C	2.39751300	0.25732600	-1.36596200	C	-2.87740800	0.04195300	0.02998800
C	1.07002000	0.25883400	-1.76507400	C	-1.85943500	0.29282900	-0.89206700
B	-2.79588400	1.83243900	0.22755100	C	-0.53609300	0.37323700	-0.48475300
O	-3.82404600	2.73816500	0.15733100	F	3.82399000	-2.26237500	-0.85384900
O	-1.53459000	2.30488100	0.41045100	O	1.45016900	-1.94288800	-0.85302400
F	4.48396000	1.12119800	0.94809600	O	2.73209600	-2.26170600	1.19958100
C	4.16729700	-0.06933300	0.38590200	F	-5.05801300	-0.85032400	0.31048700
F	4.44301100	-1.01033300	1.31268600	C	-4.30622200	0.02162700	-0.40316000
F	5.03247400	-0.25099400	-0.63249900	F	-4.91617800	1.23076100	-0.25553200
H	-1.79145600	-2.58953500	-1.19815100	F	-4.45943300	-0.30918800	-1.70397300
H	-3.70609900	-3.57376000	0.06129400	H	1.48601100	2.80551500	1.15584900
H	-5.20852200	-2.08631200	1.37221800	H	3.33953300	3.87657700	-0.14306100
H	-4.79334800	0.33863800	1.42885500	H	4.91053200	2.42708300	-1.42680100
H	-0.37030300	-0.75397700	1.15108900	H	4.61472300	-0.03714700	-1.40504300
H	1.99482800	-0.76483700	1.84803200	H	-0.97099500	-0.18643300	2.83723000
H	3.17091700	0.54093900	-2.07106200	H	-3.33981000	-0.33613600	2.10239900
H	0.78654800	0.54128800	-2.77265300	H	-2.09571900	0.40624900	-1.94455500
H	-4.67675100	2.34932600	-0.04886200	H	0.25914800	0.50961900	-1.20610400
H	-1.49985400	3.26609700	0.43000200	H	1.25364000	-2.87758300	-0.75162600
				H	2.04900300	-1.82978200	1.71764800
no imaginary frequencies				no imaginary frequencies			
-1051.144696				-1151.067402			

FIA _{ni} (kJ.mol ⁻¹)	213.3
FIA _{COF₂} (kJ.mol ⁻¹)	239.8



ω B97xd/6-31++g(d,p)							
Lewis acid				Fluorine complex			
Charge 0				Charge -1			
C	-0.94316200	0.69977000	0.72645100	C	-0.60089000	0.50075700	0.08537500
C	0.03685700	-0.26812700	0.90184400	C	0.45110800	-0.23631100	-0.46395900
C	1.21706000	-0.17472500	0.17245700	C	1.36555300	0.41606300	-1.27199500
C	1.41305800	0.86787400	-0.73178000	C	1.23946100	1.77124300	-1.54369500
C	0.41426000	1.82273000	-0.87579200	C	0.17724000	2.46467900	-0.96928000
C	-0.78925200	1.78047300	-0.15421100	C	-0.77975500	1.86919400	-0.12943200
O	-2.07056000	0.57575900	1.51334700	O	-1.41655500	-0.23690500	0.94168800
C	-3.22116900	0.10283300	0.95921700	C	-2.70792800	-0.48802300	0.62890000
C	-4.36207700	0.18410500	1.76245100	C	-3.42332400	-1.23110800	1.57448900
C	-5.57119600	-0.28770700	1.28452300	C	-4.74258100	-1.57471400	1.33578100
C	-5.65430900	-0.84379700	0.00372700	C	-5.36541400	-1.17839600	0.14952000
C	-4.51476200	-0.92562500	-0.78772600	C	-4.64742300	-0.43668200	-0.78782000
C	-3.29166800	-0.45631800	-0.31488200	C	-3.32297400	-0.09023400	-0.55925000
O	2.12145600	-1.19238100	0.34212800	O	2.41494900	-0.31391200	-1.84087400
C	3.46427000	-0.93967500	0.21476700	C	3.58544300	-0.38825000	-1.16734900
C	4.22003900	-1.85376400	-0.51095800	C	4.60505700	-1.12318700	-1.78691500
C	5.59551300	-1.67644800	-0.61390300	C	5.83874800	-1.25116300	-1.17316200
C	6.20599500	-0.58943500	0.00659800	C	6.07438700	-0.64577900	0.06496800
C	5.44033200	0.32011800	0.73757600	C	5.05727200	0.07986500	0.68004800
C	4.06830100	0.14592900	0.84972600	C	3.81360200	0.21547500	0.07269000
F	8.24145800	0.10564100	0.99182200	F	7.51263200	-2.04176800	1.33666400
C	7.68262700	-0.35553900	-0.14548300	C	7.39972900	-0.83059400	0.73378900
F	8.34643200	-1.47460500	-0.49040900	F	8.43159500	-0.75914900	-0.13998900
F	7.94763100	0.56406700	-1.10126000	F	7.63540300	0.09006900	1.69098800
F	-7.53352800	-2.23924900	0.34522700	F	-6.84576500	-2.82394400	-0.71999000
C	-6.98298600	-1.33181700	-0.49164000	C	-6.77042400	-1.59740900	-0.13111800
F	-7.88337300	-0.32614400	-0.59690700	F	-7.52358900	-1.68968600	0.99081700
F	-6.90477200	-1.91190600	-1.70404700	F	-7.41754700	-0.75268200	-0.96353800
B	-1.84648700	2.91919800	-0.37660400	B	-2.00257200	2.83257000	0.44850100
O	-2.95685000	2.99287500	0.41726700	O	-2.70995400	2.31815100	1.61666300
O	-1.57263800	3.80953700	-1.38623900	O	-2.93847700	3.02558600	-0.64451000
H	-0.11749700	-1.08442800	1.59774100	H	0.54918600	-1.29590000	-0.25272200
H	2.32786200	0.93281500	-1.31007900	H	1.96566500	2.26533200	-2.18235000
H	0.56534500	2.63563600	-1.57877500	H	0.07605300	3.52849900	-1.16192400
H	-4.27716700	0.62891100	2.74714500	H	-2.92779700	-1.51209000	2.49712600
H	-6.45810600	-0.22298500	1.90663700	H	-5.29461700	-2.14361000	2.07676700
H	-4.57185000	-1.36229700	-1.77829700	H	-5.12743700	-0.10339800	-1.70161700
H	-2.40679900	-0.52590100	-0.93689900	H	-2.79900300	0.54198700	-1.26444400
H	3.72445100	-2.69343200	-0.98484500	H	4.40552600	-1.58154300	-2.74916000
H	6.19009900	-2.38454900	-1.17981900	H	6.62588700	-1.81794400	-1.65983800
H	5.91727400	1.16074700	1.22993000	H	5.23088500	0.55250600	1.64051800
H	3.46738100	0.84185000	1.42474800	H	3.02698400	0.78567200	0.55258200
H	-3.58912800	3.68290900	0.20552400	H	-2.19454400	2.50771300	2.40221500
H	-2.20171900	4.52304000	-1.50962100	H	-3.77512200	3.29502500	-0.25743500
F				F	-1.35159800	4.08815900	0.82555200
no imaginary frequencies		-1694.214970		no imaginary frequencies		-1794.150030	

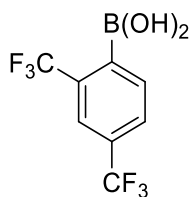
FIA _{ni} (kJ.mol ⁻¹)	245.8
FIA _{iCOF₂} (kJ.mol ⁻¹)	272.3



3.39

ωB97xd/6-31++g(d,p)							
Lewis acid				Fluorine complex			
Charge 0				Charge -1			
C	-1.27591800	-2.79077900	0.51606900	C	1.20844600	-2.54149100	-0.65908700
C	-0.91987500	-3.70229000	1.50272000	C	1.10973700	-3.07255200	-1.94502100
C	0.41536100	-4.06913400	1.64328100	C	-0.14346200	-3.32991200	-2.48621500
C	1.38334600	-3.51920200	0.81112900	C	-1.27515400	-3.04218000	-1.73050400
C	0.99122700	-2.59877400	-0.15474800	C	-1.12017600	-2.50883600	-0.45455700
C	-0.33574600	-2.21028700	-0.34734200	C	0.11203600	-2.24668200	0.15794600
O	-2.62554000	-2.53199300	0.38900100	O	2.52178100	-2.37971200	-0.21208100
C	-3.08743300	-1.24916000	0.36798300	C	3.07554300	-1.14798200	-0.16382400
C	-2.41478700	-0.18302500	0.96279000	C	2.36636700	0.04474800	-0.33455500
C	-2.96942100	1.09217300	0.90218600	C	3.04687300	1.25184000	-0.29280700
C	-4.19099400	1.29848900	0.27014400	C	4.42636700	1.29103500	-0.08072800
C	-4.86866200	0.21932700	-0.30503900	C	5.12733900	0.09774800	0.09830400
C	-4.32011400	-1.05108800	-0.25773000	C	4.45596800	-1.11388400	0.05846600
O	1.94847300	-2.10508600	-1.02596800	O	-2.29765800	-2.28688300	0.25765500
C	2.74523700	-1.07519600	-0.61751000	C	-2.95355800	-1.11919500	0.11678100
C	3.74168400	-0.68355800	-1.51527700	C	-2.51522300	-0.06197200	-0.68565500
C	4.58581500	0.36354700	-1.18764200	C	-3.28190500	1.09040800	-0.77947400
C	4.44451200	1.02502900	0.03548400	C	-4.48279800	1.20636100	-0.07962400
C	3.45254100	0.62746200	0.92464600	C	-4.91354600	0.14881100	0.72615100
C	2.59667900	-0.42176500	0.60336300	C	-4.15569900	-1.00504500	0.82513200
C	-4.76751300	2.67861100	0.14543800	C	5.14525300	2.59940400	-0.10534800
F	-4.55555100	3.20019200	-1.08750900	F	5.41390900	3.02559700	-1.37048700
F	-4.23193200	3.54390000	1.02627600	F	6.34077300	2.55504500	0.52710400
F	-6.10264600	2.69096200	0.33523800	F	4.43902000	3.59815800	0.47085200
C	5.38576800	2.14439700	0.36880900	C	-5.33446600	2.42357000	-0.22441000
F	6.65908900	1.70999400	0.51004600	F	-6.30750400	2.27631800	-1.16685700
F	5.05937000	2.77249000	1.51396300	F	-4.63252300	3.51817300	-0.59151600
F	5.41640800	3.08422400	-0.60239000	F	-5.98619800	2.74489900	0.91829500
B	-0.71168200	-1.18268700	-1.48957800	B	0.17073000	-1.58661900	1.69515600
O	-1.66683500	-1.56055200	-2.38871200	O	1.50448500	-1.47998000	2.27101200
O	-0.05818700	0.01595500	-1.49573900	O	-0.40573100	-0.26015200	1.57049700
H	-1.69269300	-4.11441300	2.14159900	H	2.02133800	-3.27718400	-2.49758500
H	0.70038000	-4.78773000	2.40434600	H	-0.23846400	-3.74955300	-3.48316900
H	2.42989800	-3.78919100	0.89883300	H	-2.27513800	-3.21965800	-2.11406800
H	-1.46259400	-0.33867600	1.45616800	H	1.28796100	0.03204900	-0.43327500
H	-2.44470400	1.92419600	1.35787900	H	2.48999300	2.17625000	-0.40645400
H	-5.82456700	0.37536600	-0.79372600	H	6.19801500	0.11491200	0.27182600
H	-4.81896500	-1.90056000	-0.70962600	H	4.98093200	-2.05160600	0.20429700
H	3.83467800	-1.20713000	-2.46006800	H	-1.56257200	-0.13083800	-1.19508100
H	5.35824000	0.66979000	-1.88549700	H	-2.92946900	1.91353200	-1.39186400
H	3.33612100	1.13847400	1.87348500	H	-5.84108400	0.23343700	1.28312600
H	1.81767900	-0.71721800	1.29559200	H	-4.45948400	-1.82758900	1.46259200
H	-1.93378200	-0.89690600	-3.02941000	H	1.74992900	-2.32496300	2.65132600
H	-0.27746200	0.62630100	-2.20347700	H	-0.13512600	0.24693500	2.33951500
				F	-0.61316000	-2.46640900	2.54266600
no imaginary frequencies				no imaginary frequencies			
-1694.214445				-1794.149665			

FIA _{ni} (kJ.mol ⁻¹)	246.2
FIA _{COF₂} (kJ.mol ⁻¹)	272.7

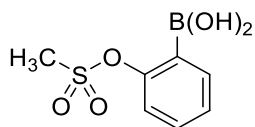


3.28

ωB97xd/6-31++g(d,p)

Lewis acid				Fluorine complex			
Charge 0				Charge -1			
C	1.25190400	-1.70145500	0.06097700	C	1.35175400	-1.65986100	0.00849200
C	0.76878900	0.65947900	-0.01773800	C	0.98794300	0.71583000	-0.02805800
C	-1.06736700	-0.94120700	0.01785400	C	-0.95137600	-0.79666600	0.03005800
C	-0.11486200	-1.96507800	0.04175700	C	-0.02004500	-1.85291200	0.03408000
H	1.96756500	-2.51495300	0.08928900	H	2.02781100	-2.51063300	0.01217500
H	1.11542200	1.68544900	-0.06388400	H	1.37945500	1.72497100	-0.05592400
H	-0.45133600	-2.99693900	0.04470200	H	-0.42442400	-2.85938500	0.06590400
B	-2.58882700	-1.37332100	0.07125100	B	-2.56607400	-1.22303700	0.00637200
O	-3.41993000	-0.73722500	0.94294200	O	-3.14484100	-1.10409100	-1.33425200
H	-4.34420700	-0.99503700	0.93376100	H	-3.35615700	-0.18345600	-1.49724400
O	-2.94139300	-2.43274100	-0.71879300	O	-2.65758400	-2.60811900	0.43122400
H	-3.84738800	-2.74098900	-0.64253000	H	-3.47357000	-2.95272900	0.06287900
C	1.68961000	-0.38426200	0.03771300	C	1.86330700	-0.36126500	-0.02495800
C	-0.59254800	0.38216700	-0.02562600	C	-0.39330100	0.49685700	-0.00569900
C	-1.54813600	1.55286200	-0.10030800	C	-1.25583600	1.73962300	0.01736400
C	3.15787700	-0.04921100	0.03368100	C	3.34232300	-0.14878200	-0.01491200
F	3.93166300	-1.13237900	0.22247500	F	3.98951600	-0.94879000	-0.89907900
F	3.46821500	0.83699500	1.00118700	F	3.90194500	-0.42232900	1.19404800
F	-0.94141300	2.66436100	-0.56443600	F	-0.54969100	2.84965200	-0.35652000
F	-2.06624700	1.87020600	1.09823100	F	-1.74102500	2.02569900	1.23893800
F	-2.58049400	1.30379700	-0.93322900	F	-2.30200400	1.69390000	-0.83103700
F	3.53528400	0.50913500	-1.13541100	F	3.70222100	1.11895300	-0.31303700
F				F	-3.27340200	-0.33962300	0.91184100
no imaginary frequencies		-1082.003555		no imaginary frequencies		-1181.937702	

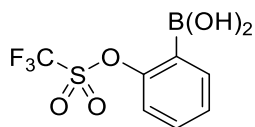
FIA _{ni} (kJ.mol ⁻¹)	243.4
FIA _{COF₂} (kJ.mol ⁻¹)	269.9



3.40

ω B97xd/6-31++g(d,p)											
Lewis acid			Charge 0			Fluorine complex			Charge -1		
C	2.7376528956	1.2241523662	0.8305831256	C	2.2934067991	0.6867812320	0.8267421329				
C	1.8088199632	2.2217708600	1.1283478128	C	1.9808851735	2.0092602526	1.1358503867				
C	0.4678504851	2.0509592607	0.7898338219	C	0.8685916274	2.6137657302	0.5648507197				
C	0.0486621682	0.8813071448	0.1516802588	C	0.0667246948	1.8978301230	-0.3176115028				
C	0.9771843015	-0.1302749920	-0.1704111113	C	0.3506064012	0.5601587574	-0.6467282816				
C	2.3363043429	0.0459285654	0.1776342541	C	1.4952492936	-0.0699816136	-0.0634813497				
O	0.6030850269	-1.2724489881	-0.8016360460	O	-0.4741982722	0.0179036298	-1.5843680559				
B	3.4228623368	-1.0709544919	-0.1159440992	B	1.9690619481	-1.5696794577	-0.3872003384				
O	4.7899966693	-0.9068659806	0.3719711011	O	3.2683110539	-1.8801255087	0.2532570343				
O	3.0609330479	-2.3177282912	-0.7878357564	O	0.9883611848	-2.5201472168	0.1452688827				
H	3.7717127861	1.3785093964	1.1137735796	H	3.1765895073	0.2703973488	1.2919763938				
H	2.1297609901	3.1277787908	1.6263408787	H	2.6127411951	2.5692603731	1.8139544120				
H	-0.2491022318	2.8281776761	1.0228665331	H	0.6337671511	3.6445351320	0.8015774713				
H	-0.9974410843	0.7892764812	-0.0940192693	H	-0.7861270904	2.3947300951	-0.7646994785				
H	4.7813099072	-1.3255578163	1.2706282601	H	3.9743755493	-1.6390133864	-0.3972700382				
H	3.2299714910	-2.1438261130	-1.7479387760	H	1.2420051557	-3.4054499273	-0.2311619229				
S	-0.8556060229	-2.1177241410	-0.5681300520	S	-1.4933878594	-1.3573009973	-1.5982173282				
O	-1.7212444886	-0.9917949230	-1.5355289178	O	-1.2593996842	-2.8935708718	-0.8736031916				
O	-1.3275951126	-3.3680268715	-1.6457720032	O	-2.2845559421	-0.8104166714	-0.1754009290				
C	0.0416734936	-3.3380309789	0.4452846499	C	-0.7329047837	-1.9196858422	-3.1684590450				
H	-0.6770406035	-4.0096253516	0.9540281569	H	-1.4128689226	-1.6651127772	-4.0059363329				
H	0.7792565362	-3.8997253591	-0.1670206042	H	0.2422549717	-1.4261188956	-3.3566155438				
H	0.5746925974	-2.8113042351	1.2644198125	H	-0.5658156197	-3.0163317599	-3.1787921443				
				F	2.1021365762	-1.7324056882	-1.8300781679				
no imaginary frequencies			-1071.066782	no imaginary frequencies			-1170.989718				

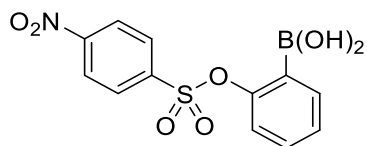
FIA _{ni} (kJ.mol ⁻¹)	213.9
FIA _{iCOF₂} (kJ.mol ⁻¹)	240.5



3.41

ω B97xd/6-31++g(d,p)							
Lewis acid		Charge 0		Fluorine complex		Charge -1	
C	1.89989500	2.82192100	-0.20454600	C	2.88753500	1.18042000	0.31096400
C	3.04897200	2.19115800	0.26506400	C	2.71208000	2.55979500	0.30661900
C	3.10228700	0.80204700	0.32174800	C	1.49778900	3.10904500	-0.11172600
C	2.02767800	-0.00178500	-0.08848200	C	0.47689100	2.25626300	-0.50985800
C	0.89078700	0.67729100	-0.53156900	C	0.70478100	0.88249600	-0.48247400
C	0.80604300	2.06003200	-0.60189700	C	1.88962100	0.27374100	-0.09375900
H	1.84790100	3.90439300	-0.25907800	O	-0.38951000	0.11292900	-0.99613300
H	3.90261900	2.78005500	0.58416500	B	2.22815600	-1.35047700	-0.00296600
H	3.99893700	0.31343800	0.68908300	O	2.26909100	-1.79480300	1.38985100
H	-0.10315000	2.52262200	-0.96851800	O	1.23312900	-2.06934300	-0.79630400
O	-0.23360800	-0.02542400	-1.01305100	H	3.83668900	0.75946600	0.63063300
B	2.17813300	-1.56792300	-0.03477800	H	3.52120600	3.21288600	0.62454700
O	3.22522700	-2.05590100	0.69960200	H	1.34588900	4.18465400	-0.12732800
H	3.33239000	-3.00920100	0.70586300	H	-0.48163000	2.63736800	-0.84717200
O	1.30394000	-2.33965700	-0.74506200	H	1.38498400	-1.69667700	1.75312200
H	1.36991300	-3.29146400	-0.64519700	H	1.32182700	-3.00465700	-0.59927800
S	-1.21576900	-0.81947600	-0.01701900	S	-1.27067600	-0.82116800	-0.07032900
O	-0.59909100	-1.04706700	1.26767500	O	-1.82812000	-1.88380500	-0.86650200
O	-1.85267400	-1.85085300	-0.78940600	O	-0.73876900	-1.00759300	1.26012700
C	-2.50772800	0.50098300	0.24750000	C	-2.70366700	0.34826400	0.18467500
F	-3.49654300	-0.01248600	0.97017100	F	-3.21184300	0.75238800	-0.98254300
F	-2.98425700	0.91880900	-0.91955400	F	-3.66869700	-0.27720100	0.86814400
F	-1.97974800	1.53509100	0.89770500	F	-2.33130400	1.42694800	0.87662700
				F	3.55676900	-1.53782400	-0.52326900
no imaginary frequencies		-1368.715185		no imaginary frequencies		-1468.642034	

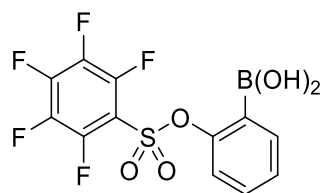
FIA _{ni} (kJ.mol ⁻¹)	224.2
FIA _{iCOF2} (kJ.mol ⁻¹)	250.7



3.42

ω B97xd/6-31++g(d,p)							
Lewis acid		Charge 0		Fluorine complex		Charge -1	
C	2.60066000	-2.95843000	0.80758800	C	1.63865000	-1.63039200	2.79714300
C	1.56817100	-2.70250200	-0.08935900	C	2.00970600	-1.94398700	1.48947300
C	1.37421400	-1.43051500	-0.64972600	C	2.06477600	-0.99107400	0.46041000
C	2.26141800	-0.42831600	-0.24271100	C	1.71065600	0.30019300	0.85348200
C	3.30232800	-0.65640300	0.64853600	C	1.36202300	0.66850200	2.14916200
C	3.47147500	-1.93407600	1.17262400	C	1.31999400	-0.31688100	3.13230200
H	2.72690700	-3.95370700	1.22116300	H	1.60552900	-2.40866000	3.55548100
H	0.88791200	-3.50114300	-0.36842000	H	2.26860700	-2.96754500	1.23488000
H	3.95289900	0.16237600	0.93175300	H	1.12961300	1.70234600	2.37889400
H	4.28006900	-2.12438200	1.87088500	H	1.04529400	-0.05269700	4.14974900
B	0.20795900	-1.22992200	-1.68808900	B	2.63399600	-1.38704200	-1.05144300
O	2.10061900	0.86365300	-0.75979200	O	1.75160000	1.29747900	-0.15789700
O	0.32687600	-0.29089000	-2.67207000	O	1.67754200	-1.03502300	-2.09375800
H	-0.40778700	-0.22388800	-3.28619600	H	2.17967500	-0.63657100	-2.80838800
O	-0.87224800	-2.06452000	-1.54781300	O	3.90059800	-0.71538400	-1.33753800
H	-1.56481900	-1.98540700	-2.20782600	H	4.61379400	-1.21734500	-0.94015500
S	1.40236600	2.00086700	0.17768400	S	0.50913200	2.26781600	-0.42062300
O	2.03210000	2.00070400	1.48163200	O	0.37857200	3.24100800	0.65614000
O	1.36746400	3.17667700	-0.65751200	O	0.67049900	2.74180300	-1.77880900
C	-0.24844300	1.35042100	0.35696500	C	-0.91215000	1.17843500	-0.32260900
C	-0.50982500	0.44793500	1.38385300	C	-1.99558000	1.58338900	0.45239800
C	-1.21358600	1.70449100	-0.58204000	C	-0.90846800	-0.01472900	-1.03887300
C	-1.76776800	-0.13756800	1.46365400	C	-3.12678600	0.77975300	0.50368400
H	0.26319800	0.19861700	2.10170800	H	-1.94163100	2.51069100	1.01097700
C	-2.47167000	1.12174200	-0.50493900	C	-2.03772800	-0.82491300	-0.97795800
H	-0.97234200	2.41944600	-1.36025100	H	-0.01896600	-0.33541800	-1.59419500
C	-2.71550700	0.20317200	0.50957500	C	-3.12430200	-0.40974100	-0.21702500
H	-2.01017500	-0.85599500	2.23608300	H	-3.99271900	1.05591800	1.09152500
H	-3.25388900	1.36588200	-1.21297200	H	-2.06807800	-1.77072700	-1.50378400
N	-4.03676500	-0.44789600	0.56521600	N	-4.32139800	-1.26213300	-0.16090100
O	-4.78524800	-0.28349100	-0.38720000	O	-4.32391500	-2.29374600	-0.81635700
O	-4.29844700	-1.11594500	1.55162300	O	-5.25716600	-0.89180400	0.53798700
				F	2.85844500	-2.82454500	-1.02546400
no imaginary frequencies		-1467.125260		no imaginary frequencies		-1567.062398	

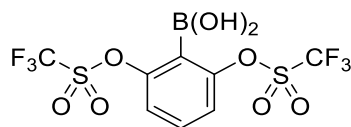
FIA _{ni} (kJ.mol ⁻¹)	251.2
FIA _{/COF₂} (kJ.mol ⁻¹)	277.7



3.43

ω B97xd/6-31++g(d,p)							
Lewis acid		Charge 0		Fluorine complex		Charge -1	
C	-5.22668300	-0.49491900	-0.60507000	C	3.45937000	2.05917100	-0.59785400
C	-4.43761400	0.64840900	-0.69131600	C	2.36239200	2.13571000	0.25152800
C	-3.04016100	0.59405400	-0.57778400	C	1.69702100	0.99976700	0.75180600
C	-2.49246800	-0.67097300	-0.35806200	C	2.22730100	-0.20893000	0.31387000
C	-3.25081100	-1.82828100	-0.25439600	C	3.33319600	-0.33686300	-0.52562900
C	-4.63299800	-1.73571600	-0.38671200	C	3.95689000	0.81315100	-0.98699300
H	-6.30426800	-0.41663300	-0.70569900	H	3.93246300	2.96905400	-0.95885200
H	-4.90725800	1.61402900	-0.84843200	H	1.98450400	3.10780600	0.55500400
H	-2.75528800	-2.77584200	-0.07581700	H	3.67134200	-1.32485800	-0.81781400
H	-5.24099100	-2.63165700	-0.31471600	H	4.81503500	0.73849400	-1.64888200
B	-2.20725300	1.92506700	-0.68860400	B	0.44411900	1.27036700	1.80418900
O	-0.87251600	1.88711100	-0.99780300	O	-0.51402400	2.12392200	1.11381800
H	-0.43046400	2.73933300	-0.99366800	H	-1.19450700	2.35577600	1.75125900
O	-2.91184400	3.08658600	-0.51251100	O	-0.24742800	0.09092400	2.31067600
H	-2.42099900	3.90619600	-0.59941500	H	0.32206300	-0.41135100	2.89580200
O	-1.09750600	-0.81808900	-0.27242100	O	1.64521200	-1.42596300	0.77043600
S	-0.40035400	-0.62674800	1.17966600	S	0.63826200	-2.22088900	-0.19501100
O	-0.92340900	0.55064900	1.82915100	O	1.26419400	-2.47328300	-1.47768000
O	-0.37442700	-1.89128300	1.87604500	O	0.15625800	-3.32596400	0.59840300
C	1.23605700	-0.30630200	0.53035500	C	-0.68693500	-1.04575700	-0.46683800
C	1.91705400	-1.32941700	-0.13351300	C	-1.82374200	-1.03656100	0.34643800
C	1.86024600	0.93554000	0.64825600	C	-0.57618400	-0.06204100	-1.45374200
C	3.18614300	-1.12898000	-0.65738900	C	-2.82117700	-0.09192900	0.15830500
C	3.13269500	1.14345000	0.12800000	C	-1.57084400	0.88514900	-1.63973200
C	3.79569700	0.11226900	-0.52249000	C	-2.69085500	0.87178000	-0.82754600
F	1.28147400	1.96676000	1.24874800	F	0.47609800	0.00903700	-2.26082500
F	3.71487700	2.33400300	0.24866200	F	-1.44637900	1.81637100	-2.58817500
F	5.00797600	0.31297900	-1.01800900	F	-3.64662500	1.78458000	-0.99482400
F	3.81744500	-2.11348400	-1.28790500	F	-3.90788000	-0.09831300	0.93683200
F	1.36221400	-2.52107900	-0.30181300	F	-2.02507200	-1.94081000	1.28970100
F				F	1.03919100	1.97741200	2.93460300
no imaginary frequencies		-1758.742436		no imaginary frequencies		-1858.685125	

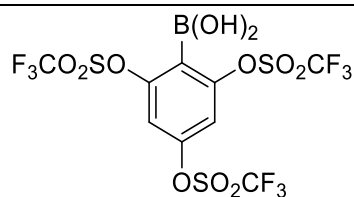
FIA _{ni} (kJ.mol ⁻¹)	265.8
FIA _{/COF₂} (kJ.mol ⁻¹)	292.3



3.44

ω B97xd/6-31++g(d,p)							
Lewis acid		Charge 0		Fluorine complex		Charge -1	
C	0.43701700	-3.04785200	-0.13427400	C	-0.00826000	-2.71299500	-0.24966400
C	-0.78124900	-2.49410900	0.24089300	C	-1.13513800	-2.00019600	0.14719000
C	-0.92978700	-1.11590400	0.18749900	C	-1.06062500	-0.61666800	0.19884500
C	0.06625300	-0.22917600	-0.22927400	C	0.06835800	0.14885700	-0.08980600
C	1.26857500	-0.84844100	-0.58193100	C	1.15315400	-0.63326400	-0.47470700
C	1.47414400	-2.22027600	-0.54627500	C	1.15123200	-2.02076300	-0.57144200
H	0.57909900	-4.12216300	-0.10374400	H	-0.03775500	-3.79572100	-0.31267600
H	-1.61299200	-3.10838900	0.56488600	H	-2.05754300	-2.50674300	0.40313200
H	2.43493600	-2.62285300	-0.84519500	H	2.04489100	-2.53801800	-0.90177800
O	2.34825400	-0.09689900	-1.07839400	O	2.35809500	-0.02437600	-0.92524000
B	-0.15776600	1.34128200	-0.30809400	B	0.03398300	1.81862900	0.06497100
O	-0.92102800	1.91866900	0.65814900	O	-0.26686300	2.11816100	1.43735500
H	-1.05111900	2.86652700	0.58414000	H	0.28542600	2.85900100	1.69423900
O	0.43755000	1.98562000	-1.35091100	O	1.28338500	2.45593800	-0.32722900
H	0.34110600	2.93987200	-1.38211300	H	1.26218000	2.66339800	-1.26308400
S	3.18052200	0.91956800	-0.14781200	S	3.41802100	0.61889800	0.08289300
O	2.38519500	1.37640400	0.96699400	O	2.93673300	0.74178600	1.43330700
O	3.88126300	1.80166400	-1.03794600	O	4.14730800	1.63485600	-0.63192400
C	4.44640300	-0.25942100	0.55562600	C	4.60937000	-0.81923100	0.14061000
F	5.32366600	0.43807800	1.26496600	F	4.06477700	-1.87648900	0.74780400
F	5.07300100	-0.89499200	-0.42685800	F	5.69879400	-0.45699500	0.82463300
F	3.84827000	-1.14957700	1.34182200	F	4.98565800	-1.18740000	-1.08646500
O	-2.17036000	-0.60048100	0.60733700	O	-2.22541500	0.06046000	0.65401000
S	-3.31224800	-0.42225800	-0.52014300	S	-3.38896000	0.48196400	-0.35161200
O	-2.85012300	0.45342400	-1.57093800	O	-3.89359800	1.78036100	0.00087300
O	-3.93647700	-1.68921000	-0.81248900	O	-3.12466200	0.05882600	-1.70528200
C	-4.46992300	0.54192400	0.58202800	C	-4.69663800	-0.68704000	0.28875700
F	-3.94725500	1.71542900	0.89830100	F	-4.89403800	-0.52350800	1.59519300
F	-4.73369100	-0.14549900	1.68335500	F	-4.36748900	-1.96491700	0.06806600
F	-5.59258800	0.72874100	-0.10496500	F	-5.84441300	-0.43990800	-0.35012300
				F	-1.01447500	2.23264500	-0.85142300
no imaginary frequencies		-2329.358708		no imaginary frequencies		-2429.296429	

FIA _{ni} (kJ.mol ⁻¹)	252.7
FIA _{iCOF₂} (kJ.mol ⁻¹)	279.3



3.45

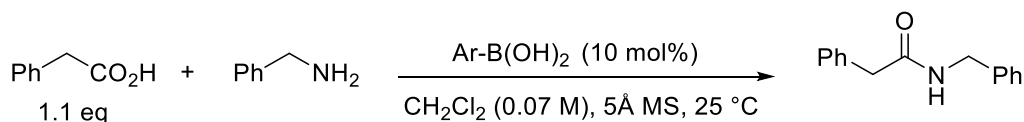
ω B97xd/6-31++g(d,p)							
Lewis acid				Fluorine complex			
Charge 0				Charge -1			
C	1.00079400	-1.18226300	0.04728200	C	-1.10811600	-1.12368600	0.12107500
C	-0.35084500	-1.19688200	-0.26180700	C	0.25048900	-1.14220900	0.40899300
C	-1.13115800	-0.05160100	-0.42937100	C	1.06505700	-0.02079900	0.58503700
C	-0.44106300	1.15322800	-0.29325500	C	0.37336300	1.17193500	0.39138900
C	0.91719000	1.24369000	-0.01704000	C	-0.97899100	1.29097800	0.08059100
C	1.60926800	0.05672000	0.16238300	C	-1.69545400	0.11784500	-0.04528800
H	1.55469100	-2.10270600	0.18022800	H	-1.68627500	-2.03574200	0.02910600
H	1.42427800	2.19908100	0.04454700	H	-1.44403600	2.25953800	-0.05556400
B	-2.68696700	-0.11091900	-0.75309600	B	2.70338600	-0.21255600	0.94000200
O	-3.06802500	-0.94031600	-1.76340000	O	2.78270500	-1.05492800	2.10509800
H	-4.01256600	-1.02204100	-1.91462300	H	3.65262700	-1.46019600	2.11223700
O	-3.49648700	0.69042000	-0.01584400	O	3.37646200	-0.82137300	-0.19290000
H	-4.43909100	0.63618100	-0.18757600	H	3.48683500	-0.16987800	-0.88922100
O	-1.15415400	2.32957400	-0.54622200	O	1.05328300	2.40882900	0.53296900
O	-0.93101100	-2.45914500	-0.44875800	O	0.84237100	-2.41218100	0.57705800
O	2.96413800	0.12046200	0.49783800	O	-3.05958300	0.17892800	-0.41658100
S	4.02360000	-0.00289700	-0.73518100	S	-4.14106800	0.34371500	0.76137000
S	-1.28033000	3.43032900	0.64522600	S	1.56467100	3.11168500	-0.80721400
S	-1.72152700	-3.12512900	0.79825800	S	0.83974800	-3.43265600	-0.64966900
O	-0.79885600	-3.50910600	1.83616000	O	-0.29063400	-4.33250000	-0.53595300
O	-2.91914400	-2.37168400	1.08682000	O	1.13751600	-2.79066100	-1.90600900
O	4.00473200	1.20204300	-1.52552100	O	-4.09975300	1.67131900	1.32597700
O	3.93277800	-1.31210100	-1.33271400	O	-4.18841000	-0.83086000	1.59827600
O	-0.10970200	4.27414000	0.64767500	O	0.51847300	3.95401100	-1.35003400
O	-1.78408700	2.82470000	1.84936100	O	2.29199900	2.20670500	-1.66373100
C	5.52796500	0.03495500	0.37129700	C	-5.60591100	0.27484300	-0.38969600
C	-2.20689500	-4.65320000	-0.15880400	C	2.32981600	-4.41213200	-0.09945300
C	-2.65459800	4.38311500	-0.18958900	C	2.78182500	4.27017400	0.00876200
F	-2.87990000	5.46315100	0.54940200	F	3.10284300	5.18713300	-0.91326000
F	-2.28022500	4.74600600	-1.40740200	F	2.21221900	4.88648800	1.04066500
F	-3.75798500	3.65624000	-0.25780200	F	3.87481500	3.65416200	0.39824900
F	5.57673000	1.17905700	1.03444500	F	-5.55479500	1.25825900	-1.27891900
F	5.49467300	-0.97982800	1.22049300	F	-5.65448500	-0.89165800	-1.01980900
F	6.59092100	-0.07353300	-0.41530800	F	-6.70302500	0.41528500	0.35361200
F	-1.12630900	-5.29043500	-0.58005900	F	2.13527700	-4.88869300	1.12667800
F	-2.97035000	-4.32580800	-1.18929000	F	3.43495500	-3.70455000	-0.13751800
F	-2.89041900	-5.43165500	0.67222400	F	2.43738300	-5.44409900	-0.94799000
F				F	3.25619200	1.09713400	1.18605100
no imaginary frequencies				no imaginary frequencies			
-3289.998718				-3389.947945			

FIA _{ni} (kJ.mol ⁻¹)	283.0
FIA _{COF₂} (kJ.mol ⁻¹)	309.5

❖ Summary of Gibbs Free Energies and FIA data:

Catalyst	$G_{\text{Lewis acid}}$ (a.u.)	G_{complex} (a.u.)	FIA_{ni} (kJ.mol ⁻¹)	$\text{FIA}_{\text{COF}_2}$ (kJ.mol ⁻¹)
3.34	-828.633042	-928.545614	186.7	213.2
3.35	-813.392501	-913.310571	201.1	227.7
3.36	-1051.144696	-1151.067402	213.3	239.8
3.37	-1388.111653	-1488.041899	233.1	259.6
3.38	-1694.214970	-1794.150030	245.8	272.3
3.39	-1694.214445	-1794.149665	246.2	272.7
3.40	-1188.900522	-1288.826970	213.9	240.5
3.41	-1368.715185	-1468.642034	224.2	250.7
3.42	-1467.125260	-1567.062398	251.2	277.7
3.43	-1758.742436	-1858.685125	265.8	292.3
3.44	-2329.358708	-2429.296429	252.7	279.3
3.45	-3289.998718	-3389.947945	283.0	309.5
3.28	1082.003555	-1181.937702	243.4	269.9

3.4.2 Determination of reaction rates



- In a 25 mL flask, under argon, phenylacetic acid 98.50% (76 mg, 0.55 mmol, 1.1 equiv.), boronic acid (0.05 mmol, 10 mol%), and 1 g of activated powdered 5 Å molecular sieves were introduced. To this mixture, 1,1,2,2-tetrachloroethane (53 µL, 0.50 mmol, 1 equiv.) and dry CH₂Cl₂ (7 mL, 0.0714 M) were added, and the mixture was stirred vigorously for 15 minutes at 25 °C. Next, benzylamine 99% (55 µL, 0.50 mmol, 1 equiv.) was introduced and the reaction was stirred at 25 °C.
- The sampling was performed by taking 0.10 mL of the reaction mixture at t = 1 h, 2 h. To each sample, 0.35 mL of CDCl₃ was added and the % NMR yield was determined from ¹H NMR integrations. The % NMR yield was determined by integrating the peak at δ 5.96 ppm (s, 2H) for the internal standard (1,1,2,2-tetrachloroethane) and the signals of the amide at δ 4.4 ppm (d, 2H, CH₂-NH), and 3.6 ppm (s, 2H, CH₂-C-C=O).
- The concentration of the amide was determined as follows: 0.0714 M × (% NMR yield/100)

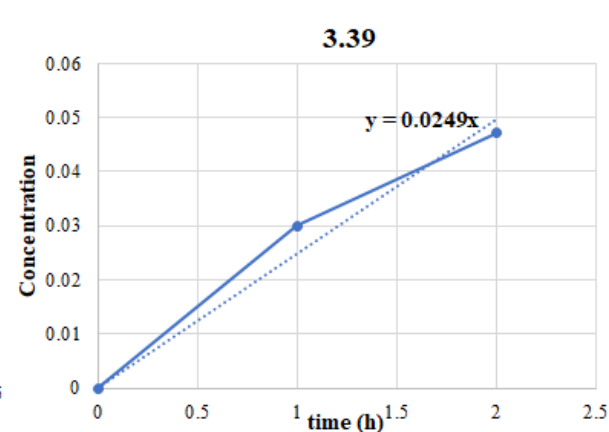
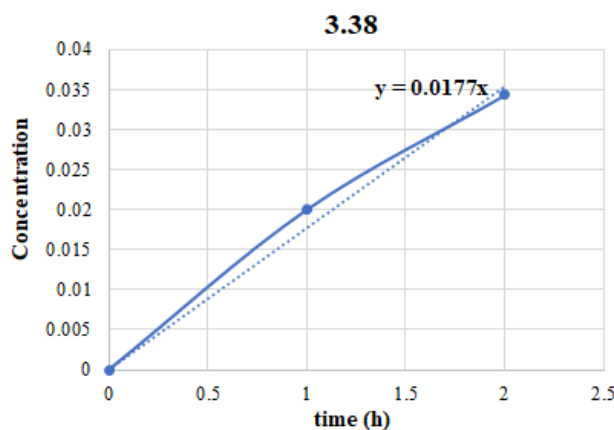
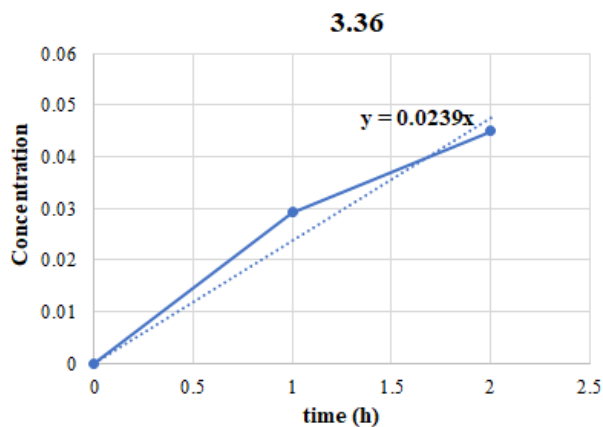
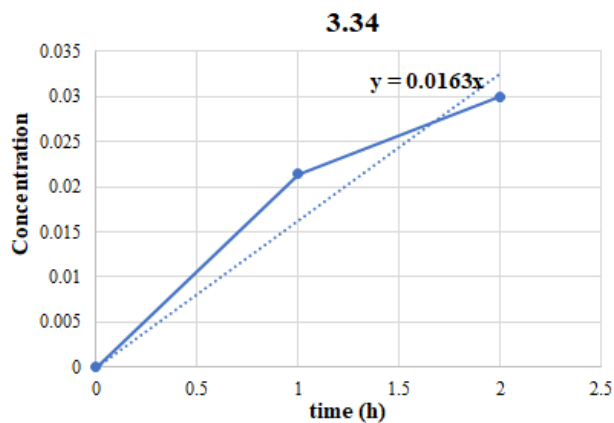
- Reaction rate is the y intercept of the trendline in the plot of concentration versus time.

- **Raw kinetic data:**

	Boronic acid 3.34		Boronic acid 3.36	
Time (h)	% NMR yield	[amide] (M)	% NMR yield	[amide] (M)
1	30	0.0214	41	0.0293
2	42	0.0300	63	0.0450

	Boronic acid 3.38		Boronic acid 3.39	
Time (h)	% NMR yield	[amide] (M)	% NMR yield	[amide] (M)
1	28	0.0200	42	0.0300
2	48	0.0343	66	0.0471

- **Graphs of amide concentration versus time**



**Chapter 4. Novel class of (sulfonate)-
functionalized arylboronic acid catalysts for
amide bond formation**

Table of Contents

4.1 Introduction	165
4.2 Preparation of the (sulfonyloxy)phenylboronic acids	166
4.2.1 Mono-substituted-(sulfonyloxy)phenylboronic acids	166
4.2.2 2,6-Bis(sulfonyloxy)phenylboronic acids	169
4.2.3 2,4-Bis(sulfonyloxy)phenylboronic acid.....	178
4.2.4 2,4,6-Tris-(sulfonyloxy)phenylboronic acid	179
4.3 Kinetic Studies for catalytic activity evaluation	180
4.3.1 Catalytic activity assessment of mono-substituted arylboronic acids.....	180
4.3.2 Catalytic activity assessment of di-substituted arylboronic acids.....	182
4.3.3 Comparative catalytic activity study with the state-of-the-art boronic acids.....	183
4.4 Investigation of the catalyst stability during the amidation reaction	185
4.4.1 The case of 2-(triflyloxy)phenylboronic acid.....	185
4.4.2 The case of 2,6-bis(triflyloxy)phenylboronic acid.....	187
4.5 Selection of catalyst for scope examination	189
4.6 Optimization of reaction conditions for low-temperature amide synthesis	190
4.6.1 Effect of the nature of molecular sieves.....	190
4.6.2 Catalyst loading.....	195
4.7 Scope and limitations of low-temperature amide synthesis	196
4.8 Optimization of high-temperature amidation conditions	198
4.8.1 Effect of catalyst loading.....	198
4.8.2 Effect of the solvent	199
4.8.3 Effect of the solvent concentration.....	201
4.9 Scope of the high-temperature amides synthesis	202
4.10 Mechanistic investigation.....	204
4.11 Conclusions	211
4.12 Future Perspective	212

4.13 Experimental Section	214
4.13.1 General Methods	214
4.13.2 Preparation and characterization of <i>ortho</i> -(sulfonyloxy)phenylboronic acids.....	215
4.13.2.1 General procedure A for the preparation of 2-(sulfonyloxy)phenylboronic acid pinacol ester.....	215
4.13.2.2 General procedure B for the deprotection of 2-(sulfonyloxy)phenylboronic acid pinacol ester with NaIO ₄	215
4.13.2.3 General procedure C for the deprotection of 2-(sulfonyloxy)phenylboronic acid pinacol ester with diethanolamine.....	216
4.13.3 Preparation and characterization of <i>para</i> -(sulfonyloxy)phenylboronic acid and its pinacol ester.....	224
4.13.4 Synthesis and characterization of 2,6-bis(sulfonyloxy)phenylboronic acid and its synthetic intermediates	226
4.13.5 Synthesis and characterization of 2,4-bis(mesyloxy)phenylboronic acid.....	235
4.13.6 General procedure for kinetic studies and raw kinetic data	239
4.13.7 Synthesis of the protodeboration products	240
4.13.8 Scope of the low-temperature amides synthesis	242
4.13.8.1 General procedure D for Low-temperature amide synthesis	242
4.13.8.2 Synthesis and characterization of amide substrates	242
4.13.9 Scope of the High-temperature amide synthesis	253
4.13.9.1 General procedure E for amide synthesis under azeotropic reflux	253
4.13.9.2 Synthesis and characterization of amide substrates	253
4.13.10 Synthesis and characterization of mixed anhydride intermediates	261

4.1 Introduction

The boronic acid-catalyzed direct amidation reaction has been one of the most extensively studied approaches for amide bond formation. A multitude of arylboronic acid catalysts have been reported since the seminal work of Ishihara *et al.* on the catalytic application of arylboronic acids in amides synthesis.⁴⁴ Later, a milestone was achieved by Hall *et al.* when they reported the first room-temperature amide synthesis using 2-iodo (**4.1**) and 2-iodo-5-methoxy- (**4.2**) phenylboronic acids (Figure 22).^{54,55} This study has encouraged the search for boronic acid catalysts that could allow the dehydrative condensation of carboxylic acids and amines at room temperature. The reported boronic catalysts that enabled amide synthesis at 25 °C are displayed in Figure 22.^{57,60,61,64,67}

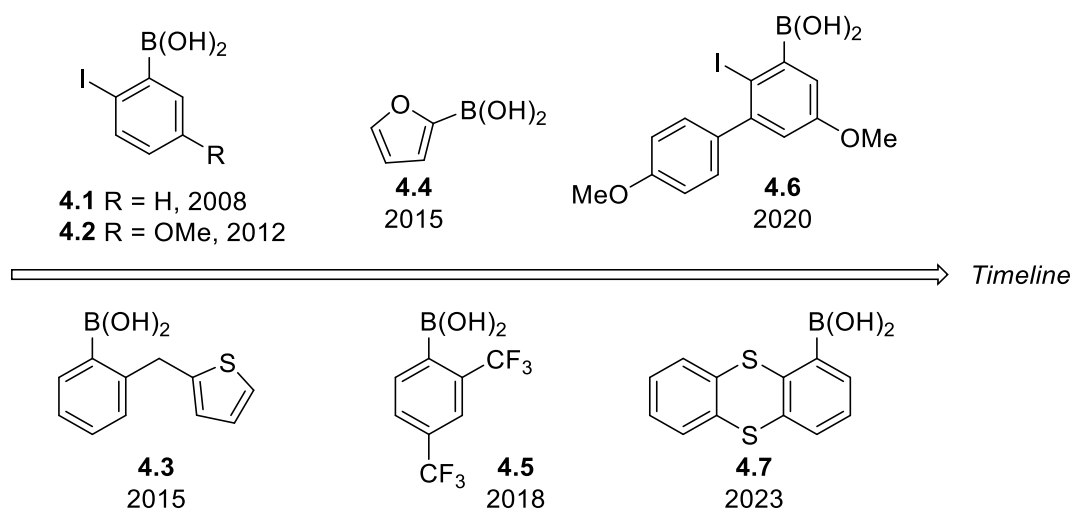
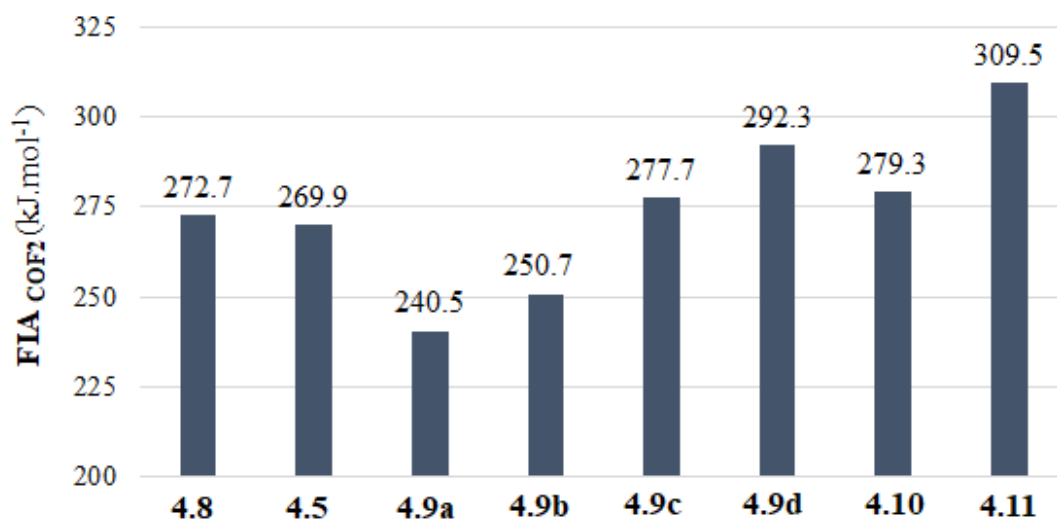
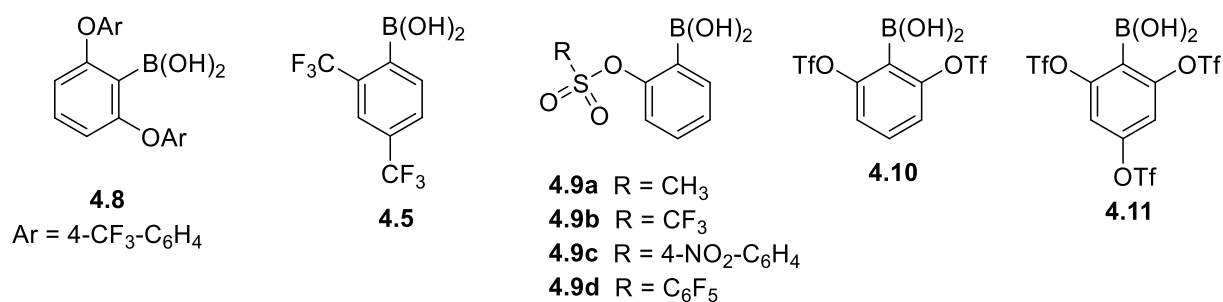


Figure 22

In this context, we are interested in developing arylboronic acid catalysts that promote amide bond formation at 25 °C and compete with the existing state-of-the-art boronic acids. In Chapter 2, the catalytic efficiency of a group *ortho*-(aryloxy)phenylboronic acids was examined. However, these catalysts did not compare favorably with the current state-of-the-art boronic acids, represented by **4.2** and **4.5**. Later, in Chapter 3, the Lewis acidity estimation of *ortho*-(sulfonate)phenylboronic acids, using fluorine ion affinity, revealed that this class of arylboronic acids (**4.9-4.11**) have a FIA_{COF_2} range of 240.5-309.5 $\text{kJ}\cdot\text{mol}^{-1}$, which encompasses that of the best-performing biarylether-based boronic acid **4.8** (272.7 $\text{kJ}\cdot\text{mol}^{-1}$), and more importantly, the highly competent boronic acid **4.5** (269.9 $\text{kJ}\cdot\text{mol}^{-1}$) (Figure 23).



FIA calculations were performed at the ω B97XD/6-31++(d,p) level of theory

Figure 23

The encouraging FIA profile prompted the preparation and evaluation of the *ortho*-(sulfonyloxy)phenylboronic acids **4.9-4.11**.

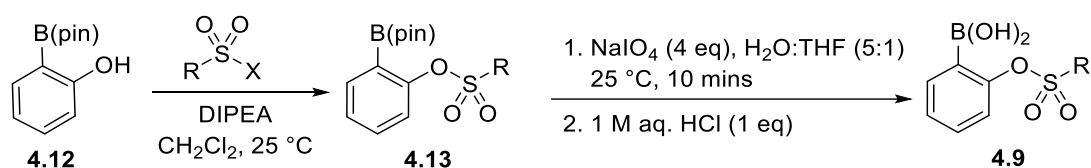
4.2 Preparation of the (sulfonyloxy)phenylboronic acids

4.2.1 Mono-substituted-(sulfonyloxy)phenylboronic acids

2-(Sulfonyloxy)phenylboronic acids **4.9a-d** were prepared through a facile and reliable strategy (Scheme 109). Firstly, the substituted pinacol boronates **4.13a-d** were obtained in 92-99% yields from the reaction of commercially available 2-(hydroxy)phenylboronic acid pinacol ester **4.12** with the suitable sulfonyl chloride or anhydride.¹⁵⁶ Secondly, the pinacol boronates **4.13**

¹⁵⁶ Sumida, Y.; Kato, T.; Hosoya, T. *Org. Lett.* **2013**, *15*, 2806–2809.

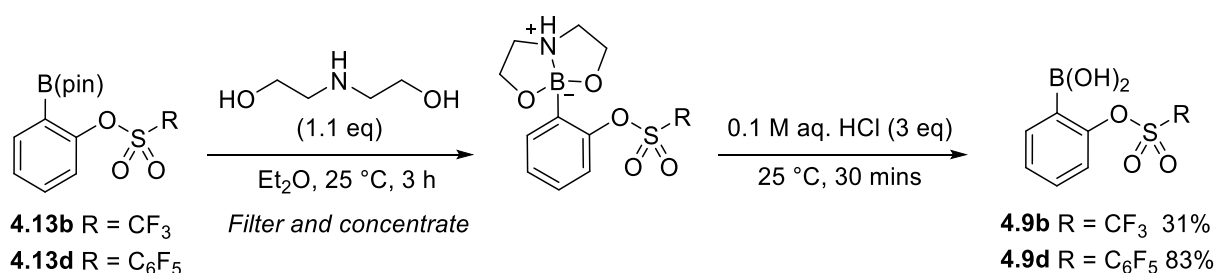
were deprotected via electrophilic oxidative cleavage, using sodium periodate,¹⁵⁶ to furnish the target boronic acids **4.9** in variable yields (33-80%) depending on the nature of the substrate.



RSO ₂ X	4.13 (yield)	4.9 (yield)
CH ₃ SO ₂ Cl	4.13a (99%)	4.9a (80%)
(CF ₃ SO ₂) ₂ O	4.13b (92%)	4.9b (37%)
4-NO ₂ C ₆ H ₄ SO ₂ Cl	4.13c (93%)	4.9c (33%)
C ₆ F ₅ SO ₂ Cl	4.13d (98%)	4.9d (40%)

Scheme 109

Due to the inefficient deprotection of pinacol boronates **4.13b-d** (33-40%) using the oxidative cleavage method (Scheme 109), alternative protocols were evaluated. A two-step deprotection procedure via transesterification with diethanolamine followed by acidic hydrolysis was first attempted.¹⁵⁷ When this method was applied for the deprotection of **4.13b**, the diethanolamine complex was obtained in a quantitative yield, but the subsequent acidic hydrolysis caused side product formation (> 50%)¹⁵⁸. As a consequence, the boronic acid **4.9b** was isolated in a non-improved 31% yield (Scheme 110). On the other hand, this protocol offered a substantial improvement in the deprotection of **4.13d** where the boronic acid **4.9d** was isolated in an 83% yield (Scheme 110).

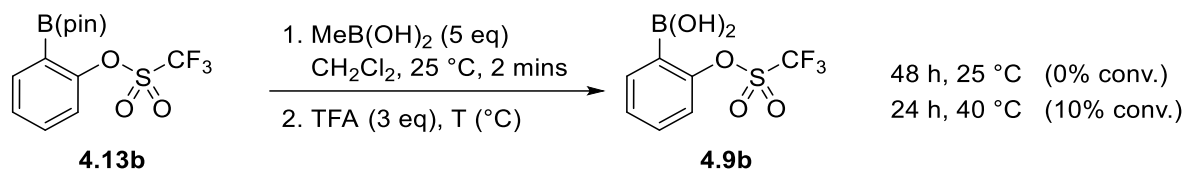


Scheme 110

¹⁵⁷ Sun, J.; Perfetti, M. T.; Santos, W. L. *J. Org. Chem.* **2011**, *76*, 3571–3575.

¹⁵⁸ The % of side product is estimated roughly from ¹H NMR of the crude residue. The formed side products are unidentified, however, no protodeborylation product was observed.

Additionally, a monophasic transesterification with methylboronic acid was tested. This method has been described to facilitate product isolation by making use of the volatility of methylboronic acid and its pinacol ester.¹⁵⁹ Nonetheless, when this protocol was applied in the case of the deprotection of **4.13b**, no conversion into **4.9b** was observed at 25 °C, and most of **4.13b** was recovered unchanged (Scheme 111). Also, using a higher temperature of 40 °C resulted in only 10% conversion.

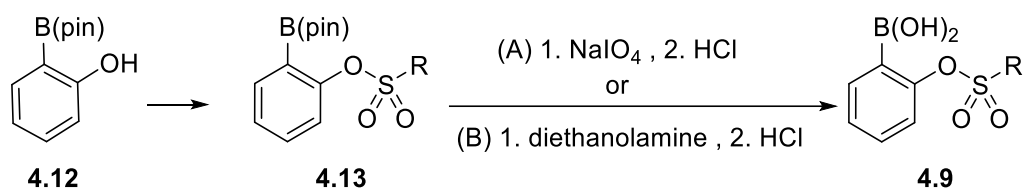


Scheme 111

In order to determine whether the absence of conversion with **4.13b** is due to the used reaction conditions or if it is substrate-dependent, the deprotection of **4.12**, which is one of the reported substrates with this protocol,¹⁵⁹ was reproduced. Therefore, the deprotection of pinacol boronate **4.12** was performed using MeB(OH)₂ (5 eq) and TFA (3 eq) for 1 h, at 25 °C, and it afforded the desired boronic acid in a 96% yield, which is consistent with the reported one (93%)¹⁵⁹. It can be suggested that due to the reduced electron density in the boronic acid **4.9b**, the electrophilic boron center has a high tendency to re-associate with the free pinacol, resulting in the regeneration of starting pinacol boronate.

As a result, with the exception of **4.13d**, where diethanolamine-transesterification works best, the oxidative cleavage protocol was adopted to deprotect the pinacol boronates **4.13a-c** (Scheme 112). Overall yields ranged from 31% to 81% depending on the nature of the sulfonate-group (Scheme 112).

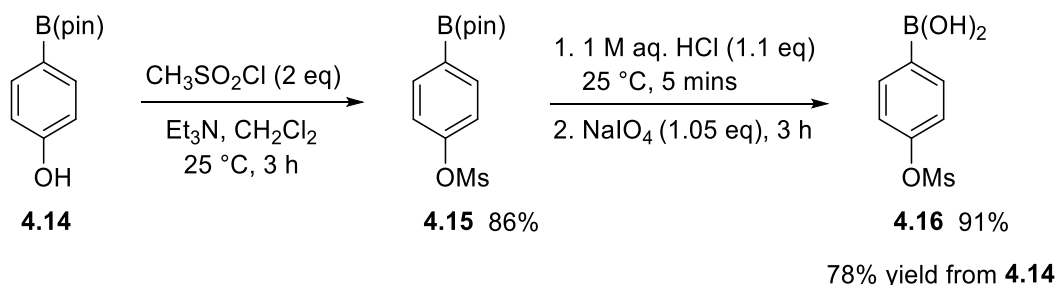
¹⁵⁹ Hinkes, S. P. A.; Klein, C. D. P. *Org. Lett.* **2019**, *21*, 3048–3052.



R	deprotection method	yield 4.9	overall yield
CH ₃	A	80%	79%
CF ₃	A	37%	34%
4-NO ₂ C ₆ H ₄	A	33%	31%
C ₆ F ₅	B	83%	81%

Scheme 112

Furthermore, *para*-regioisomer **4.16** was prepared to probe the role of the *ortho*-substituent as a key feature for the catalyst design. Starting from the commercially available pinacol ester **4.14**, the mesylation of **4.14** provided the pinacol boronate **4.15** in 86% yield (Scheme 113). The subsequent deprotection of **4.15** furnished the desired boronic acid **4.16** in 91% yield and an overall yield of 78% (from **4.14**) (Scheme 113).

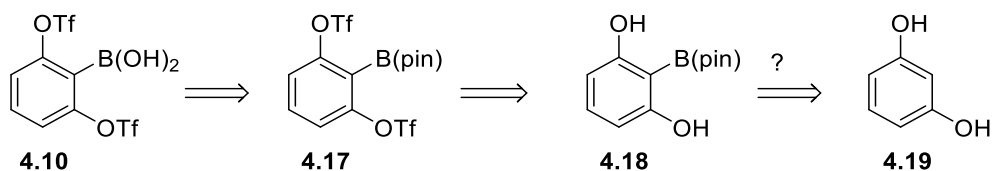


Scheme 113

4.2.2 2,6-Bis(sulfonyloxy)phenylboronic acids

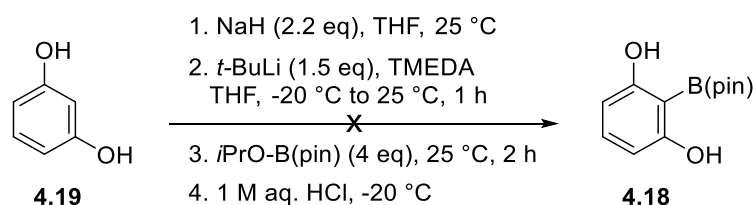
The 2,6-bis(sulfonyloxy)phenylboronic acid **4.10** represents an interesting target since it has FIA_{COF2} of 279.3 kJ.mol⁻¹, which is higher than that of its mono-triflate analog **4.9b** (250.7 kJ.mol⁻¹). Moreover, in Chapter 2, the 2,6-bis(aryloxy)phenyl boronic acid **4.8** displayed a superior catalytic performance to its mono-aryloxy derivative.

A synthetic route was developed for the preparation of 2,6-disubstituted boronic acid **4.10** where 2,6-dihydroxybenzeneboronic acid pinacol ester **4.18** was identified as a precursor (Scheme 114). It is worth noting that the pinacol boronate **4.18** is commercially available, however, at a very high price,¹⁶⁰ therefore, we opted to synthesize it from readily available resorcinol **4.19**.



Scheme 114

Preliminarily, a direct *ortho*-lithiation of resorcinol **4.19** with *t*-Buli, followed by electrophilic trapping of the anionic species with isopropoxyboronic acid pinacol ester, led to a complete recovery of the starting material **4.19** (Scheme 115). This suggests that either metalation did not occur or the generated tris-anion was not sufficiently stable to react with *i*PrO-B(pin). However, the phenoxide is recognized as a weak directing metalation group.¹⁶¹ *Ortho*-lithiation reactions involving a phenoxide as a directing *ortho*-metalation (DoM) group are usually not successful,¹⁶² or low yielding,¹⁶³ which was attributed to the reduced acidity of the *ortho*-hydrogen and the insolubility of lithium salts of phenols.¹⁶⁴



Scheme 115

An alternative path was considered, which involved the borylation of protected resorcinol. Initially, this path was investigated starting from dimethoxybenzene **4.20** since the methoxy

¹⁶⁰ 2,6-Di(hydroxy)benzeneboronic acid pinacol ester is supplied by Enamine (1 g for 591 USD) and Aurora Chemicals (1 mg for 1,590 USD).

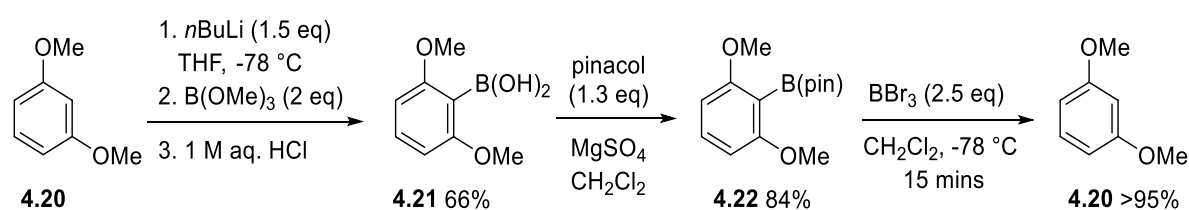
¹⁶¹ Gilman, H.; Morton Jr., J. W. The Metalation Reaction with Organolithium Compounds. In *Organic Reactions*; John Wiley & Sons, Ltd, **2011**; pp 258–304.

¹⁶² Gilman, H.; Bebb, R. L. *J. Am. Chem. Soc.* **1939**, 61, 109–112.

¹⁶³ Posner, G. H.; Canella, K. A. *J. Am. Chem. Soc.* **1985**, 107, 2571–2573

¹⁶⁴ Narasimhan, N. S.; Mali, R. S. *Synthesis* **1983**, 1983, 957–986.

group is a good directing *ortho*-metalation group.¹⁶⁵ First, the regioselective borylation of **4.20** was followed by the protection of the obtained boronic acid **4.21** in the form of a pinacol boronate **4.22** with a 55% yield (2 steps) (Scheme 116). Next, the demethylation of the methoxy group in the presence of a boronic acid or pinacol boronate moieties is not trivial and poorly described in the literature. There are few examples reported and they all include the use of BBr₃ at -78 °C,^{166,167} however, no yield was described in any of them. In our case, attempts of demethylation of pinacol boronate **4.22** using BBr₃ selectively yielded the protodeborylation product **4.20** (Scheme 116). It ought to be noted that demethylation of boronic acid **4.21** with BBr₃ was also tested and, similarly, resulted in complete C-B bond cleavage.



Scheme 116

In order to avoid the use of the strongly acidic boron tribromide, a methoxymethyl acetal (MOM) protecting group was used since it can be cleaved under milder acidic conditions using trifluoroacetic acid. First, the MOM groups were introduced in a 96% yield by nucleophilic substitution with freshly prepared methoxymethyl chloride (Scheme 117).¹⁶⁸ Next, the regioselective borylation of the MOM-protected resorcinol **4.23** provided the pinacol boronate **4.24** in 66% yield. Afterwards, the MOM-groups of **4.24** were deprotected with trifluoroacetic acid, which, while mild and quick, produced a considerable amount of degradation byproducts (~ 40%)¹⁶⁹. However, in this case, no protodeborylation product **4.23** was detected. Moreover, conducting the MOM-deprotection step at 0 °C or for a shorter reaction time of 15 mins did not improve the yield. The subsequent triflation of crude **4.18** furnished the bis(triflate)benzene

¹⁶⁵ For a review on directed *ortho*-metalation, see: Snieckus, V. *Chem. Rev.* **1990**, *90*, 879–933.

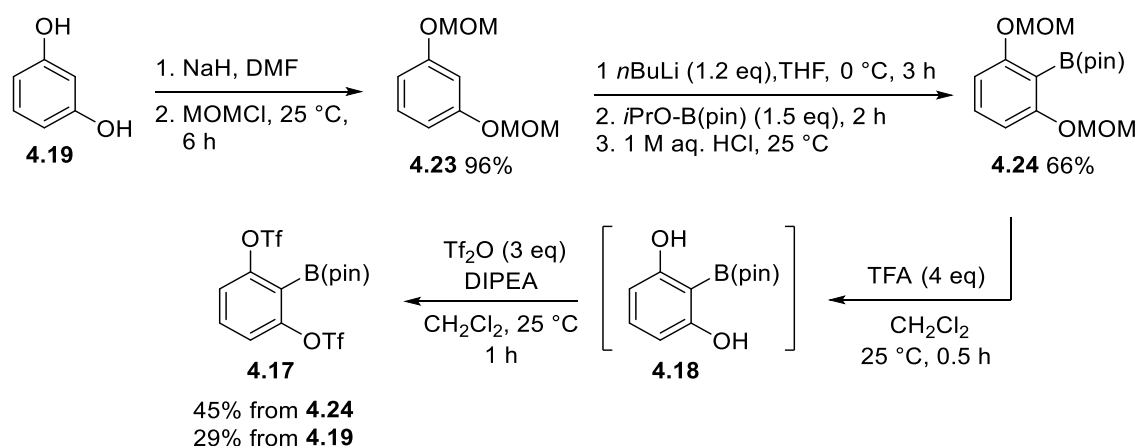
¹⁶⁶ Vishnumurthy, K.; Makriyannis, A. *J. Comb. Chem.* **2010**, *12*, 664–669.

¹⁶⁷ Makriyannis, A.; Vemuri, V. K. US10221164B2, March 5, 2019.

¹⁶⁸ Yamada, S.; Kawasaki, M.; Fujihara, M.; Watanabe, M.; Takamura, Y.; Takioku, M.; Nishioka, H.; Takeuchi, Y.; Makishima, M.; Motoyama, T.; Ito, S.; Tokiwa, H.; Nakano, S.; Kakuta, H. *J. Med. Chem.* **2019**, *62*, 8809–8818.

¹⁶⁹ % of degradation products is estimated from ¹H NMR of the crude residue. The crude residue was obtained after extraction with CH₂Cl₂ and H₂O.

pinacol boronate **4.17** in 45% yield (2 steps) (Scheme 117). Overall, the intermediate pinacol boronate **4.17** was obtained in 29% yield from resorcinol **4.19**.



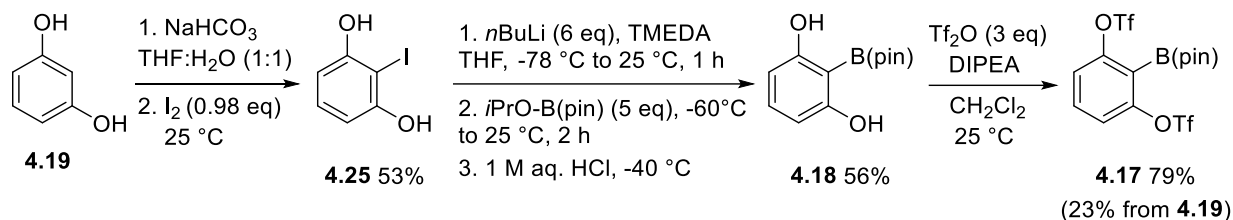
Scheme 117

The acidic deprotection protocols used for **4.22** and **4.24** demonstrated poor compatibility with the boronic acid group or its pinacol ester, hence resulting in undesired protodeborylation or degradation. Therefore, a protecting group-free synthesis was devised to avoid the use of acidic deprotection.

In the protecting group-free strategy, the precursor **4.18** is obtained from resorcinol **4.19** through a 2-iodoresorcinol intermediate **4.25** (Scheme 118). The selective iodination of resorcinol provided **4.25** in 53% yield.¹⁷⁰ This moderate yield results from the non-selective polyiodination side products. In an attempt to minimize the polyiodination, the reaction was conducted with a slight excess of resorcinol (1.02 eq), however, a similar 53% yield was obtained. Furthermore, the separation of 2-iodoresorcinol **4.25** from the polyiodination byproducts resulted in mass loss caused by their nearly identical polarities and solubilities, thus making purification by chromatography or crystallization difficult. Afterward, the lithium-iodine exchange and electrophilic trapping of the lithium tris-anion provided **4.18** in 56% yield (Scheme 118). This step necessitated the use of 6 equiv. of *n*BuLi whereby trials using 3, 4, or 5 equiv. produced mixtures of the halogenated starting material **4.25** and resorcinol **4.19**. Supposedly, the large quantity of *n*BuLi serves to solubilize the highly polar lithium tris-anion. Moreover, the generation of such tris-anion is not well documented. The only report described the halogen-metal exchange of resorcinols using 14 equiv. of *n*BuLi, followed by trapping the

¹⁷⁰ Thomsen, I.; Torssell, K. B. G.; Lund, H.; O'Reilly, K. P. J.; Ertan, A.; Kleinpeter, E. *Acta Chem. Scand.* **1991**, *45*, 539–542.

tris-anion with an electrophile (-CHO, -SMe) to give the desired products in variable yields (15-76%).¹⁷¹ In these cases, the protonation of the lithium carbanion was found to be difficult to avoid.

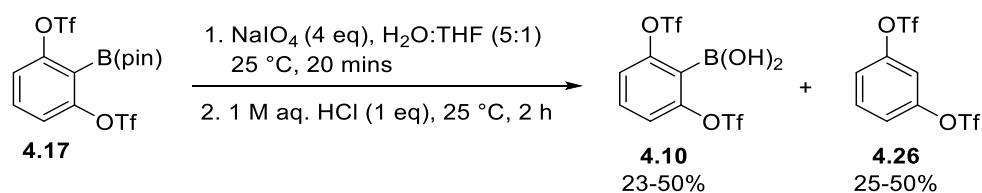


Scheme 118

Finally, the triflation of **4.18** afforded the desired product **4.17** in 79% yield (Scheme 118). This synthetic route provided the intermediate pinacol boronate **4.17** in a 23% overall yield from **4.19**.

On the whole, the first methodology (Scheme 117) provided the target pinacol ester **4.17** in a slightly higher overall yield (29%) than the protecting group-free one (23%) (Scheme 118), yet the latter generated the intermediate **4.17** in fewer steps.

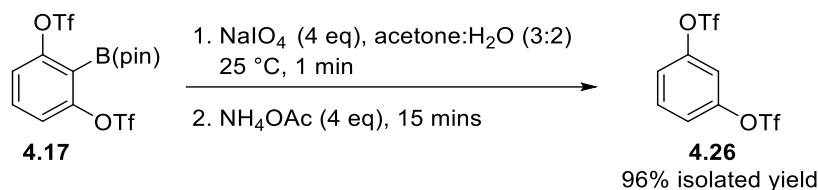
Subsequently, the deprotection of the pinacol ester **4.17** was performed, but it was not straightforward and required some optimization. First, the NaIO₄-mediated deprotection was implemented for the pinacol ester **4.17** (Scheme 119). However, the boronic acid **4.10** was obtained in variable yields, under the same conditions, that never exceeded 50%, accompanied by the formation of 1,3-bis(triflate)benzene **4.26** (25-50%) and degradation products each time.



Scheme 119

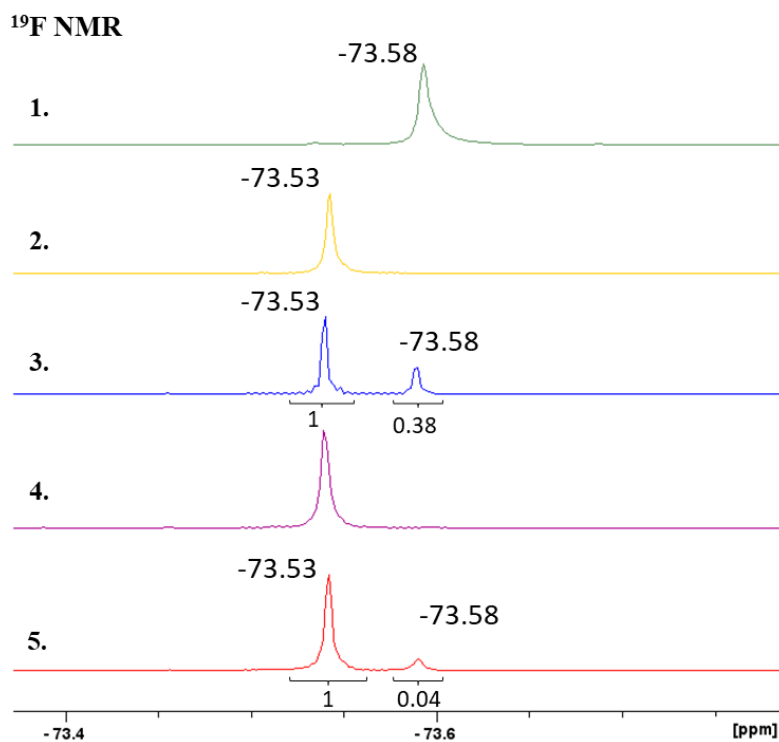
It was originally proposed that boronic acid **4.10** might be unstable in the presence of aqueous HCl (1 M). As a result, the use of a weaker acid, ammonium acetate, was examined (Scheme 120). Surprisingly, after 15 minutes, complete deboronation into **4.26** occurred under these conditions.

¹⁷¹ Saá, J. M.; Morey, J.; Suñer, G.; Frontera, A.; Costa, A. *Tetrahedron Lett.* **1991**, 32, 7313–7316.



Scheme 120

In order to determine the conditions responsible for the protodeborylation, control experiments were performed.¹⁷² Firstly, the addition of solid NaIO_4 (4 eq) to acetone: water solution of **4.17** caused a 73% protodeborylation into **4.26** (^{19}F $\delta = -73.53$ ppm) after 2 mins at 25 °C (Entry 3, Scheme 121). In this case, the medium was found to be mildly acidic (pH = 4). The successive introduction of NH_4OAc (4 eq) led to complete deboronation (^{19}F $\delta = -73.53$ ppm) (Entry 4, Scheme 121), which is in line with the previous result in Scheme 120.



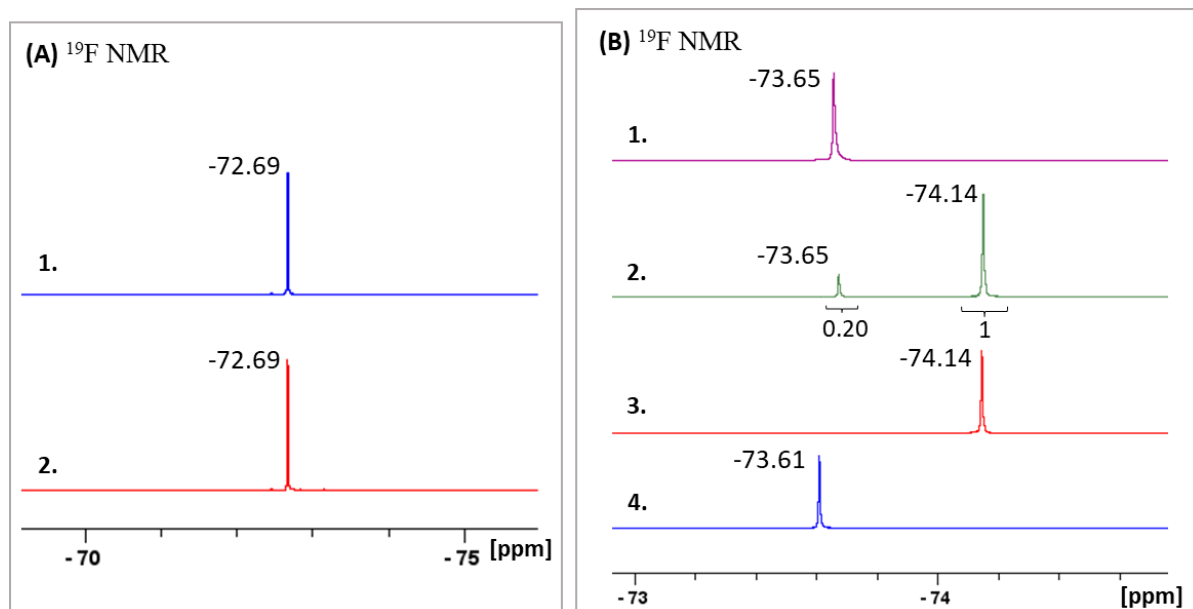
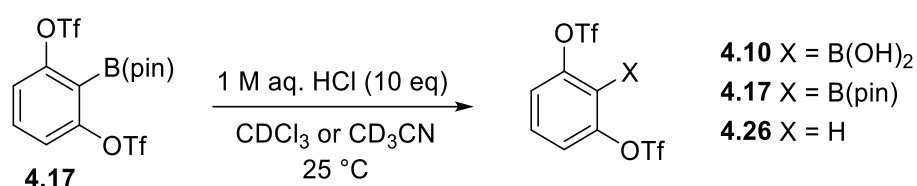
1. Pure **4.17** in acetone- d_6 ; 2. Pure **4.26** in acetone- d_6 ; 3. **4.17** (0.1 mmol) + NaIO_4 (4 eq), acetone: H_2O (3:2), 25 °C, 2 mins; 4. Mixture of entry 3 + NH_4OAc (4 eq), 25 °C, 15 mins; 5. **4.17** (0.1 mmol) + NH_4OAc (4 eq), acetone: H_2O (3:2), 25 °C, 10 mins

Scheme 121

¹⁷² In the control experiments, the % conversion of **4.17** into **4.26** or **4.10** was determined by ^{19}F NMR, and confirmed by ^1H NMR data. In all cases, the conversions determined from ^{19}F NMR matched exactly those from ^1H NMR.

At that point it was unclear if NH_4OAc participated to the deboronation of **4.17**. Therefore, NH_4OAc (4 eq) was added to **4.17** in acetone: water (pH = 7) and, after 10 mins, 96% conversion from **4.17** (^{19}F δ = -73.58 ppm) into **4.26** (^{19}F δ = -73.53 ppm) was detected (Entry 5, Scheme 121). This shows that both NaIO_4 and NH_4OAc caused the protodeboronation of **4.17**.

Next, the effect of aqueous HCl was investigated. The addition of an aqueous HCl solution (1 M, 10 eq) to a solution of **4.17** in CDCl_3 , followed by vigorous mixing, produced a biphasic medium in which no change was observed (^{19}F δ = -72.69 ppm) (Entry 2, Scheme 122A).



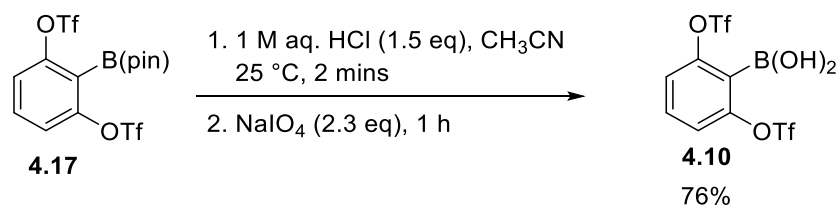
(A) 1. Pure **4.17** in CDCl_3 ; 2. **4.17** (0.1 mmol), 1 M aq HCl (10 eq), CDCl_3 , 25 °C, 30 mins
 (B) 1. Pure **4.17** in CD_3CN ; 2. **4.17** (0.1 mmol), 1 M aq HCl (10 eq), CD_3CN , 25 °C, 1 h; 3. Pure **4.10** in CD_3CN ; 4. Pure **4.26** in CD_3CN

Scheme 122

In contrast, when the same experiment was conducted in CD_3CN , 83% conversion into **4.10** was achieved in 1 h, which was determined by the formation of a new signal in ^{19}F NMR at -74.14 ppm relating to the boronic acid **4.10** (Entry 2, Scheme 122B). More importantly, protodeborylation was not detected, confirmed by the absence of the signal of **4.26** at -73.61 ppm (Entry 2, Scheme 122B).

The finding that 2,6-disubstituted boronic acid **4.10** has enhanced stability in aqueous HCl (1 M) is not unusual. To emphasize, Lloyd Jones has investigated the protodeboronation of fluorinated arylboronic acids in dioxane: water (1:1) with KOH (2 eq), at 70 °C.¹⁷³ In this study, the 2,6-di(fluoro)phenylboronic acid protodeborylated under neutral conditions in a solution of dioxane: water (1:1) before the addition of KOH. Hence, the solution of 2,6-di(fluoro)phenylboronic acid in dioxane: water (1:1) was acidified with TFA (10 mol%) before KOH addition to avoid C-B bond cleavage. This is consistent with our result, where boronic acid **4.10** protodeborylated under neutral (with NH₄OAc) or mildly acidic (with NaIO₄) conditions and that this undesired side reaction was circumvented when HCl (1 M) was introduced first.

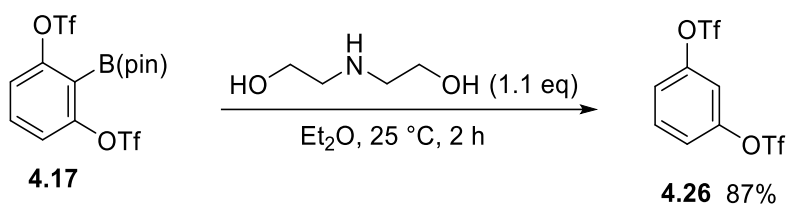
In light of these facts and the experimental findings, the electrophilic oxidative cleavage was re-attempted with a reverse order of addition, where HCl is added before NaIO₄ to avoid the protodeborylation pathway. Through applying this protocol, boronic acid **4.10** was isolated in a reproducible 76% yield (Scheme 123).



Scheme 123

It is worth noting that the deprotection of pinacol boronate **4.17** was examined with another strategy besides oxidative cleavage. When the transesterification of pinacol boronate **4.17** with diethanolamine was tested, it was observed that the addition of diethanolamine to a solution of **4.17**, in Et₂O, induced the precipitation of viscous oily material. When checked by ¹H NMR, the precipitated material comprised degradation products and diethanolamine. On the other hand, the Et₂O phase contained the protodeborylation product **4.26**, which was isolated in 87% yield, and no conversion into the boronic acid was detected (Scheme 124).

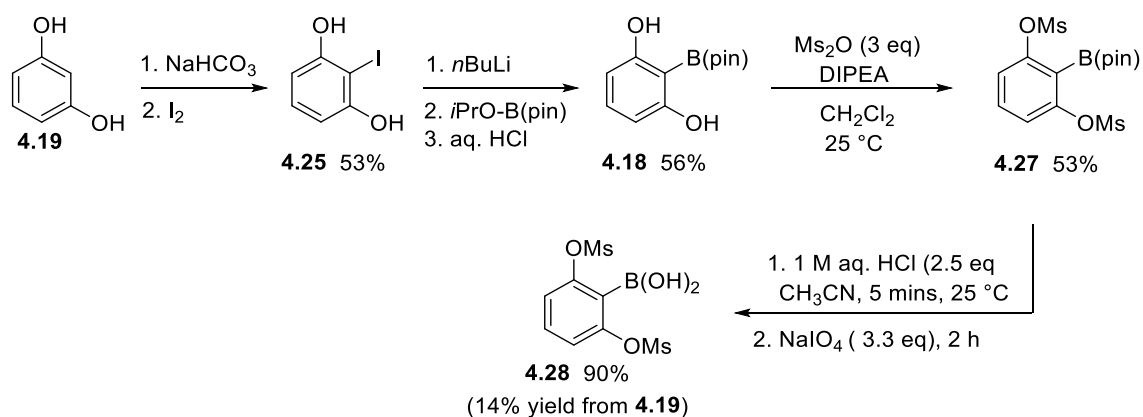
¹⁷³ Cox, P. A.; Reid, M.; Leach, A. G.; Campbell, A. D.; King, E. J.; Lloyd-Jones, G. C. *J. Am. Chem. Soc.* **2017**, *139*, 13156–13165.



Scheme 124

As a consequence, the oxidative cleavage deprotection methodology was selected for boronic acid **4.10**, provided that the reaction medium is acidified with 1 M aqueous HCl prior to the addition of NaIO₄.

Due to the competing protodeborylation issue encountered during the synthesis of **4.10**, it was proposed that a 2,6-di(mesyloxy)phenylboronic acid **4.28** would have lower Lewis acidity than **4.10** and possibly higher stability against protodeborylation. Subsequently, the 2,6-bis(mesyloxy)phenylboronic acid **4.28** was synthesized using a similar route to that of **4.10** (Scheme 125). First, the pinacol boronate **4.18** was synthesized from **4.19** in a 30% yield (2 steps). The reaction of **4.18** with methanesulfonyl anhydride afforded **4.27** in a non-optimized 53% yield. Next, the deprotection of **4.27** was performed using the optimized pinacol deprotection conditions of **4.10**. Therefore, the solution of **4.27** in CH₃CN was acidified with aqueous HCl (1 M), then NaIO₄ was added, which provided the boronic **4.28** in 90% yield. Overall, the boronic acid **4.28** was prepared in a 14% overall yield from **4.19** (Scheme 125).



Scheme 125

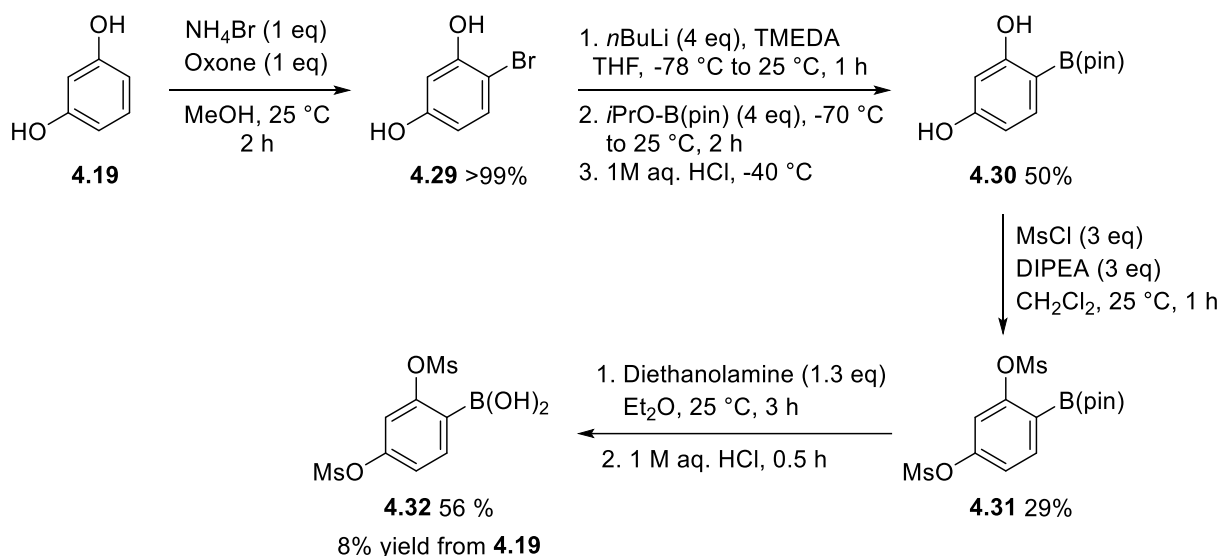
The boronic acid **4.28** was prepared near the end of the Ph.D., and due to time limitations, we were unable to assess its catalytic activity. As a result, besides its synthesis, it will not be

discussed in this manuscript. However, catalytic efficiency studies of **4.28** will be conducted in our group soon.

4.2.3 2,4-Bis(sulfonyloxy)phenylboronic acid

The study on 2,4-di(aryloxy)phenylboronic acids in Chapter 2 revealed that 2,4-disubstitution could either increase or lower the catalytic efficiency based on the electronic properties of the substituents. Consequently, we decided to synthesize and study the 2,4-disubstituted boronic acid **4.32**.

2,4-Bis(mesyloxy)phenylboronic acid **4.32** was synthesized using a similar approach to that of the 2,6-regioisomer **4.10**. First, the selective mono-bromination of resorcinol **4.19** was achieved in a quantitative yield using *in situ*-generated bromine from NH_4Br and oxone (Scheme 126).¹⁷⁴ Successively, 4-bromoresorcinol **4.29** was treated with *n*BuLi to produce a tris-anion, which, upon electrophilic quenching, delivered the pinacol boronate **4.30** in 50% yield. Later, the nucleophilic substitution of **4.30** with methanesulfonyl chloride afforded **4.31** in a non-optimized 29% yield. This step was low yielding due to the precipitation of an insoluble material during the reaction, which could result from the polymerization of phenolic species.



Scheme 126

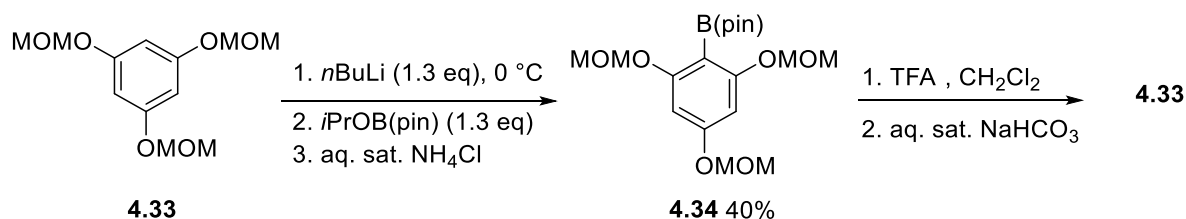
¹⁷⁴ Narender, N.; Mohan, K. V. V. K.; Kulkarni, S. J.; Raghavan, K. V. J. *Chem. Res.* **2003**, 2003, 597–598.

Lastly, the boronic acid **4.32** was obtained upon transesterification of the pinacol ester **4.31** with diethanolamine and subsequent acidic hydrolysis, in a 56% yield (Scheme 126). The boronic acid **4.32** was synthesized in an overall yield of 8% from **4.19**.

4.2.4 2,4,6-Tris-(sulfonyloxy)phenylboronic acid

According to the computational studies, the 2,4,6-tris(triflyloxy)benzeneboronic acid **4.11** could be a very interesting target since it was estimated to have the highest Lewis acidity ($FIA_{COF_2} = 309.5 \text{ kJ.mol}^{-1}$) among the candidate (sulfonyloxy)phenylboronic acids.

The synthesis attempts of **4.11** were conducted by Tom Septvents.¹⁷⁵ In the first approach, the borylation of 2,4,6-tris(triflyloxy)phenyl lithium failed presumably due to the uncontrolled formation of arynes.^{176,177} Alternatively, MOM-protected derivatives were used for the synthesis of **4.11**. The pinacol boronate **4.34** was obtained from the borylation of MOM-protected phloroglucinol **4.33** in a non-optimized 40% yield (Scheme 127). Consequently, the MOM-deprotection of **4.34** was tested using various amounts of TFA, reaction times, and temperatures, all of which resulted in selective protodeborylation into **4.33** (Scheme 127). Furthermore, the use of TMSBr led to the formation of insoluble Bakelite-like polymeric material.¹⁷⁸



Scheme 127

As a result, the intermediate tris-(hydroxy)benzeneboronic acid pinacol ester was found to be too vulnerable to protodeborylation and uncontrolled polymerization, thus preventing the synthesis of **4.11**.

¹⁷⁵ Third year bachelor internship student at the LCMT, group of Pr. Jacques Rouden (2 May-31 May 2022)

¹⁷⁶ Sumida, Y.; Kato, T.; Hosoya, T. *Org. Lett.* **2013**, *15*, 2806–2809.

¹⁷⁷ Nakamura, Y.; Ozawa, S.; Yoshida, S.; Hosoya, T. *Chem. Lett.* **2019**, *48*, 1296–1299.

¹⁷⁸ Hanessian, S.; Delorme, D.; Dufresne, Y. *Tetrahedron Lett.* **1984**, *25*, 2515–2518.

4.3 Kinetic Studies for catalytic activity evaluation

The novel sulfonyloxyphenylboronic acids **4.9-4.10** were then evaluated for the catalytic direct coupling of carboxylic acids and amines. Their activity was assessed using kinetic data, collected from the model reaction of synthesis of *N*-benzylphenylacetamide, at 25 °C.

At a specific time (h), a sample of the reaction mixture was taken and analyzed by ¹H NMR. The % NMR yield was determined from ¹H NMR integrations of the signals of the amide at 4.4 ppm (d, 2H, CH₂-NH) and 3.6 ppm (s, 2H, CH₂-C-C=O) and the internal standard (1,1,2,2-tetrachloroethane) at 5.96 ppm (s, 2H).

Furthermore, each catalyst was subjected to the kinetic study twice, and the % NMR yields were found to be identical in both cases, with only a 1% difference in the yields in some cases.

4.3.1 Catalytic activity assessment of mono-substituted arylboronic acids

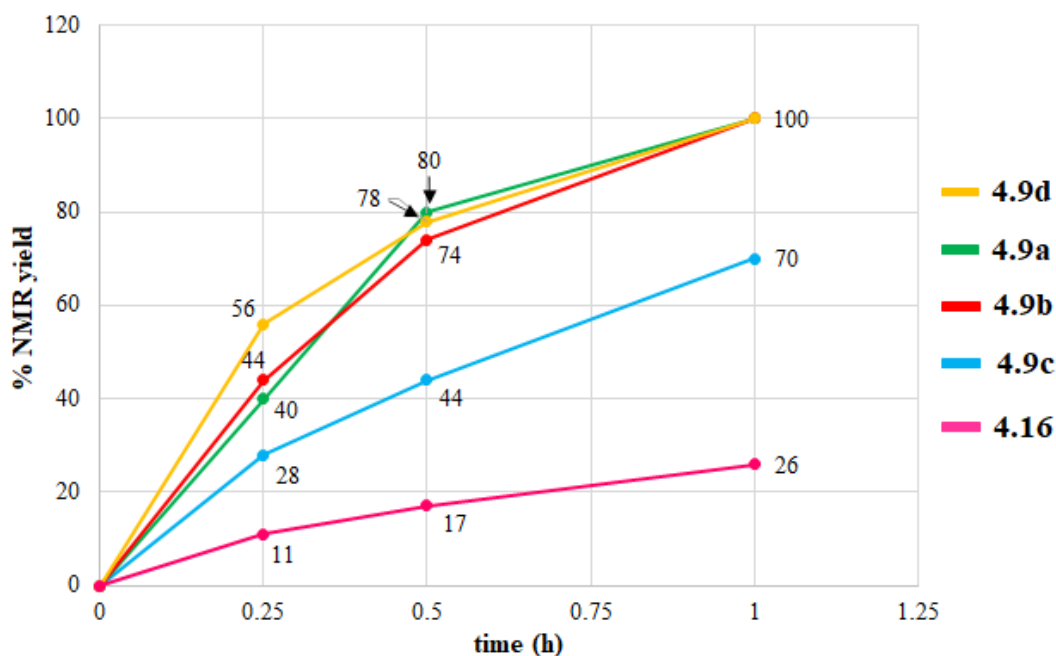
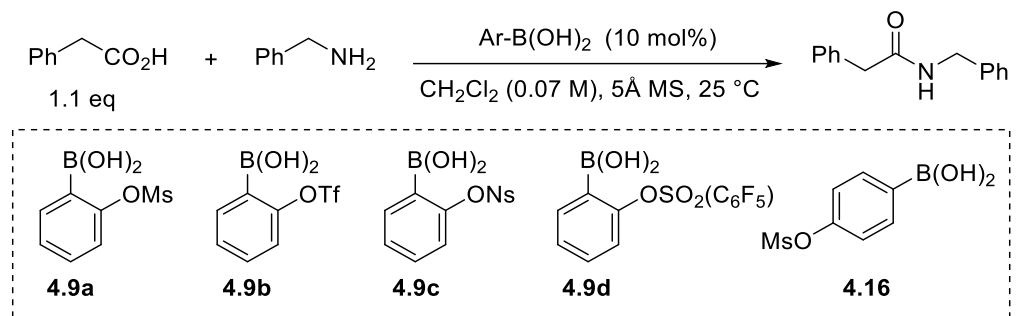
The boronic acid **4.9a** afforded an 80% NMR yield in 30 minutes, which is slightly higher than that achieved by **4.9b** (74% NMR yield) and **4.9d** (78% NMR yield) (Scheme 128). Moreover, these three catalysts (**4.9a,b,d**) have enabled the reaction to be complete after only 1 hour at 25 °C.

Although **4.9d** has a higher Lewis acidity (FIA_{COF₂} = 292.3 kJ.mol⁻¹) than **4.9a** (FIA_{COF₂} = 240.5 kJ.mol⁻¹) and **4.9b** (FIA_{COF₂} = 250.7 kJ.mol⁻¹), it still provided 100% NMR yield in 1 h, as did **4.9a** and **4.9b**. Therefore, despite having higher Lewis acidity than **4.9a** and **4.9b**, catalyst **4.9d** did not demonstrate significantly better performance than them. This can be explained by the fact that the catalytic activity of a Lewis acid is governed not only by the electronic effects, but also by steric repulsion and secondary interactions.¹⁵⁰

Moreover, the nosyl-substituted boronic acid **4.9c** displayed a reduced catalytic activity providing 70% NMR yield in 1 h instead of 100% with the other *ortho*-substituted derivatives **4.9a,b,d** (Scheme 128). This lower reactivity could be associated to the presence of nitro group that might interact with boron center through an intermolecular pathway.¹⁷⁹

¹⁷⁹ An example of a reaction between nitro compound and a Lewis acid include the Lewis acid catalyzed Henry reaction: Palomo, C.; Oiarbide, M.; Laso, A. *Angew. Chem. Int. Ed. Engl.* **2005**, *44*, 3881–3884.

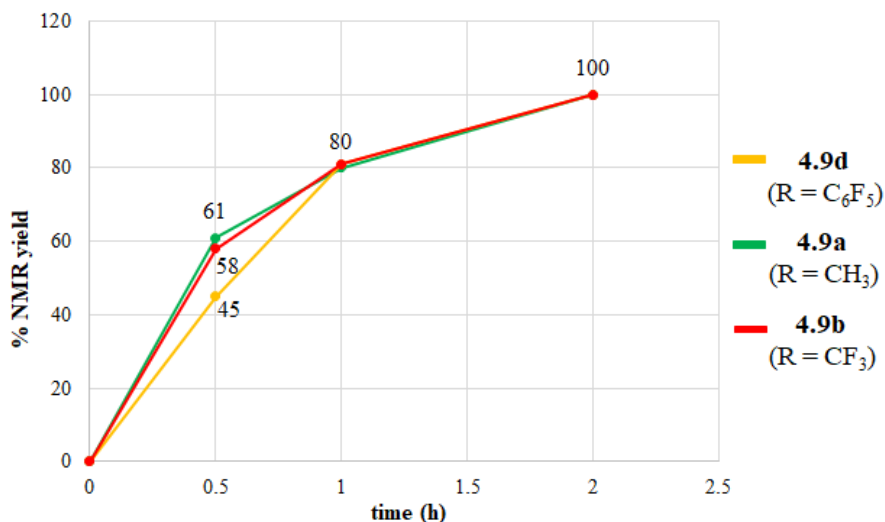
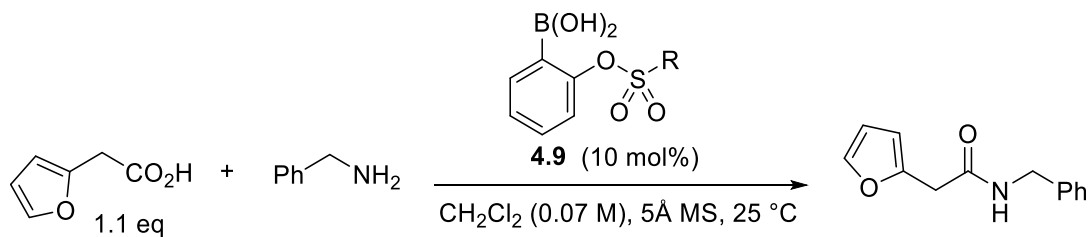
Lastly, the *para*-regioisomer **4.16** provided 26% NMR yield in 1 h, which was significantly lower than that of its *ortho*-counterpart **4.9a** that allowed a complete conversion (Scheme 128). The drastically reduced catalytic efficiency of **4.16** confirmed the relevance of the *ortho*-substitution in the arylboronic acid to promote amidation reactions.



Scheme 128

As a result, the arylboronic acids bearing 2-mesyloxy (**4.9a**), 2-triflyloxy (**4.9b**), and 2-pentafluorosulfonyloxy (**4.9d**) groups were found to be highly competent catalysts, with complete reaction achieved in 1 h. Furthermore, these boronic acids exhibit very comparable performance, with a range of 74-80% NMR yield recorded within 30 minutes.

In an attempt to distinguish between **4.9a**, **4.9b**, and **4.9d**, additional kinetic data were collected from the reaction of 2-furanacetic acid and benzylamine. In this case, these boronic acids displayed also similar activity where they provided 80% NMR yield after 1 h, and 100% NMR yield after 2 h (Scheme 129).



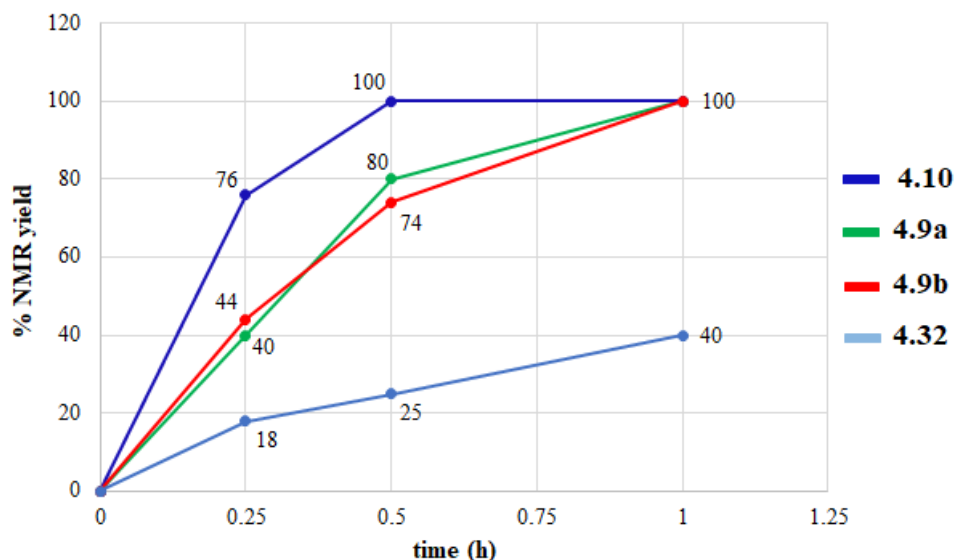
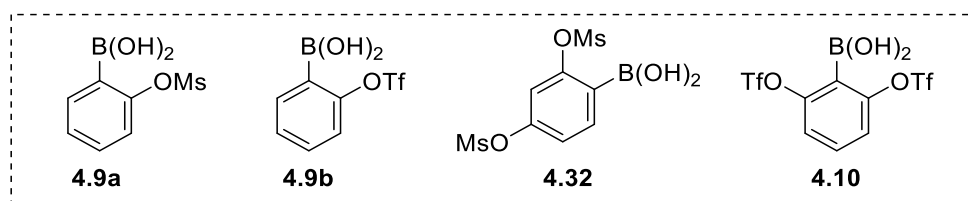
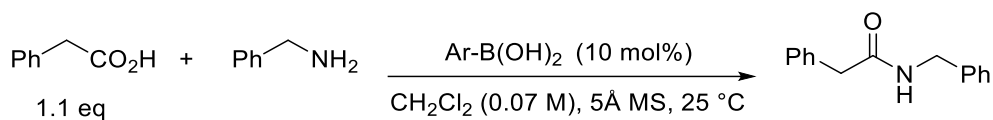
Scheme 129

Eventually, **4.9a** and **4.9b** were selected for further studies since the synthesis of **4.9c** requires the use of the relatively expensive pentafluorobenzenesulfonyl chloride.

4.3.2 Catalytic activity assessment of di-substituted arylboronic acids

Consequently, the catalytic performance of the disubstituted arylboronic acids **4.10** and **4.32** was examined (Scheme 130). First, the 2,4-bis(mesyloxy)phenylboronic acid **4.32** afforded a 40% NMR yield in 1 h, which was considerably lower than the 2-(mesyloxy) derivative **4.9a** which provided a 100% NMR yield.

On the other hand, the use of 2,6-bis(triflyloxy)phenylboronic acid **4.10** has allowed the reaction to be complete in 30 mins, which is half the time needed by the 2-(triflyloxy)phenylboronic acid **4.9b** (Scheme 130). As a result, **4.10** provided a superior performance to **4.9b** and it was distinguished as the most catalytically competent boronic acid of this study.



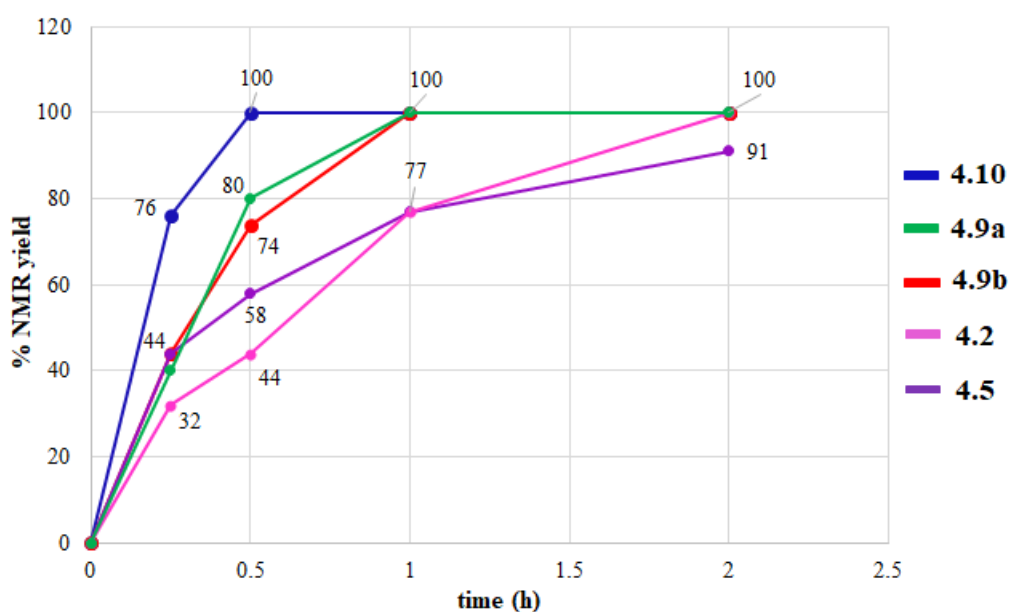
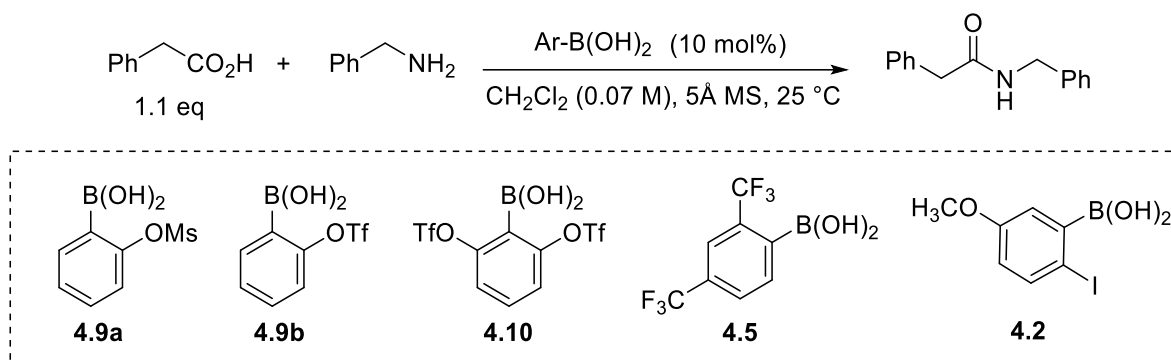
Scheme 130

Next, the activity of the (sulfonyloxy)phenylboronic acids **4.9a**, **4.9b** and **4.10** was compared with those of the actual state-of-the-art boronic acids for the direct condensation of carboxylic acids and amines.

4.3.3 Comparative catalytic activity study with the state-of-the-art boronic acids

After identifying the most competent catalysts in the group of sulfonate-based boronic acids, it was critical to determine whether or not the state-of-the-art boronic acids, represented by **4.2** and **4.5**, had been bested. It should be noted that amidation reactions involving catalyst **4.5** were reported using 3Å MS⁶¹ and those catalyzed by **4.2** used 4Å MS.⁵⁵ However, in order to compare the performance of those boronic acids with the sulfonate-based arylboronic acids, comparative catalytic activity studies were performed using 5 Å MS.

It was observed that after 2 h, boronic acid **4.2** provided complete conversion into the amide (Scheme 131). However, **4.5** gave 91% NMR yield in 2 h and full conversion in 4 h.¹⁸⁰ Notably, the boronic acid catalysts **4.9a** and **4.9b** completed the reaction in 1 h, and **4.10** achieved 100% NMR yield in 0.5 h (Scheme 131). These results revealed that boronic acid catalysts **4.9a**, **4.9b**, and **4.10** compared favorably to Hall's catalyst **4.2** and Ishihara's **4.5**.



Scheme 131

Prior to examining the scope of the amidation reaction, the stability of catalysts **4.9b** and **4.10** during the amidation reaction was monitored. The purpose of this study is to determine if there is side protodeborylation reaction that might interfere with the performance of the catalysts.

¹⁸⁰ The % NMR yields after 4 h are displayed in the raw kinetic data in the experimental part.

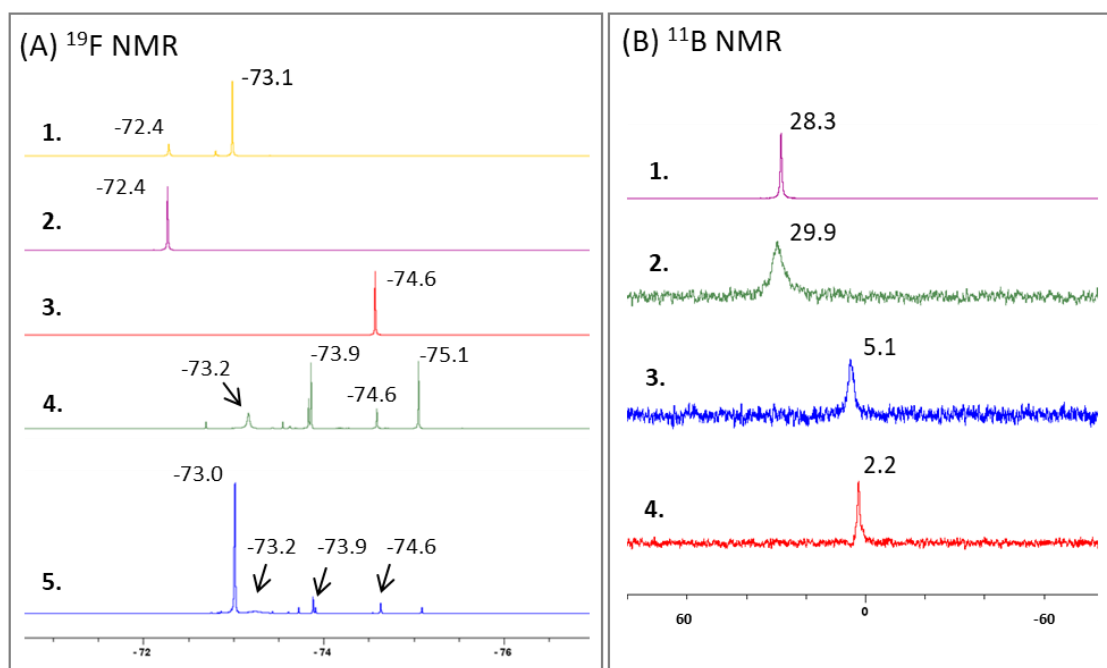
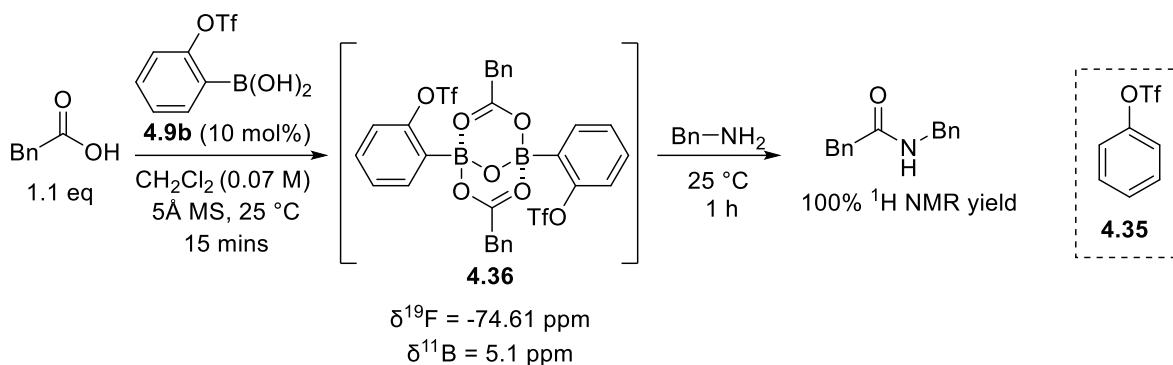
4.4 Investigation of the catalyst stability during the amidation reaction

In order to investigate the stability of the (sulfonyloxy)phenylboronic acids during the amidation reaction, samples of the amidation reaction mixture were examined via NMR spectroscopy. In ^1H NMR, the aromatic proton signals of boronic acids **4.9a**, **4.9b** and **4.10** overlap with those of phenylacetic acid and benzylamine, which makes it difficult to analyze the present species. Therefore, the catalyst stability study was performed on boronic acids **4.9b** and **4.10** which contain a CF_3 -group thus allowing for the examination of the formed species through ^{19}F NMR. Additionally, ^{11}B NMR was simultaneously recorded in all cases.

4.4.1 The case of 2-(triflyloxy)phenylboronic acid

Before conducting the amidation reaction, the ^{19}F and ^{11}B NMR signals of the boronic acid **4.9b** and its boroxine were identified. A solution of boronic acid **4.9b** in CDCl_3 displayed two ^{19}F NMR signals at -73.1 ppm and -72.4 ppm (Entry 1, Scheme 132A). The ^{11}B NMR of this solution showed a signal at 28.3 ppm (Entry 1, Scheme 132B). The addition of activated powdered 5Å MS (20 mg) allowed the appearance of the ^{19}F NMR signal at -72.4 ppm only (Entry 2, Scheme 132A). Therefore, the ^{19}F peak at -72.4 ppm corresponds to the boroxine and that at -73.1 ppm relates to **4.9b**. Also, the boroxine displayed an ^{11}B NMR signal at 29.9 ppm (Entry 2, Scheme 132B). Moreover, benzene triflate **4.35** was prepared and characterized, in order to identify its presence in case of protodeboronation of **4.9b**. It had a signal at -73.0 ppm in ^{19}F NMR.

Next, the amidation reaction was conducted and samples of the reaction mixture were taken, diluted with CDCl_3 , and analyzed by ^{19}F NMR and ^{11}B NMR. First, the boronic acid **4.9b** (10 mol%) was added to phenylacetic acid (1.1 eq) and activated powdered 5Å activated MS (1 g), in CH_2Cl_2 , and the mixture was stirred vigorously for 15 mins. The ^{19}F NMR analysis of a sample of this mixture showed a signal at -74.6 ppm (Entry 3, Scheme 132A). The signal at -74.6 ppm did not match the ^{19}F δ of boronic (-73.1 ppm), boroxine (-72.4 ppm), or benzene triflate (-73.0 ppm), and it was accompanied by a signal at 5.1 ppm in ^{11}B NMR (Entry 3, Scheme 132B). According to Whiting's mechanistic investigations,⁵⁹ the mixed carboxylic boronic complex is observed at 5 ppm in ^{11}B NMR. Therefore, the signals at -74.6 ppm in ^{19}F NMR and 5.1 ppm in ^{11}B NMR were attributed to complex **4.36** (Scheme 132).



1. Pure **4.9b** in CDCl_3 ; 2. **4.9b** (0.05 mmol), activated powdered 5Å MS (20 mg), CDCl_3 ; 3. Phenylacetic acid (0.55 mmol, 1.1 eq), **4.9b** (0.05 mmol, 10 mol%), activated powdered 5Å MS (1 g), 15 mins, 25 °C; 4. Mixture of entry 3 + benzylamine (0.5 mmol, 1 eq), 1 h, 25 °C; 5. Mixture of entry 4 + 4 mg of pure **4.35**, 2 mins, 25 °C

Scheme 132

Afterwards, benzylamine (1 eq) was added and a sample of the reaction mixture was examined after 1 h, when complete conversion was observed by ^1H NMR. The ^{19}F NMR of this mixture shows various signals, of which only that of complex **4.36** (-74.6 ppm) can be identified (Entry 4, Scheme 132A). These signals could arise from different potential interactions of the amine with the organoboron species in the reaction medium. One possible interaction is the formation of a complex similar to **4.36**, which contains a B-N-B linkage instead of a B-O-B motif. Whiting proposed the formation of a B-N-B bridged complex based on the observation of an ^{11}B NMR signal at 2.5 ppm. However, his study did not provide any further evidence. Therefore, the ^{11}B

NMR peak at 2.2 ppm is cautiously assigned to a B-N-B bridged complex (Entry 4, Scheme 132B).

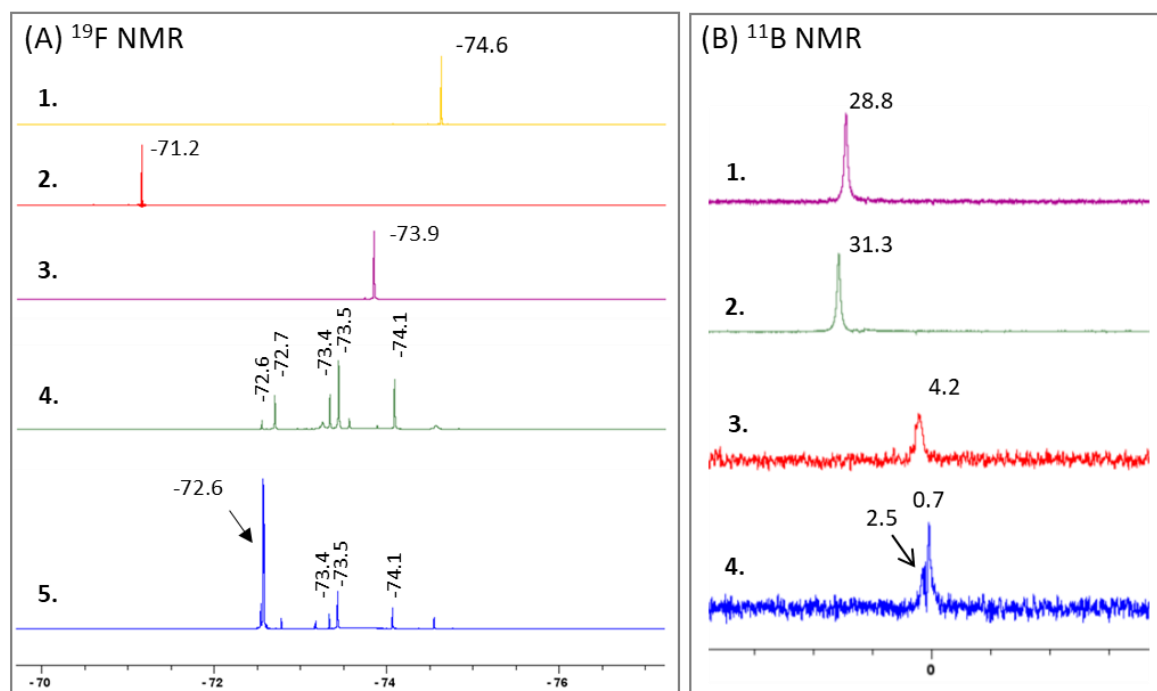
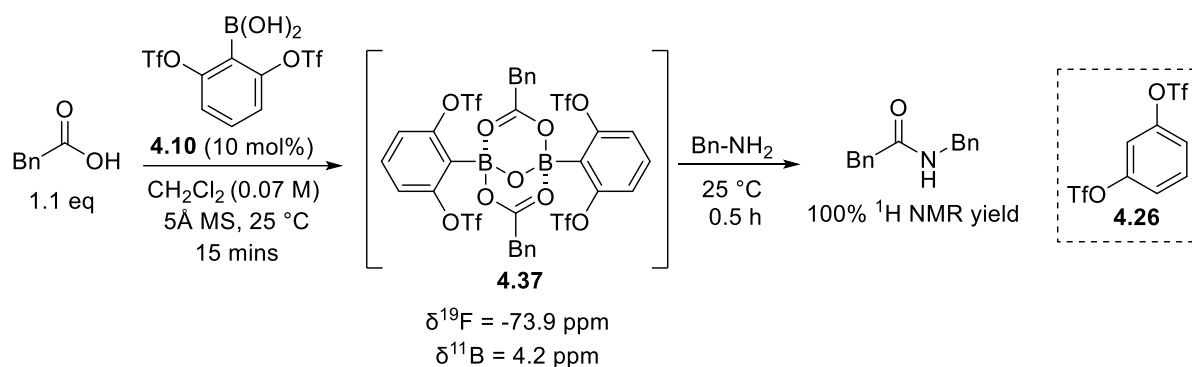
To a sample of the mixture of the amidation mixture of Entry 4, 4 mg of pure benzene triflate **4.35** were added. Importantly, the signal of **4.35** at -73.0 ppm (Entry 5, Scheme 132A) was absent in the amidation mixture, suggesting that protodeborylation of **4.9b** did not take place.

This reveals that catalyst **4.9b** effectively forms the catalytically active intermediate **4.36**, and more importantly, it does not undergo deboronation during the reaction.

4.4.2 The case of 2,6-bis(triflyloxy)phenylboronic acid

Similar to the stability study of boronic acid **4.9b**, the signals of boronic acid **4.10** and its boroxine were first characterized. The ^{19}F NMR of a solution of **4.10** in CDCl_3 revealed a signal at -74.6 ppm (Entry 1, Scheme 133A). Additionally, the ^{11}B NMR of this solution showed a signal at 28.8 ppm (Entry 1, Scheme 133B). Afterwards, activated powdered 5Å MS (20 mg) were added to the solution of **4.10** in CDCl_3 , and ^{19}F NMR signal at -71.2 ppm and ^{11}B NMR peak at 31.3 ppm were recorded (Entries 2, Scheme 133). The latter signals correspond to the boroxine. Additionally, 1,3-bis(triflate) benzene **4.26**, protodeboronation product of **4.10**, was prepared and it showed a ^{19}F NMR signal at -72.6 ppm.

The amidation reaction was then performed and samples of the reaction mixture were taken, diluted with CDCl_3 , and analyzed by ^{19}F NMR and ^{11}B NMR. When boronic acid **4.10** (10 mol%) was mixed with phenylacetic acid (1.1 eq) and activated powdered 5Å MS (1 g), a ^{19}F NMR signal appeared at -73.9 ppm (Entry 3, Scheme 133A). This signal differs from the ^{19}F peaks of **4.10** (-74.6 ppm), its boroxine (-71.2 ppm), or **4.26** (-72.6 ppm). Furthermore, the ^{11}B NMR of this sample displayed a chemical shift of 4.2 ppm (Entry 3, Scheme 133B). Using similar reasoning as for complex **4.36** (Scheme 132), the ^{19}F NMR signal at -73.9 ppm and ^{11}B NMR signal at 4.2 ppm were assigned to complex **4.37** (Scheme 133).



1. Pure **4.10** in CDCl_3 ; **2.** **4.10** (0.05 mmol), activated powdered 5Å MS (20 mg), CDCl_3 ; **3.** Phenylacetic acid (0.55 mmol, 1.1 eq), **4.10** (0.05 mmol, 10 mol%), activated powdered 5Å MS (1 g), 15 mins, 25 °C; **4.** Mixture of entry 3 + benzylamine (0.5 mmol, 1 eq), 0.5 h, 25 °C; **5.** Mixture of entry 4 + 4 mg of pure **4.26**, 2 mins, 25 °C

Scheme 133

Next, benzylamine (1 eq) was introduced and a sample of the reaction mixture was examined after 0.5 h, when complete conversion was detected by ^1H NMR. The ^{19}F NMR of the mixture shows several unidentified new signals, and the disappearance of the signal of **4.53** at -73.9 ppm (Entry 4, Scheme 133A). Additionally, the ^{11}B NMR of this sample displayed two signals at 2.5 ppm and 0.7 ppm (Entry 4, Scheme 133B). Based on Whiting's study,⁵⁹ the ^{11}B NMR signal at 2.5 ppm was cautiously attributed to a B-N-B bridged complex. However, the signal at 0.7 ppm was not identified at this point.

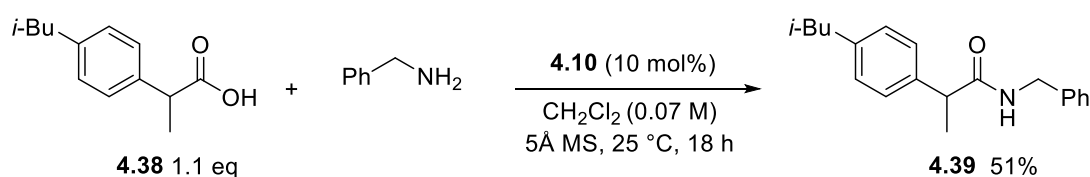
To a sample of the amidation mixture after 0.5 h from benzylamine addition, 4 mg of pure **4.26** were added (Entry 5, Scheme 133A). Unfortunately, the ^{19}F NMR signal of **4.26** at -72.6 ppm was present in the reaction mixture of Entry 4 (Scheme 133A), which indicates that protodeborylation is taking place. Nonetheless, the presence of several unidentified signals in this mixture (Entry 4) makes it difficult to determine the ratio of **4.26**. It can be suggested that the protodeborylation is a minor event given the intensity of the signal of **4.26**.

Furthermore, the cleavage of the C-B bond in **4.10** results in the formation of boric acid and **4.26**. Since the deboronation of **4.10** was observed after 30 mins, it is presumed that the ^{11}B signal at 0.7 ppm (Entry 4, Scheme 133B) corresponds to a boric acid-related complex. In the control experiments conducted by Whiting, a mixture of boric acid and benzylamine (1:1 ratio) was added to CDCl_3 .⁵⁹ Initially, this mixture was insoluble and did not provide any signal in ^{11}B NMR. However, when phenylacetic acid was introduced, the solubility improved, and an ^{11}B NMR signal was observed at 1 ppm. Therefore, it is suggested that the signal at 0.7 ppm is associated with an interaction between boric acid, benzylamine, and phenylacetic acid.

At first, boronic acid **4.10** was intended to be selected for scope examination since it displayed the highest catalytic efficiency on the model amidation reaction. However, since it is observed that **4.10** undergone minor protodeborylation during this reaction, we were curious to look into if this protodeborylation issue is substrate dependent or stems from the intrinsic properties of **4.10**. Therefore, its performance was evaluated on different amidation reactions.

4.5 Selection of catalyst for scope examination

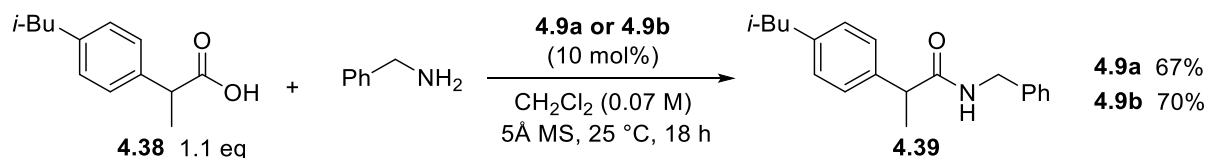
First, the coupling of racemic ibuprofen **4.38** and benzylamine was tested since this reaction was reported with catalyst **4.5**,⁶¹ which allowed for an additional comparison of the isolated yields. The use of catalyst **4.10** afforded the amide **4.39** in a 51% yield after 18 h (Scheme 134). Such result was unsatisfactory owing to the fact that boronic acid **4.5** provided a 97% yield for the same reaction.⁶¹ Importantly, during the purification of the amidation reaction mixture, the bis(triflate)benzene **4.26** was isolated in a 53% yield (from **4.10**).



Scheme 134

Therefore, the use of **4.10** for further scope investigation was discontinued due to competing protodeborylation.

Afterwards, preliminary testing on the coupling of racemic ibuprofen and benzylamine using stable boronic acids **4.9a** and **4.9b**, has afforded 67% and 70% yields respectively (Scheme 135). In both cases, no protodeborylation product was isolated during chromatographic purification.



Scheme 135

Due to the observation that the stable and catalytically proficient boronic acids **4.9a** and **4.9b** showed almost identical performance in kinetic studies and very close yields of isolated amide **4.39**, they were both chosen to investigate the optimization of amidation reaction conditions and for scope investigations.

4.6 Optimization of reaction conditions for low-temperature amide synthesis

The effect of the catalyst loading and the nature of the molecular sieves on the amidation reaction were investigated in order to identify the optimal reaction conditions for the scope examination.

4.6.1 Effect of the nature of molecular sieves

Molecular sieves are synthetic zeolite materials engineered with pores of uniform structure and size.¹⁸¹ This allows them to adsorb molecules based on molecular size. The importance of the molecular sieves is that they can act as efficient dehydrating agents.

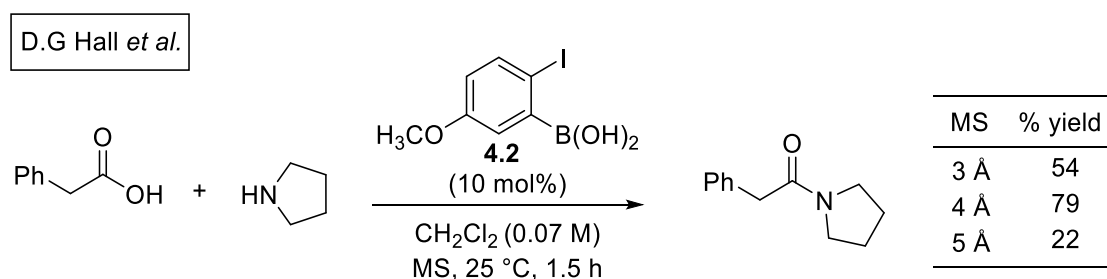
¹⁸¹ Flanigen, E. M. Chapter 2 Zeolites and Molecular Sieves: A Historical Perspective. In *Studies in Surface Science and Catalysis*; van Bekkum, H., Flanigen, E. M., Jacobs, P. A., Jansen, J. C., Eds.; Introduction to Zeolite Science and Practice; Elsevier, 2001; Vol. 137, pp 11–35.

The different types of molecular sieves commonly used as dehydrating agents in amide synthesis, which are 3Å, 4Å, and 5Å, differ by their chemical composition (Table 3).^{181,182} The 4 Å MS is a sodium aluminosilicate while the 5 Å MS is obtained by exchanging replaceable Na ions in 4 Å with Ca ions, and the 3 Å MS are produced by exchanging replaceable Na ions in 4 Å MS with K ions.¹⁸³ It should be noted that the composition of the molecular sieves, more particularly the SiO₂/Al₂O₃ ratio can differ from one source to the other depending on the synthesis procedure.¹⁸²

Type	Pore diameter	Composition	Ref.
3Å	3	K _n Na _{12-n} [(AlO ₂) ₁₂ (SiO ₂) ₁₂] · xH ₂ O	Sigma-Aldrich
4Å	4	Na ₂ O·Al ₂ O ₃ ·2SiO ₂ ·xH ₂ O	[183]
		Na ₁₂ [(AlO ₂) ₁₂ (SiO ₂) ₁₂]·27 H ₂ O	[182]
5Å	5	1/3Na ₂ O·2/3CaO·Al ₂ O ₃ ·2SiO ₂ ·xH ₂ O	[183]

Table 3

In most of the reports about the boronic acid-catalyzed amidation reactions, the 4Å molecular sieves are used as dehydrating agents,^{55,60,67} since they provided better yields than 3Å or 5Å. To illustrate, Hall has examined the effect of the molecular sieves of different pore diameters on the yield of the amide synthesis using catalyst **4.2**.⁵⁵ It was revealed that 4Å MS afforded higher isolated yield (79%) than 3Å (54%) or 5Å (22%) molecular sieves (Scheme 136).



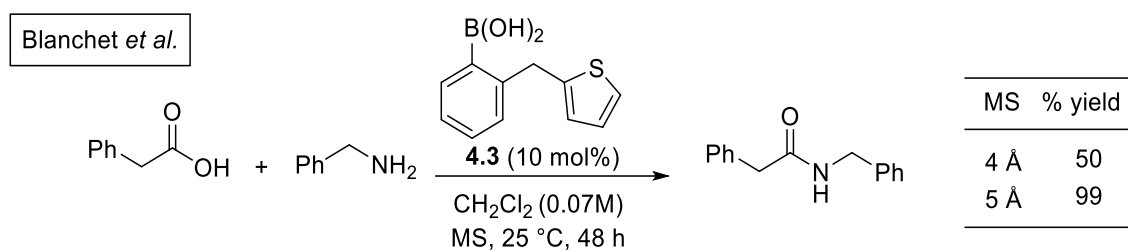
Scheme 136

Nonetheless, previous studies conducted by our research group revealed that 5Å MS afforded the highest yields.^{57,103} Using the boronic acid **4.3**, the *N*-benzylphenylacetamide was isolated

¹⁸² Broach, R. W.; Jan, D.-Y.; Lesch, D. A.; Kulprathipanja, S.; Roland, E.; Kleinschmit, P. Zeolites. In *Ullmann's Encyclopedia of Industrial Chemistry*; John Wiley & Sons, Ltd, **2012**.

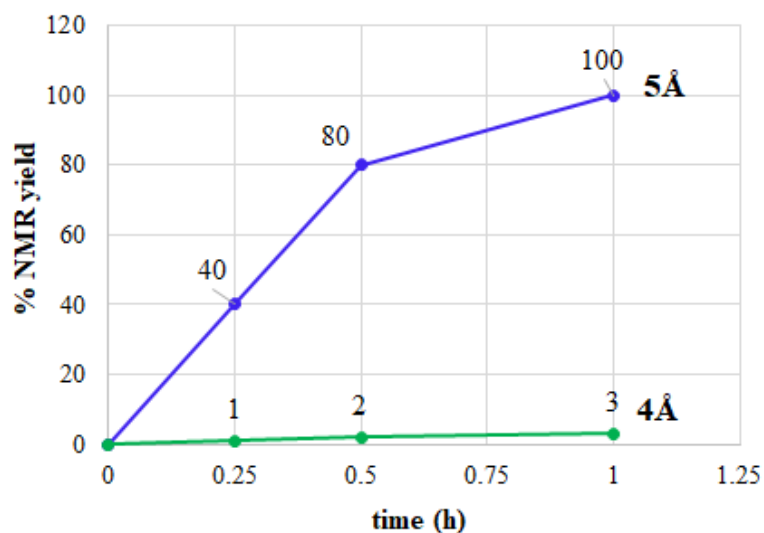
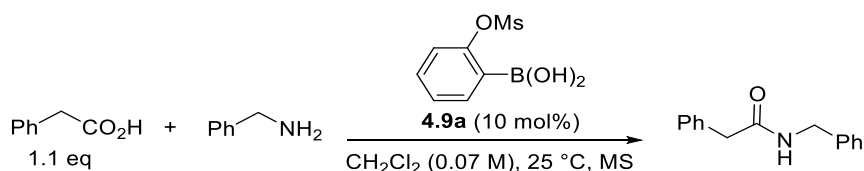
¹⁸³ Broussard, L.; Shoemaker, D. P. *J. Am. Chem. Soc.* **1960**, 82, 1041–1051.

in a 99% yield using 5Å MS, however, a considerable decrease in the yield to 50% was obtained with the 4 Å MS (Scheme 137).



Scheme 137

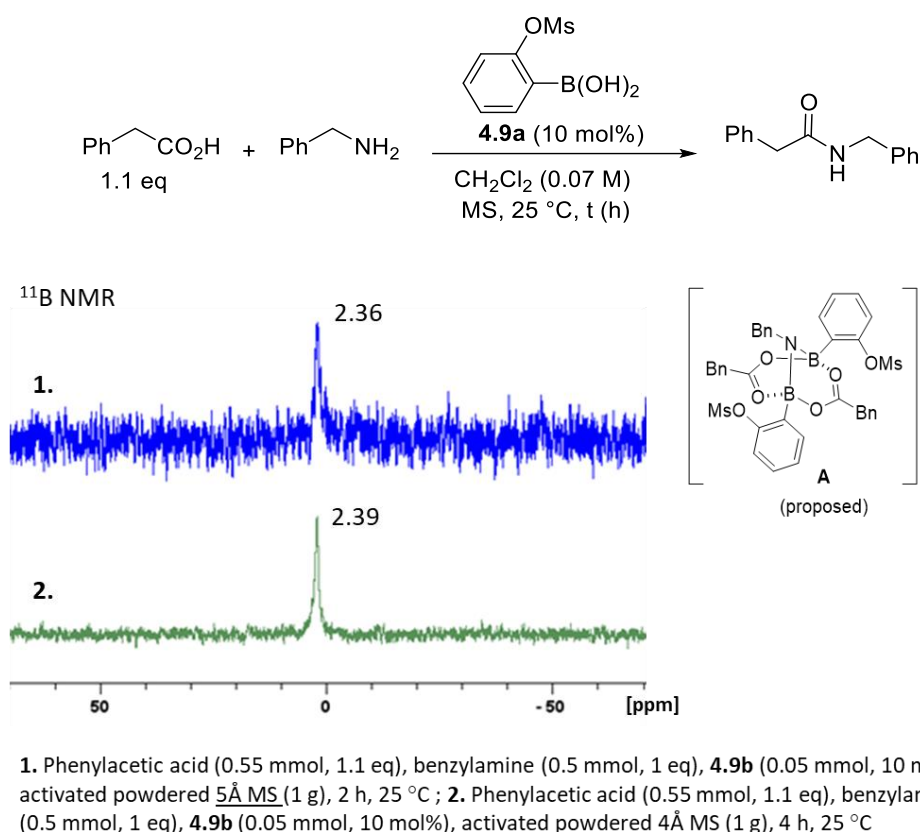
Accordingly, in our case, both 4Å and 5Å molecular sieves were examined in order to determine the optimal dehydrating agent. By employing 5Å MS, catalyst **4.9a** accomplished reaction completion in 1 h, however, the use of 4Å MS dramatically reduced the rate of the reaction, with an NMR yield as low as 3% noted after 1 h (Scheme 138).



Scheme 138

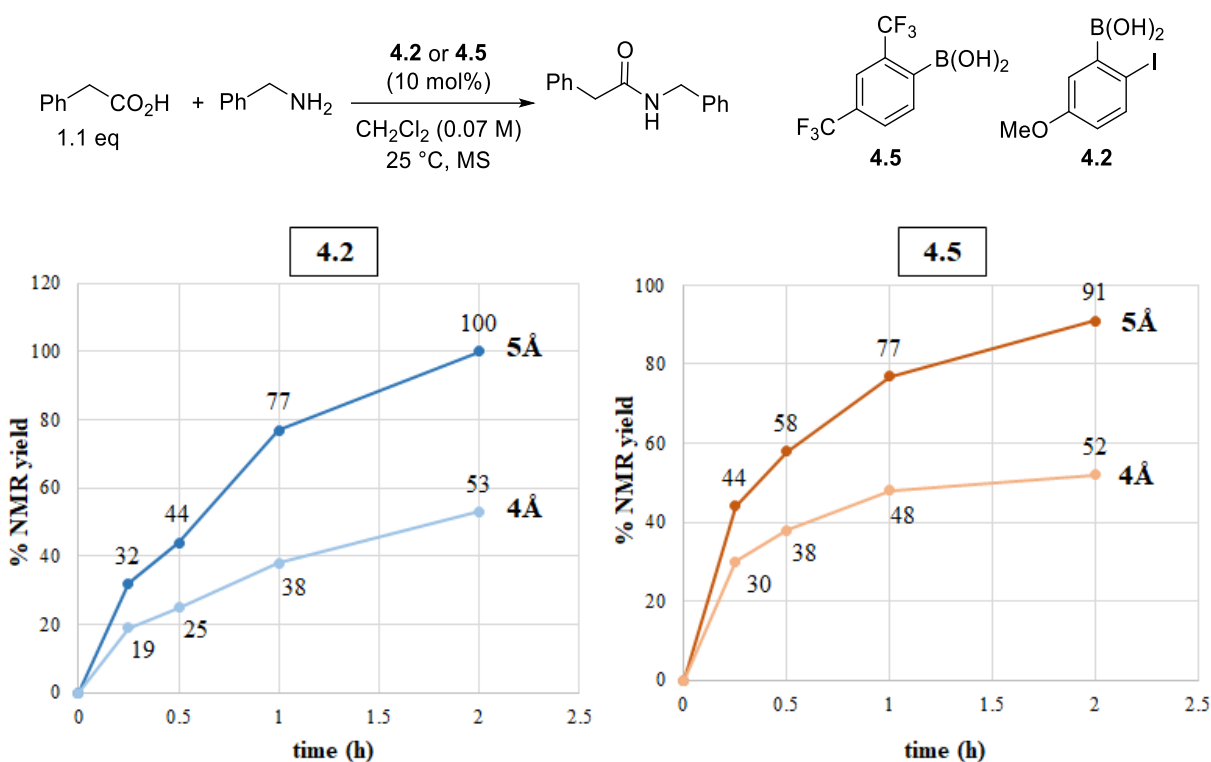
In an attempt to understand this huge gap in the catalytic performance upon using 5Å and 4Å MS, the ^{11}B NMR of the reaction mixture was examined. When 5Å MS were used, the ^{11}B NMR of the amidation mixture was recorded after 1 h from the addition of benzylamine and a signal at 2.36 ppm was detected (Entry 1, Scheme 139). Based on Whiting's mechanistic study,

the ^{11}B NMR signal at 2.5 ppm is related to an amine-bridged bicyclic complex which is catalytically active.⁵⁹ Thus, it is proposed that the signal at 2.36 ppm is likely to belong to complex **A** (Scheme 139), however, this claim is not definitive. Moreover, the ^{11}B NMR spectrum of the amidation mixture, when 4Å MS was used, shows a similar signal at 2.39 ppm after 4 h from benzylamine addition (Entry 2, Scheme 139). It was also proposed that the signal at 2.39 ppm corresponds to **A**, based on the same reasoning as with 5Å MS. As a consequence, the ^{11}B NMR signal of the amidation mixture with 5Å MS or 4Å MS was similar, and it did not provide an explanation for the decrease in activity observed when using 4Å MS.



Scheme 139

Given that boronic acids **4.2** and **4.5** are reported to be highly active with 4Å MS,^{55,61} their reactivity was examined using the same batch of powdered activated 4Å MS that was used for testing **4.9a**. In the case of boronic acid **4.2**, its catalytic activity was significantly reduced with the use of 4Å MS where it afforded 53% yield after 2 h in place of 100% with 5Å MS (Scheme 140). Similarly, the use of 4Å MS with catalyst **4.5** caused the reaction rate to drop, affording 52% NMR yield after 2 h, in place of 91% with the 5Å MS (Scheme 140).



Scheme 140

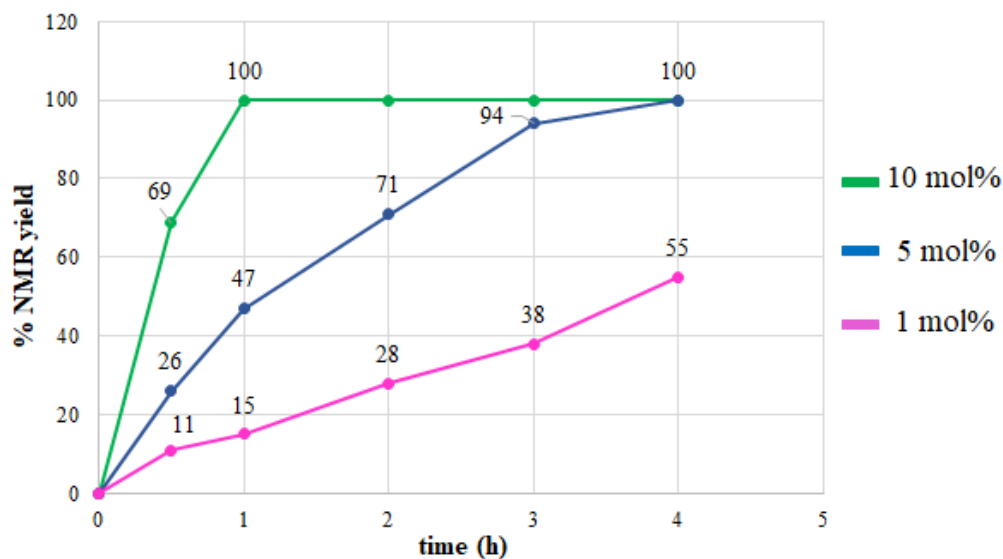
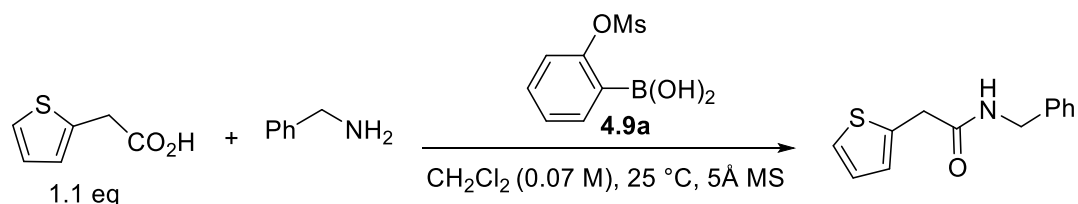
Given that the function of the molecular sieves is to trap the water produced during the reaction, using activated 4 Å or 5 Å MS should not result in such a huge discrepancy in catalytic performance. However, it was noticed none of the previously cited studies has mentioned specification of the molecular sieves besides their pore size and morphology (bead/powder). This is due to the fact that important parameters such as the SiO₂/Al₂O₃ ratio, pH levels or bulk density of the molecular sieves are not usually provided by the manufacturers. For the moment, it could be proposed that molecular sieves of the same pore diameter may differ in their SiO₂/Al₂O₃ ratio, mesh particle size or pH levels, depending on the manufacturer. This could presumably lead to inconsistencies in the results. However, more work should be done in this direction in order to gain further insight on the effect of the nature of the molecular sieves on the catalytic activity.

Finally, according to the results obtained in this section, 5 Å molecular sieves was selected for further scope examination.

4.6.2 Catalyst loading

When 2-mesyloxyphenylboronic acids **4.9a** was used at 10 mol% loading, it enabled a fast reaction. Reduced loadings of **4.9a** were tested to determine if they can still provide synthetically useful reaction times.

Firstly, the use of 5 mol% **4.9a** resulted in a decline in the reaction rate where 100% NMR yield was reached after 4 h, compared to 1 h with 10 mol% (Scheme 141). Moreover, decreasing the catalyst loading to 1 mol% considerably slowed down the reaction whereby 15% NMR yield was detected after 1 h, instead of full conversion with 10 mol% of **4.9a** (Scheme 141). Additionally, with the use of 1 mol% **4.9a**, 88% NMR yield was obtained after 24 h (not shown on graph).



Scheme 141

It is interesting that **4.9a** allowed the reaction to progress even when a quantity as low as 1 mol% was used. However, the catalyst loading of 10% mol% was selected in anticipation that more challenging aromatic or sterically hindered substrates would require longer reaction times.

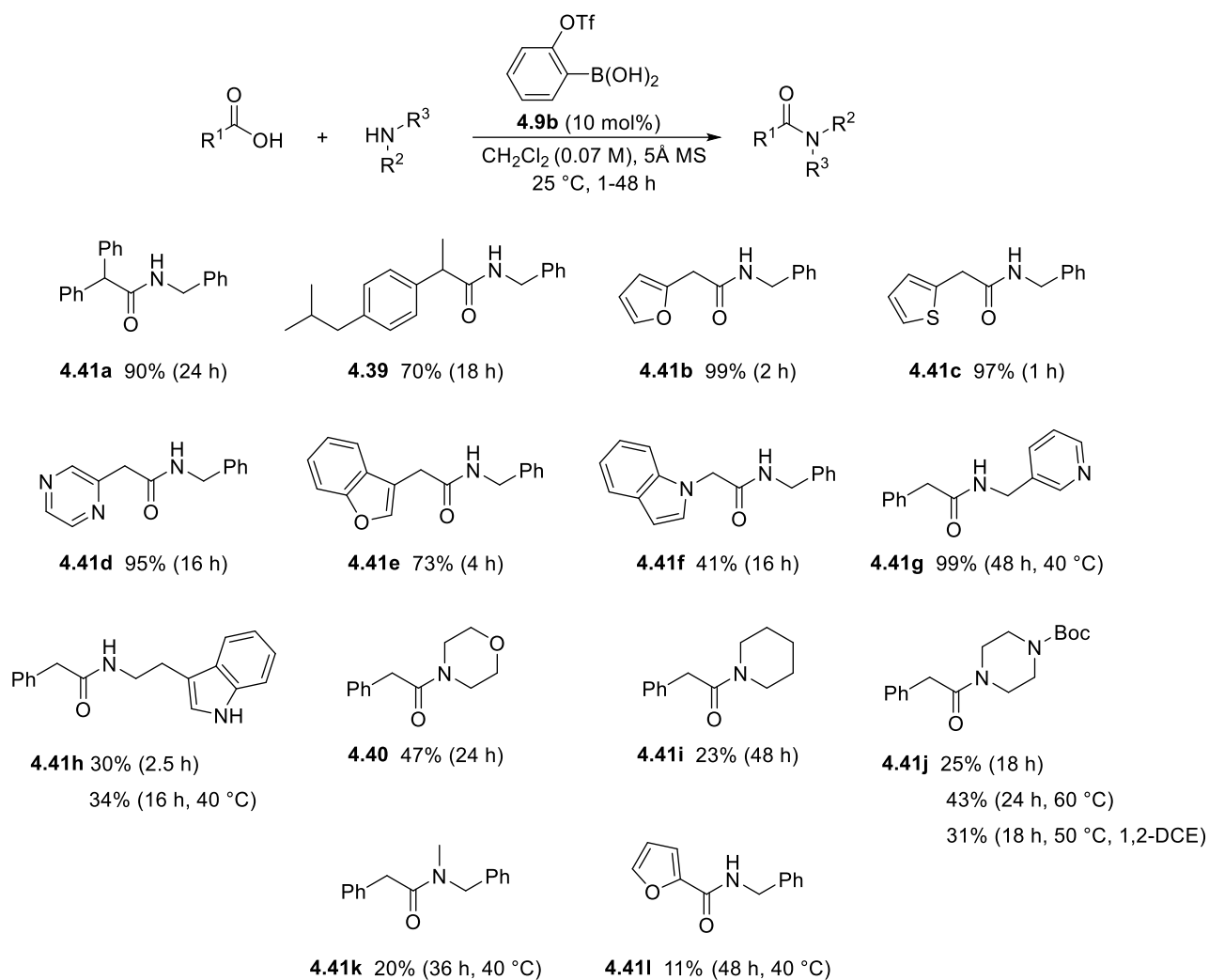
4.7 Scope and limitations of low-temperature amide synthesis

The optimal conditions were exploited for the synthesis of a diverse range of amides (Scheme 142). In the case of **4.41a** and **4.39**, the coupling of α -substituted carboxylic acids in 70-90% yields signifies a level of tolerance for steric hindrance. Furthermore, acetic acid derivatives functionalized with various heterocycles, such as furan (**4.41b**), thiophene (**4.41c**), pyrazine (**4.41d**), and benzofuran (**4.41e**), were well tolerated where the respective amides were obtained in up to 99% yields. Remarkably, the presence of a heterocycle on the amine partner was also tolerated, in which 3-picolyamine produced the amide **4.41g** in 99% yield, albeit demanding higher temperature of 40 °C.

Unexpectedly, an indole moiety, whether on the acid (**4.41f**) or amine (**4.41h**) partner, reduced the solubility of the reaction medium resulting in low yields (30-41%). In an effort to overcome this solubility issue, gentle heating at 40 °C was applied for **4.41h**, however, a marginally improved yield of 34% was obtained.

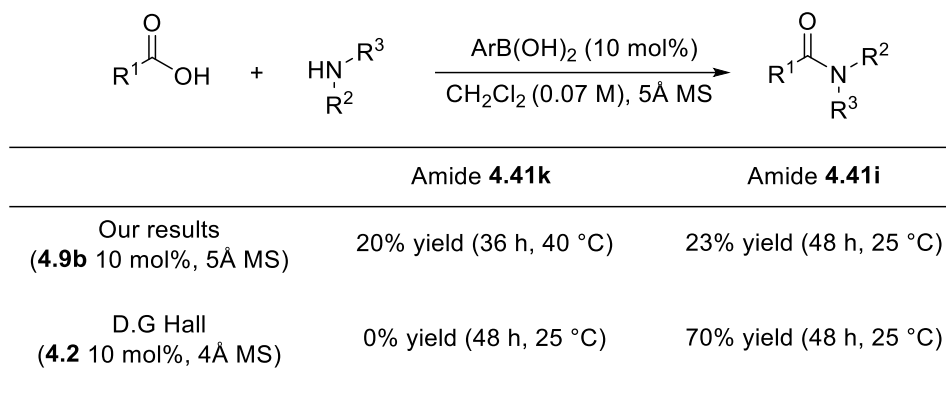
Moreover, the reactions with secondary amines were examined. The coupling of phenylacetic acid with morpholine or piperidine provided the corresponding amide products in 47% (**4.40**) and 23% (**4.41i**) yields, respectively. Besides, *N*-Boc-piperazine gave the amide **4.41j** in a 25% yield, which was marginally improved to 43% upon heating at 60 °C. The synthesis of **4.41j** was also tested in 1,2-dichloroethane at 50 °C and, in this case, the amide was obtained in a 31% yield. Moreover, *N*-methylbenzylamine afforded the target amide **4.41k** in a 20% yield at 40 °C. Generally, secondary amines proved to be challenging substrates for this approach, affording unsatisfactory yields, even when higher temperatures (40-60 °C) were applied.

Furthermore, the reaction of furoic acid and benzylamine provided the amide **4.41l** in 11% yield after 48 h at 40 °C. Therefore, the coupling of aromatic acids was another limitation of this method.



Scheme 142

After reviewing existing reports for boronic acid-catalyzed amide synthesis, it was discovered that some secondary amines could be difficult substrates. For instance, **4.41k** was obtained in 0% yield after 48 h at 25 °C using **4.2** as a catalyst (Scheme 143).⁵⁵ In our case, a slightly higher temperature of 40 °C afforded the amide **4.41k** in 20% yield. On the other hand, there are instances where secondary amines can be efficiently coupled to produce the desired amides in good yields. For example, amide **4.41i** was synthesized in 70% yield using catalyst **4.2**,⁵⁵ however, in our case, this amide was obtained in a lower 23% yield (Scheme 143).



Scheme 143

As a consequence, the coupling of secondary amines and aromatic acids are identified limitations for the room-temperature amide synthesis, using molecular sieves. Further scope investigations were conducted at higher temperatures and using a Dean-Stark trap for water removal in place of molecular sieves.

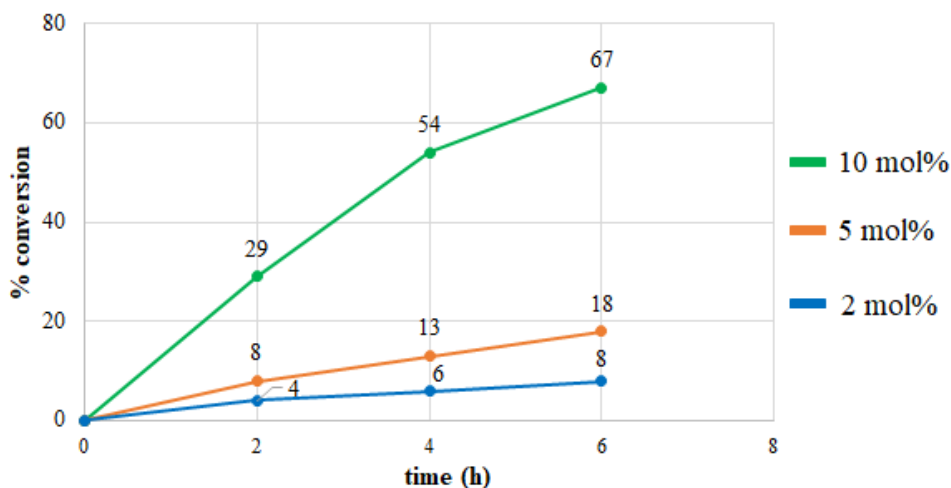
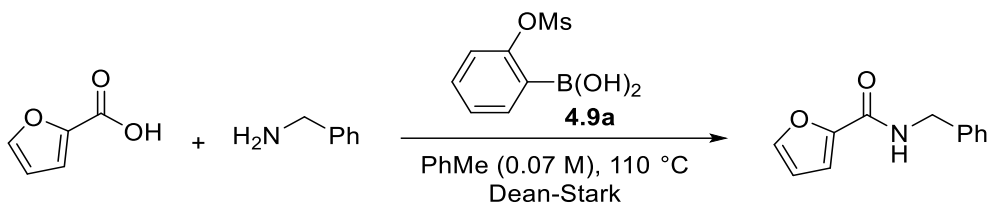
Prior to examining the scope of amides synthesis under the azeotropic reflux conditions, several reaction parameters were studied in order to identify the ideal ones.

4.8 Optimization of high-temperature amidation conditions

The optimization of the reaction parameters was performed using the coupling of furoic acid and benzylamine as the model reaction, since the corresponding amide **4.41i** was obtained in a low 11% yield under the low-temperature amidation conditions.

4.8.1 Effect of catalyst loading

Different loading of **4.9a** were examined, with toluene as the reaction solvent (Scheme 144) at 110 °C. The use of a 10 mol% loading provided a 67% conversion in 6 h, however, catalyst loadings of 5 mol% and 2 mol% led to slower reactions with conversions of 18% and 8% recorded in 6 h, respectively (Scheme 144).



Scheme 144

Consequently, 10 mol% of **4.9a** was selected as the optimal catalyst loading.

4.8.2 Effect of the solvent

The most frequently utilized solvent for amide synthesis under azeotropic reflux conditions is toluene (110 °C).^{39,63} Nevertheless, other solvents with varying polarities and lower boiling points have been investigated for amide synthesis through the utilization of a Dean-Stark trap.^{184,185,65} The physical properties of the tested solvents, which are the boiling point (bp), azeotrope temperature (T_{AZ})¹⁸⁶ of the system with water and azeotrope composition^{187,188} are displayed in Table 4.

¹⁸⁴ Sabatini, M. T.; Boulton, L. T.; Sheppard, T. D. *Sci. Adv.* **2017**, *3*, e1701028.

¹⁸⁵ Coomber, C. E.; Laserna, V.; Martin, L. T.; Smith, P. D.; Hailes, H. C.; Porter, M. J.; Sheppard, T. D. *Org. Biomol. Chem.* **2019**, *17*, 6465–6469.

¹⁸⁶ Azeotrope temperatures (T_{AZ}) and boiling points (bp) of all the mentioned solvents are from the following sources: (a) Horsley, L. H. *Anal. Chem.* **1949**, *21*, 831–873. (b) Lide D.R. *CRC Handbook of Chemistry and Physics*, 85th ed., CRC Press: Boca Raton, FL, **2005**.

¹⁸⁷ Horsley, L. H. *Anal. Chem.* **1949**, *21*, 831–873.

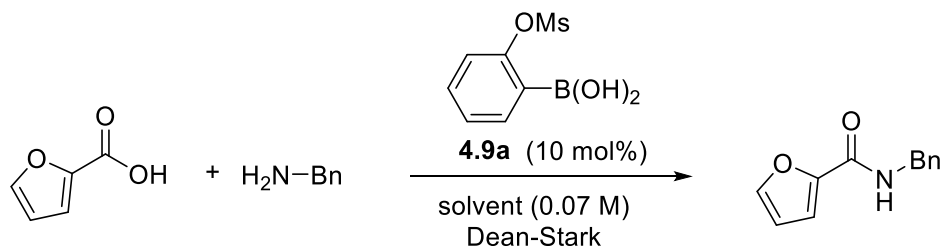
¹⁸⁸ Lide D.R. *CRC Handbook of Chemistry and Physics*, 85th ed., CRC Press: Boca Raton, FL, **2005**.

Solvent	PhMe	<i>t</i> -BuOAc	TAME ^(a)	PhF	1,2-DCE ^(b)
bp (°C)	110.6	97	86	85	83.5
T _{AZ} (°C)	84.1	86.6	73.8	60.2	72.3
% weight (H ₂ O)	19.6	19.4	9	not found	19.5

(a) TAME = *tert*-amyl methyl ether ; (b) 1,2-DCE = 1,2-dichloroethane

Table 4

When toluene (T_{AZ} = 84.1 °C) was used as the reaction solvent, 67% conversion was recorded in 6 h and full conversion was achieved after 24 h (Table 5). Moreover, *t*-BuOAc, which has a close T_{AZ} (86.6 °C) to toluene, allowed slightly lower conversions than toluene where 50% conversion was achieved in 6 h and 93% in 24 h (Table 5). On the other hand, the use of TAME (T_{AZ} = 73.8 °C) resulted in a slower reaction, providing 25% conversion in 6 h, compared to 67% conversion with toluene. Also, when PhF (T_{AZ} = 60.2 °C) was employed, only 8% conversion was achieved after 6 h and 52% in 24 h. Finally, 1,2-DCE (T_{AZ} = 72.3 °C) considerably decelerated the reaction, providing 8% conversion in 24 hours.



% Conversion					
t (h)	PhMe	<i>t</i> -BuOAc	TAME	PhF	1,2-DCE
2 h	29%	27%	8%	4%	3%
6 h	67%	50%	25%	8%	4%
24 h	100%	93%	86%	52%	8%

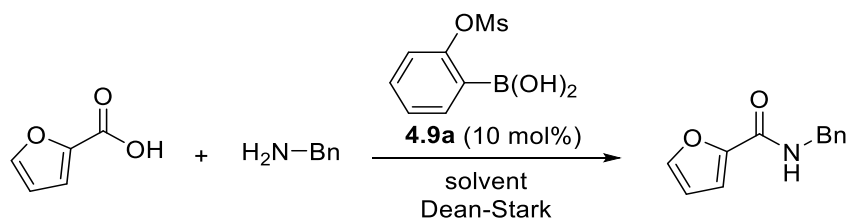
Table 5

As a result, the screening of several reaction solvents with varying boiling points and polarities revealed that toluene and *t*-BuOAc are the optimal solvents, and they were selected for further optimization studies.

4.8.3 Effect of the solvent concentration

The effect of the concentration of the reaction medium on the rate of the reaction was studied using toluene and *t*-BuOAc (Table 6). First, when toluene was used at 0.07 M, it provided 67% conversion in 6 h, however, at 0.14 M a higher conversion of 95% was recorded. An increase in the concentration of toluene to 0.5 M provided similar conversions to that of 0.14 M where 94% was achieved in 6 h. Therefore, the optimal concentration of toluene is 0.14 M.

Next, when *t*-BuOAc was examined at 0.07 M concentration, 50% conversion was achieved in 6 h. The use of higher concentration of 0.14 M provided very close conversions, affording 54% conversion in 6 h. Therefore, in this case, no rate enhancement was observed with the increase in concentration of *t*-BuOAc from 0.07 M and 0.14 M.



		PhMe			<i>t</i> -BuOAc	
t \ C	0.07 M	0.14 M	0.5 M	0.07 M	0.14 M	
2h	29%	47%	46%	27%	25%	
4h	54%	75%	75%	40%	41%	
6h	67%	95%	94%	50%	54%	
24h	100%	100%	100%	93%	90%	

Table 6

To conclude, these optimization studies have revealed that the most suitable conditions involve the use of 10 mol% loading of **4.9a**, in toluene and at 0.14 M concentration. These conditions are implemented in the following section to investigate the scope of amides synthesis with azeotropic removal of water.

4.9 Scope of the high-temperature amides synthesis

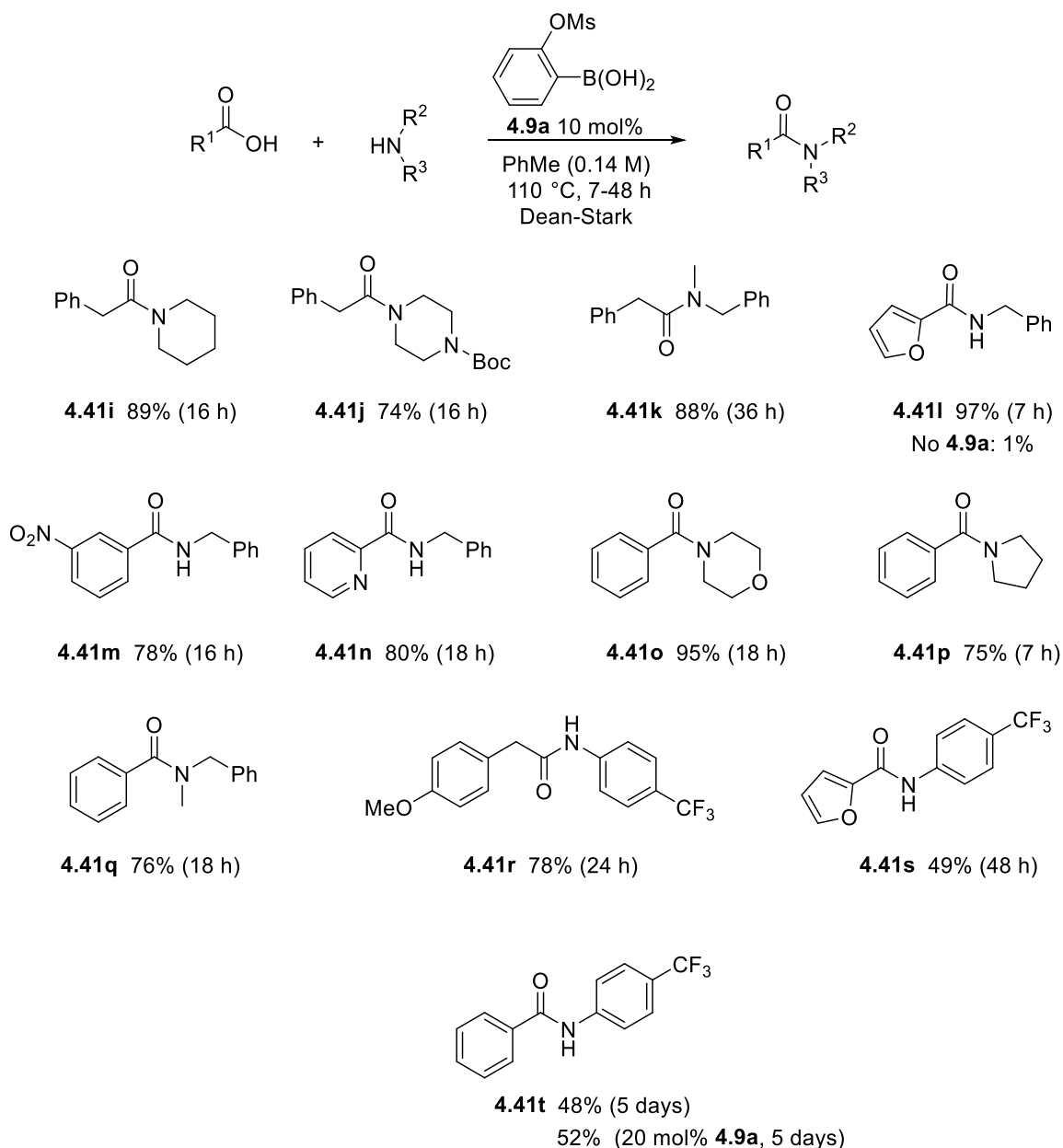
First, the reactions of phenylacetic acid with secondary amines were tested (Scheme 145). The coupling of phenylacetic acid with piperidine afforded the amide **4.41i** in 89% yield. Moreover, the reaction with *N*-Boc-piperazine provided the target amide **4.41j** in 74% yield. Interestingly, *N*-methylbenzylamine gave 88% yield of amide **4.41k**. Therefore, secondary amines efficiently reacted with phenylacetic acid under azeotropic reflux conditions.

Furthermore, the reaction of furoic acid with benzylamine, which afforded only 11% yield of **4.41l** at 40 °C in the presence of molecular sieves, delivered an improved 97% yield (Scheme 145). Notably, the control thermal reaction was carried out with the catalyst **4.9a** and it afforded **4.41l** in 1% yield only.

The applicability of this methodology has been broadened to include aryl and heteroaryl carboxylic acids (Scheme 145). The reaction of 3-nitrobenzoic acid with benzylamine furnished amide **4.41m** in 78% yield. Also, **4.41n** was obtained in an 80% yield from picolinic acid. It can be observed that aromatic acids reacted smoothly regardless of the aromatic ring's electron density since electron-poor 3-nitrobenzoic acid and picolinic acid provided good yields as did the electron-rich furoic acid.

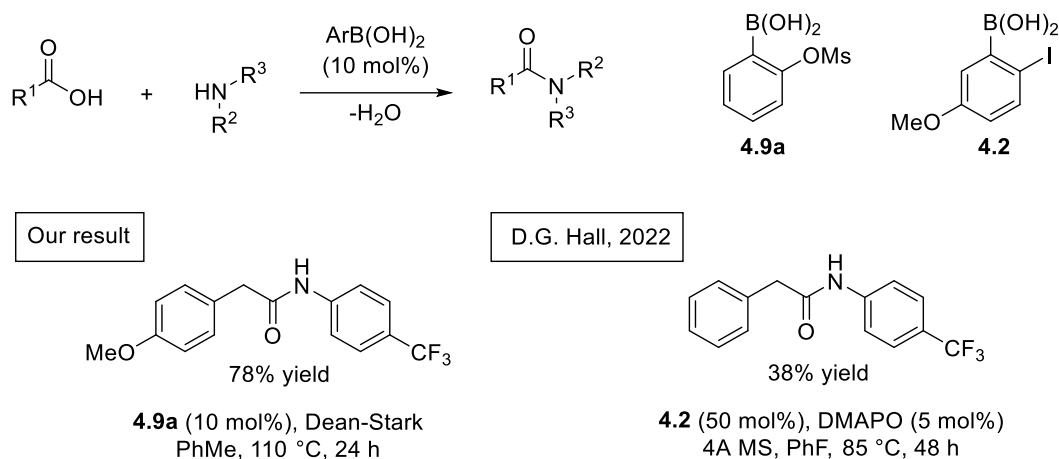
Moreover, secondary amines were reacted with benzoic acid (Scheme 145). First, the coupling with morpholine and pyrrolidine furnished the desired amides in 95% (**4.41o**) and 75% (**4.41p**) yields, respectively. Also, the reaction involving *N*-methylbenzylamine provided 76% of amide **4.41q**.

Lastly, the amides synthesis from anilines was investigated. The electron-deficient 4-trifluoromethylaniline successfully reacted with 4-methoxyphenylacetic acid to produce **4.41r** in 78% yield (Scheme 145). However, the coupling of 4-trifluoromethylaniline with aromatic carboxylic acids such as furoic acid (**4.41s**, 49%) and benzoic acid (**4.41t**, 48%) required very long reaction times ranging from 2 to 5 days. In the case of amide **4.41t**, higher catalyst loading of 20 mol% gave a marginally improved 52% yield (Scheme 145).



Scheme 145

Anilines are well-known to be challenging substrates for the amidation reaction, and reported examples of boronic acid-catalyzed approaches involved the use of either non-substituted aniline⁶³ or highly nucleophilic 4-methoxyaniline.^{65,61} The only example involving the coupling of an electron-deficient aniline was recently reported by Hall, in which phenylacetic acid is coupled with 4-(trifluoromethyl)aniline.⁶⁵ However, 50 mol% of **4.2** was required, along with a DMAPO co-catalyst, to achieve 38% yield in 48 h (Scheme 146).



Scheme 146

Overall, the amidation reaction under azeotropic removal of water was applicable to a variety of aromatic carboxylic acids and amines. It can be deduced that issue of low yields with secondary amines and aromatic acids that was encountered with the use of molecular sieves, was resolved through the implementation of the azeotropic reflux process for amide synthesis. Additionally, the challenges encountered with the coupling of anilines calls for an improvement of this methodology. One of the solutions that can be proposed is to use DMAPO co-catalyst, which has been reported to enhance the isolated yields of amides under azeotropic reflux conditions.¹⁸⁹ Lastly, aside from the synthetic utility, the exclusion of molecular sieves as a dehydrating agent in this protocol helps improve the practicality of amide-bond formation reactions.

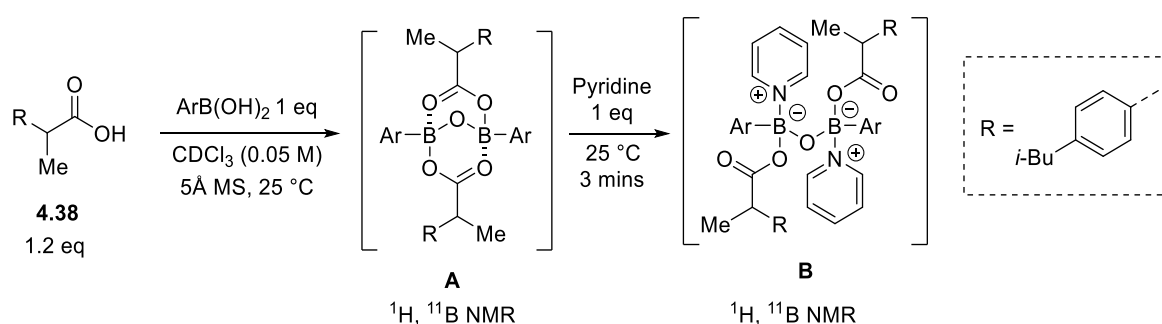
4.10 Mechanistic investigation

In our study, we were inspired by the mechanistic investigations of Whiting and Ishihara (discussed in Chapter 1) to gain insight into the mechanism of action of (sulfonyloxy)phenylboronic acid catalysts in amide synthesis. Besides examining the formed intermediates during the reaction, this mechanism was proposed to understand the significantly different catalytic efficiency between *ortho*-mesyloxyphenyl boronic acid **4.9a** and its *para*-regioisomer **4.16**. To recall, boronic acid **4.9a** afforded 100% NMR yield in 1 h on the reaction

¹⁸⁹ Ishihara K. *Chem. Sci.* **2016**, 7, 1276-1280.

of synthesis of *N*-benzyl-2-phenylacetamide, whereas boronic acid **4.16** provided only 26% NMR yield.

The general methodology used for the mechanistic studies was as follows (Scheme 147): first, the boronic acid (0.025 mmol) was added to a vial containing (*S*)-ibuprofen 99% (1.2 eq) and activated powdered 5Å MS (50 mg) in CDCl₃ (0.05 M, 0.5 ml). This mixture was vigorously stirred at 25 °C for 30 mins. Then, the reaction mixture was transferred to an NMR tube, and analyzed by ¹H and ¹¹B NMR. If the conversion into the B-O-B bridged complex **A** was complete, pyridine (1 eq) was added to the NMR tube, and after vigorous shaking for 3 mins, the mixture was analyzed by ¹H and ¹¹B NMR. Then, the % conversion from complex **A** to **B** was determined by the integration of the CH₃SO₂-signals of **A** and **B**. If conversion into **A** was not complete, then more (*S*)-ibuprofen was added until full conversion into **A**. Afterward, pyridine (1 eq) was added and the same experimental procedure as above was followed.



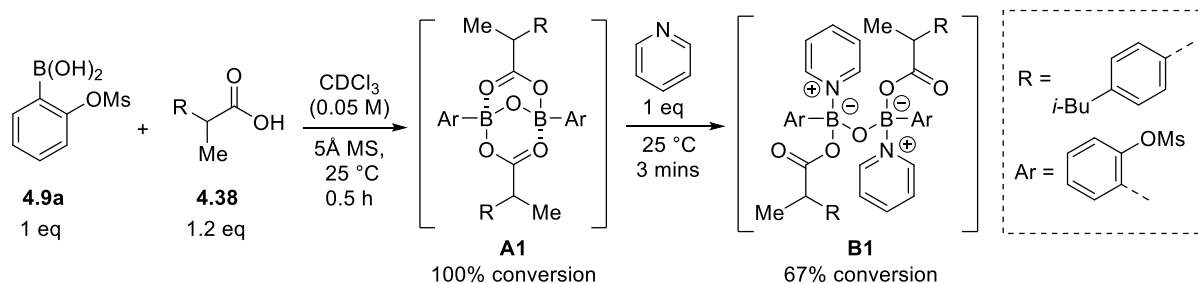
Scheme 147

It is important to mention that the assignment of complexes **A** and **B** was made based on a combination of ¹H and ¹¹B NMR data. Herein, the ¹H NMR data will be presented initially, followed by the ¹¹B NMR spectra, for presentation purposes.

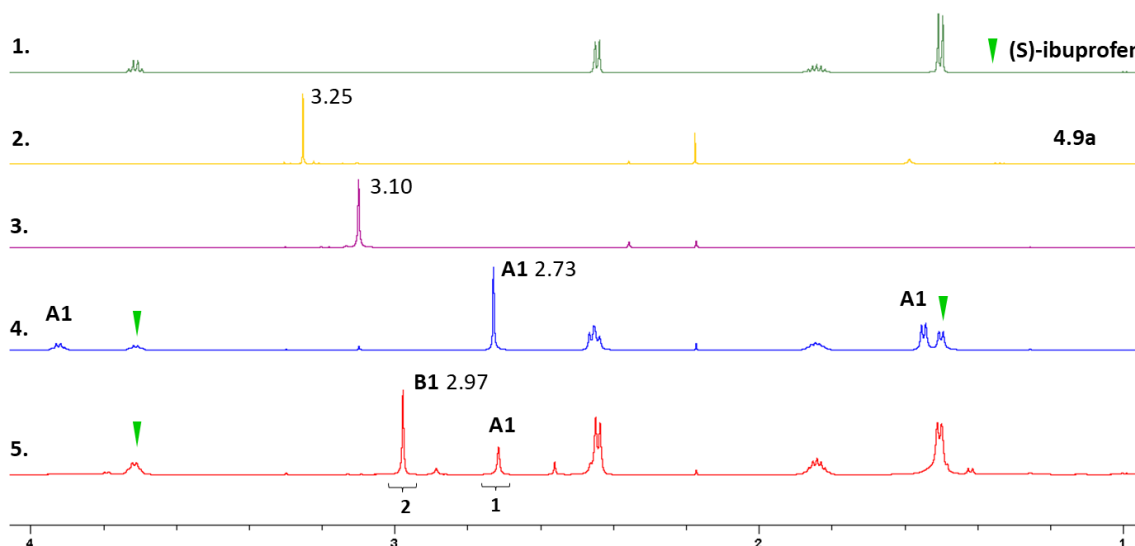
First, the boronic acid **4.9a** and its boroxine were characterized by ¹H and ¹¹B NMR to be able to identify their signals. A solution of boronic acid **4.9a** in CDCl₃ showed a mesyl (CH₃SO₂) signal at 3.25 ppm in ¹H NMR (Entry 2, Scheme 148). When activated powdered 5Å MS was added to this solution, a new mesyl signal appeared at 3.10 ppm corresponding to the boroxine (Entry 3, Scheme 148).

Next, the reaction of formation of **A1** was conducted. The boronic acid **4.9a** (0.025 mmol), (*S*)-ibuprofen 99% (1.2 eq), and activated powdered 5Å MS (50 mg) were added to CDCl₃ (0.05 M). When this mixture was stirred at 25 °C for 30 mins, the formation of a new mesyl signal at 2.73 ppm was observed in ¹H NMR (Entry 4, Scheme 148). Moreover, the ¹H NMR signal at

2.73 ppm did not correspond to **4.9a** (3.25 ppm) or its boroxine (3.10 ppm). Therefore, full conversion of **4.9b** into **A1** was achieved and the complex **A1** was characterized by ^1H , and ^{13}C NMR by subtracting the surplus signals from (S)-ibuprofen in the reaction mixture (described in the experimental section).



^1H NMR (1-4 ppm)

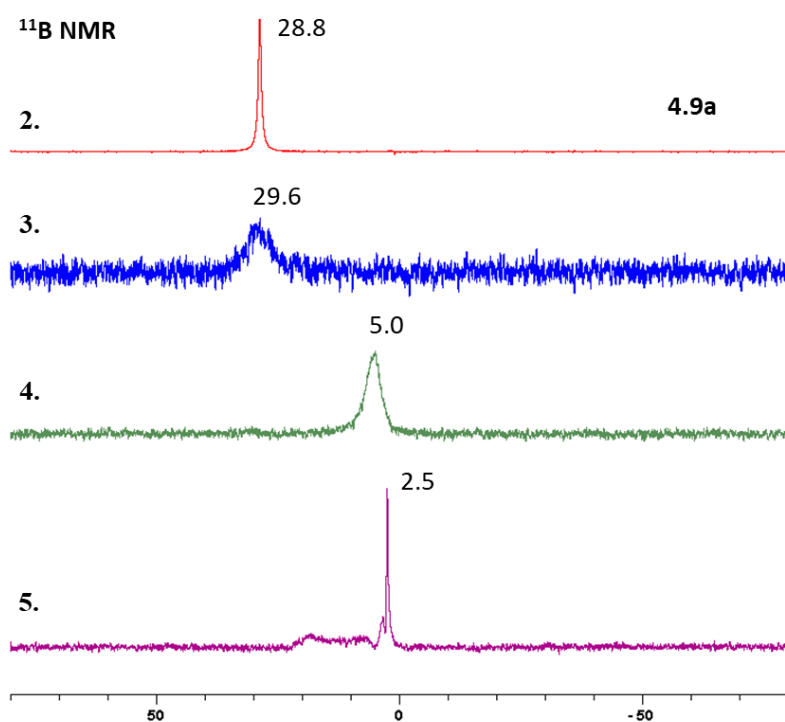


1. Pure (S)-ibuprofen in CDCl_3 ; 2. Pure boronic acid **4.9a** in CDCl_3 ; 3. Boronic acid **4.9a**, 5Å powdered activated MS (20 mg), CDCl_3 , 25 °C, 10 sec 4. Boronic acid **4.9a** (5.4 mg, 0.025 mmol), (S)-ibuprofen (6.3 mg, 0.03 mmol, 1.2 eq), 5Å activated powdered MS (50 mg) in CDCl_3 , 25 °C, 30 mins 5. Mixture of entry 4 + pyridine (2 μL , 2 mg, 0.025 mmol, 1 eq), 25 °C, 3 mins.

Scheme 148

Subsequently, pyridine (1 eq) was introduced, and after vigorous shaking for 3 mins at 25 °C, the sample was analyzed. In ^1H NMR, two mesyl signals were observed, one at 2.73 ppm which corresponded to the remaining **A1** and another at 2.97 ppm which was suggested to belong to complex **B1** (Entry 5, Scheme 148). Based on the ^1H integrations of **A1** and **B1**, there was a 67% conversion of **A1** into the pyridinium-boronate complex **B1** (Entry 5, Scheme 148).

The ^{11}B NMR of a solution of **4.9a** in CDCl_3 shows a signal at 28.8 ppm (Entry 2, Scheme 149). Once activated powdered 5 Å MS was added, a new signal appeared at 29.6 ppm corresponding to the boroxine (Entry 3, Scheme 149). Moreover, the mixture of **4.9a** with (S)-ibuprofen and activated powdered 5 Å MS displayed a signal at 5.0 ppm in ^{11}B NMR, after 30 mins reaction at 25 °C (Entry 4, Scheme 149). Based on Whiting's mechanistic investigations, the signal around 5 ppm in ^{11}B NMR was diagnostic of a catalytically active intermediate bearing a B-O-B linkage.⁵⁹ This showed that **A1** was indeed the formed complex. Furthermore, after the addition of pyridine (1 eq), a major signal at 2.5 ppm appeared which was indicative of a tetrahedral boron species (Entry 5, Scheme 149). This supported the formation of complex **B1** (Entry 5, Scheme 149).

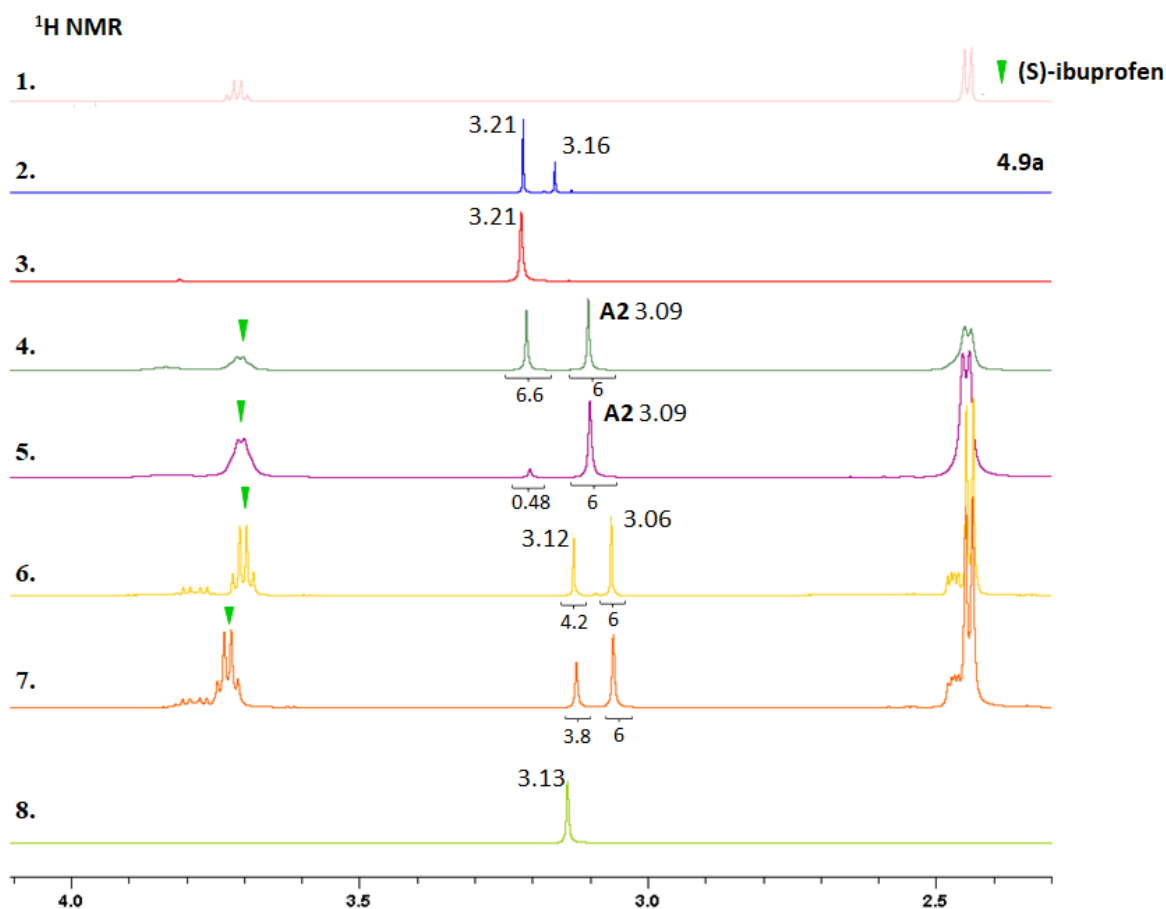
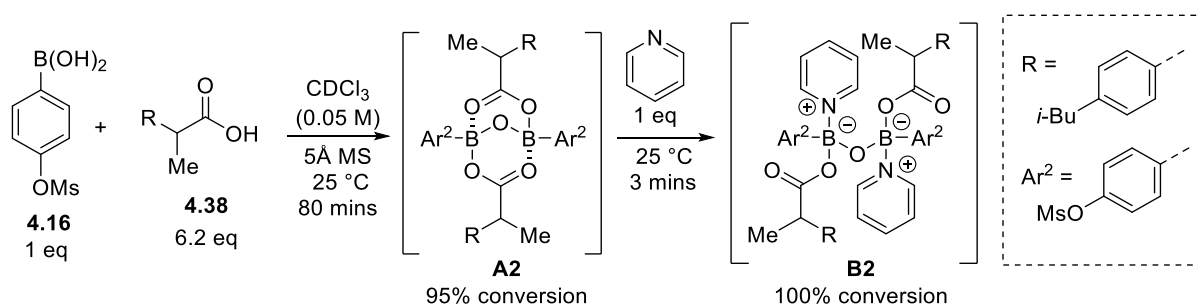


2. Pure boronic acid **4.9a** in CDCl_3 ; 3. Boronic acid **4.9a**, 5 Å powdered activated MS (20 mg), CDCl_3 , 25 °C, 10 sec 4. Boronic acid **4.9a** (5.4 mg, 0.025 mmol), (S)-ibuprofen (6.3 mg, 0.03 mmol, 1.2 eq), 5 Å activated powdered MS (50 mg) in CDCl_3 , 25 °C, 30 mins 5. Mixture of entry 4 + pyridine (2 μL , 2 mg, 0.025 mmol, 1 eq), 25 °C, 3 mins.

Scheme 149

Consequently, the *para*-(mesyloxy)phenylboronic acid **4.16** was studied using a similar experiment to that of **4.9a**. The ^1H NMR of a solution of **4.16** in CDCl_3 , showed two mesyl signals at 3.21 ppm and 3.16 ppm (Entry 2, Scheme 150). When activated powdered 5 Å MS

was added, a single mesyl signal appeared at 3.21 ppm (Entry 3, Scheme 150). Therefore, the peak at 3.21 ppm corresponded to the boroxine, and that at 3.16 was for boronic acid **4.16**.



1. Pure (S)-ibuprofen in CDCl_3 ; 2. Pure boronic acid **4.16** in CDCl_3 ; 3. Boronic acid **4.16**, 5Å powdered activated MS (20 mg), CDCl_3 , 25 °C, 10 sec 4. Boronic acid **4.16** (5.4 mg, 0.025 mmol), (S)-ibuprofen (6.3 mg, 0.03 mmol, 1.2 eq), 5Å activated powdered MS (50 mg) in CDCl_3 , 25 °C, 30 mins 5. Sequential (S)-ibuprofen addition until 95% conversion to **A2** after a total of 6.2 eq (S)-ibuprofen; 6. Mixture of entry 5 + pyridine (2 μL , 2 mg, 0.025 mmol, 1 eq), 25 °C, 3 mins; 7. Mixture of entry 6 + 5 eq pyridine, 25 °C, 15 mins; 8. Boronic acid **4.16** (5.4 mg, 0.025 mmol), pyridine (2 μL , 2 mg, 0.025 mmol, 1 eq), 5Å activated powdered MS (50 mg) in CDCl_3 , 25 °C, 5 sec.

Scheme 150

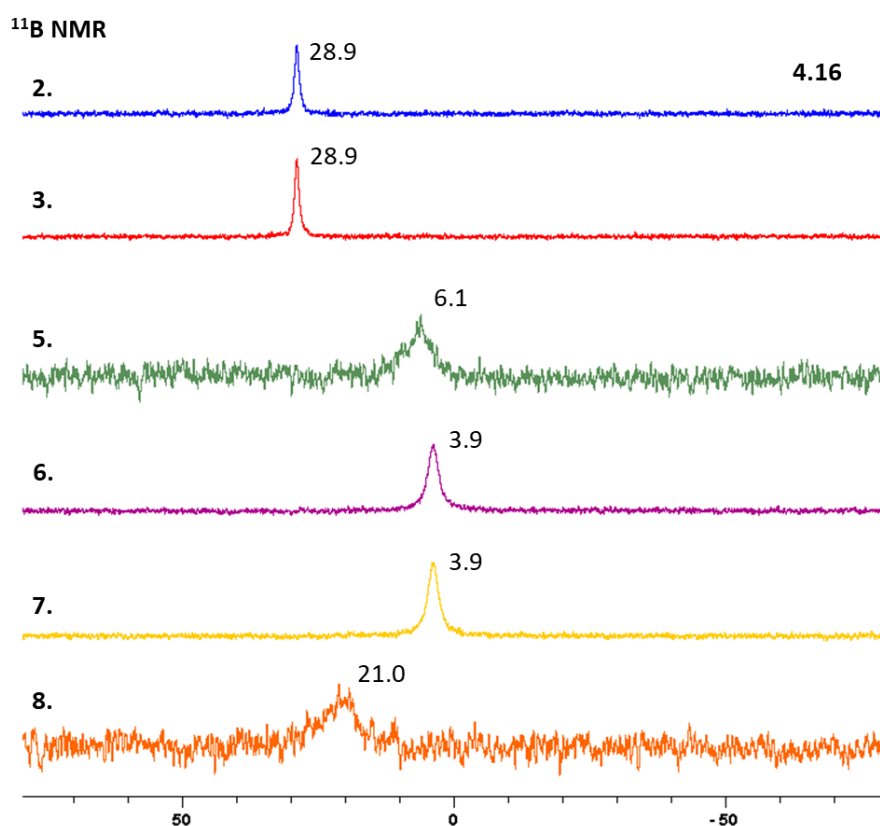
Next, a mixture of **4.16** (0.025 mmol), (S)-ibuprofen (1.2 eq), and activated powdered 5Å MS (50 mg), in CDCl_3 (0.05 M), was vigorously stirred for 30 mins at 25 °C. In this case, a new

signal appeared at 3.09 ppm, which was attributed to complex **A2**, alongside the signal of the boroxine at 3.21 ppm (Entry 4, Scheme 150). Based on the ^1H NMR integrations of the mesyl signals of **A2** (3.09 ppm, $2\times\text{CH}_3$) and boroxine (3.21 ppm, $3\times\text{CH}_3$), there was a 58% conversion into **A2**. Afterward, sequential addition of **4.38** portions (1 eq each), followed by vigorous mixing for 10 mins after each addition was performed. After a total of 6.2 eq of **4.38** and 80 minutes reaction time, 95% conversion into **A2** was achieved (Entry 5, Scheme 150). Complex **A2** was characterized by ^1H NMR by subtracting the surplus signals from (S)-ibuprofen in the reaction mixture (described in the experimental section).

To this mixture, pyridine (1 eq) was added and the mixture was vigorously shaken for 3 mins. In ^1H NMR, the signal of **A2** at 3.09 disappeared, indicating full consumption of **A2** (Entry 6, Scheme 150). Moreover, 2 new peaks appeared at 3.12 ppm and 3.06 ppm, one of which should belong to **B2**. Initially, it was assumed that one of these signals could represent a structure with only one pyridinium-boronate group. Therefore, an excess of pyridine (5 eq total) was added to this sample. In this case, the ratio of the peaks at 3.12 ppm and 3.06 ppm changed marginally from 4.2:6 to 3.8: 6 (Entry 7, Scheme 150). Since a very minor change in the ratio of these two peaks was observed, we ruled out a mixture of complex derived from **A2** bearing one molecule of pyridine. Furthermore, a control experiment, in which pyridine (1 eq) was added to **4.16** and 5Å MS, revealed a signal of CH_3SO_2 at 3.13 ppm that was assigned for a boroxine-pyridine complex (Entry 8, Scheme 150). As a result, the signal at 3.12 ppm (Entry 6, Scheme 150) was attributed to a boroxine-pyridine complex, and that at 3.09 ppm was assigned to **B2**.

Furthermore, the ^{11}B NMR data provided further confirmation of the nature of the formed intermediates. The ^{11}B NMR of **4.16** in CDCl_3 showed a signal at 28.9 ppm (Entry 2, Scheme 151). When activated powdered 5Å MS was added, the boroxine was formed and it displayed a similar signal at 28.9 ppm (Entry 3, Scheme 151). The mixture of **4.16**, (S)-ibuprofen (6.2 eq total), and activated powdered 5Å MS had a signal at 6.1 ppm, which confirmed the formation of B-O-B bridged complex **A2** (Entry 5, Scheme 151). Additionally, upon the introduction of pyridine (1 eq), a signal at 3.9 ppm appeared (Entry 6, Scheme 151). This signal remained unchanged after the amount of the pyridine was increased by 5 equivalents (Entry 7, Scheme 151). Hence, the ^{11}B NMR peak at 3.9 ppm was related to **B2**. Lastly, when pyridine (1 eq) was added to **4.16** and 5Å MS, a very weak signal was detected at 21 ppm (Entry 8, Scheme 151). Whiting has reported that the boroxine-pyridinium complexes have appeared in ^{11}B NMR at 15-20 ppm.⁵⁹ Hence ^{11}B NMR signal of 21 ppm belonged to a boroxine-pyridinium complex.

It is worth noting that the peak at 21 ppm was not observed in Entries 6 and 7 (Scheme 151), most likely due to its very low intensity.



2. Pure boronic acid **4.16** in CDCl_3 ; **3.** Boronic acid **4.16**, 5Å powdered activated MS (20 mg), CDCl_3 , 25 °C, 10 sec **5.** Boronic acid **4.16** (5.4 mg, 0.025 mmol), (S)-ibuprofen (6.2 eq total), 5Å activated powdered MS (50 mg) in CDCl_3 , 25 °C, 30 mins (95% conversion to **A2**) ; **6.** Mixture of entry 5 + pyridine (2 μL , 2 mg, 0.025 mmol, 1 eq), 25 °C, 3 mins ; **7.** Mixture of entry 6 + 5 eq pyridine, 25 °C, 15 mins ; **8.** Boronic acid **4.16** (5.4 mg, 0.025 mmol), pyridine (2 μL , 2 mg, 0.025 mmol, 1 eq), 5Å activated powdered MS (50 mg) in CDCl_3 , 25 °C, 5 sec.

Scheme 151

Overall, these findings suggest that the formation of the catalytically active B-O-B complex from boronic acid **4.16** is more demanding than its formation from **4.9a**. Hence, it can be presumed that one of the reasons for the poor catalytic performance of **4.16** is its low efficiency in activating the carboxylic acid. Additionally, while the *para*-mesyloxy derivative **4.16** has enabled higher conversion (100%) into the catalytically inactive pyridinium-boronate complex than its *ortho*-mesyloxy analog **4.9a** (67%), this difference is insufficient to solely account for the big difference in terms of catalytic activity. Hence, it can be proposed that the combination of electronic and steric properties of **4.16** that makes the formation of the active catalytic complex difficult and the generation of inactive boronate complex facile, could result in this

low catalytic efficiency. This confirms the role of the *ortho*-substitution as a key element for a competent catalyst design.

4.11 Conclusions

The majority of research on arylboronic acid catalysts for direct amide synthesis has entailed the use of commercially available boronic acids or those whose design was guided by a trial and error process. In this study, we devised a strategy for rational catalyst development. To begin, fluorine-ion affinity (FIA), a computationally driven metric, can be used to predict the Lewis acidity (LA) trend of plausible arylboronic acid candidates. Following that, the FIA values can be compared to those of proficiently performing, reference boronic acids to identify the candidates that may offer good catalytic activity and those that do not.

Applying this strategy, a new group of *ortho*-(sulfonyloxy)phenylboronic acid catalysts was uncovered. It was discovered that while boronic acids with higher LA, provided enhanced activity in many cases, such correlation was not always direct due to the interference of steric effects and instability issues. For instance, the 2,6-bis(triflyoxy)phenyl boronic acid **4.10**, possesses higher LA and much improved kinetic activity than the 2-triflyoxy derivative **4.9b**; however, the former's remarkable catalytic performance was restricted due to its high susceptibility to protodeborylate.

Importantly, this class of catalysts compared favorably with the established state-of-the-art boronic acids. Moreover, the 2-mesyloxy- **4.9a** and 2-triflyoxy- **4.9b** phenylboronic acids, which provided the best compromise between proficient catalytic activity and stability, were exploited to study the scope and limitations of this methodology. It was revealed that a wide range of aliphatic acids, including those bearing heterocycles and α -substitution can be well tolerated under dehydrative conditions achieved using molecular sieves. Remarkably, challenging aromatic acids and anilines were efficiently coupled, albeit requiring higher temperatures and the switch to azeotropic reflux conditions.

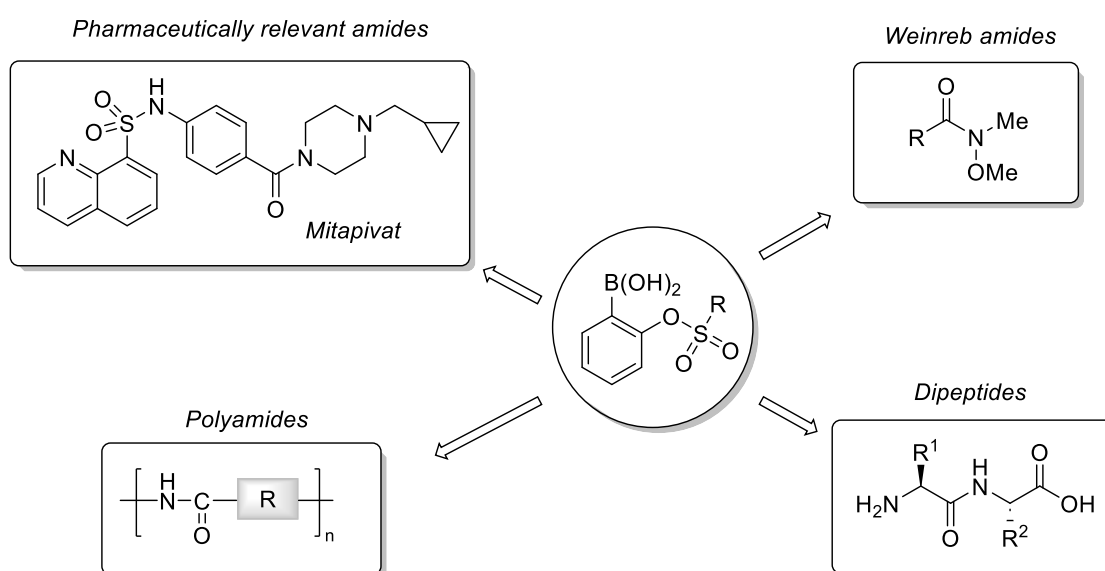
Lastly, the study of the interaction between boronic acid and the reaction components, i.e. acid and amine partners, revealed that the carboxylic acid is activated via a dimeric intermediate bridged by a B-O-B linkage. Furthermore, comparative mechanistic studies between the *ortho*-substituted boronic acid **4.9a** and its *para*-analog **4.16** revealed that, while steric effects

imposed by the *ortho*-group do contribute to minimizing the formation of a catalytically inactive species, they aren't the sole variables influencing the performance of the catalyst.

4.12 Future Perspective

For the purpose of a more reliable predictive catalyst design, it would be very valuable if a quantitative estimation of the substituents' steric effects could also be performed. Very recently, a study has been reported on the quantification of the steric properties of Lewis acids based on the percentage of buried volume ($\%V_{\text{Bur}}$) of their fluoride adducts.¹⁹⁰ Given that the same input structure for FIA calculations can be used to estimate steric properties, it can be suggested that a correlation between the FIA and $\%V_{\text{Bur}}$ would provide beneficial information on steric-electronic properties, permitting more robust catalyst development.

Nonetheless, it is anticipated that the current work will lead to further accomplishments, whether at the level of developing novel arylboronic acid catalysts or in terms of their catalytic utility. Preliminarily, it can be proposed that the application of (sulfonyloxy)phenylboronic acids could be broadened to include the synthesis of pharmaceutically relevant amides such as Mitapivat (Scheme 152).



Scheme 152

¹⁹⁰ Zapf, L.; Riethmann, M.; Föhrenbacher, S. A.; Finze, M.; Radius, U. *Chem. Sci.* **2023**, *14*, 2275–2288.

The formation of dipeptides and Weinreb amides is another appealing application area (Scheme 152). With the exception of a recent report involving the use of diboronic acids for Weinreb amide synthesis,¹⁹¹ the latter has not yet been examined under boronic acid catalysis. Finally, given that the only document on boronic acid-catalyzed polyamide synthesis dates back to 1996,¹⁹² the use of such catalysts for the fabrication of polymeric materials (Scheme 152) might very well present an opportunity to lower the energy requirements of this process.

¹⁹¹ Shimada, N.; Takahashi, N.; Ohse, N.; Koshizuka, M.; Makino, K. *Chem. Commun.* **2020**, 56, 13145–13148.

¹⁹² Ishihara, K.; Ohara, S.; Yamamoto, H. *Macromolecules* **2000**, 33, 3511–3513.

4.13 Experimental Section

4.13.1 General Methods

Dry solvents (THF, dichloromethane, diethyl ether, acetonitrile, and toluene) were dried from a double-cartridge solvent purification system. Fluorobenzene and anhydrous DMF were purchased from Sigma-Aldrich. Analytical thin layer chromatographies were performed on silica gel 60 F254 plates. ^1H NMR spectra were recorded on BRUKER Avance III (500 MHz) and BRUKER NEO (600 MHz) spectrometers. ^1H NMR spectral data were recorded as follows: chemical shift in ppm from internal tetramethylsilane on the δ scale, multiplicity (s = singlet; br s = broad singlet; d = doublet; t = triplet; q = quartet; sept = septet; m = multiplet, dd = doublet of doublet, dt = doublet of triplet, etc.), coupling constant (Hz), and integration. The residual solvent protons (in ^1H NMR) were used as internal standards (CDCl_3 at 7.26 ppm, CD_3CN at 1.94 ppm, and $\text{DMSO-}d_6$ at 2.50 ppm). ^{13}C NMR spectra were taken on a BRUKER Avance III (125 MHz) and BRUKER NEO (150 MHz) spectrometers. Chemical shifts were recorded in ppm from the solvent resonance employed as the internal standard (CDCl_3 at 77.16 ppm, CD_3CN at 1.32 and 118.26 ppm, and $\text{DMSO-}d_6$ at 39.52 ppm). ^{11}B NMR spectra were taken on BRUKER Avance III (160 MHz) and BRUKER NEO (193 MHz) spectrometers. ^{19}F NMR spectra were taken on a BRUKER Avance III (470 MHz) and BRUKER NEO (565 MHz) spectrometers. Chemical shifts recorded in NMR experiments were performed in deuterated solvents (CDCl_3 with 0.04% TMS, CD_3CN , or $\text{DMSO-}d_6$) purchased from Eurisotop. In some mentioned cases, a drop of deuterated water was added in order to minimize the formation of the corresponding boronic anhydrides. Because of their low intensity (resulting from quadrupolar coupling), ^{13}C signals arising from the quaternary carbon bearing the boronic acid group were not observed in most cases (unless otherwise mentioned).

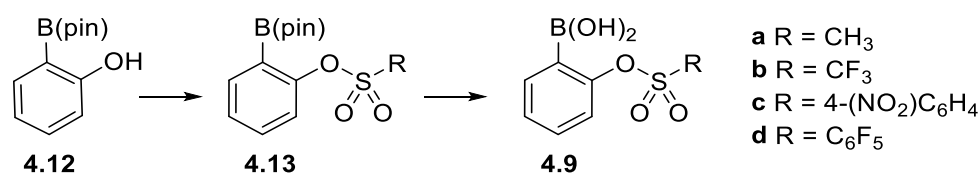
Mass spectrometry analysis were conducted using a Q-ToF APCI analyzer equipped with an atmospheric pressure chemical ionization (APCI) source. The used instrument was the UPLC H-ClassXevo G2-XS QToF (WATERS) spectrometer. High-resolution mass spectra were recorded using either atmospheric solids analysis probe (ASAP) or electrospray ionization (ESI) techniques.

Infrared spectra were recorded using a PerkinElmer Spectrum Two Fourier Transform Infrared (FT-IR) Spectrometer equipped with a diamond attenuated total reflectance (ATR) accessory.

Measurements were conducted in the mid-infrared region (4000-450 cm^{-1}) with a resolution of 4 cm^{-1} . Each spectrum was obtained by accumulating 50 scans to improve the signal-to-noise ratio. Baseline correction was performed by acquiring a blank spectrum without the sample and subtracting it from the sample spectrum to remove any instrument or background noise. The IR spectra were reported as frequencies expressed in cm^{-1} .

5Å molecular sieves were purchased from Sigma-Aldrich (CAS 69912-79-4), reference 233676-500G (powder, undried). This reference is no more available. 4Å molecular sieves were purchased from Sigma-Aldrich (CAS 70955-01-0), reference 688363-500G (powder, activated, -325 mesh particle size). The molecular sieves were activated under a high vacuum (1 mbar) at 250 °C using a Kugelrohr distillation instrument for 2 hours.

4.13.2 Preparation and characterization of *ortho*-(sulfonyloxy)phenylboronic acids



4.13.2.1 General procedure A for the preparation of 2-(sulfonyloxy)phenylboronic acid pinacol ester

To a solution of 2-hydroxyphenylboronic acid pinacol ester (1 equiv.) in dry CH_2Cl_2 (0.2 M), under argon, was added *N,N*-diisopropylethylamine (2 equiv.), and the properly substituted sulfonylchloride or anhydride (2 equiv.) at 0 °C. After stirring for 10 mins at 0 °C, the mixture was allowed to warm to 25 °C and stirred for 2-16 h (progress of the reaction was monitored by TLC in Cy/EtOAc (80:20)). Then, H_2O (20 mL) was added, and the mixture was extracted with CH_2Cl_2 (3×25 mL). The combined organic extracts were dried over MgSO_4 and the filtrate was concentrated under reduced pressure to afford the crude residue. The latter was purified by flash silica-gel column chromatography using Cy/EtOAc (80:20) to afford the pure product.

4.13.2.2 General procedure B for the deprotection of 2-(sulfonyloxy)phenylboronic acid pinacol ester with NaIO_4

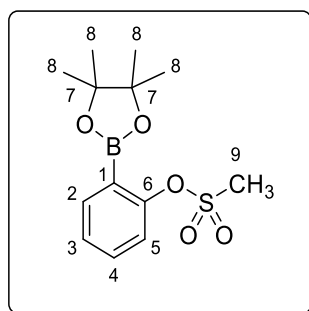
To a solution of the corresponding pinacol boronate (1 equiv.) in THF: H_2O (5:1; 0.2M) was added sodium periodate (4 equiv.) at 25 °C. Then, aqueous HCl (1 M, 1 equiv.) was added and

this mixture was stirred for 2-16 h at 25 °C (progress of the reaction was monitored by TLC in Cy/EtOAc 90:10). Once the conversion is complete, water (10 mL) was added and the mixture was extracted with EtOAc (3×20 mL). The combined organic extracts were dried over MgSO₄, and after filtration, the filtrate was concentrated under reduced pressure to afford the crude residue. The residual oil was purified by trituration using Cy: CHCl₃ (1:1; 5 mL) to afford the pure boronic acid.

4.13.2.3 General procedure C for the deprotection of 2-(sulfonyloxy)phenylboronic acid pinacol ester with diethanolamine.

To a solution of the corresponding pinacol boronate (1 equiv.) in Et₂O (0.1 M) was added diethanolamine (1.1 equiv.) at 25 °C. The precipitation of a pale-yellow solid (diethanolamine-boronate complex) is observed within minutes after the addition of diethanolamine. This mixture was stirred until the disappearance of the starting pinacol boronate in the supernatant (the reaction progress was monitored by TLC in Cy/EtOAc 90:10). Once the reaction is complete, the precipitate was collected through decantation, and the crude complex was used for the hydrolysis step without further purification. Next, aqueous HCl (0.1 M, 3 eq) was added to a suspension of the diethanolamine-boronate complex (1 equiv.) in diethyl ether (2 mL). The mixture was stirred at 25 °C for 30 mins, then the organic phase was collected by washing with EtOAc (3×10 mL). The organic layers were collected, washed with brine (15 mL), dried over MgSO₄, and concentrated under reduced pressure to afford pure boronic acid.

(2-((Methylsulfonyl)oxy)phenyl)boronic acid pinacol ester 4.13a



The title compound was prepared from 2-hydroxyphenylboronic acid pinacol ester **4.12** (660 mg, 3 mmol, 1 equiv.), DIPEA (1.05 mL, 6 mmol, 2 equiv.) and methanesulfonyl chloride (0.46 mL, 6 mmol, 2 equiv.) after 4 h at 25 °C, according to general procedure **A**. The product **4.13a** was obtained pure after the extractive work-up as a pale-yellow oil that crystallizes at 25 °C to

give a pale-yellow crystalline solid (885 mg, 2.97 mmol, **99% yield**). The ^1H and ^{13}C NMR data match those reported in the literature.¹⁵⁶

Rf (Cy/EtOAc 80:20) = 0.6

$\text{C}_{13}\text{H}_{19}\text{BO}_5\text{S}$, **M.W**: 298.16 g/mol. **M.p**: 60-62 °C.

^1H NMR (600 MHz; CDCl_3): δ 7.82 (dd, $J = 7.4, 1.8$ Hz, 1H, H^2), 7.49 (ddd, $J = 8.2, 7.4, 1.8$ Hz, 1H, H^4), 7.34 (dd, $J = 8.2, 0.9$ Hz, 1H, H^5), 7.31 (td, $J = 7.4, 0.9$ Hz, 1H, H^3), 3.20 (s, 3H, H^9), 1.36 (s, 12H, H^8).

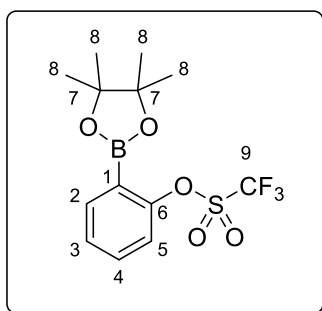
^{13}C NMR (150 MHz; CDCl_3) δ 153.3 (C_{qAr} , C^6), 137.2 (CH_{Ar} , C^2), 132.8 (CH_{Ar} , C^4), 126.9 (CH_{Ar} , C^3), 122.6 (CH_{Ar} , C^5), 84.3 (2 C_{q} , C^7), 37.8 (CH_3 , C^9), 25.0 (4 CH_3 , C^8). C^1 was not observed due to quadrupolar relaxation.

^{11}B NMR (192.5 MHz, CDCl_3) δ 30.1 ppm.

HRMS (ESI-TOF) m/z : $[\text{M} + \text{Na}]^+$ Calcd for $\text{C}_{13}\text{H}_{19}\text{O}_5\text{SBNa}$: 321.0944; Found: 321.0948.

IR (neat)/ cm^{-1} ν_{max} 3396, 3032, 2981, 2949, 1609, 1439, 1367, 1351, 1153, 1118, 1065, 962, 792, 774.

(2-(((Trifluoromethyl)sulfonyl)oxy)phenyl)boronic acid pinacol ester **4.13b**



The title compound was prepared from 2-hydroxyphenylboronic acid pinacol ester **4.12** (660 mg, 3 mmol, 1 equiv.), DIPEA (1.05 mL, 6 mmol, 2 equiv.) and Tf_2O (1 mL, 1.692 g, 6 mmol, 2 equiv.) after 2 h at 25 °C, according to general procedure **A**. The residual oil (1.30 g) obtained after extractive work-up was purified by flash silica-gel column chromatography (Cy/EtOAc 90:10) to afford the pure product **4.13b** as a colorless oil (973 mg, 2.76 mmol, **92% yield**). The ^1H and ^{13}C NMR data match those reported in the literature.¹⁵⁶

Rf (Cy/EtOAc 80:20) = 0.5

$C_{13}H_{16}BO_5F_3S$, **M.W.**: 352.13 g/mol.

1H NMR (600 MHz; $CDCl_3$): δ 7.87 (dd, $J = 7.4, 1.8$ Hz, 1H, H^2), 7.51 (ddd, $J = 8.3, 7.4, 1.8$ Hz, 1H, H^4), 7.38 (td, $J = 7.4, 0.9$ Hz, 1H, H^3), 7.22 (d, $J = 8.3$ Hz, 1H, H^5), 1.37 (s, 12H, H^8).

^{13}C NMR (150 MHz; $CDCl_3$) δ 154.4 (C_{qAr} , C^6), 137.3 (CH_{Ar} , C^2), 133.1 (CH_{Ar} , C^4), 127.9 (CH_{Ar} , C^3), 121.1 (q, $^5J_{C-F} = 1.2$ Hz, C^5), 119.0 (q, $^1J_{C-F} = 321.0$ Hz, C^9), 84.7 (2 Cq , C^7), 24.9 (4 CH_3 , C^8). C^1 was not observed due to quadrupolar relaxation.

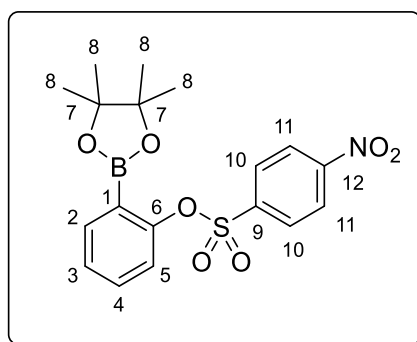
^{19}F NMR (565 MHz, $CDCl_3$) δ -73.1 ppm.

^{11}B NMR (192.5 MHz, $CDCl_3$) δ 29.9 ppm

HRMS (ASAP-TOF) m/z : $[M]^+$ Calcd for $C_{13}H_{16}BO_5F_3S$: 352.0764; Found: 352.0776.

IR (neat)/ cm^{-1} ν_{max} 2982, 1613, 1422, 1382, 1356, 1334, 1247, 1119, 1058, 856, 780.

(2-(((4-Nitrophenyl)sulfonyl)oxy)phenyl)boronic acid pinacol ester **4.13c**



The title compound was prepared from 2-hydroxyphenylboronic acid pinacol ester **4.12** (611 mg, 2.5 mmol, 1 equiv.), DIPEA (0.87 mL, 5 mmol, 2 equiv.) and 4-nitrobenzenesulfonyl chloride (1.166 g, 5 mmol, 2 equiv.) after 16 h at 25 °C, according to general procedure **A**. The crude yellow powder (1.02 g) obtained after extraction was purified by flash silica-gel column chromatography (Cy/EtOAc 90:10) to afford the pure product **4.13c** as a pale-yellow amorphous powder (942 mg, 2.32 mmol, **93% yield**).

Rf (Cy/EtOAc 80:20) = 0.7

$C_{18}H_{20}BNO_7S$, **M.W.**: 405.23 g/mol. **M.p.**: 139-142 °C.

¹H NMR (600 MHz; CDCl₃): δ 8.35 (d, *J* = 9.0 Hz, 2H, H¹¹), 8.11 (d, *J* = 9.0 Hz, 2H, H¹⁰), 7.80 (dd, *J* = 7.4, 1.8 Hz, 1H, H²), 7.37 (ddd, *J* = 8.1, 7.4, 1.8 Hz, 1H, H⁴), 7.30 (td, *J* = 7.4, 1.0 Hz, 1H, H³), 6.90 (dd, *J* = 8.1, 1.0 Hz, 1H, H⁵), 1.33 (s, 12H, H⁸).

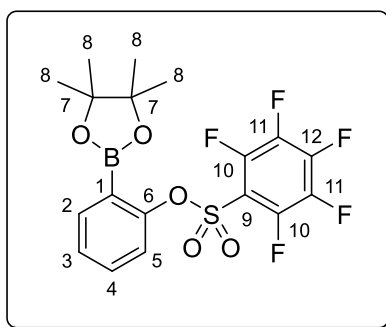
¹³C NMR (150 MHz; CDCl₃) δ 153.2 (C_{qAr}, C⁶), 150.9 (C_{qAr}, C¹²), 142.0 (C_{qAr}, C⁹), 137.3 (CH_{Ar}, C²), 132.6 (CH_{Ar}, C⁴), 130.1 (2CH_{Ar}, C¹⁰), 127.3 (CH_{Ar}, C³), 124.2 (2CH_{Ar}, C¹¹), 121.7 (CH_{Ar}, C⁵), 84.4 (2C_q, C⁷), 24.9 (4CH₃, C⁸). C¹ was not observed due to quadrupolar relaxation.

¹¹B NMR (192.5 MHz, CDCl₃) δ 30.1 ppm

HRMS (ESI-TOF) *m/z*: [M + Na]⁺ Calcd for C₁₈H₂₀BNO₇SNa: 428.0951; Found: 428.0952.

IR (neat)/cm⁻¹ *v*_{max} 3114, 2982, 1608, 1528, 1484, 1439, 1379, 1351, 1333, 1196, 1153, 1063, 857, 790.

(2-(((Perfluorophenyl)sulfonyl)oxy)phenyl)boronic acid pinacol ester **4.13d**



The title compound was prepared from 2-hydroxyphenylboronic acid pinacol ester **4.12** (611 mg, 2.5 mmol, 1 equiv.), DIPEA (0.87 mL, 5 mmol, 2 equiv.) and pentafluorobenzenesulfonyl chloride (0.74 mL, 1.33 g, 5 mmol, 2 equiv.) after 16 h at 25 °C, according to general procedure A. After extraction, the crude residue was obtained as an orange oil (1.17 g) that was purified by flash silica-gel column chromatography (Cy/EtOAc 90:10) to afford the pure product **4.13d** as an orange amorphous powder (1.11 g, 2.46 mmol, **98% yield**).

Rf (Cy/EtOAc 80:20) = 0.6

C₁₈H₁₆BF₅O₅S, **M.W.**: 450.18 g/mol. **M.p.**: 92-95 °C.

¹H NMR (600 MHz; CDCl₃): δ 7.81 (dd, *J* = 7.4, 1.8 Hz, 1H, H²), 7.45 (ddd, *J* = 8.2, 7.4, 1.8 Hz, 1H, H⁴), 7.34 (td, *J* = 7.4, 1.0 Hz, 1H, H³), 7.10 (dd, *J* = 8.2, 1.0 Hz, 1H, H⁵), 1.29 (s, 12H, H⁸).

¹³C NMR (150 MHz; CDCl₃) δ 153.1 (C_{qAr}, C⁶), 145.4 (ddd, *J*_{C-F} = 264.5, 13.1, 4.5 Hz, C¹⁰), 145.0 (dtd, *J*_{C-F} = 263.9, 13.1, 4.6 Hz, C¹¹), 137.9 (dtt, *J*_{C-F} = 262.0, 12.4, 4.6 Hz, C¹²), 137.4 (CH_{Ar}, C²), 132.8 (CH_{Ar}, C⁴), 127.6 (CH_{Ar}, C³), 123.7 (br, C¹), 121.4 (CH_{Ar}, C⁵), 112.9 (m, C⁹), 84.4 (2C_q, C⁷), 24.8 (4CH₃, C⁸).

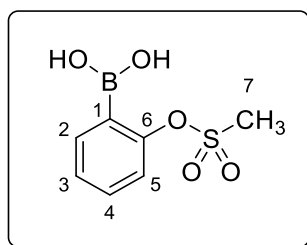
¹⁹F NMR (565 MHz, CDCl₃) δ -132.2 - -132.3 (m, 2F, F^{10/11}), -143.30 (tt, *J* = 21.2, 7.5 Hz, 1F, F¹²), -158.2 - -158.3 (m, 2F, F^{10/11}).

¹¹B NMR (192.5 MHz, CDCl₃) δ 30.0 ppm

HRMS (ESI-TOF) *m/z*: [M + Na]⁺ Calcd for C₁₈H₁₆BF₅O₅SNa: 473.0629; Found: 473.0633.

IR (neat)/cm⁻¹ *v*_{max} 3500, 2983, 1645, 1610, 1521, 1499, 1439, 1399, 1354, 1201, 1143, 1103, 1065, 991, 881, 855, 779.

(2-((Methylsulfonyl)oxy)phenyl)boronic acid **4.9a**



The title compound was prepared from the deprotection of 2-(mesyloxy)phenylboronic acid pinacol ester **4.13a** (745 mg, 2.5 mmol, 1 equiv.) using NaIO₄ (2.140 g, 10 mmol, 4 equiv.) and aqueous HCl (2.5 mL, 2.5 mmol, 1 M, 1equiv.) in THF: H₂O (10 mL: 2 mL), after a 16 h reaction at 25 °C, according to general procedure **B**. The residual orange oil (546 mg) obtained after extraction was purified by crystallization from toluene (8 mL) to afford the pure boronic acid **4.9a** as a beige amorphous solid (432 mg, 2.0 mmol, **80% yield**).

C₇H₉BO₅S, **M.W.**: 216.01 g/mol. **M.p.**: 112-114 °C.

¹H NMR (600 MHz; CD₃CN): δ 7.71 (dd, *J* = 7.4, 1.8 Hz, 1H, H²), 7.51 (ddd, *J* = 8.2, 7.4, 1.8 Hz, 1H, H⁴), 7.37 (td, *J* = 7.4, 1.0 Hz, 1H, H³), 7.31 (dd, *J* = 8.2, 1.0 Hz, 1H, H⁵), 6.19 (br s, 2H, OH), 3.20 (s, 3H, H⁷).

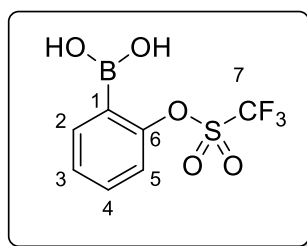
¹³C NMR (150 MHz; CD₃CN) δ 153.4 (C_{qAr}, C⁶), 136.7 (CH_{Ar}, C²), 132.7 (CH_{Ar}, C⁴), 127.9 (CH_{Ar}, C³), 123.1 (CH_{Ar}, C⁵), 38.3 (CH₃, C⁷). C¹ was not observed due to quadrupolar relaxation.

¹¹B NMR (192.5 MHz, CD₃CN) δ 28.5 ppm

HRMS (ASAP-TOF) *m/z*: [M - H]⁻ Calcd for C₇H₈BO₅S: 215.0185; Found: 215.0186.

IR (neat)/cm⁻¹ *v*_{max} 3534 (br), 3334 (br), 3037, 1607, 1443, 1388, 1356, 1334, 1142, 960, 872, 774.

(2-(((Trifluoromethyl)sulfonyl)oxy)phenyl)boronic acid **4.9b**



The title compound was obtained upon deprotection of 2-(triflyloxy)phenylboronic acid pinacol ester **4.13b** (880 mg, 2.5 mmol, 1 equiv.) using NaIO₄ (2.140 g, 10 mmol, 4 equiv.) and aqueous HCl (2.5 mL, 2.5 mmol, 1 M, 1equiv.) in THF: H₂O (10 mL: 2 mL), after a 4 h reaction at 25 °C, according to general procedure **B**. The residual pale-yellow oil (711 mg) obtained after extraction was purified by crystallization from toluene (10 mL) to afford the pure boronic acid **4.9b** as a colorless amorphous powder (252 mg, 0.933 mmol, **37% yield**). The ¹H and ¹³C NMR data match those reported in the literature.¹⁵⁶

R_f (Cy/EtOAc 70:30) = 0.2

C₇H₆BF₃O₅S, **M.W:** 269.99 g/mol. **M.p:** 91-94 °C.

¹H NMR (600 MHz; CD₃CN): δ 7.76 (dd, *J* = 7.4, 1.8 Hz, 1H, H²), 7.57 (ddd, *J* = 8.3, 7.4, 1.8 Hz, 1H, H⁴), 7.45 (td, *J* = 7.4, 1.0 Hz, 1H, H³), 7.30 (d, *J* = 8.3 Hz, 1H, H⁵), 6.35 (br s, 2H, OH).

^{13}C NMR (150 MHz; CD_3CN) δ 154.4 (C_{qAr} , C^6), 137.0 (CH_{Ar} , C^2), 133.2 (CH_{Ar} , C^4), 129.1 (CH_{Ar} , C^3), 122.1 (q, $^5J_{\text{C-F}} = 1.1$ Hz, C^5), 119.8 (q, $^1J_{\text{C-F}} = 320.0$ Hz, C^7). C^1 was not observed due to quadrupolar relaxation.

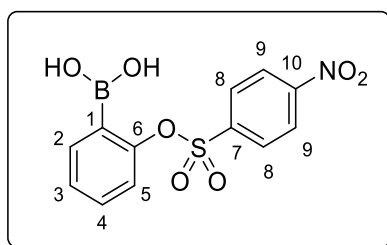
^{19}F NMR (565 MHz, CD_3CN) δ -74.3 ppm.

^{11}B NMR (192.5 MHz, CD_3CN) δ 28.0 ppm

HRMS (ESI-TOF) m/z : $[\text{M} + \text{Cl}]^+$ Calcd for $\text{C}_7\text{H}_6\text{BO}_5\text{SClF}_3$ 304.9670; Found: 304.9666.

IR (neat)/ cm^{-1} ν_{max} 3338 (br), 1610, 1443, 1418, 1337, 1250, 1195, 1139, 1062, 885, 772.

(2-(((4-Nitrophenyl)sulfonyl)oxy)phenyl)boronic acid **4.9c**



The title compound was prepared from the deprotection 2-(nosyloxy)phenylboronic acid pinacol ester **4.13c** (203 mg, 0.5 mmol, 1 equiv.) using NaIO_4 (428 mg, 2 mmol, 4 equiv.) and aqueous HCl (0.5 mL, 0.5 mmol, 1 M, 1equiv.) in $\text{THF}:\text{H}_2\text{O}$ (10 mL: 2 mL), after a 4 h reaction at 25 °C, according to general procedure **B**. The residual yellow oil (170 mg) obtained after the extractive work-up was purified by crystallization from toluene (5 mL) to afford the pure boronic acid **4.9c** as a pale-yellow amorphous solid (53 mg, 0.164 mmol, **33% yield**).

Rf (Cy/EtOAc 70:30) = 0.2

$\text{C}_{12}\text{H}_{10}\text{BNO}_7\text{S}$, **M.W.**: 323.08 g/mol. **M.p.**: 107-109 °C.

^1H NMR (600 MHz; CD_3CN): δ 8.34 (d, $J = 9.0$ Hz, 2H, H^9), 7.99 (d, $J = 9.0$ Hz, 2H, H^8), 7.58 (dd, $J = 7.4, 1.8$ Hz, 1H, H^2), 7.41 (ddd, $J = 8.2, 7.4, 1.8$ Hz, 1H, H^4), 7.33 (td, $J = 7.4, 1.0$ Hz, 1H, H^3), 7.03 (dd, $J = 8.2, 1.0$ Hz, 1H, H^5), 6.00 (br s, 2H, OH).

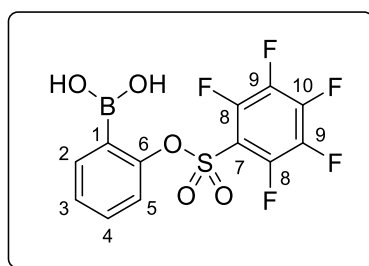
^{13}C NMR (150 MHz; CD_3CN) δ 153.3 (C_{qAr} , C^6), 152.3 (C_{qAr} , C^{10}), 141.3 (C_{qAr} , C^7), 136.5 (CH_{Ar} , C^2), 132.6 (CH_{Ar} , C^4), 131.2 (2 CH_{Ar} , C^8), 128.2 (CH_{Ar} , C^3), 125.6 (2 CH_{Ar} , C^9), 123.2 (CH_{Ar} , C^5). C^1 was not observed due to quadrupolar relaxation.

^{11}B NMR (192.5 MHz, CD_3CN) δ 28.1 ppm

HRMS (ESI-TOF) m/z : $[\text{M} + \text{Cl}]^+$ Calcd for $\text{C}_{12}\text{H}_{10}\text{BClNO}_7\text{S}$: 357.9960; Found: 357.9954.

IR (neat)/ cm^{-1} ν_{max} 3623 (br), 1606, 1530, 1480, 1442, 1374, 1348, 1312, 1194, 1149, 1091, 872, 787.

(2-(((Perfluorophenyl)sulfonyl)oxy)phenyl)boronic acid **4.9d**



The title compound was obtained upon the deprotection of **4.13d** (220 mg, 0.49 mmol, 1 equiv.) using general procedure **C**. First, the diethanolamine complex was synthesized from **4.13d** (220 mg, 0.49 mmol), and diethanolamine (57 mg, 0.539 mmol, 1.1 equiv.) in Et_2O (5 ml), after a 3 h reaction at 25 °C. Then, the diethanolamine-boronate complex was collected as a pale-yellow solid (230 mg, 0.53 mmol). The latter contains diethanolamine, however, it was used for the next step without further purification. Next, upon hydrolysis with aqueous HCl (14.7 mL, 0.1 M, 1.47 mmol, 3 eq) and extractive workup, the pure boronic acid **4.9d** was collected as a colorless amorphous powder (150 mg, 0.407 mmol, **83% yield**).

Rf (Cy/EtOAc 60:40) = 0.2

$\text{C}_{12}\text{H}_6\text{BF}_5\text{O}_5\text{S}$, **M.W**: 368.04 g/mol. **M.p**: 92°C.

^1H NMR (600 MHz; CD_3CN): δ 7.63 (dd, $J = 7.4, 1.8$ Hz, 1H, H^2), 7.47 (ddd, $J = 8.2, 7.4, 1.8$ Hz, 1H, H^4), 7.39 (td, $J = 7.4, 1.0$ Hz, 1H, H^3), 7.16 (dd, $J = 8.2, 1.0$ Hz, 1H, H^5), 6.16 (br s, 2H, OH).

^{13}C NMR (150 MHz; CD_3CN) δ 153.1 (C_{qAr} , C^6), 146.6 (m, $^1J_{\text{C-F}} = 262.6$ Hz, C^{10}), 146.4 (m, $^1J_{\text{C-F}} = 264.2$ Hz, C^8), 139.3 (m, $^1J_{\text{C-F}} = 262.6$ Hz, C^9), 136.6 (CH_{Ar} , C^2), 132.8 (CH_{Ar} , C^4), 128.7 (CH_{Ar} , C^3), 123.2 (CH_{Ar} , C^5), 112.3 (m, C_{qAr} , C^7). C^1 was not observed due to quadrupolar relaxation.

The signals of C⁸, C⁹, and C¹⁰ are in the form of multiplets, however, only ¹J_{C-F} can be distinguished due to low-intensity signals arising from the C-F coupling and overlapping signals.

¹⁹F NMR (565 MHz, CD₃CN) δ -135.5 - -135.6 (m, 2F, F^{8/9}), -144.98 (tt, *J* = 20.4, 8.4 Hz, 1F, F¹⁰), -160.3 - -160.5 (m, 2F, F^{8/9}).

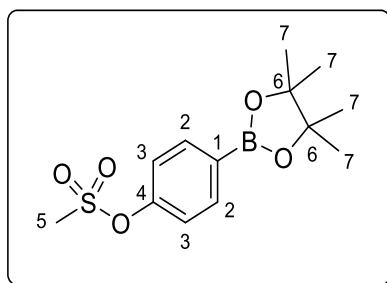
¹¹B NMR (192.5 MHz, CD₃CN) δ 28.1 ppm.

HRMS (ESI-TOF) *m/z*: [M + Cl]⁺ Calcd for C₁₂H₆BO₅F₅S ³⁵Cl: 402.9638; Found: 402.9633.

IR (neat)/cm⁻¹ ν_{max} 3514 (br), 3431 (br), 1644, 1606, 1525, 1505, 1442, 1392, 1325, 1198, 1156, 1110, 1082, 998, 889, 788.

4.13.3 Preparation and characterization of *para*-(sulfonyloxy)phenylboronic acid and its pinacol ester

4-(Methanesulfonyloxy)phenylboronic pinacol ester 4.15



The title compound was prepared from 4-hydroxyphenylboronic acid pinacol ester **4.14** (440 mg, 2 mmol, 1 equiv.), Et₃N (0.56 mL, 4 mmol, 2 equiv.) and CH₃SO₂Cl (0.31 mL, 4 mmol, 2 equiv.) after a 3 h reaction, employing the conditions of general procedure A. The crude residue (1.10 g) was purified by flash-silica gel column chromatography using Cy/EtOAc 80:20 to afford the desired product as a colorless amorphous powder (515 mg, 1.72 mmol, **86% yield**).

R_f (Cy/EtOAc 80:20) = 0.25

C₁₃H₁₉BO₅S, **M.W**: 298.16 g/mol. **M.p**: 118-122°C.

¹H NMR (500 MHz; CDCl₃): δ 7.86 (d, *J* = 8.5 Hz, 2H, H³), 7.28 (d, *J* = 8.5 Hz, 2H, H²), 3.11 (s, 3H, H⁵), 1.33 (s, 12H, H⁷).

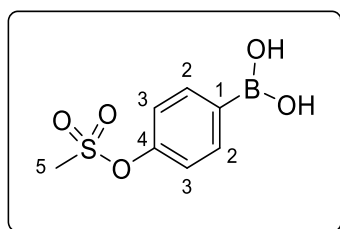
^{13}C NMR (125 MHz; CDCl_3) δ 151.6 (C_{qAr} , C^4), 136.7 (CH_{Ar} , C^3), 121.2 (CH_{Ar} , C^2), 84.1 (C_{q} , C^6), 37.3 (CH_3 , C^5), 24.8 (CH_3 , C^7). C^1 was not observed due to quadrupolar relaxation.

^{11}B NMR (192.5 MHz, CDCl_3) δ 30.6 ppm

HRMS (ASAP-TOF) m/z : $[\text{M} + \text{H}]^+$ Calcd for $\text{C}_{13}\text{H}_{20}\text{BO}_5\text{S}$: 299.1124 ; Found: 299.1137.

IR (neat)/ cm^{-1} ν_{max} 3023, 2986, 2972, 2936, 1601, 1471, 1394, 1355, 1138, 1087, 976, 868, 787.

4-(Methanesulfonyloxy)phenylboronic acid **4.16**



To a solution of 4-(mesyloxy)phenylboronic acid pinacol ester **4.15** (298 mg, 1 mmol, 1equiv.) in $\text{CH}_3\text{CN}:\text{H}_2\text{O}$ (1:1 ; 3 mL) was added HCl (1.1 mL, 1 M, 1.1 mmol, 1.1 equiv.) at 25 °C. The mixture was stirred for 5 mins before the addition of NaIO_4 (225 mg, 1.05 mmol, 1.05 equiv.). After 3 h at 25 °C, full conversion was attained. Consequently, the mixture was diluted with distilled H_2O (10 mL) and extracted with EtOAc (3 \times 20 mL). The combined EtOAc phases were washed with brine (10 mL), dried over MgSO_4 , filtered, and concentrated under reduced pressure to afford the pure boronic **4.16** acid as a colorless amorphous powder (196 mg, 0.91 mmol, **91% yield**).

$\text{C}_7\text{H}_9\text{BO}_5\text{S}$, **M.W.**: 216.01 g/mol. **M.p.**: 240-244 °C.

In CD_3CN , there's a mixture of boroxine: boronic (1.3:1). One drop of D_2O was added to obtain selectively the boronic acid.

^1H NMR (600 MHz; $\text{CD}_3\text{CN} + \text{D}_2\text{O}$): δ 7.85 (d, $J = 8.6$ Hz, 2H, H^3), 7.30 (d, $J = 8.6$ Hz, 2H, H^2), 3.19 (s, 3H, H^5).

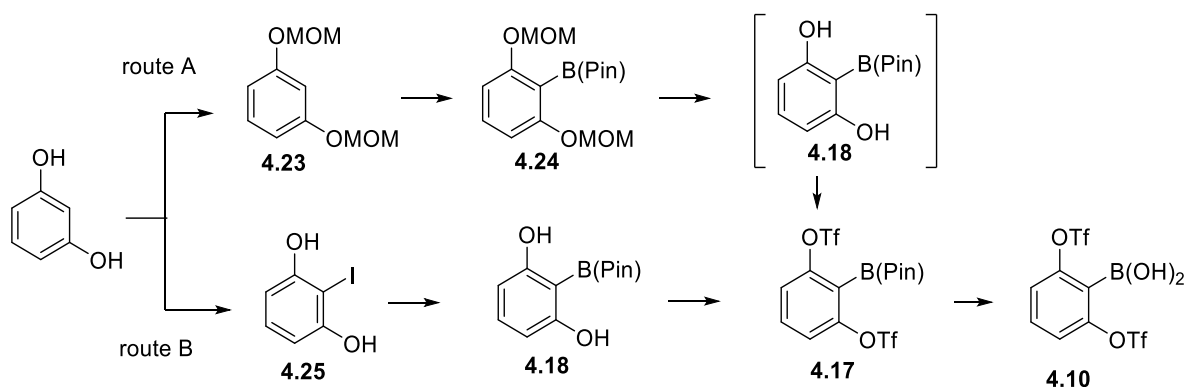
^{13}C NMR (150 MHz; $\text{CD}_3\text{CN} + \text{D}_2\text{O}$) δ 152.3 (C_{qAr} , C^4), 136.9 (CH_{Ar} , C^3), 122.3 (CH_{Ar} , C^2), 38.0 (CH_3 , C^5). C^1 was not observed due to quadrupolar relaxation.

^{11}B NMR (192.5 MHz, $\text{CD}_3\text{CN} + \text{D}_2\text{O}$) δ 28.4 ppm

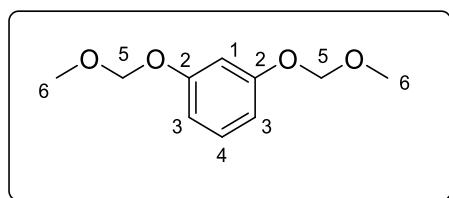
HRMS (ESI-TOF) m/z: $[M - H]^-$ Calcd for $C_7H_8BO_5S$: 215.0185; Found: 215.0183.

IR (neat)/ cm^{-1} ν_{max} 3500 (br), 3350 (br), 3045, 3031, 1599, 1383, 1367, 1332, 1153, 968, 866, 793.

4.13.4 Synthesis and characterization of 2,6-bis(sulfonyloxy)phenylboronic acid and its synthetic intermediates



1,3-Bis(methoxymethoxy)benzene 4.23 (route A)



To a suspension of NaH (60% in oil; 3.03 g, 126.1 mmol, 3 equiv.) in dry DMF (20 mL) was added a solution of resorcinol (2.83 g, 25.2 mmol, 1 equiv.) in dry DMF (15 mL). The mixture was stirred at 0 °C, under an argon atmosphere, for 30 min. Then chloromethyl methyl ether solution in toluene (36 mL, 2.24 M, 75.7 mmol, 3 equiv.) was added very slowly (vigorous evolution of gas), and stirring was continued at 25 °C for 6 h. The reaction mixture was quenched with NH_4Cl (50 mL) and extracted with Et_2O (3×100 mL). The organic layers were collected, washed with brine (100 mL), dried over $MgSO_4$, and filtered. The filtrate was concentrated under reduced pressure to afford the crude residue (7 g). This residue was purified

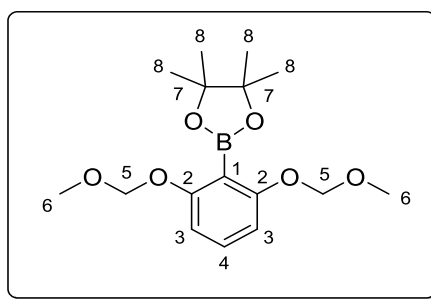
by flash silica-gel column chromatography using Cy/EtOAc 90:10 to afford the pure product **4.23** as a colorless oil (4.80 g, 24.2 mmol, **96% yield**).

The ^1H and ^{13}C NMR data match those reported in the literature.¹⁹³

^1H NMR (600 MHz; CDCl_3): δ 7.15 (t, $J = 8.2$ Hz, 1H, H^4), 6.73 (t, $J = 2.3$ Hz, 1H, H^1), 6.68 (dd, $J = 8.2, 2.3$ Hz, 2H, H^3), 5.11 (s, 4H, H^5), 3.43 (s, 6H, H^6).

^{13}C NMR (150 MHz; CDCl_3) δ 158.3 (C_{qAr} , C^2), 129.9 (CH_{Ar} , C^4), 109.5 (CH_{Ar} , C^3), 104.9 (CH_{Ar} , C^1), 94.3 (CH_2 , C^5), 55.8 (CH_3 , C^6).

(2,6-Bis(methoxymethoxy)phenyl)boronic acid pinacol ester **4.24** (route A)



In a 25 mL oven-dried flask, under argon, 1,3-bis-(methoxymethyl) resorcinol **4.23** (793 mg, 4 mmol, 1 equiv.) was dissolved in dry THF (5 mL, 0.8 M). At 0 °C, *n*BuLi (2.25 mL, 4.80 mmol, 2.13 M, 1.2 equiv.) was introduced slowly and the mixture was stirred at 25 °C for 3 h. After cooling down to 0 °C, 2-isopropoxy-4,4,5,5-tetramethyl-1,3,2-dioxaborolane (1.22 mL, 6 mmol, 1.5 equiv.) was added and the mixture was stirred at 25 °C for 2 h. Next, the reaction mixture was quenched with aqueous HCl (1 M, 12 mL) at 0 °C and once it warms up to room temperature, it was extracted with EtOAc (3×30 mL). The combined organic extracts were washed with brine (20 mL), dried over MgSO_4 , filtered, and concentrated under reduced pressure to give the crude residue (1.56 g). The latter was purified by flash silica-gel column chromatography using Cy/EtOAc 80:20 to afford the pure product **4.24** as a pale-yellow oil (860 mg, 2.65 mmol, **66% yield**).

¹⁹³ (a) Yamada, S.; Kawasaki, M.; Fujihara, M.; Watanabe, M.; Takamura, Y.; Takioku, M.; Nishioka, H.; Takeuchi, Y.; Makishima, M.; Motoyama, T.; Ito, S.; Tokiwa, H.; Nakano, S.; Kakuta, H. *J. Med. Chem.* **2019**, *62*, 8809–8818. (b) Donnelly, A. C.; Mays, J. R.; Burlison, J. A.; Nelson, J. T.; Vielhauer, G.; Holzbeierlein, J.; Blagg, B. S. *J. J. Org. Chem.* **2008**, *73*, 8901–8920.

Rf (Cy/EtOAc 80:20) = 0.35

C₁₆H₂₅BO₆, M.W: 324.18 g/mol.

¹H NMR (600 MHz; CDCl₃): δ 7.19 (t, *J* = 8.3 Hz, 1H, H⁴), 6.67 (d, *J* = 8.3 Hz, 2H, H³), 5.14 (s, 4H, H⁵), 3.46 (s, 6H, H⁶), 1.38 (s, 12H, H⁸).

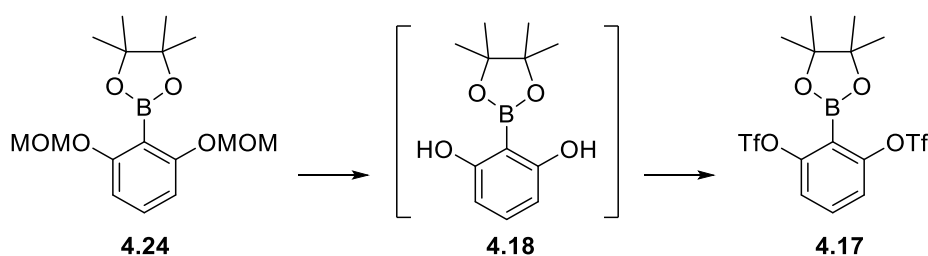
¹³C NMR (150 MHz; CDCl₃) δ 160.8 (2C_{qAr}, C²), 131.4 (CH_{Ar}, C⁴), 107.7 (2CH_{Ar}, C³), 94.4 (2CH₂, C⁵), 83.9 (2C_q, C⁷), 56.1 (2CH₃, C⁶), 24.8 (4CH₃, C⁸). C¹ was not observed due to quadrupolar relaxation.

¹¹B NMR (192.5 MHz, CDCl₃) δ 31.7 ppm

HRMS (ASAP-TOF) *m/z*: [M + H]⁺ Calcd for C₁₆H₂₆BO₆ 325.1822; Found: 325.1815.

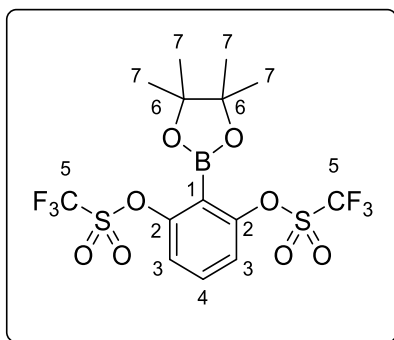
IR (neat)/cm⁻¹ *v*_{max} 2975, 2899, 2828, 1603, 1459, 1342, 1243, 1144, 1100, 1034, 918, 855, 780.

(2,6-Bis(((trifluoromethyl)sulfonyl)oxy)phenyl)boronic acid pinacol ester 4.17 (Route A)



Under argon atmosphere, (2,6-bis(methoxymethoxy)phenyl)boronic acid pinacol ester **4.24** (369 mg, 1.14 mmol, 1 equiv.) was dissolved in dry CH₂Cl₂ (5 mL). Next, trifluoroacetic acid (350 μL, 4.56 mmol, 4 equiv.) was added dropwise at 0 °C and the mixture was stirred at 25 °C for 30 mins (complete conversion is attained). After quenching with NaHCO₃ (aq. sat.; 5 mL), the phases were separated through extraction with CH₂Cl₂ (3 × 15 mL). The organic phases were collected, washed with brine (15 mL), dried over MgSO₄, filtered, and concentrated under reduced pressure to afford the crude residue containing pinacol boronate **4.18** (260 mg, 1.10 mmol). The latter residue was used for the triflation step without further purification. Next, to the crude mixture of (2,6-Dihydroxyphenyl)boronic acid pinacol ester **4.18** (260 mg, 1.10 mmol) in CH₂Cl₂ (5 ml, 0.2 M), was added *N,N*-diisopropylethylamine (575 μL, 427 mg, 3.30 mmol, 3 equiv.) and Tf₂O (554 μL, 931 mg, 3.30 mmol, 3 equiv.) at 0 °C. The mixture was stirred at 25 °C for 1 h. Then, H₂O (10 ml) was added and the mixture was extracted with CH₂Cl₂ (3 × 25 ml). The combined organic extracts were dried over MgSO₄ and, after filtration,

the filtrate was concentrated under reduced pressure to afford the crude residue as a brown oil (686 mg, 1.37 mmol). This residue was purified by flash silica-gel column chromatography using Cy/EtOAc (80:20) to afford the pure product **4.17** as a yellow oil that solidifies at 25 °C to give a yellow crystalline solid (254 mg, 0.51 mmol) in 45% yield over two steps (from **4.24**).



R_f (Cy/EtOAc 90:10) = 0.25

C₁₄H₁₅BF₆O₈S₂, **M.W:** 500.19 g/mol. **M.p:** 50-53 °C.

¹H NMR (600 MHz; CDCl₃): δ 7.58 (t, *J* = 8.4 Hz, 1H, H⁴), 7.31 (d, *J* = 8.4 Hz, 2H, H³), 1.39 (s, 12H, H⁷).

¹³C NMR (150 MHz; CDCl₃) δ 153.9 (2C_{qAr}, C²), 133.2 (CH_{Ar}, C⁴), 121.6 (q, ⁵*J*_{C-F} = 1.0 Hz, 2CH_{Ar}, C³), 118.9 (q, ¹*J*_{C-F} = 321.3 Hz, C⁵), 85.6 (2C_q, C⁶), 24.9 (4CH₃, C⁷). C¹ was not observed due to quadrupolar relaxation.

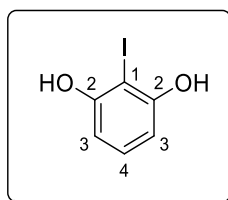
¹⁹F NMR (565 MHz, CDCl₃) δ -72.7 ppm

¹¹B NMR (192.5 MHz, CDCl₃) δ 28.8 ppm

HRMS (ESI-TOF) *m/z*: [M + Na]⁺ Calcd for C₁₄H₁₅BO₈NaS₂F₆: 523.0103; Found: 523.0110.

IR (neat)/cm⁻¹ *v*_{max} 2986, 1615, 1423, 1376, 1340, 1249, 1201, 1134, 801, 759.

2-Iodobenzene-1,3-diol **4.25** (route B)



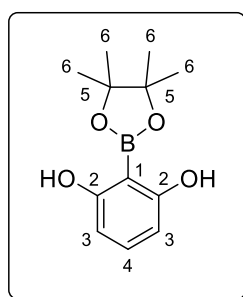
Under ambient atmosphere, NaHCO₃ (3.917 g, 46.64 mmol, 1.1 equiv.) was added to a solution of resorcinol (4.764 g, 43.265 mmol, 1 equiv.) in H₂O: THF (1:1; 60 mL). After stirring for 30 mins at 25 °C, Iodine (10.761 g, 42.4 mmol, 0.98 equiv.) was introduced in portions and the mixture was stirred for 16 h at 25 °C. Then Na₂SO₃ (aq. sat., 50 mL) was added and the mixture was stirred for 1h, after which it was extracted with EtOAc (3×100 mL). The organic phases were washed with brine (100 mL), dried over MgSO₄, filtered, and concentrated under reduced pressure to afford the crude mixture as a brown oil (10.3 g). The residual oil was purified by flash silica-gel column chromatography using Cy/EtOAc (80:20), to separate the unreacted resorcinol from the iodinated resorcinol derivatives, followed by crystallization from toluene (15 mL) to afford the pure 2-iodoresorcinol **4.25** as colorless crystalline solid (5.30 g, 22.5 mmol, **53% yield**).¹⁹⁴

Rf (Cy/EtOAc 80:20) = 0.25

¹H NMR (600 MHz; CDCl₃): δ 7.11 (t, *J* = 8.1 Hz, 1H, H⁴), 6.55 (d, *J* = 8.1 Hz, 2H, H³), 5.30 (br s, 2H, OH).

¹³C NMR (150 MHz; CDCl₃) δ 155.8 (2C_{qAr}, C²), 130.5 (CH_{Ar}, C⁴), 107.4 (2CH_{Ar}, C³), 77.8 (C_{qAr}, C¹).

(2,6-Dihydroxyphenyl)boronic acid pinacol ester **4.18** (route B)



To a solution of 2-iodoresorcinol **4.25** (118 mg, 0.5 mmol, 1 equiv.) and TMEDA (0.45 mL, 3 mmol, 6 equiv.) in dry THF (4 mL) at -78 °C, was added *n*BuLi (1.40 mL, 3 mmol, 2.13 M, 6 equiv.). The mixture was stirred at 25 °C for 1 h. Then, at -60 °C, 2-isopropoxy-4,4,5,5-tetramethyl-1,3,2-dioxaborolane (510 μl, 2.5 mmol, 5 equiv.) was introduced and the mixture

¹⁹⁴ (a) Hamura, T.; Hosoya, T.; Yamaguchi, H.; Kuriyama, Y.; Tanabe, M.; Miyamoto, M.; Yasui, Y.; Matsumoto, T.; Suzuki, K. *Helv. Chim. Acta* **2002**, 85, 3589–3604. (b) Shi, J.; Xu, H.; Qiu, D.; He, J.; Li, Y. *J. Am. Chem. Soc.* **2017**, 139, 623–626.

was stirred at 25 °C for 2 h. Lastly, aqueous HCl (1 M, 12 mL) was added at -40 °C to quench the reaction, and it was left to stir at 25 °C for 10 mins. The phases were next separated through extraction with EtOAc (3×30 mL). The combined EtOAc phases were washed with brine (20 mL), dried over MgSO₄, filtered, and concentrated to afford crude residue as a yellow oil (360 mg). The latter was purified by flash silica-gel column chromatography using Cy/EtOAc (80:20) to afford the pure product **4.18** as a colorless oil that crystallizes eventually at 25 °C to give a colorless crystalline solid (66 mg, 0.28 mmol, **56% yield**).

Rf (Cy/EtOAc 80:20) = 0.3

C₁₂H₁₇BO₄, **M.W:** 236.07 g/mol. **M.p:** 50 °C.

¹H NMR (600 MHz; CDCl₃): δ 7.59 (br s, 2H, OH), 7.24 (t, *J* = 8.2 Hz, 1H, H⁴), 6.41 (d, *J* = 8.2 Hz, 2H, H³), 1.40 (s, 12H, H⁶).

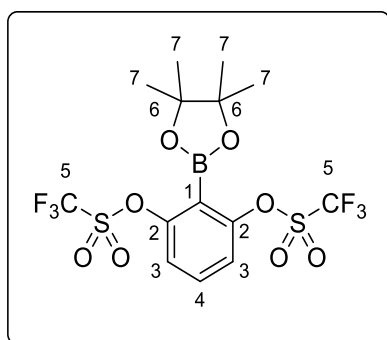
¹³C NMR (150 MHz; CDCl₃) δ 164.3 (2C_{qAr}, C²), 135.4 (CH_{Ar}, C⁴), 107.1 (2CH_{Ar}, C³), 85.4 (2C_q, C⁵), 24.9 (4CH₃, C⁶). C¹ was not observed due to quadrupolar relaxation.

¹¹B NMR (192.5 MHz, CDCl₃) δ 30.6 ppm

HRMS (ESI-TOF) *m/z*: [M - H]⁻ Calcd for C₁₂H₁₆BO₄: 235.1142; Found: 235.1139.

IR (neat)/cm⁻¹ *v*_{max} 3410, 2982, 1633, 1484, 1378, 1273, 1130, 1090, 849, 795.

(2,6-Bis(((trifluoromethyl)sulfonyl)oxy)phenyl)boronic acid pinacol ester **4.17** (Route B)



To a solution of 1,3-dihydroxybenzene pinacol boronate **4.18** (1.5 g, 3 mmol, 1 equiv.) in CH₂Cl₂ (15 mL, 0.2 M), was added DIPEA (1.57 mL, 9 mmol, 3 equiv.) and Tf₂O (1.51 mL, 9 mmol, 3 equiv.) at 0 °C. The mixture was stirred at 25 °C for 1 h. Next, water (20 mL) was added and the mixture was extracted with CH₂Cl₂ (3×25 mL). The combined organic extracts

were dried over MgSO₄, filtered, and concentrated under reduced pressure to afford the crude product as a brown oil (2 g). The residual oil was purified by flash silica-gel column chromatography using Cy/EtOAc (90:10) to afford the pure product **4.17** as a yellow oil that solidifies at 25 °C to give a yellow crystalline solid (1.18 g, 2.36 mmol, **79% yield**).

Rf (Cy/EtOAc 90:10) = 0.25

C₁₄H₁₅BF₆O₈S₂, **M.W:** 500.19 g/mol. **M.p:** 50-53 °C.

¹H NMR (600 MHz; CDCl₃): δ 7.58 (t, *J* = 8.4 Hz, 1H, H⁴), 7.31 (d, *J* = 8.4 Hz, 2H, H³), 1.39 (s, 12H, H⁷).

¹³C NMR (150 MHz; CDCl₃) δ 153.9 (2C_{qAr}, C²), 133.2 (CH_{Ar}, C⁴), 121.6 (q, ⁵*J*_{C-F} = 1.0 Hz, 2CH_{Ar}, C³), 118.9 (q, ¹*J*_{C-F} = 321.3 Hz, C⁵), 85.6 (2C_q, C⁶), 24.9 (4CH₃, C⁷). C¹ was not observed due to quadrupolar relaxation.

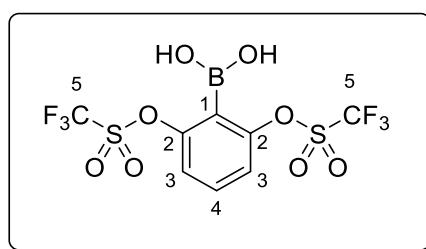
¹⁹F NMR (565 MHz, CDCl₃) δ -72.7 ppm

¹¹B NMR (192.5 MHz, CDCl₃) δ 28.8 ppm

HRMS (ESI-TOF) m/z: [M + Na]⁺ Calcd for C₁₄H₁₅BO₈NaS₂F₆: 523.0103; Found: 523.0110.

IR (neat)/cm⁻¹ ν_{max} 2986, 1615, 1423, 1376, 1340, 1249, 1201, 1134, 801, 759.

(2,6-Bis(((trifluoromethyl)sulfonyl)oxy)phenyl)boronic acid **4.10** (Routes A and B)



To a solution of 2,6-bis(triflyloxy)phenylboronic acid pinacol ester **4.17** (400 mg, 0.8 mmol, 1equiv.) in CH₃CN (5 mL) was added aqueous HCl (1.2 mL, 1 M, 1.2 mmol, 1.5 equiv.) at 25 °C. The mixture was stirred for 5 mins before the addition of NaIO₄ (394 mg, 1.84 mmol, 2.3 equiv.). It's mandatory to acidify the medium using HCl (pH=1) before NaIO₄ addition to avoid the protodeboronation of the starting material. The reaction progress was monitored by ¹H and ¹⁹F NMR in CD₃CN. After 1 h at 25 °C, full conversion was attained. Consequently, the mixture

was diluted with distilled H₂O (10 mL) and extracted with EtOAc (3×30 mL). The combined EtOAc phases were dried over MgSO₄, filtered, and concentrated under reduced pressure to afford the crude residue as an orange oil. Note that the organic phase should not be washed with NaCl (aq. sat.) because it induces protodeboronation (there was a 7% protodeboronated product when the organic phase was washed with brine). Finally, the residual oil was purified by trituration using a 1:1 mixture of cyclohexane: CHCl₃ (10 mL total) to afford the pure boronic acid **4.10** as an off-white amorphous powder (255 mg, 0.61 mmol, **76% yield**).

C₈H₅BF₆O₈S₂, **M.W:** 418.04 g/mol. **M.p:** 98-102 °C.

¹H NMR (600 MHz; CD₃CN): δ 7.67 (t, *J* = 8.4 Hz, 1H, H⁴), 7.47 (d, *J* = 8.4 Hz, 2H, H³), 6.82 (br s, 2H, OH).

¹³C NMR (150 MHz; CD₃CN) δ 152.9 (2C_{qAr}, C²), 133.7 (CH_{Ar}, C⁴), 122.6 (q, ⁵*J*_{C-F} = 1.0 Hz, 2CH_{Ar}, C³), 119.6 (q, ¹*J*_{C-F} = 319.8 Hz, C⁵). C¹ was not observed due to quadrupolar relaxation.

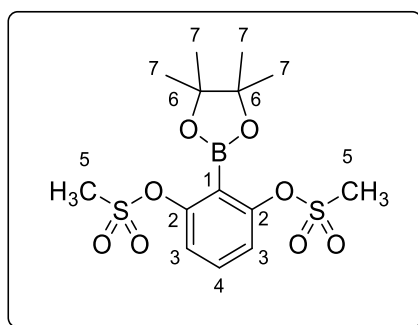
¹⁹F NMR (565 MHz, CD₃CN) δ -74.2 ppm

¹¹B NMR (192.5 MHz, CD₃CN) δ 27.1 ppm

HRMS (ESI-TOF) *m/z*: [M + Cl]⁺ Calcd for C₈H₅BO₈F₆S₂Cl 452.9112; Found: 452.9094.

IR (neat)/cm⁻¹ *v*_{max} 3327 (br), 1613, 1448, 1415, 1339, 1207, 1198, 1133, 1072, 872, 790.

(2,6-Bis(((methyl)sulfonyl)oxy)phenyl)boronic acid pinacol ester **4.27**



To a solution of 1,3-dihydroxyphenylpinacolboronate **4.18** (236 mg, 1 mmol, 1 equiv.) in CH₂Cl₂ (5 mL) was added DIPEA (0.70 mL, 4 mmol, 4 equiv.) and (CH₃SO₂)₂O (0.76 mL, 697 mg, 4 mmol, 4 equiv.) at 0 °C, under argon. The mixture was stirred at 25 °C for 2 h. Next, H₂O (20 mL) was added and the mixture was extracted with CH₂Cl₂ (3×25 mL). The combined

organic extracts were dried over MgSO_4 , filtered, and concentrated under reduced pressure to afford the crude residue as a yellow oil (560 mg). The residual oil was purified by flash silica-gel column chromatography using Cy/EtOAc (60:40) to afford the pure pinacol ester **4.27** as a colorless powder (209 mg, 0.53 mmol, **53% yield**).

Rf (Cy/EtOAc 60:40) = 0.35

$\text{C}_{14}\text{H}_{21}\text{BO}_8\text{S}_2$, **M.W.**: 392.24 g/mol. **M.p.**: 154-158 °C.

$^1\text{H NMR}$ (600 MHz; CDCl_3): δ 7.50 (t, $J = 8.2$ Hz, 1H, H^4), 7.40 (d, $J = 8.2$ Hz, 2H, H^3), 3.19 (s, 6H, H^5), 1.39 (s, 12H, H^7).

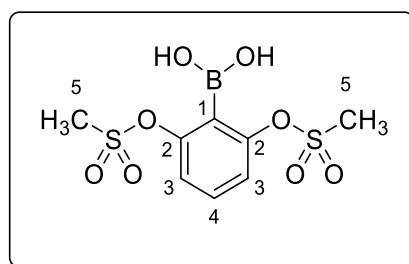
$^{13}\text{C NMR}$ (150 MHz; CDCl_3) δ 153.2 (2 C_{qAr} , C^2), 132.6 (CH_{Ar} , C^4), 121.2 (2 CH_{Ar} , C^3), 85.0 (2 C_{q} , C^6), 37.8 (2 CH_3 , C^5), 25.1 (4 CH_3 , C^7). C^1 was not observed due to quadrupolar relaxation.

$^{11}\text{B NMR}$ (192.5 MHz, CDCl_3) δ 29.6 ppm.

HRMS (ASAP-TOF) m/z : [M] Calcd for $\text{C}_{14}\text{H}_{21}\text{BO}_8\text{S}_2$ 392.0771; Found: 392.0775.

IR (neat)/ cm^{-1} ν_{max} 3026, 2987, 2946, 1610, 1445, 1371, 1349, 1211, 1174, 1140, 822, 793.

(2,6-Bis(((methyl)sulfonyl)oxy)phenyl)boronic acid **4.28**



To a solution of 2,6-di(mesyloxy)phenylboronic acid pinacol ester **4.27** (50 mg, 0.127 mmol, 1equiv.) in CH_3CN (2 mL) was added aqueous HCl (318 μL , 0.318 mmol, 1 M, 2.5 equiv.). The mixture was stirred at 25 °C for 5 mins before the addition of NaIO_4 (90 mg, 0.419 mmol, 3.3 equiv.). The reaction progress was monitored by $^1\text{H NMR}$ in CD_3CN and full conversion was achieved after 2 h at 25 °C. The mixture was extracted with EtOAc (3 \times 5 mL). The EtOAc phases were collected, dried over MgSO_4 , filtered, and concentrated under reduced pressure to afford the crude residue as a yellow powder (45 mg). Based on $^1\text{H NMR}$, the crude residue contains the desired boronic acid + 10% impurities (no protodeboronation byproduct). The

crude mixture was purified by trituration with CHCl_3 (1 mL, 25 °C) to afford the pure boronic acid as a pale-yellow powder (35 mg, 0.113 mmol, **90% yield**).

$\text{C}_8\text{H}_{11}\text{BO}_8\text{S}_2$, **M.W:** 310.10 g/mol. **M.p:** 137-141 °C.

$^1\text{H NMR}$ (600 MHz; CD_3CN): δ 7.54 (t, $J = 8.2$ Hz, 1H, H^4), 7.36 (d, $J = 8.2$ Hz, 2H, H^3), 6.47 (br s, 2H, OH), 3.21 (s, 6H, H^5).

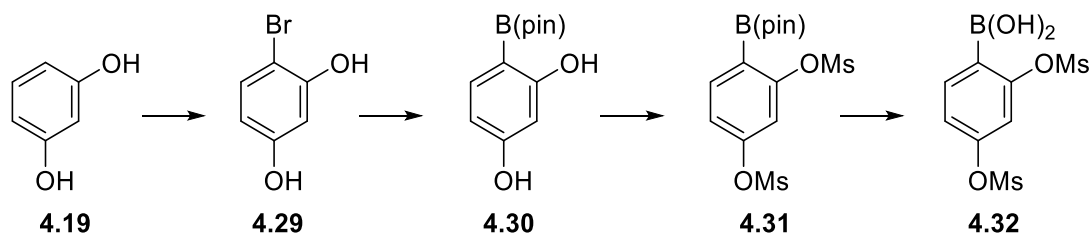
$^{13}\text{C NMR}$ (150 MHz; CD_3CN) δ 152.8 (2C_{qAr} , C^2), 132.5 (CH_{Ar} , C^4), 121.8 (2CH_{Ar} , C^3), 38.5 (2CH_3 , C^5). C^1 was not observed due to quadrupolar relaxation.

$^{11}\text{B NMR}$ (192.5 MHz, CD_3CN) δ 27.9 ppm.

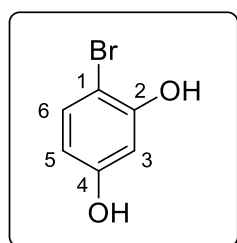
HRMS (ESI-TOF) m/z : $[\text{M}-\text{H}]^-$ Calcd for $\text{C}_8\text{H}_{10}\text{BO}_8\text{S}_2$ 308.9910; Found: 308.9915.

IR (neat)/ cm^{-1} ν_{max} 3524 (br), 3030, 2936, 1607, 1446, 1357, 1304, 1206, 1169, 1079, 824, 786.

4.13.5 Synthesis and characterization of 2,4-bis(mesyloxy)phenylboronic acid



4-bromobenzene-1,3-diol 4.29



To a solution of resorcinol (1.348 g, 12 mmol, 1 equiv.) in MeOH (15 mL) was added NH_4Br (1.175 g, 12 mmol, 1 equiv.) and oxone® (7.380 g, 12 mmol, 1 equiv.) and the mixture was

stirred at 25 °C for 2 h. After MeOH evaporation, the reaction mixture was dissolved in EtOAc and quenched with Na₂SO₃ (aq. sat.; 5 mL). Later, after extraction with EtOAc (3×50 mL), the EtOAc phases were collected, washed with brine (25 mL), dried over MgSO₄, filtered, and concentrated under reduced pressure to afford the desired bromobenzene (2.27 g, 12.01 mmol, > 99% yield).

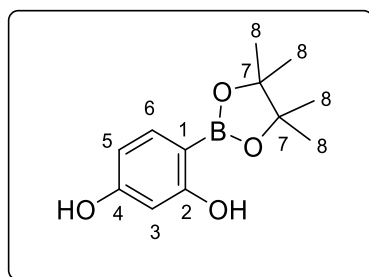
The ¹H, and ¹³C NMR spectra match the reported ones.¹⁹⁵

C₆H₅BrO₂, M.W: 189.01 g/mol.

¹H NMR (500 MHz; CDCl₃): δ 7.28 (d, *J* = 8.7 Hz, 1H, H⁶), 6.54 (d, *J* = 2.9 Hz, 1H, H³), 6.35 (dd, *J* = 8.7, 2.9 Hz, 1H, H⁵), 5.31 (br s, 2H, OH).

¹³C NMR (125 MHz; CDCl₃) δ 156.6 (C_{qAr}, C²), 153.2 (C_{qAr}, C⁴), 132.4 (CH_{Ar}, C⁶), 109.6 (CH_{Ar}, C⁵), 103.6 (CH_{Ar}, C³), 101.3 (C_{qAr}, C¹).

(2,4-Dihydroxyphenyl)boronic acid pinacol ester 4.30



To a solution of 4-bromoresorcinol **4.29** (2.0 g, 10.60 mmol, 1 equiv.) and TMEDA (3.17 mL, 21.2 mmol, 2 equiv.) in dry THF (15 mL) at -78 °C, was added *n*BuLi (25 mL, 1.67M, 42.4 mmol, 4 equiv.) dropwise. The mixture was stirred at 25 °C for 1 h. Then, at -70°C, 2-isopropoxy-4,4,5,5-tetramethyl-1,3,2-dioxaborolane (8.65 mL, 42.4 mmol, 4 equiv.) was added and the mixture was stirred at 25 °C for 2 h. Next, the mixture was quenched with HCl (1 M, 25 mL) at -40 °C and it was left to stir at 25 °C for 10 mins. After extraction with EtOAc (3×50 mL), the EtOAc phases were washed with brine (50 mL), dried over MgSO₄, filtered, and concentrated under reduced pressure to afford the crude residue (3.25 g). The latter residue was purified by flash silica-gel column chromatography using Cy/EtOAc (80:20) to afford the pure

¹⁹⁵ Dalai, P. G.; Palit, K.; Panda, N. *Adv. Synth. Catal.* **2022**, *364*, 1031–1038.

pinacol boronate as a colorless oil that crystallizes at 25 °C to give a colorless crystalline solid (1.25 g, 5.30 mmol, **50% yield**).

R_f (Cy/EtOAc 80:20) = 0.25

C₁₂H₁₇BO₄, **M.W.**: 236.07 g/mol. **M.p.**: 39-40 °C.

¹H NMR (600 MHz; CDCl₃): δ 7.90 (br s, 1H, OH_{ortho}), 7.47 (d, *J* = 8.1 Hz, 1H, H⁶), 6.38 (dd, *J* = 8.1, 2.3 Hz, 1H, H⁵), 6.34 (d, *J* = 2.3 Hz, 1H, H³), 5.48 (br s, 1H, OH_{para}), 1.34 (s, 12H, H⁸).

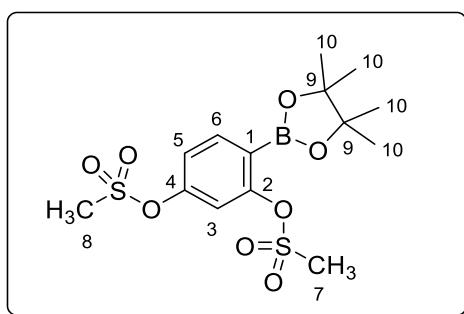
¹³C NMR (150 MHz; CDCl₃) δ 165.6 (C_{qAr}, C²), 160.8 (C_{qAr}, C⁴), 137.4 (CH_{Ar}, C⁶), 107.9 (CH_{Ar}, C⁵), 102.2 (CH_{Ar}, C³), 84.4 (C_q, C⁷), 24.9 (CH₃, C⁸). C¹ was not observed due to quadrupolar relaxation.

¹¹B NMR (192.5 MHz, CDCl₃) δ 30.57 ppm.

HRMS (ESI-TOF) *m/z*: [M - H]⁻ Calcd for C₁₂H₁₆BO₄ 235.1142; Found: 235.1149.

IR (neat)/cm⁻¹ *v*_{max} 3429 (br), 2979, 2932, 1624, 1457, 1371, 1267, 1141, 1066, 962, 852.

(2,4-Bis((methylsulfonyl)oxy)phenyl)boronic acid pinacol ester **4.31**



To a solution of 2,4-dihydroxyphenylboronic acid pinacol ester **4.30** (438 mg, 1.86 mmol, 1 equiv.) in dichloromethane (5 mL), was added DIPEA (0.98 mL, 5.6 mmol, 3 equiv.) and methanesulfonylchloride (0.434 mL, 5.6 mmol, 3 equiv.) at 25 °C. The mixture was then stirred at 25 °C for 3 h. After complete conversion, water (15 mL) was added and the mixture was extracted with CH₂Cl₂ (3×15 mL). The combined organic extracts were dried over MgSO₄ and the filtrate was concentrated under reduced pressure to afford the crude residue (690 mg). The residual oil was purified by flash silica-gel column chromatography using Cy/EtOAc 80:20 to afford the pure product as a colorless oil (213 mg, 0.54 mmol, **29% yield**).

Rf (Cy/EtOAc 80:20) = 0.2

$C_{14}H_{21}BO_8S_2$, **M.W.**: 392.24 g/mol.

1H NMR (600 MHz; $CDCl_3$): δ 7.88 (d, J = 8.1 Hz, 1H, H^6), 7.28 (dd, J = 8.1, 2.2 Hz, 1H, H^5), 7.27 (d, J = 2.2 Hz, 1H, H^3), 3.23 (s, 3H, H^7), 3.16 (s, 3H, H^8), 1.34 (s, 12H, H^{10}).

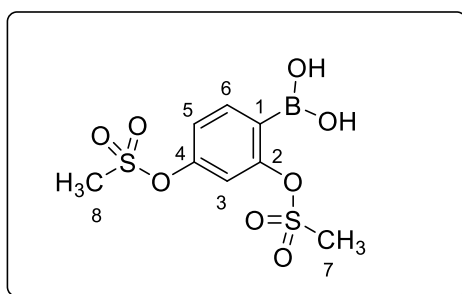
^{13}C NMR (150 MHz; $CDCl_3$) δ 153.7 (C_{qAr} , C^2), 151.8 (C_{qAr} , C^4), 138.4 (CH_{Ar} , C^6), 120.6 (CH_{Ar} , C^5), 116.9 (CH_{Ar} , C^3), 84.5 (Cq , C^9), 38.1 (CH_3 , C^7), 37.8 (CH_3 , C^8), 25.0 (CH_3 , C^{10}). C^1 was not observed due to quadrupolar relaxation.

^{11}B NMR (192.5 MHz, $CDCl_3$) δ 29.8 ppm.

HRMS (ESI-TOF) m/z : $[M + Na]^+$ Calcd for $C_{14}H_{21}BO_8NaS_2$ 415.0669 ; Found: 415.0673.

IR (neat)/ cm^{-1} ν_{max} 2981, 2940, 1605, 1495, 1406, 1330, 1216, 1172, 1109, 882, 852.

(2,4-Bis((methylsulfonyl)oxy)phenyl)boronic acid **4.32**



To a solution of 2,4-(mesyloxy)phenylboronic acid pinacol ester **4.31** (78.5 mg, 0.2 mmol, 1 equiv.) in Et_2O (1 ml, 0.2M), was added diethanolamine (29 ml, 32 mg, 0.3 mmol, 1.5 equiv.) at 25 °C. This mixture was stirred for 24 h, and the precipitated diethanolamine complex was collected by decantation and washing with Et_2O (3×5 mL). The crude diethanolamine complex (96 mg, 0.25 mmol) contains residual diethanolamine and it was used for the hydrolysis step without further purification. Next, HCl (1.2 mL, 0.5M, 0.6 mmol, 3 eq) was added to a suspension of the diethanolamine-boronate complex (96 mg) in Et_2O (2 ml) and the mixture was stirred at 25 °C for 30 mins. After washing with EtOAc (3×10 mL), the organic phases were collected, washed with brine (10 mL), dried over $MgSO_4$, and concentrated under reduced pressure to afford the pure boronic acid **4.32** as an amorphous colorless powder (35 mg, 0.11 mmol, **56% yield**).

$C_8H_{11}BO_8S_2$, **M.W:** 310.10 g/mol. **M.p:** 130-134 °C.

1H NMR (600 MHz; CD_3CN): δ 7.79 (d, $J = 8.2$ Hz, 1H, H^6), 7.33 (dd, $J = 8.2, 2.2$ Hz, 1H, H^5), 7.30 (d, $J = 2.2$ Hz, 1H, H^3), 6.26 (br s, 2H, OH), 3.24 (s, 3H, H^7), 3.23 (s, 3H, H^8).

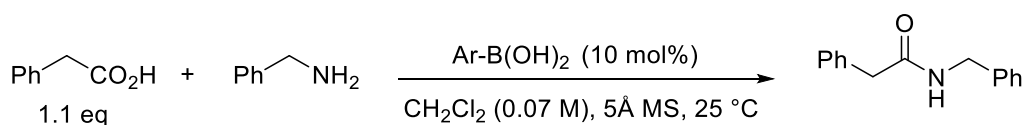
^{13}C NMR (150 MHz; CD_3CN) δ 153.7 (C_{qAr} , C^2), 152.0 (C_{qAr} , C^4), 137.9 (CH_{Ar} , C^6), 121.6 (CH_{Ar} , C^5), 117.5 (CH_{Ar} , C^3), 38.4 (CH_3 , C^7), 38.2 (CH_3 , C^8). C^1 was not observed due to quadrupolar relaxation.

^{11}B NMR (192.5 MHz, CD_3CN) δ 28.1 ppm.

HRMS (ESI-TOF) m/z : $[M - H]^-$ Calcd for $C_8H_{10}BO_8S_2$ 308.9910; Found: 308.9915.

IR (neat)/ cm^{-1} ν_{max} 3373 (br), 3038, 2939, 1604, 1490, 1412, 1344, 1212, 1166, 1121, 949, 838.

4.13.6 General procedure for kinetic studies and raw kinetic data



General procedure: In a 25 mL flask, under argon, phenylacetic acid 98.50% (76 mg, 0.55 mmol, 1.1 equiv.), boronic acid (0.05 mmol, 10 mol%), and 1g of activated 5 Å powdered molecular sieves were introduced. The molecular sieves were activated before each use, using the Kugelrohr instrument for 2 hours at 250 °C (0-1 mbar), after which they were left at <2 mbar until they cooled down to 25 °C, and then, used immediately. To this mixture, 1,1,2,2-tetrachloroethane (53 μ l, 0.50 mmol, 1 equiv.) and dry CH_2Cl_2 (7 mL, 0.0714 M) were added, and the mixture was stirred vigorously for 15 minutes at 25 °C. Next, benzylamine 99% (55 μ l, 0.50 mmol, 1 equiv.) was introduced and the mixture was stirred at 25 °C, under argon.

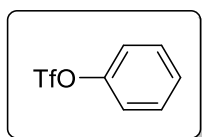
The sampling was performed by taking a sample of 0.10 mL of the reaction mixture each time. To each sample, 0.35 mL of $CDCl_3$ was added and the % NMR yield was determined from 1H NMR integrations. The % NMR yield was determined by integrating the peak at δ 5.96 ppm (s, 2H) for the internal standard (1,1,2,2-tetrachloroethane) and the signals of the amide at δ 4.4 ppm (d, 2H, CH_2), and 3.6 ppm (s, 2H, CH_2).

❖ Raw kinetic data:

Catalyst	% NMR yield				
	0.25 h	0.5 h	1 h	2 h	4 h
4.9a	40	80	100	100	100
4.9b	44	74	100	100	100
4.9c	28	44	70	100	100
4.9d	56	78	100	100	100
4.16	11	17	26	32	39
4.10	76	100	100	100	100
4.32	18	25	40	65	100
4.2	32	44	77	100	100
4.5	44	58	77	91	100

4.13.7 Synthesis of the protodeboronation products

Phenyl triflate 4.53



Under argon, a solution of phenol (188 mg, 2 mmol, 1 equiv.) was dissolved in CH₂Cl₂ (6 ml, 0.33 M). Then, *N,N*-diisopropylethylamine (0.52 ml, 3 mmol, 1.5 equiv.) and Tf₂O (0.50 ml, 3 mmol, 1.5 equiv.) were added at 0 °C. The mixture was allowed to warm to 25 °C and stirred at this temperature for 3 h. Next, H₂O (10 ml) was added and the mixture was extracted with CH₂Cl₂ (15 ml × 3). The combined organic extracts were dried over MgSO₄, filtered, and concentrated under reduced pressure to the crude residue as a brown oil (530 mg). The latter was purified by flash silica-gel column chromatography using Cy/EtOAc (90:10) to afford the pure benzene triflate as a colorless oil (400 mg, 1.77 mmol, **89% yield**).

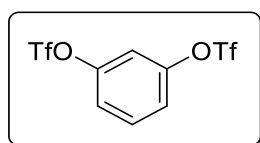
Rf (Cy/EtOAc 90:10) = 0.4

C₇H₅F₃O₃S, **M.W**: 226.17 g/mol. The ¹H and ¹⁹F NMR data are consistent with those reported in the literature.¹⁹⁶

¹H NMR (500 MHz; CDCl₃) δ 7.49-7.43 (m, 2H_{Ar}), 7.42-7.37 (m, 1H_{Ar}), 7.31-7.24 (m, 2H_{Ar}).

¹⁹F NMR (470 MHz; CDCl₃) δ -73.0 ppm.

1,3-Phenylene ditriflate 4.26



Under argon, a solution of resorcinol (220 mg, 2 mmol, 1 equiv.) was dissolved in CH₂Cl₂ (6 ml, 0.33 M). Then, pyridine (0.48 ml, 6 mmol, 3 equiv.) and Tf₂O (1 ml, 6 mmol, 3 equiv.) were added at 0 °C. The mixture was allowed to warm to 25 °C and stirred at this temperature for 2 h. Next, H₂O (10 ml) was added and the mixture was extracted with CH₂Cl₂ (15 ml × 3). The combined organic extracts were dried over MgSO₄, filtered, and concentrated under reduced pressure to the crude residue as a yellow oil (900 mg). The latter was purified by flash silica-gel column chromatography using Cy/EtOAc (90:10) to afford the pure benzene triflate as a colorless oil (683 mg, 1.83 mmol, **91% yield**).

R_f (Cy/EtOAc 90:10) = 0.35.

C₈H₄F₆O₆S₂, **M.W**: 374.22 g/mol. The ¹H and ¹⁹F NMR data are consistent with those reported in the literature.¹⁹⁷

¹H NMR (500 MHz; CDCl₃) δ 7.59 (t, *J* = 8.4 Hz, 1H_{Ar}), 7.37 (dd, *J* = 8.4, 2.3 Hz, 2H_{Ar}), 7.26 (t, *J* = 2.3 Hz, 1H_{Ar}).

¹⁹F NMR (470 MHz; CDCl₃) δ -72.6 ppm.

¹⁹⁶ Gui, Y.-Y.; Liao, L.-L.; Sun, L.; Zhang, Z.; Ye, J.-H.; Shen, G.; Lu, Z.-P.; Zhou, W.-J.; Yu, D.-G. *Chem. Commun.* **2017**, 53, 1192–1195.

¹⁹⁷ Duan, J.; Wang, K.; Xu, G.-L.; Kang, S.; Qi, L.; Liu, X.-Y.; Shu, X.-Z. *Angew. Chem. Int. Ed.* **2020**, 59, 23083–23088.

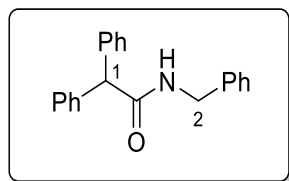
4.13.8 Scope of the low-temperature amides synthesis

4.13.8.1 General procedure D for Low-temperature amide synthesis

In a 25 mL flask, under argon, a carboxylic acid (0.55 mmol, 1.1 equiv.), boronic acid **4.9b** (14 mg, 0.05 mmol, 10 mol%), and 1 g of 5 Å powdered activated molecular sieves were introduced. Then 7 mL of dry CH₂Cl₂ (0.0714 M) was added, and the mixture was stirred vigorously for 15 minutes at 25 °C. Next, an amine (0.50 mmol, 1 equiv.) was added and the mixture was stirred under argon. After **t (h)**, the reaction was stopped and the mixture was filtered through a celite pad (~1 cm) and washed with EtOAc (2×10 mL) and CH₂Cl₂ (2×10 mL). The filtrate was concentrated under reduced pressure to give a residue. The latter was purified by flash silica-gel column chromatography to afford the pure amide.

4.13.8.2 Synthesis and characterization of amide substrates

N-Benzyl-2,2-diphenylacetamide **4.41a**



The title compound was prepared from diphenylacetic acid 99% (118 mg, 0.55 mmol, 1.1 equiv.) and benzylamine 99% (55 μ l, 54 mg, 0.50 mmol, 1 equiv.) after 24 h at 25 °C using the general procedure **D** and purified by flash silica-gel column chromatography using Cy/EtOAc 80:20 to afford the pure amide as a colorless solid (136 mg, 0.45 mmol, **90% yield**).

Rf (Cy/EtOAc 80:20) = 0.35

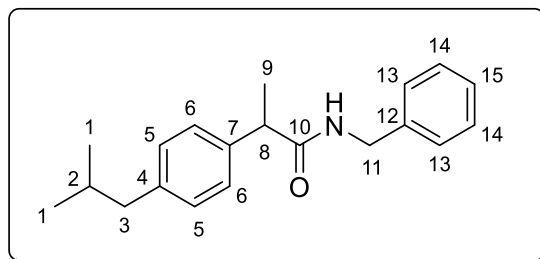
C₂₁H₁₉NO, **M.W.**: 301,39 g/mol. The ¹H and ¹³C NMR data are consistent with those reported in the literature.⁵⁷

¹H NMR (500 MHz; CDCl₃) δ 7.29-7.17 (m, 13H_{Ar}), 7.12 (dd, J = 6.6, 1.6 Hz, 2H_{Ar}), 6.32 (br s, 1H, NH), 4.91 (s, 1H, H¹), 4.34 (d, J = 5.8 Hz, 2H, H²).

¹³C NMR (150 MHz; CDCl₃) δ 172.0 (C=O), 139.5 (C_{qAr}), 138.2 (C_{qAr}), 128.9 (CH_{Ar}), 128.7 (CH_{Ar}), 128.6 (CH_{Ar}), 127.6 (CH_{Ar}), 127.4 (CH_{Ar}), 127.2 (CH_{Ar}), 58.8 (CH, C¹), 43.7 (CH₂, C²).

HRMS (ESI-TOF) m/z: $[M + H]^+$ Calcd for $C_{21}H_{20}NO$ 302.1545; Found: 302.1544.

(S)-N-Benzyl-2-(4-isobutylphenyl)propenamide 4.39



The title compound was prepared from ibuprofen 99% (115 mg, 0.55 mmol, 1.1 equiv.) and benzylamine 99% (55 μ l, 54 mg, 0.50 mmol, 1 equiv.) after 18 h at 25 °C using the general procedure **D** and purified by flash silica-gel column chromatography using Cy/EtOAc 80:20 to afford the pure amide as a colorless solid (103 mg, 0.349 mmol, **70% yield**).

Rf (Cy/EtOAc 80:20) = 0.3

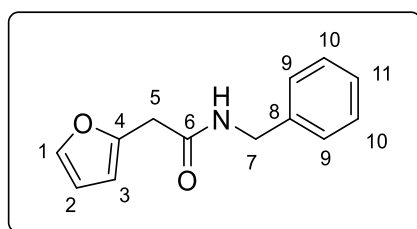
$C_{20}H_{25}NO$, **M.W:** 295,43 g/mol. The 1H and ^{13}C NMR data are consistent with those reported in the literature.⁶¹

1H NMR (500 MHz; $CDCl_3$) δ 7.27-7.18 (m, 5H), 7.13-7.09 (m, 4H), 5.71 (brs, 1H, NH), 4.37 (m, 2H, H^{11}), 3.57 (q, $J = 7.2$ Hz, 1H, H^8), 2.44 (d, $J = 7.2$ Hz, 2H, H^3), 1.84 (nonaplet/m, $J = 6.7$ Hz, 1H, H^2), 1.53 (d, $J = 7.2$ Hz, 3H, H^9), 0.89 (d, $J = 6.7$ Hz, 6H, H^1).

^{13}C NMR (150 MHz; $CDCl_3$) δ 174.5 (C=O, C^{10}), 140.9 (C_{qAr} , C^4), 138.6 (C_{qAr} , C^{12}), 138.5 (C_{qAr} , C^7), 129.8 (CH_{Ar}), 128.7 (CH_{Ar}), 127.5 (CH_{Ar}), 127.47 (CH_{Ar}), 127.4 (CH_{Ar}), 46.9 (CH, C^8), 45.1 (CH_2 , C^3), 43.6 (CH_2 , C^{11}), 30.3 (CH, C^2), 22.5 (CH_3 , C^1), 18.5 (CH_3 , C^9).

HRMS (ESI-TOF) m/z: $[M + H]^+$ Calcd for $C_{20}H_{26}NO$ 296.2014; Found: 296.2013.

N-Benzyl-2-(furan-2-yl)acetamide 4.41b



The title compound was prepared from 2-furanacetic acid (69 mg, 0.55 mmol, 1.1 equiv.) and benzylamine 99% (55 μ l, 54 mg, 0.50 mmol, 1 equiv.) after 2 h at 25 °C using the general procedure **D** and purified by flash silica gel column chromatography using Cy/EtOAc 60:40 to afford the pure amide as a colorless solid (106.5 mg, 0.494 mmol, **99% yield**).

Rf (Cy/EtOAc 60:40) = 0.4

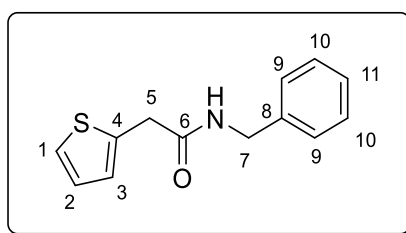
C₁₃H₁₃NO₂, **M.W**: 215,25 g/mol. The ¹H and ¹³C NMR data are consistent with those reported in the literature.⁵⁷

¹H NMR (500 MHz; CDCl₃) δ 7.34 (dd, J = 1.9, 0.8 Hz, 1H, H¹), 7.31-7.26 (m, 2H_{Ar}, H¹⁰), 7.24 (tt, J = 7.4, 1.7 Hz, 1H, H¹¹), 7.21-7.17 (m, 2H, H⁹), 6.32 (dd, J = 3.2, 1.9 Hz, 1H, H²), 6.29 (br s, 1H, NH), 6.20 (ddt, J = 3.2, 1.5, 0.8 Hz, 1H, H³), 4.38 (d, J = 5.8 Hz, 2H, H⁷), 3.60 (s, 2H, H⁵).

¹³C NMR (150 MHz; CDCl₃) δ 168.6 (C=O, C⁶), 148.7 (C_{qAr}, C⁴), 142.4 (CH_{Ar}, C¹), 138.1 (C_{qAr}, C⁸), 128.7 (CH_{Ar}, C¹⁰), 127.5 (CH_{Ar}, C⁹), 127.4 (CH_{Ar}, C¹¹), 110.8 (CH_{Ar}, C²), 108.6 (CH_{Ar}, C³), 43.6 (CH₂, C⁷), 36.2 (CH₂, C⁵).

HRMS (ESI-TOF) m/z : [M + H]⁺ Calcd for C₁₃H₁₄NO₂ 216.1025; Found: 216.1025.

***N*-Benzyl-2-(thiophen-2-yl)acetamide 4.41c**



The title compound was prepared from 2-thiopheneacetic acid (78 mg, 0.55 mmol, 1.1 equiv.) and benzylamine 99% (55 μ l, 54 mg, 0.50 mmol, 1 equiv.) after 1 h at 25 °C using the general procedure **D** and purified by flash silica gel column chromatography using Cy/EtOAc 60:40 (**Rf** in Cy/EtOAc 60:40 = 0.45) to afford the pure amide as a pale-yellow solid (115 mg, 0.497 mmol, **99% yield**).

Rf (Cy/EtOAc 60:40) = 0.45

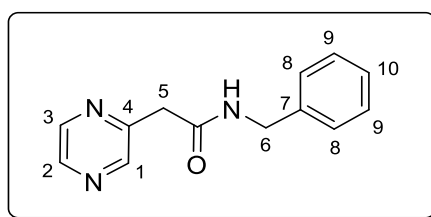
C₁₃H₁₃NOS, **M.W**: 231.31 g/mol. The ¹H and ¹³C NMR data are consistent with those reported in the literature.⁵⁷

¹H NMR (500 MHz; CDCl₃) δ 7.31-7.27 (m, 2H_{Ar}, H¹⁰), 7.26-7.23 (m, 1H_{Ar}, H¹¹), 7.22 (dd, *J* = 5.1, 1.2 Hz, 1H, H¹), 7.20-7.17 (m, 2H_{Ar}, H⁹), 6.96 (dd, *J* = 5.1, 3.5 Hz, 1H, H²), 6.92 (ddt, *J* = 3.5, 1.2, 0.6 Hz, 1H, H³), 6.13 (br s, 1H, NH), 4.40 (d, *J* = 5.8 Hz, 2H, H⁷), 3.79 (d, *J* = 0.6 Hz, 2H, H⁵).

¹³C NMR (150 MHz; CDCl₃) δ 169.9 (C=O, C⁶), 138.1 (C_{qAr}, C⁸), 136.2 (C_{qAr}, C⁴), 128.7 (CH_{Ar}, C¹⁰), 127.6 (CH_{Ar}, C⁹), 127.54 (CH_{Ar}, C¹¹), 127.48 (CH_{Ar}, C³), 127.4 (CH_{Ar}, C²), 125.7 (CH_{Ar}, C¹), 43.7 (CH₂, C⁷), 37.6 (CH₂, C⁵).

HRMS (ESI-TOF) *m/z*: [M + H]⁺ Calcd for C₁₃H₁₄NOS 232.0796; Found: 232.0797.

***N*-Benzyl-2-(pyrazin-2-yl)acetamide 4.41d**



The title compound was prepared from 2-pyrazineacetic acid 95% (79 mg, 0.55 mmol, 1.1 equiv.) and benzylamine 99% (55 μl, 54 mg, 0.50 mmol, 1 equiv.) after 16 h at 25 °C using the general procedure **D** and purified by flash silica gel column chromatography to afford the pure amide as a yellow solid (108 mg, 0.475 mmol, **95% yield**).

R_f (Cy/EtOAc 60:40) = 0.4

C₁₃H₁₃N₃O, **M.W**: 227.27 g/mol. **M.p**: 140-143 °C.

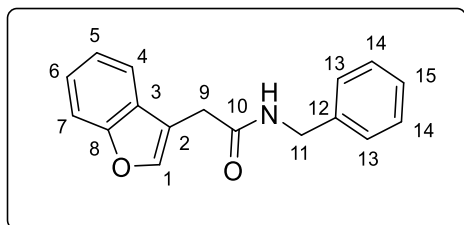
¹H NMR (500 MHz; CDCl₃) δ 8.57 (d, *J* = 0.8 Hz, 1H, H¹), 8.47-8.44 (m, 2H_{Ar}, H²⁻³), 7.36 (br s, 1H, NH), 7.31-7.19 (m, 5H_{Ar}, H⁸⁻¹⁰), 4.42 (d, *J* = 5.7 Hz, 2H, H⁶), 3.75 (s, 2H, H⁵).

¹³C NMR (150 MHz; CDCl₃) δ 168.2 (C=O), 151.3 (C_{qAr}, C⁴), 145.3 (CH_{Ar}, C¹), 143.7 (CH_{Ar}, C^{2/3}), 143.2 (CH_{Ar}, C^{2/3}), 138.0 (C_{qAr}, C⁷), 128.6 (CH_{Ar}, C⁸), 127.6 (CH_{Ar}, C⁹), 127.4 (CH_{Ar}, C¹⁰), 43.7 (CH₂, C⁶), 42.6 (CH₂, C⁵).

HRMS (ESI-TOF) m/z : $[M + H]^+$ Calcd for $C_{13}H_{14}N_3O$ 228.1137; Found: 228.1135.

IR (neat) ν_{\max} 3433 (br), 3078, 2967, 1769, 1604, 1533, 1439, 1364, 1245, 1181, 903, 857, 761.

2-(Benzofuran-3-yl)-*N*-benzylacetamide **4.41e**



The title compound was prepared from 2-(benzofuran-3-yl)acetic acid (99 mg, 0.55 mmol, 1.1 equiv.) and benzylamine 99% (55 μ l, 54 mg, 0.50 mmol, 1 equiv.) after 4 h at 25 °C using the general procedure **D** and purified by flash silica gel column chromatography using Cy/EtOAc 60:40 to afford the pure amide as a colorless solid (100 mg, 0.375 mmol, **75% yield**).

R_f (Cy/EtOAc 60:40) = 0.3

$C_{17}H_{15}NO_2$, **M.W.**: 265.31 g/mol. **M.p.**: 119-121 °C.

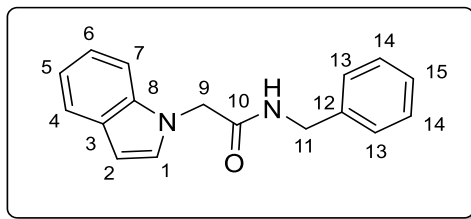
¹H NMR (500 MHz; $CDCl_3$) δ 7.57 (t, , J = 0.8 Hz, 1H, H¹), 7.53 (ddd, J = 7.7, 1.2, 0.7 Hz, 1H, H⁴), 7.48 (ddd, J = 8.2, 1.6, 0.7 Hz, 1H, H⁷), 7.32 (ddd, J = 8.2, 7.4, 1.2 Hz, 1H, H⁶), 7.28-7.20 (m, 4H, H⁵⁻¹⁴⁻¹⁵), 7.14 (ddd, J = 7.7, 1.4, 0.7 Hz, 2H, H¹³), 6.04 (br s, 1H, NH), 4.39 (d, J = 5.9 Hz, 2H, H¹¹), 3.67 (d, J = 0.8 Hz, 2H, H⁹).

¹³C NMR (150 MHz; $CDCl_3$) δ 169.7 (C=O, C¹⁰), 155.5 (C_{qAr}, C⁸), 143.3 (CH_{Ar}, C¹), 138.1 (C_{qAr}, C¹²), 128.7 (CH_{Ar}, C¹⁴), 127.7 (CH_{Ar}, C¹³), 127.6 (CH_{Ar}, C¹⁵), 127.3 (C_{qAr}, C³), 125.0 (CH_{Ar}, C⁶), 123.1 (CH_{Ar}, C⁵), 119.7 (CH_{Ar}, C⁴), 113.9 (C_{qAr}, C²), 111.8 (CH_{Ar}, C⁷), 43.7 (CH₂, C¹¹), 31.8 (CH₂, C⁹).

HRMS (ESI-TOF) m/z : $[M + H]^+$ Calcd for $C_{17}H_{16}NO_2$ 266.1181; Found: 266.1187.

IR (neat) ν_{\max} 3480 (br), 3177, 2989, 1758, 1617, 1601, 1583, 1476, 1438, 1366, 1261, 1212, 1129, 1105, 872, 801, 745.

***N*-Benzyl-2-(1*H*-indol-1-yl)acetamide 4.41f**



The title compound was prepared from indole-1-acetic acid 96% (99 mg, 0.55 mmol, 1.1 equiv.) and benzylamine 99% (55 μ l, 54 mg, 0.50 mmol, 1 equiv.) after 16 h at 25 °C using the general procedure **D** and purified by flash silica gel column chromatography using Cy/EtOAc 50:50 to afford the pure amide as a colorless solid (54 mg, 0.204 mmol, **41% yield**).

R_f (Cy/EtOAc 50:50) = 0.4

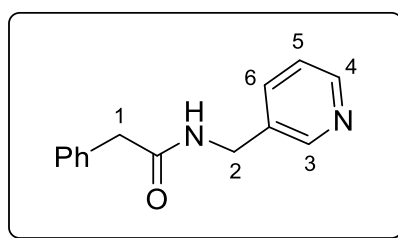
$C_{17}H_{16}N_2O$, **M.W.**: 264.33 g/mol. The 1H and ^{13}C NMR data are consistent with those reported in the literature.⁵⁵

1H NMR (500 MHz; $CDCl_3$) δ 7.63 (ddd, $J = 7.9, 1.0$, Hz, 1H, H^7), 7.30-7.18 (m, 5H_{Ar}), 7.15 (ddd, $J = 7.9, 6.7, 1.3$ Hz, 1H, H^6), 7.04 (d, $J = 3.2$ Hz, 1H, H^1), 7.04-7.01 (m, 2H_{Ar}), 6.58 (dd, $J = 3.2, 0.6$ Hz, 1H, H^2), 5.75 (br s, 1H, NH), 4.79 (s, 2H, H^9), 4.33 (d, $J = 6.1$ Hz, 2H, H^{11}).

^{13}C NMR (150 MHz; $CDCl_3$) δ 168.4 (C=O, C^{10}), 137.6 (C_{qAr}, C^{12}), 136.3 (C_{qAr}, C^8), 128.9 (CH_{Ar}, $C^{14/15}$), 128.7 (CH_{Ar}, $C^{14/15}$), 128.3 (CH_{Ar}, C^4), 127.5 (CH_{Ar}, C^1), 127.3 (CH_{Ar}, C^{13}), 122.8 (CH_{Ar}, C^5), 121.5 (CH_{Ar}, C^7), 120.6 (CH_{Ar}, C^6), 109.3 (C_{qAr}, C^3), 103.8 (CH_{Ar}, C^2), 50.1 (CH₂, C^9), 43.2 (CH₂, C^{11}).

HRMS (ESI-TOF) m/z : $[M + H]^+$ Calcd for $C_{17}H_{17}N_2O$ 265.1341; Found: 265.1342.

2-Phenyl-*N*-(pyridin-3-ylmethyl)acetamide 4.41g



The title compound was prepared from phenylacetic acid 98.5% (76 mg, 0.55 mmol, 1.1 equiv.) and 3-(aminomethyl)pyridine $\geq 99\%$ (52 μ l, 54 mg, 0.50 mmol, 1 equiv.) after 48 h at 40 °C

using the general procedure **D** and purified by flash silica gel column chromatography using Cy/EtOAc 70:30 to afford the pure amide as an off-white solid (113 mg, 0.499 mmol, > **99% yield**).

Rf (Cy/EtOAc 70:30) = 0.3

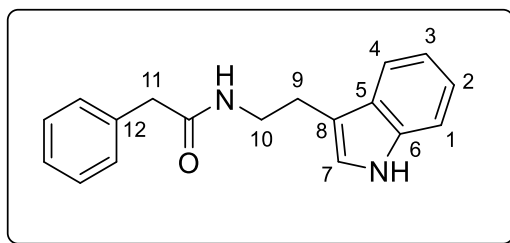
C₁₄H₁₄N₂O, **M.W.**: 226,28 g/mol. The ¹H and ¹³C NMR data are consistent with those reported in the literature.¹⁹⁸

¹H NMR (500 MHz; CDCl₃) δ 8.47 (dd, *J* = 4.8, 1.6 Hz, 1H, H⁴), 8.41 (d, *J* = 2.2 Hz, 1H, H³), 7.50 (ddd, *J* = 7.8, 2.2, 1.6 Hz, 1H, H⁶), 7.36-7.31 (m, 2H_{Ar}), 7.31-7.24 (m, 3H_{Ar}), 7.21 (dd, *J* = 7.8, 4.8 Hz, 1H, H⁵), 6.07 (br s, 1H, NH), 4.39 (d, *J* = 6.1 Hz, 2H, H²), 3.61 (s, 2H, H¹).

¹³C NMR (150 MHz; CDCl₃) δ 171.4 (C=O), 148.2 (CH_{Ar}), 147.9 (CH_{Ar}), 135.8 (CH_{Ar}), 134.8 (C_{qAr}), 134.4 (C_{qAr}), 129.1 (CH_{Ar}), 128.7 (CH_{Ar}), 127.1 (CH_{Ar}), 123.6 (CH_{Ar}), 43.2 (CH₂, C²), 40.7 (CH₂, C¹).

HRMS (ESI-TOF) *m/z*: [M + H]⁺ Calcd for C₁₄H₁₅N₂O 227.1184; Found: 227.1182.

N-(2-(1H-indol-3-yl)ethyl)-2-phenylacetamide **4.41h**



The title compound was prepared from phenylacetic acid 98.5% (76 mg, 0.55 mmol, 1.1 equiv.) and tryptamine 98% (82 mg, 0.50 mmol, 1 equiv.) after 2.5 h at 25 °C using the general procedure **D** and purified by flash silica gel column chromatography using Cy/EtOAc 50:50 to afford the pure amide as a colorless solid (42 mg, 0.151 mmol, **30% yield**). When the reaction was conducted for 16 h at 40 °C, a **34% yield** was obtained (47 mg, 0.169 mmol).

Rf (Cy/EtOAc 50:50) = 0.35

¹⁹⁸ Gernigon, N.; Zheng, H.; Hall, D. G. *Tetrahedron Lett.* **2013**, *54*, 4475–4478.

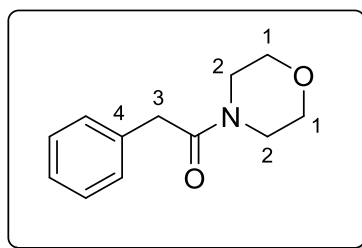
C₁₈H₁₈N₂O, **M.W**: 278,36 g/mol. The ¹H and ¹³C NMR data are consistent with those reported in the literature.⁵⁵

¹H NMR (500 MHz; CDCl₃) δ 8.16 (br s, 1H, NH_{indole}), 7.52 (d, *J* = 7.8 Hz, 1H), 7.33 (d, *J* = 8.1 Hz, 1H), 7.29-7.22 (m, 3H_{Ar}), 7.18 (ddd, *J* = 8.1, 7.1, 1.0 Hz, 1H), 7.15-7.07 (m, 3H_{Ar}), 6.75 (d, *J* = 2.6 Hz, 1H, H⁷), 5.48 (br s, 1H, NH_{amide}), 3.53 (q, *J* = 6.6 Hz, 2H, H¹⁰), 3.50 (s, 2H, H¹¹), 2.88 (t, *J* = 6.6 Hz, 2H, H⁹).

¹³C NMR (150 MHz; CDCl₃) δ 171.0 (C=O), 136.4 (C_{qAr}, C⁶), 134.9 (C_{qAr}, C¹²), 129.5 (CH_{Ar}), 128.9 (CH_{Ar}), 127.2 (C_{qAr}, C⁵), 122.2 (CH_{Ar}), 122.0 (CH_{Ar}, C⁷), 119.5 (CH_{Ar}), 118.7 (CH_{Ar}), 112.7 (C_{qAr}, C⁸), 111.3 (CH_{Ar}), 43.9 (CH₂, C¹⁰), 39.8 (CH₂, C¹¹), 25.1 (CH₂, C⁹).

HRMS (ESI-TOF) *m/z*: [M + H]⁺ Calcd for C₁₈H₁₉N₂O 279.1497; Found: 279.1501.

1-Morpholino-2-phenylethanone 4.40



The title compound was prepared from phenylacetic acid 98.5% (76 mg, 0.55 mmol, 1.1 equiv.) and morpholine 99% (43.5 μl, 44 mg, 0.50 mmol, 1 equiv.) after 24 h at 25 °C using the general procedure **D** and purified by flash silica gel column chromatography using Cy/EtOAc 50:50 to afford the pure amide as an off-white solid (48 mg, 0.234 mmol, **47% yield**).

R_f (Cy/EtOAc 50:50) = 0.45

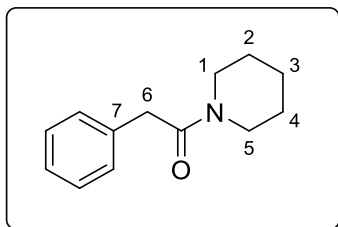
C₁₂H₁₅NO₂, **M.W**: 205.26. The ¹H and ¹³C NMR data are consistent with those reported in the literature.⁵⁷

¹H NMR (500 MHz; CDCl₃) δ 7.34-7.27 (m, 2H_{Ar}), 7.26-7.20 (m, 3H_{Ar}), 3.72 (s, 2H, H³), 3.63 (s, 4H, H¹), 3.48-3.38 (m, 4H, H²).

¹³C NMR (150 MHz; CDCl₃) δ 169.8 (C=O), 134.8 (C_{qAr}, C⁴), 128.9 (CH_{Ar}), 128.6 (CH_{Ar}), 126.9 (CH_{Ar}), 66.8 (CH₂, C¹), 66.5 (CH₂, C¹), 46.6 (CH₂, C²), 42.2 (CH₂, C²), 40.9 (CH₂, C³).

HRMS (ESI-TOF) m/z: $[M + H]^+$ Calcd for $C_{12}H_{16}NO_2$ 206.1181; Found: 206.1181.

2-Phenyl-1-(piperidin-1-yl)ethanone 4.41i



The title compound was prepared from phenylacetic acid 98.5% (76 mg, 0.55 mmol, 1.1 equiv.) and piperidine 99% (50 μ l, 43 mg, 0.50 mmol, 1 equiv.) after 48 h at 25 °C using the general procedure **D** and purified by flash silica gel column chromatography using Cy/EtOAc 50:50 to afford the pure amide as a colorless solid (23 mg, 0.113 mmol, **23% yield**).⁵⁵

Rf (Cy/EtOAc 50:50) = 0.45

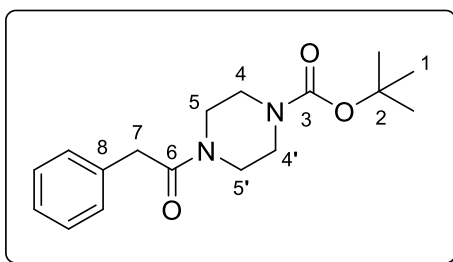
$C_{13}H_{17}NO$, **M.W:** 203,29. The 1H and ^{13}C NMR data are consistent with those reported in the literature.⁵⁵

1H NMR (500 MHz; $CDCl_3$) δ 7.31-7.26 (m, 2H_{Ar}), 7.25-7.18 (m, 3H_{Ar}), 3.71 (s, 2H, H⁶), 3.55 (t, $J = 5.5$ Hz, 2H, H^{1/5}), 3.34 (t, $J = 5.5$ Hz, 2H, H^{1/5}), 1.58-1.52 (m, 2H, H^{2/4}), 1.51-1.45 (m, 2H, H^{2/4}), 1.35-1.28 (m, 2H, H³).

^{13}C NMR (150 MHz; $CDCl_3$) δ 169.6 (C=O), 135.4 (C_{qAr}, C⁷), 128.8 (CH_{Ar}), 128.7 (CH_{Ar}), 126.8 (CH_{Ar}), 47.4 (CH₂, C⁶), 43.1 (CH₂), 41.2 (CH₂), 26.2 (CH₂), 25.6 (CH₂), 24.5 (CH₂).

HRMS (ESI-TOF) m/z: $[M + H]^+$ Calcd for $C_{13}H_{18}NO$ 204.1388; Found: 204.1386.

Tert-butyl 4-(2-phenylacetyl)piperazine-1-carboxylate 4.41j



The title compound was prepared from phenylacetic acid 98.5% (76 mg, 0.55 mmol, 1.1 equiv.) and 1-Boc-piperazine 97% (93 μ l, 96 mg, 0.50 mmol, 1 equiv.) using the general procedure **D** and purified by flash silica gel column chromatography using Cy/EtOAc 60:40 to afford the pure amide as a colorless solid. Several conditions were tested: a reaction for 18 h at 25 °C afforded the amide in **25% yield** (38 mg, 0.125 mmol), a reaction of 24 h at 60 °C provided the amide in **43% yield** (66 mg, 0.217 mmol), and the amidation reaction in 1,2-dichloroethane (7 ml, 0.0714 M) for 18 h at 50 °C afforded **31% yield** (47 mg, 0.154 mmol).

Rf (Cy/EtOAc 60:40) = 0.35

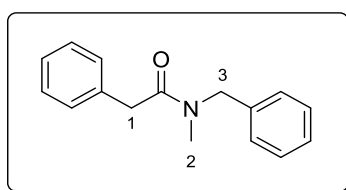
C₁₇H₂₄N₂O₃, **M.W.**: 304,39. The ¹H and ¹³C NMR data are consistent with those reported in the literature.¹⁹⁹

¹H NMR (500 MHz; CDCl₃) δ 7.34-7.28 (m, 2H_{Ar}), 7.27-7.21 (m, 3H_{Ar}), 3.74 (s, 2H, H⁷), 3.63-3.57 (m, 2H, H^{4/4'}), 3.44-3.33 (m, 4H, H⁵ and H^{5'}), 3.24-3.16 (m, 2H, H^{4/4'}), 1.44 (s, 9H, H¹).

¹³C NMR (150 MHz; CDCl₃) δ 174.8 (C=O, C³), 169.9 (C=O, C⁶), 134.8 (C_{qAr}, C⁸), 128.9 (CH_{Ar}), 128.6 (CH_{Ar}), 127.1, 127.0 (CH_{Ar}), 80.4 (C_{qAr}, C²), 46.0 (2CH₂, C^{5-5'}), 43.6 (CH₂, C^{4/4'}), 41.7 (CH₂, C^{4/4'}), 41.2 (CH₂, C⁷), 28.4 (3CH₃, C¹).

HRMS (ESI-TOF) m/z: [M + Na]⁺ Calcd for C₁₇H₂₄N₂O₃Na 327.1685; Found: 327.1688.

***N*-Benzyl-*N*-methyl-2-phenylacetamide 4.41k**



The title compound was prepared from phenylacetic acid 98.5% (76 mg, 0.55 mmol, 1.1 equiv.) and *N*-methylbenzylamine 99% (64.5 μ l, 60.6 mg, 0.50 mmol, 1 equiv.) after 36 h at 40°C using the general procedure **D**, and it was purified by flash silica-gel column chromatography using Cy/EtOAc 70:30 to afford the pure amide as a pale-yellow oil (24 mg, 0.10 mmol, **20% yield**).

Rf (Cy/EtOAc 70:30) = 0.3

¹⁹⁹ Cassidy, M. P.; Raushel, J.; Fokin, V. V. *Angew. Chem. Int. Ed.* **2006**, *45*, 3154–3157.

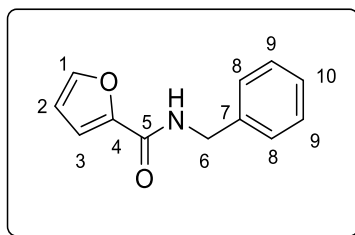
C₁₆H₁₇NO, **M.W**: 239.32. The ¹H and ¹³C NMR data are consistent with those reported in the literature.²⁰⁰

¹H NMR (500 MHz; CDCl₃, mixture of 2 rotamers 1:0.7) δ (Major rotamer) 7.36-7.06 (m, 10H_{Ar}), 4.60 (s, 2H, H³), 3.77 (s, 2H, H¹), 2.88 (s, 3H, H²); (Minor rotamer) 7.36-7.06 (m, 10H_{Ar}), 4.51 (s, 2H, H³), 3.74 (s, 2H, H¹), 2.94 (s, 3H, H²).

¹³C NMR (150 MHz; CDCl₃, mixture of 2 rotamers 1:0.7) δ (Major rotamer) 171.1 (C=O), 137.3 (C_{qAr}), 135.0 (C_{qAr}), 128.8 (2CH_{Ar}), 128.67 (2CH_{Ar}), 128.6 (2CH_{Ar}), 128.1 (2CH_{Ar}), 127.4 (CH_{Ar}), 126.78 (CH_{Ar}), 50.9 (CH₂, C³), 41.2 (CH₂, C¹), 35.2 (CH₃, C²); (Minor rotamer) 171.5 (C=O), 136.5 (C_{qAr}), 135.1 (C_{qAr}), 128.9 (2CH_{Ar}), 128.79 (2CH_{Ar}), 128.7 (2CH_{Ar}), 127.6 (CH_{Ar}), 126.8 (CH_{Ar}), 126.4 (2CH_{Ar}), 53.6 (CH₂, C³), 40.8 (CH₂, C¹), 34.0 (CH₃, C²).

HRMS (ESI-TOF) m/z: [M + H]⁺ Calcd for C₁₆H₁₈NO : 240.1388; Found: 240.1387.

***N*-Benzylfuran-2-carboxamide 4.411**



The title amide was prepared from 2-furoic acid (61.6 mg, 0.55 mmol, 1.1 equiv.) and benzylamine 99% (55 μl, 54 mg, 0.50 mmol, 1 equiv.) after a 48 h reaction at 40 °C using the general procedure **D** and purified by flash silica-gel column chromatography (Cy/EtOAc 60:40) to afford the pure amide as a colorless powder (11 mg, 0.055 mmol, **11% yield**).

R_f (Cy/EtOAc 60:40) = 0.25

C₁₂H₁₁NO₂, **M.W**: 201.23 g/mol. The ¹H and ¹³C NMR data are consistent with those reported in the literature.²⁰¹

²⁰⁰ Braddock, D. C.; Davies, J. J.; Lickiss, P. D. *Org. Lett.* **2022**, *24*, 1175–1179.

²⁰¹ Sawant, D. N.; Bagal, D. B.; Ogawa, S.; Selvam, K.; Saito, S. *Org. Lett.* **2018**, *20*, 4397–4400.

¹H NMR (500 MHz; CDCl₃) δ 7.38 (dd, *J* = 1.7, 0.8 Hz, 1H, H¹), 7.34-7.30 (m, 4H, H⁸⁻⁹), 7.30-7.24 (m, 1H, H¹⁰), 7.12 (dd, *J* = 3.5, 0.8 Hz, 1H, H³), 6.82 (br s, 1H, NH), 6.47 (dd, *J* = 3.5, 1.7 Hz, 1H, H²), 4.58 (d, *J* = 6.0 Hz, 2H, H⁶).

¹³C NMR (150 MHz; CDCl₃) δ 158.4 (C=O, C⁵), 147.9 (C_{qAr}, C⁴), 143.9 (CH_{Ar}, C¹), 138.1 (C_{qAr}, C⁷), 128.8 (CH_{Ar}, C⁹), 127.9 (CH_{Ar}, C⁸), 127.6 (CH_{Ar}, C¹⁰), 114.4 (CH_{Ar}, C³), 112.2 (CH_{Ar}, C²), 43.1 (CH₂, C⁶).

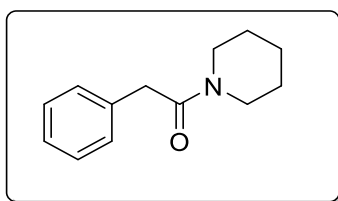
4.13.9 Scope of the High-temperature amide synthesis

4.13.9.1 General procedure E for amide synthesis under azeotropic reflux

A 10 mL oven-dried flask, equipped with a magnetic stirring bar, was charged with carboxylic acid (0.55 mmol, 1.1 equiv), boronic acid **4.9a** (11 mg, 0.05 mmol, 10 mol%), and dry toluene (3.5 mL, 0.143 M), followed by the addition of the amine (0.5 mmol, 1 equiv). The resulting suspension was stirred at reflux temperature, and the water formed during the reaction was removed using a Dean-Stark trap. After *t* (h), the reaction was allowed to cool down to room temperature, then, toluene was evaporated and the residue was purified by flash silica-gel column chromatography to afford the pure amide.

4.13.9.2 Synthesis and characterization of amide substrates

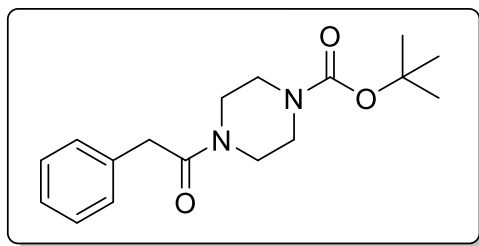
2-Phenyl-1-(piperidin-1-yl)ethanone **4.41i**



The title compound was prepared from phenylacetic acid 98.5% (76 mg, 0.55 mmol, 1.1 equiv.) and piperidine 99% (50 μl, 43 mg, 0.50 mmol, 1 equiv.) using the general procedure E, after a 16 h reaction, and purified by flash silica gel column chromatography using Cy/EtOAc 50:50 (**R_f** in Cy/EtOAc 50:50 = 0.45) to afford the pure amide as a colorless solid (90 mg, 0.443 mmol, **89% yield**).

The ^1H and ^{13}C NMR data are consistent with those reported in the literature.⁵⁵

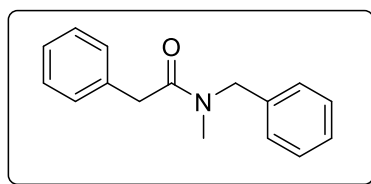
***Tert*-butyl 4-(2-phenylacetyl)piperazine-1-carboxylate 4.41j**



The title compound was prepared from phenylacetic acid 98.5% (76 mg, 0.55 mmol, 1.1 equiv.) and 1-Boc-piperazine 97% (93 μl , 96 mg, 0.50 mmol, 1 equiv.) using the general procedure **E**, after a 16 h reaction, and purified by flash silica gel column chromatography using Cy/EtOAc 60:40 (**Rf** in Cy/EtOAc 60:40 = 0.35) to afford the pure amide as a colorless solid (113 mg, 0.37 mmol, **74% yield**).

The ^1H and ^{13}C NMR data are consistent with those reported in the literature.¹⁹⁹

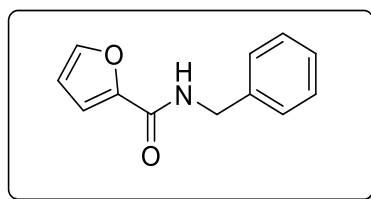
***N*-Benzyl-*N*-methyl-2-phenylacetamide 4.41k**



The title compound was prepared from phenylacetic acid 98.5% (76 mg, 0.55 mmol, 1.1 equiv.) and *N*-methylbenzylamine 99% (64.5 μl , 60.6 mg, 0.50 mmol, 1 equiv.) using the general procedure **E**, after a 36 h reaction, and it was purified by flash silica-gel column chromatography using Cy/EtOAc 70:30 (**Rf** in Cy/EtOAc 70:30 = 0.3) to afford the pure amide as a pale-yellow oil (105 mg, 0.439 mmol, **88% yield**).

The ^1H and ^{13}C NMR data are consistent with those reported in the literature.²⁰⁰

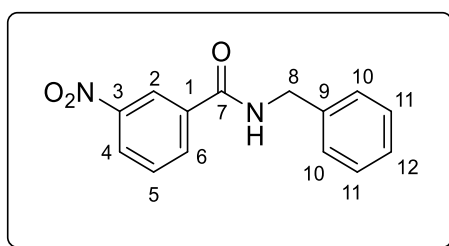
***N*-Benzylfuran-2-carboxamide 4.41l**



The title compound was prepared from 2-furoic acid (61.6 mg, 0.55 mmol, 1.1 equiv.) and benzylamine 99% (55 μ l, 54 mg, 0.50 mmol, 1 equiv.) using the general procedure **E**, after a 7 h reaction, and purified by flash silica gel column chromatography using Cy/EtOAc 60:40 (**Rf** in Cy/EtOAc 60:40 = 0.25) to afford the pure amide as a colorless solid (98 mg, 0.487 mmol, **97% yield**).

The ^1H and ^{13}C NMR data are consistent with those reported in the literature.²⁰¹

***N*-Benzyl-3-nitrobenzamide 4.41m**



The title compound was prepared from 3-nitrobenzoic acid (92 mg, 0.55 mmol, 1.1 equiv.) and benzylamine 99% (55 μ l, 54 mg, 0.50 mmol, 1 equiv.) using the general procedure **E**, after a 16 h reaction, and purified by flash silica gel column chromatography using Cy/EtOAc 60:40 (**Rf** in Cy/EtOAc 60:40 = 0.4) to afford the pure amide as a colorless solid (100 mg, 0.39 mmol, **78% yield**).

Rf (Cy/EtOAc 60:40) = 0.4

$\text{C}_{14}\text{H}_{12}\text{N}_2\text{O}_3$, **M.W.**: 256.26 g/mol. The ^1H and ^{13}C NMR data are consistent with those reported in the literature.²⁰²

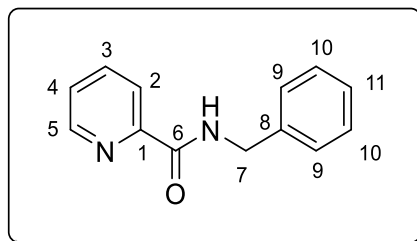
^1H NMR (500 MHz; CDCl_3) δ 8.60 (s, 1H, H^2), 8.30 (d, $J = 7.7$ Hz, 1H, H^4), 8.15 (d, $J = 7.7$ Hz, 1H, H^6), 7.58 (t, $J = 7.7$ Hz, 1H, H^5), 7.38-7.23 (m, 5H, $\text{H}^{10-11-12}$), 7.16 (br s, 1H, NH), 4.61 (d, $J = 5.1$ Hz, 2H, H^8).

^{13}C NMR (150 MHz; CDCl_3) δ 165.2 (C=O, C^7), 148.2 (C_{qAr} , C^3), 137.7 (C_{qAr} , C^9), 136.0 (C_{qAr} , C^1), 133.4 (CH_{Ar} , C^6), 129.9 (CH_{Ar} , C^5), 128.9 (CH_{Ar} , C^{11}), 127.9 (CH_{Ar} , C^{10}), 127.8 (CH_{Ar} , C^{12}), 126.1 (CH_{Ar} , C^4), 122.0 (CH_{Ar} , C^2), 44.4 (CH_2 , C^8).

²⁰² Hamstra, D. F. J.; Lenstra, D. C.; Koenders, T. J.; Rutjes, F. P. J. T.; Mecinović, J. *Org. Biomol. Chem.* **2017**, *15*, 6426–6432.

HRMS (ESI-TOF) m/z: $[M + H]^+$ Calcd for $C_{14}H_{13}N_2O_3$ 257.0926; Found: 257.0925.

***N*-Benzylpicolinamide 4.41n**



The title compound was prepared from picolinic acid (68 mg, 0.55 mmol, 1.1 equiv.) and benzylamine 99% (55 μ l, 54 mg, 0.50 mmol, 1 equiv.) using the general procedure E, after an 18 h reaction, and purified by flash silica gel column chromatography using Cy/EtOAc 60:40 (**Rf** in Cy/EtOAc 60:40 = 0.35) to afford the pure amide as a colorless solid (85 mg, 0.4 mmol, **80% yield**).

Rf (Cy/EtOAc 60:40) = 0.35

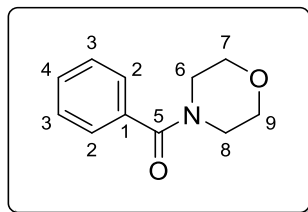
$C_{13}H_{12}N_2O$, **M.W**: 212.25 g/mol. The 1H and ^{13}C NMR data are consistent with those reported in the literature.²⁰¹

1H NMR (500 MHz; $CDCl_3$) δ 8.50 (ddd, $J = 4.8, 1.7, 0.9$ Hz, 1H, H^5), 8.41 (br s, 1H, NH), 8.23 (ddd, $J = 7.8, 1.3, 0.9$ Hz, 1H, H^2), 7.83 (td, $J = 7.7, 1.7$ Hz, 1H, H^3), 7.39 (ddd, $J = 7.6, 4.8, 1.3$ Hz, 1H, H^4), 7.38-7.31 (m, 4H, H^{9-10}), 7.27 (tt, $J = 7.1, 2.2$ Hz, 1H, H^{11}), 4.66 (d, $J = 6.1$ Hz, 2H, H^7).

^{13}C NMR (150 MHz; $CDCl_3$) δ 164.3 (C=O, C^6), 149.9 (C_{qAr} , C^1), 148.1 (CH_{Ar} , C^5), 138.3 (C_{qAr} , C^8), 137.4 (CH_{Ar} , C^3), 128.7 (CH_{Ar} , C^{10}), 127.9 (CH_{Ar} , C^9), 127.5 (CH_{Ar} , C^{11}), 126.3 (CH_{Ar} , C^4), 122.4 (CH_{Ar} , C^2), 43.5 (CH_2 , C^7).

HRMS (ESI-TOF) m/z: $[M + H]^+$ Calcd for $C_{13}H_{13}N_2O$ 213.1028; Found: 213.1029.

Morpholino(phenyl)methanone 4.41o



The title compound was prepared from benzoic acid > 99% (68 mg, 0.55 mmol, 1.1 equiv.) and morpholine 99% (43.5 μ l, 44 mg, 0.50 mmol, 1 equiv.) using the general procedure E, after an 18 h reaction, and purified by flash silica gel column chromatography using Cy/EtOAc 60:40 (**Rf** in Cy/EtOAc 60:40 = 0.2) to afford the pure amide as a yellow oil (91 mg, 0.476 mmol, **95% yield**).

Rf (Cy/EtOAc 60:40) = 0.2

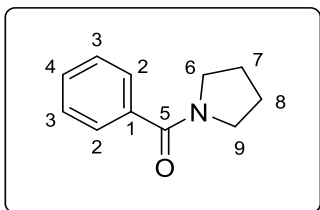
$C_{11}H_{13}NO_2$, **M.W.**: 191.23 g/mol. The 1H and ^{13}C NMR data are consistent with those reported in the literature.²⁰³

1H NMR (500 MHz; $CDCl_3$) δ 7.43-7.35 (m, 5H_{Ar}), 3.90-3.51 (m, 6H, H⁶, H⁸ and H^{7/9}), 3.42 (s, 2H, H^{7/9}).

^{13}C NMR (150 MHz; $CDCl_3$) δ 170.5 (C=O, C⁵), 135.3 (C_{qAr}, C¹), 129.9 (CH_{Ar}, C^{2/3/4}), 128.6 (CH_{Ar}, C^{2/3/4}), 127.1 (CH_{Ar}, C^{2/3/4}), 66.9, 48.3, 42.6.

HRMS (ESI-TOF) m/z: [M + H]⁺ Calcd for $C_{11}H_{14}NO_2$ 192.1025; Found: 192.1022.

Phenyl(pyrrolidin-1-yl)methanone 4.41p



²⁰³ Braddock, D. C.; Lickiss, P. D.; Rowley, B. C.; Pugh, D.; Purnomo, T.; Santhakumar, G.; Fussell, S. J. *Org. Lett.* **2018**, *20*, 950–953.

The title compound was prepared from benzoic acid > 99% (68 mg, 0.55 mmol, 1.1 equiv.) and pyrrolidine 99% (41.5 μ l, 36 mg, 0.50 mmol, 1 equiv.) using the general procedure **E**, after a 7 h reaction, and purified by flash silica gel column chromatography using Cy/EtOAc 60:40 (**Rf** in Cy/EtOAc 60:40 = 0.3) to afford the pure amide as a colorless oil (66 mg, 0.377 mmol, **75% yield**).

Rf (Cy/EtOAc 60:40) = 0.3

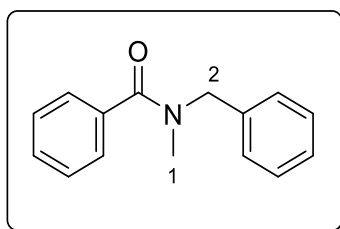
$C_{11}H_{13}NO$, **M.W.**: 175.23 g/mol. The 1H and ^{13}C NMR data are consistent with those reported in the literature.²⁰¹

1H NMR (500 MHz; $CDCl_3$) δ 7.51-7.46 (m, 2H_{Ar}, H²), 7.41-7.33 (m, 3H_{Ar}, H³⁻⁴), 3.62 (t, J = 7.0 Hz, 2H, H⁶), 3.39 (t, J = 6.7 Hz, 2H, H⁹), 1.93 (tt, J = 7.0, 6.7 Hz, 2H, H⁷), 1.83 (pentet, J = 6.7 Hz, 2H, H⁸).

^{13}C NMR (150 MHz; $CDCl_3$) δ 169.8 (C=O, C⁵), 137.2 (C_{qAr}, C¹), 129.8 (CH_{Ar}, C⁴), 128.3 (CH_{Ar}, C³), 127.1 (CH_{Ar}, C²), 49.7 (CH₂, C⁹), 46.2 (CH₂, C⁶), 26.4 (CH₂, C⁸), 24.5 (CH₂, C⁷).

HRMS (ESI-TOF) m/z : $[M + H]^+$ Calcd for $C_{11}H_{14}NO$ 176.1075; Found: 176.1074.

***N*-Benzyl-*N*-methylbenzamide 4.41q**



The title amide was prepared from benzoic acid > 99% (68 mg, 0.55 mmol, 1.1 equiv.) and *N*-methylbenzylamine 99% (64.5 μ l, 61 mg, 0.50 mmol, 1 equiv.) using the general procedure **E**, after an 18 h reaction, and purified by flash silica gel column chromatography using Cy/EtOAc 80:20 (**Rf** in Cy/EtOAc 80:20 = 0.2) to afford the pure amide as a colorless oil (86 mg, 0.38 mmol, **76% yield**).

Rf (Cy/EtOAc 80:20) = 0.2

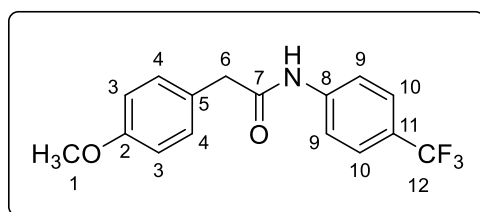
$C_{15}H_{15}NO$, **M.W.**: 225.29 g/mol. The 1H and ^{13}C NMR data are consistent with those reported in the literature.²⁰¹

¹H NMR (600 MHz; CDCl₃, mixture of two rotamers 1:1) δ 7.49-7.27 (m, 18H_{Ar}), 7.21-7.12 (m, 2H_{Ar}), 4.76 (s, 2H, H²), 4.51 (s, 2H, H²), 3.03 (s, 3H, H¹), 2.85 (s, 3H, H¹).

¹³C NMR (150 MHz; CDCl₃, mixture of two rotamers 1:1) δ 172.4 (C=O), 171.7 (C=O), 137.1 (C_{qAr}), 136.6 (C_{qAr}), 136.3 (C_{qAr}), 136.2 (C_{qAr}), 129.7 (CH_{Ar}), 128.9 (CH_{Ar}), 128.8 (CH_{Ar}), 128.5 (CH_{Ar}), 128.4 (CH_{Ar}), 128.3 (CH_{Ar}), 128.2 (CH_{Ar}), 127.7 (CH_{Ar}), 127.6 (CH_{Ar}), 127.1 (CH_{Ar}), 126.84 (CH_{Ar}), 126.8 (CH_{Ar}), 55.2 (CH₂), 50.8 (CH₂), 37.1 (CH₃), 33.2 (CH₃).

HRMS (ESI-TOF) m/z: [M + H]⁺ Calcd for C₁₅H₁₆N O : 226.1232; Found: 226.1230.

4-Methoxy-*N*-(4-(trifluoromethyl)phenyl)benzeneacetamide **4.41r**



The title amide was prepared from 4-methoxyphenylacetic acid (91.4 mg, 0.55 mmol, 1.1 equiv.) and 4-trifluoromethylaniline 99% (63.4 μL, 81.4 mg, 0.5 mmol, 1 equiv.) using the general procedure **E**, after a 24 h reaction, and purified by flash silica gel column chromatography using Cy/EtOAc 70:30 to afford the pure amide as a colorless solid (121 mg, 0.39 mmol, **78% yield**).

R_f (Cy/EtOAc 70:30) = 0.3

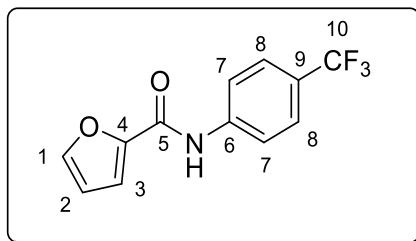
C₁₆H₁₄F₃NO₂, **M.W.**: 309.29 g/mol.

¹H NMR (600 MHz; CDCl₃) δ 7.54 (d, *J* = 8.9 Hz, 2H, H¹⁰), 7.52 (d, *J* = 8.9 Hz, 2H, H⁹), 7.31 (br s, NH), 7.24 (d, *J* = 8.6 Hz, 2H, H⁴), 6.93 (d, *J* = 8.6 Hz, 2H, H³), 3.83 (s, 3H, H¹), 3.69 (s, 2H, H⁶).

¹³C NMR (150 MHz; CDCl₃) δ 170.0 (C=O, C⁷), 159.4 (C_{qAr}, C²), 140.8 (q, ⁵*J*_{C-F} = 1.3 Hz, C⁸), 130.8 (CH_{Ar}, C⁴), 126.3 (q, ³*J*_{C-F} = 3.8 Hz, C¹⁰), 126.2 (q, ²*J*_{C-F} = 32.7 Hz, C¹¹), 125.9 (C_{qAr}, C⁵), 124.2 (q, ¹*J*_{C-F} = 272.0 Hz, C¹²), 119.4 (CH_{Ar}, C⁹), 114.9 (CH_{Ar}, C³), 55.5 (CH₃, C¹), 44.1 (CH₂, C⁶).

¹⁹F NMR (565 MHz; CDCl₃) δ -62.1.

N-(4-(Trifluoromethyl)phenyl)-2-furancarboxamide **4.41s**



The title amide was prepared from furoic acid (61.6 mg, 0.55 mmol, 1.1 equiv.) and 4-trifluoromethylaniline 99% (63.4 μ L, 81.4 mg, 0.5 mmol, 1 equiv.) using the general procedure **E**, after a 48 h reaction, and purified by flash silica gel column chromatography using Cy/EtOAc 60:40 to afford the pure amide as a colorless solid (62 mg, 0.24 mmol, **49% yield**).

$C_{12}H_8F_3NO_2$, **M.W.**: 255.20 g/mol.

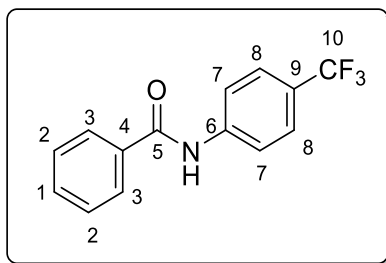
R_f (Cy/EtOAc 60:40) = 0.4

¹H NMR (500 MHz; $CDCl_3$) δ 8.27 (br s, NH), 7.78 (d, $J = 8.5$ Hz, H⁸), 7.60 (d, $J = 8.5$ Hz, H⁷), 7.51 (dd, $J = 1.7, 0.8$ Hz, H¹), 7.26 (dd, $J = 3.6, 0.8$ Hz, H³), 6.57 (dd, $J = 3.6, 1.7$ Hz, H²).

¹³C NMR (125 MHz; $CDCl_3$) δ 156.3 (C=O, C⁵), 147.4 (C_{qAr}, C⁴), 144.7 (CH_{Ar}, C¹), 140.6 (C_{qAr}, C⁶), 126.5 (q, $^3J_{C-F} = 3.8$ Hz, C⁸), 124.2 (q, $^1J_{C-F} = 271.7$ Hz, C¹⁰), 122.1 (q, $^2J_{C-F} = 32.3$ Hz, C⁹), 119.6 (CH_{Ar}, C⁷), 116.1 (CH_{Ar}, C²), 112.9 (CH_{Ar}, C³).

¹⁹F NMR (470 MHz; $CDCl_3$) δ -62.1.

N-(4-(Trifluoromethyl)phenyl)benzamide **4.41t**



The title amide was prepared from benzoic acid > 99% (68 mg, 0.55 mmol, 1.1 equiv.) and 4-trifluoromethylaniline 99% (63.4 μ L, 81.4 mg, 0.5 mmol, 1 equiv.) using the general procedure **E**, after a 5 days reaction, and purified by flash silica gel column chromatography using Cy/EtOAc 70:30 to afford the pure amide as a colorless solid (64 mg, 0.24 mmol, **48% yield**).

The use of higher loading of boronic acid **4.9a** (21.6 mg, 0.1 mmol, 20 mol%) for a reaction time of 5 days afforded the amide **4.54t** in **52% yield** (69 mg, 0.26 mmol).

Rf (Cy/EtOAc 70:30) = 0.3

C₁₄H₁₀F₃NO, **M.W**: 265.24 g/mol. The ¹H and ¹³C NMR data are consistent with those reported in the literature.²⁰⁴

¹H NMR (500 MHz; DMSO-*d*₆) δ 10.60 (br s, 1H, NH), 8.02 (d, *J* = 8.5 Hz, 2H, H⁷), 7.98 (dd, *J* = 7.2, 1.3 Hz, 2H, H³), 7.73 (d, *J* = 8.5 Hz, 2H, H⁸), 7.63 (tt, *J* = 7.3, 1.3 Hz, 1H, H¹), 7.59-7.53 (m, 2H, H²),

¹³C NMR (150 MHz; CDCl₃) δ 166.5 (C=O, C⁵), 143.3 (q, ⁵*J*_{C-F} = 1.31 Hz, C⁶), 134.9 (Cq_{Ar}, C⁴), 132.4 (CH_{Ar}, C¹), 128.9 (CH_{Ar}, C²), 128.3 (CH_{Ar}, C³), 126.4 (q, ³*J*_{C-F} = 3.8 Hz, C⁸), 125.1 (q, ¹*J*_{C-F} = 271.1 Hz, C¹⁰), 124.0 (q, ²*J*_{C-F} = 32.1 Hz, C⁹), 120.5 (CH_{Ar}, C⁷).

¹⁹F NMR (470 MHz; DMSO-*d*₆) δ -60.3

HRMS (ESI-TOF) *m/z*: [M + H]⁺ Calcd for C₁₄H₁₁F₃NO 266.0793; Found: 266.0794.

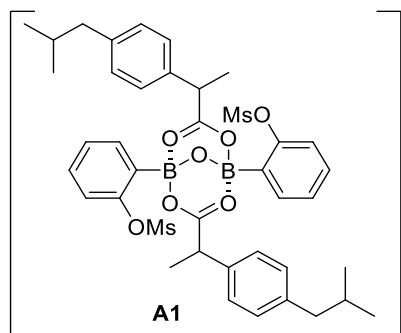
4.13.10 Synthesis and characterization of mixed anhydride intermediates

Intermediate A1

To a 1.5 mL sealed vial, boronic acid **4.9a** (5.4 mg, 0.025 mmol), (S)-ibuprofen (6.3 mg, 0.03 mmol, 1.2 equiv) and activated powdered 5 Å molecular sieves (50 mg) were added. Then CDCl₃ (0.5 mL, 0.05 M) was added and the mixture was vigorously stirred at 25 °C for 30 minutes. Next, the reaction mixture was transferred into an NMR tube and characterized by ¹H, ¹³C and ¹¹B NMR.

In this case, the reaction mixture contains the complex **A1** and remaining ibuprofen. Hence, intermediate **A1** was not obtained in a pure form. But its ¹H, and ¹³C NMR signals were identified by subtracting the surplus signals of ibuprofen.

²⁰⁴ Brittain, W. D. G.; Cobb, S. L. *Org. Lett.* **2021**, *23*, 5793–5798.



^1H NMR (600 MHz, CDCl_3) δ 7.61 (dd, $J = 7.4, 1.3$ Hz, 2H), 7.43 (d, $J = 8.1$ Hz, 2H), 7.37 (ddd, $J = 8.1, 7.4, 1.5$ Hz, 2H), 7.24 (t, $J = 7.4$ Hz, 2H), 7.16 (d, $J = 7.8$ Hz, 4H), 7.10 (d, $J = 7.8$ Hz, 4H), 3.92 (q, $J = 7.1$ Hz, 2H), 2.73 (s, 6H), 2.46 (d, $J = 7.5$ Hz, 4H), 1.89-1.79 (m, 2H), 1.55 (d, $J = 7.1$ Hz, 6H), 0.89 (d, $J = 6.5$ Hz, 12H).

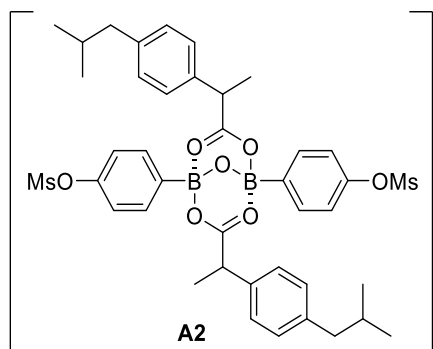
^{13}C NMR (150 MHz, CDCl_3) δ 187.8, 153.3, 141.9, 135.0, 134.2, 130.3, 129.9, 127.6, 126.5, 121.3, 46.4, 45.1, 44.9, 37.4, 22.5, 17.4.

^{11}B NMR (193 MHz, CDCl_3) δ 5.0 ppm.

Intermediate A2

To a 1.5 mL sealed vial, boronic acid **4.16** (5.4 mg, 0.025 mmol), (S)-ibuprofen (6.3 mg, 0.03 mmol, 1.2 equiv) and activated powdered 5Å molecular sieves (50 mg) were added. Then CDCl_3 (0.5 mL, 0.05 M) was added and the mixture was vigorously stirred at 25 °C for 30 minutes. Next, the reaction mixture was transferred into an NMR tube and characterized by ^1H and ^{11}B NMR. In this case, there is 58% conversion to **A2** (from ^1H NMR). Next (S)-ibuprofen was added sequentially until complete conversion into **A2**. The total of (S)-ibuprofen needed is (32 mg, 0.155 mmol, 6.2 equiv).

In this case, the reaction mixture contains the complex **A2** and excess ibuprofen. Hence, intermediate **A2** was not obtained in a pure form. But its ^1H NMR signals were identified by subtracting the surplus signals of ibuprofen. Additionally, ^{11}B NMR spectrum was recorded. The ^{13}C NMR spectrum of this mixture was not satisfactory for a proper description even after conducting 1024 scans on a 600 MHz spectrometer, due to the low solubility of **4.16** in CDCl_3 . Hence it is not described here.



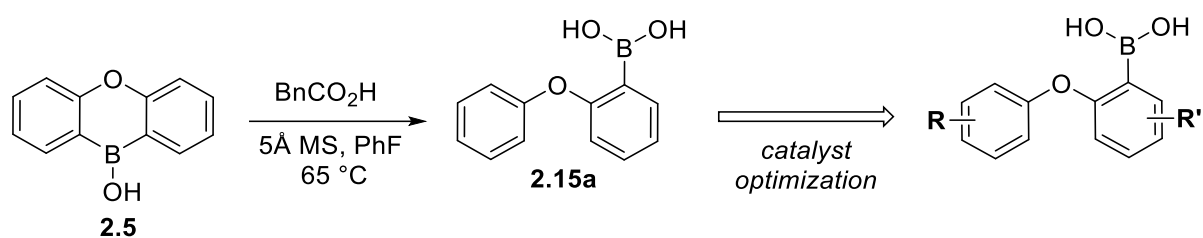
¹H NMR (600 MHz, CDCl₃) δ 7.61 (d, *J* = 8.0 Hz, 4H), 7.24 (d, *J* = 8.0 Hz, 4H), 7.22-7.17 (m, 2H), 7.12-7.04 (m, 6H), 3.91-3.76 (m, 2H), 3.09 (s, 6H), 2.44 (d, *J* = 6.7 Hz, 4H), 1.89-1.79 (m, 2H), 1.49 (d, *J* = 7.1 Hz, 6H), 0.89 (d, *J* = 6.5 Hz, 12H).

¹¹B NMR (193 MHz, CDCl₃) δ 6.1 ppm.

General Conclusion

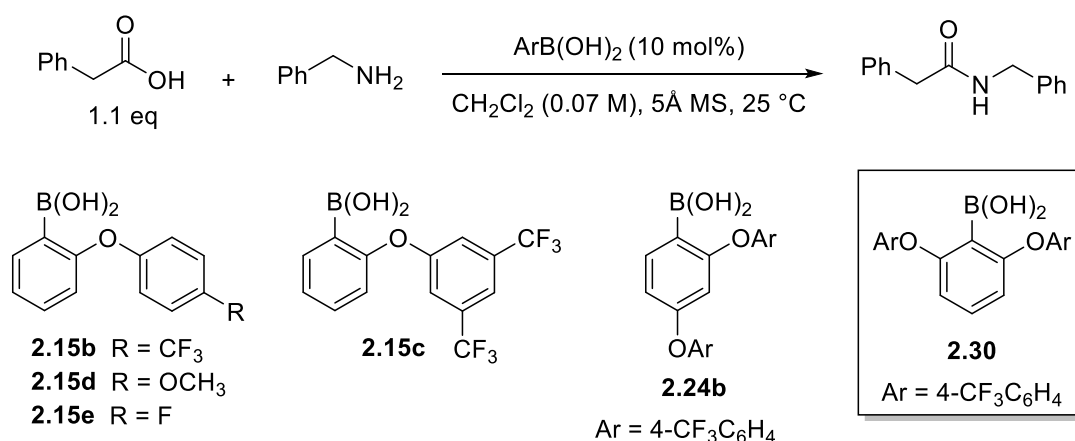
At the end of every chapter, a detailed conclusion was provided. Herein, we present a brief recap and draw overall conclusions about the thesis findings.

Firstly, the study on cyclic borinic acids revealed that they do not display catalytic activity unless they protodeborylate into the respective boronic acid, which in turn facilitates the amidation reaction. The phenoxyphenylboronic acid, generated from the protodeboronation of oxaboreanthracene, displayed catalytic activity in the amidation reaction at 25 °C, which prompted the investigation of an array of aryloxyphenylboronic acids having variable electronic properties (Scheme 153).



Scheme 153

Among various biarylether-based boronic acid catalysts (Scheme 154), 2,6-disubstituted boronic acid **2.30** was the best-performing catalyst. Although **2.30** displayed interesting kinetic activity on the reaction of formation of *N*-benzylphenylacetamide at 25 °C, such catalytic activity was restricted, resulting in low yields when different amides were tested.

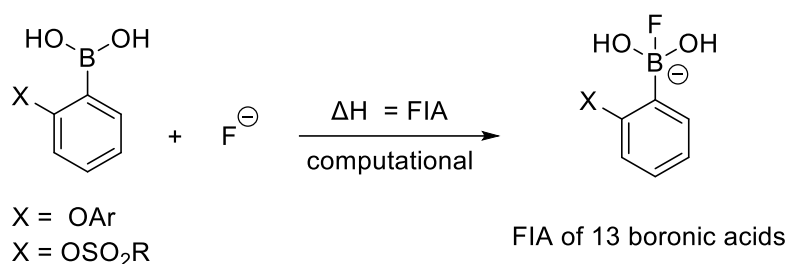


Scheme 154

Nonetheless, the emerging reactivity trend, in which 2,6-disubstitution enhances the catalytic efficiency, goes against the previously reported trend in the literature. This indicates that a specific combination of *ortho*-steric and electronic effects is needed for di(*ortho*)-substitution

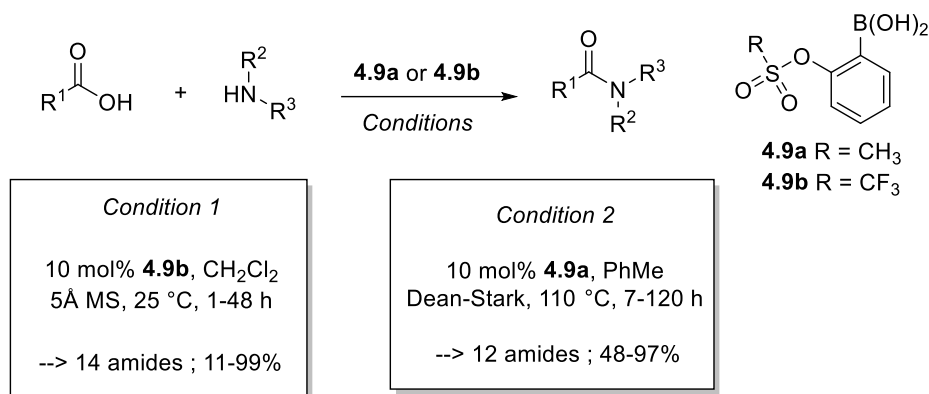
to be favorable. To illustrate, there should be sufficient steric hindrance to prevent the deactivation of the active trigonal boron center, and an electron-withdrawing effect to increase the Lewis acidity of the boronic acid.

Next, the Lewis acidity quantification of the biarylether boronic acids was performed using the fluoride-ion affinity (FIA) (Scheme 155). Notably, the correlation between the FIA scale of biarylether boronic acids and their catalytic activity demonstrated that the FIA can serve as an indicator of whether a boronic acid is a potential catalyst candidate. However, it cannot be related to the catalytic efficiency, as the FIA calculation does not consider secondary interactions and dispersive forces that impact the catalyst's activity. Moreover, the theoretical Lewis acidity study provided valuable insights that guided the development of a new group of *ortho*-(sulfonate)benzeneboronic acids.



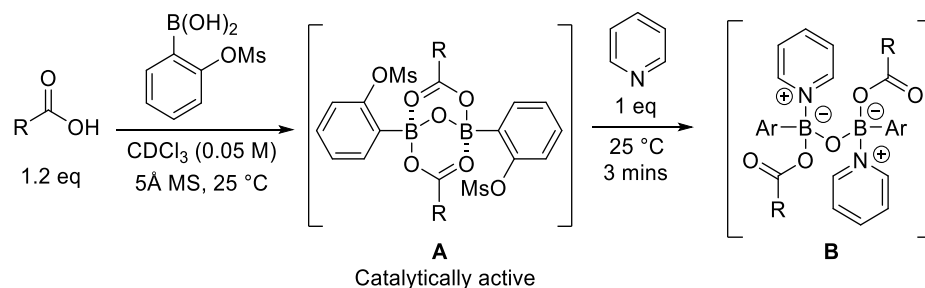
Scheme 155

Lastly, the *ortho*-(sulfonate)benzeneboronic acids were investigated as catalysts for the direct amidation reaction (Scheme 156). The catalyst **4.9b** enabled the coupling of α -branched, and heterocycle-containing aliphatic carboxylic acid with aliphatic amines, at 25 °C, in up to 99% yield. Nonetheless, the coupling of secondary amines or aromatic acids constituted a limitation for the low-temperature conditions using molecular sieves, affording the amides in 11-47% yields. Importantly, by employing Dean-stark dehydration conditions, the substrate scope was broadened to include more challenging aromatic and heteroaromatic carboxylic acids as well as secondary amines and anilines (Scheme 156).



Scheme 156

Furthermore, mechanistic investigations offered valuable insight into the significance of *ortho*-substitution in arylboronic acid catalysts. Briefly, the *ortho*-(mesyloxy)phenylboronic acid enabled easier activation of the carboxylic acid in comparison to its *para*-regioisomer, accomplished by the formation of a mixed anhydride intermediate **A** (Scheme 157). The *ortho*-substitution also mitigated the deactivation of the catalytically active species **A** to some extent by hindering the addition of the amine to the active boron center.



Scheme 157

In summary, this thesis has made advancements in investigating new boronic acid catalysts for amide synthesis and determining the theoretical Lewis acidity of arylboronic acids. Furthermore, additional research is required to extend the application of these boronic acid catalysts and to gain further information on the relationship between their Lewis acidity and catalytic properties.

Abstract

Amide bond formation reactions constitute a pivotal tool in organic synthesis owing to the versatility of the amide bond. Arylboronic acids represent one of the most distinguished classes of molecules studied for the catalytic direct amidation reaction. In this context, the catalytic activity of a group of biarylether-based boronic acids was examined and the findings of this study revealed some valuable insights into the trends of reactivity of boronic acid catalysts. Furthermore, the computational fluoride-ion affinity (FIA) was used for Lewis acidity assessment of several arylboronic acids and it assisted the design of a new class of *ortho*-(sulfonate)benzeneboronic acids whose catalytic performance compared favorably with the current state-of-the-art boronic acids. Importantly, the *ortho*-(sulfonate)benzeneboronic acids were efficiently used for the coupling of aliphatic, aromatic, and heteroaromatic carboxylic acids, as well as aliphatic amines, and anilines. Lastly, mechanistic investigations provided valuable information on the role of the *ortho*-substitution in arylboronic acid catalysis.

Keywords: Amide synthesis, boronic acid catalyst, *ortho*-substitution, Lewis acidity.

Résumé

Les réactions de formation de liaisons amides constituent un outil essentiel de la synthèse organique en raison de la polyvalence de la liaison amide. Les acides arylboroniques représentent l'une des classes les plus distinguées de molécules étudiées pour la réaction d'amidation catalytique directe. Dans ce contexte, l'activité catalytique d'un groupe d'acides boroniques à base de biaryléther a été examinée dans cette thèse et les résultats de cette étude ont abouti à une compréhension des tendances de la réactivité des catalyseurs à base d'acides boroniques. En outre, le calcul de l'affinité de l'ion fluor (FIA) a été utilisé pour évaluer l'acidité de Lewis de plusieurs acides arylboroniques et a contribué à la conception d'une nouvelle classe d'acides *ortho*-(sulfonate)benzénoboroniques dont les performances catalytiques se comparent favorablement à celles des acides boroniques actuels les plus récents. Il est important de noter que les acides *ortho*-(sulfonate)benzèneboroniques ont été utilisés efficacement pour le couplage d'acides carboxyliques aliphatiques, aromatiques et hétéroaromatiques, ainsi que d'amines aliphatiques et d'anilines. Enfin, les études mécanistiques ont fourni des informations précieuses sur le rôle de la substitution *ortho* dans la catalyse de l'acide arylboronique.

Mots-clés : Synthèse des amides, catalyse de l'acide boronique, *ortho*-substitution, acidité de Lewis.